Unified Total Site Heat Integration: Targeting, Optimisation and Network Design

A thesis

submitted in fulfilment

of the requirements for the degree

of

Doctor of Philosophy in Engineering

at

The University of Waikato

by

AMIR HOSSEIN TARIGHALESLAMI

THE UNIVERSITY OF
WAIKATO
Te Whare Wānanga o Waikato

2018

اقْرَأْ بِاسْمِ رَبِّكَ الَّذِي خَلَقَ ﴿١﴾ خَلَقَ الْإِنْسَانَ مِنْ عَلَقٍ ﴿٢﴾ اقْرَأْ وَرَبُّكَ الْأَكْرَمُ ﴿٣﴾ الَّذِي عَلَّمَ بِالْقَلَمِ ﴿٤﴾ عَلَّمَ الْإِنْسَانَ مَا لَمْ يَعْلَمْ ﴿٥﴾.

In the name of Allah, Most Gracious, Most Merciful

Read (Prophet Muhammad) in the Name of your Lord who created, (1) created the human from a (blood) clot. (2) Read! Your Lord is the Most Generous, (3) who taught by the pen, (4) taught the human what he did not know. (5)

به نام خداوند بخشاینده مهربان

بخوان به نام پروردگارت که بیافرید(۱). آدمی را از نخته خونی بیافرید(۲). بخوان، و پروردگار تو ارجمندترین است(۳). خدایی که به وسیله قلم آموزش داد(٤)، به آدمی آنچه را که نمی دانست بیاموخت(۵).

Abstract

Process industries in New Zealand use 214.3 PJ of process heat, of which approximately 65 % is fossil fuels. Despite increasing energy demands, depleting fossil fuel resources, and pressure to reduce Greenhouse Gas emissions, low grade heat in large-scale processing sites is still not fully utilised. This thesis presents methods to target, optimise and design more practical heat recovery systems for large industrial sites, i.e. Total Sites, and overcome technical limitations of current methods. Original contributions of this thesis to literature include novel developments and applications in six areas: i) a new Total Site Heat Integration (TSHI) targeting method – Unified Total Site Targeting (UTST) – which sets realistic targets for isothermal and non-isothermal utilities and heat recovery via the utility system; ii) a new TSHI optimisation and utility temperature selection method to optimise Total Cost of the utility system; iii) a new Utility Exchanger Network synthesis and design method based on the targets achieved by the UTST method and optimal temperatures from optimisation method; iv) a new method for calculating assisted heat transfer and shaft work to further improve TSHI cogeneration and performance; v) examination of heat transfer enhancement techniques in TSHI to achieve higher heat recovery and lower required area by substituting conventional utility mediums by nanofluids in the utility system; and vi) a spreadsheet software tool called Unified Total Site Integration to apply the developed methods to real industrial cases.

The developed methods have been applied to three large industrial case studies. Results confirms that heat recovery and utility targets obtained from the UTST method were lower but more realistic to achieve in practice when compared to conventional TSHI methods. The three industrial case studies represent a wide variety of processing industries. In summary, the over-estimation of TSHI targets for the three case studies from using the conventional method compared to the new method are 0.2 % for the Södra Cell Värö Kraft Pulp Mill, 22 % for a New Zealand Dairy Factory, and 0.1 % for Petrochemical Complex. The Total Annualised Costs (TAC) for the three case studies are minimised using a new derivative based approach. Results show TAC reductions 4.6 % for Kraft Pulp Mill, 0.6 % for Dairy Factory, and 3.4 % for Petrochemical Complex case studies. In addition, sensitivity

analysis for the optimisation is undertaken. The UTST method with its modified targeting procedure is demonstrated to generate simpler Utility Exchanger Network designs compared to conventional methods, which confirm the original targets are realistic and achievable. A new method for calculating assisted heat integration targets applied to an example Total Site problem increased heat recovery by 1,737 kW, which is a 21% increase in Total Site heat recovery, and increased shaft work by 80 kW. Lastly, the addition of nanoparticles to create a closed nanofluid heat recovery systems shows heat recovery from liquid-liquid heat exchangers increases of 5 % to 9 % using an intermediate fluid with 1.5 vol. % CuO/water.

Acknowledgments

I am ever grateful to the God for his graces and blessing upon me. I could never have stand where I am today without the faith in you.

First and foremost, I would like to express my sincerest gratitude to my chief supervisor Professor Michael R. W. Walmsley who supported me throughout my PhD research with his endless patience, motivation and knowledge, whilst allowing me the space to work in my own way. I also would like to acknowledge my co-supervisors, special thanks to Dr Martin J. Atkins for his valuable input, brilliant comments, flexibility and suggestions. Many thanks to Dr Timothy G. Walmsley for his patience and ongoing support during daily discussions. I deeply appreciate his help, especially with coding my software tool. This thesis would not have been possible to be done on time without your constant help and encouragement and supports. Thanks for always being there and having time for me. I would like to thank Dr James R. Neale for his technical advice, suggestions, and continuous encouragements.

I would like to thank Dr Peng Yen Liew from Malaysia-Japan International Institute of Technology (MJIIT), Universiti Teknologi Malaysia for his contribution to technical discussions and valuable input and suggestions regarding the case study.

I would like to acknowledge Energy Research Centre, University of Waikato, where my PhD research took place and Professor Peter J. J. Kamp, former director of Energy Research Centre for granting financial support as study research award.

Moreover, I would like to thank the members of my examination panel, Associate Professor Andrew Hoadley from Monash University and Dr Andreja Nemet from University of Maribor for making my oral examination a pleasant session, and for your brilliant suggestions, thank you.

In my daily work, I have been blessed with friendly and cheerful colleagues and friends and PhD students at Energy Research Centre. I want to thank research officer Mr Lance Wong, and my mates Mr Akash Lokhande, Mr Benjamin Ong, Mr Nathan Lal, Ms Danielle Bertram, and Mr Yihan Wu. You have been such amazing friends.

I would like to extend my acknowledgement and recognition to the Dean of School of Engineering, Professor Mark Dyer, former Associate Dean Professor Janis Swan, Associate Dean in postgraduate Associate Professor Michael Mucalo, and postgraduate coordinator Dr James Carson for welcoming me to the School of Engineering, Faculty of Science and Engineering, University of Waikato. A very special thanks to Administrator of the School of Engineering Ms Mary Dalbeth for being such a lovely and helpful during these years and Ms Cheryl Ward the librarian of the School of Engineering for her support. I also recognise and thank the School of Engineering for financial support to attend the 2016 Conference PRES in Prague, Czech Republic.

Since my wife and I arrived in New Zealand we faced a very warm welcome from a very kind and lovely people. We never felt we are thousands of kilometres away from friends, relatives and family. We would like to take this opportunity to show our heartfelt love and thanks to Neale, Walmsley, and Atkins families who accepted us as part of their family. Especially, Gill and Trevor Neale, and Fiona and Puti Walmsley. We love you all!

My prayers to the soul of my late father Mr Reza Tarighaleslami, who has been and will inspire my life. He was a great man who always encouraged me to achieve the highest success. Unfortunately, he is not here to celebrate this achievement with us, but I am confident that he is looking at us from the Heaven.

I would like to express my great gratitude to my family and friends. Many thanks to my lovely mother, Mohtaram, for her unconditional and endless love, and moral support. I would also like to thank my brother, Mohsen, for always being there for me, and for your enormous supports and kindness.

Thanks to my in-laws for their constant support and encouragements.

Last but not least, thanks to my beloved wife, Nasim, for providing me with your pure love and unwavering support. This work would not have been possible without your support, understanding, patience and help.

Amir Hossein Tarighaleslami

Contributing Publications

The bulk of the results contained in this thesis have been published in respectable international engineering journals and conferences. Chapter 4 is published in Energy [1]. Chapter 5 is published in Chemical Engineering Transactions [2] and in Energy [3]. Chapter 6 is published in Chemical Engineering Transactions [4] and also in Energy [5]. Chapter 7 is published as three individual papers, half of the chapter is published in Chemical Engineering Transactions [6], and the other half is published in Applied Thermal Engineering [7] and Chemical Engineering Transactions [8]. Research comprising this thesis has been presented at several local and international conferences, such as the Conference on Process Integration, Modelling and Optimisation for Energy Saving and Pollution Reduction (PRES series 2015-2017), through both oral and poster presentation. Most notably, the second half of Chapter 7 was awarded best student poster, Zdenek Burianec Memorial Award, at PRES 2015 conference. In parallel to the main objective of the thesis, significant contributions as a co-author have also resulted in three additional journal papers – two in Energy [11, 12] and one in Chemical Engineering Transactions [13] – and these articles are presented in Appendix B.

Journal Articles

[1] **A. H. Tarighaleslami**, T. G. Walmsley, M. J. Atkins, M. R. W. Walmsley, P. Y. Liew, J. R. Neale, 2017, A Unified Total Site Heat Integration targeting method for isothermal and non-isothermal utilities, *Energy*, 119, 10–25.

[2] **A. H. Tarighaleslami**, T. G. Walmsley, M. J. Atkins, M. R. W. Walmsley, J. R. Neale, 2016, Optimisation of Non-Isothermal Utilities using the Unified Total Site Heat Integration Method, *Chemical Engineering Transactions*, 52, 457–462.

[3] **A. H. Tarighaleslami**, T. G. Walmsley, M. J. Atkins, M. R. W. Walmsley, J. R. Neale, 2017, Total Site Heat Integration: Utility Selection and Optimisation Using Cost and Exergy Derivative Analysis, *Energy*, 141, 949-963.

[4] **A. H. Tarighaleslami**, T. G. Walmsley, M. J. Atkins, M. R. W. Walmsley, J. R. Neale, 2017, A Comparison of Utility Heat Exchanger Network Synthesis for Total Site Heat Integration Methods, *Chemical Engineering Transactions*, 61, 775–780.

[5] **A. H. Tarighaleslami**, T. G. Walmsley, M. J. Atkins, M. R. W. Walmsley, J. R. Neale, 2018, Utility exchanger Network Synthesis for Total Site Heat Integration, *Energy*, 153, 1000-1015.

[6] T. G. Walmsley, M. J. Atkins, **A. H. Tarighaleslami**, P. Y. Liew, 2016, Assisted Heat Transfer and Shaft Work Targets for Increased Total Site Heat Integration, *Chemical Engineering Transactions*, 52, 403–408.

[7] **A. H. Tarighaleslami**, T. G. Walmsley, M. J. Atkins, M. R. W. Walmsley, J. R. Neale, 2016, Heat Transfer Enhancement for site level indirect heat recovery systems using nanofluids as the intermediate fluid, *Applied Thermal Engineering*, 105, 923–930.

[8] **A. H. Tarighaleslami**, T. G. Walmsley, M. R. W. Walmsley, M. J. Atkins, J. R. Neale, 2015, Heat Transfer Enhancement in Heat Recovery Loops Using Nanofluids as the Intermediate Fluid, *Chemical Engineering Transactions*, 45, 991–996.

Conference Presentations

[9] **A. H. Tarighaleslami**, Implementation of the Heat Integration as an Energy Auditing Tool in Industrial Plants, *Conference of Energy Management Association of New Zealand (EMANZ)*, 23 -24 May 2017, Wellington, New Zealand.

[10] **A. H. Tarighaleslami**, Utility Heat Exchanger Network Design for a Kraft Pulp Mill Plant using the Unified Total Site Heat Integration Method, *Waikato Young Research Engineers Symposium (WYRES)*, 16 -17 November 2017, Hamilton, New Zealand, *accepted for oral presentation*.

Additional Publications in the Appendix

[11] T. G. Walmsley, M. R. W. Walmsley, **A. H. Tarighaleslami**, M. J. Atkins, J. R. Neale, 2015, Integration options for solar thermal with low temperature industrial heat recovery loops, *Energy*, 90, Part 1, 113–121.

[12] T. G. Walmsley, M. R. W. Walmsley, M. J. Atkins, J. R. Neale, **A. H. Tarighaleslami**, 2015, Thermo-economic optimisation of industrial milk spray dryer exhaust to inlet air heat recovery, *Energy*, 90, Part 1, 95–104.

[13] E. Shekarian, M. R. Jafari Nasr, **A. H. Tarighaleslami**, T. G. Walmsley, M. J. Atkins, N. Sahebjamee, M. Alaghehbandan, 2016, Impact of Hybrid Heat Transfer Enhancement Techniques in Shell and Tube Heat Exchanger Design, *Chemical Engineering Transactions*, 52, 1159–1164.

Table of Contents

List of Tables

List of Figures

Nomenclature

Roman

A	heat transfer area (m^2)
a	cost coefficient (NZD)
b	cost coefficient (NZD/m^{2c})
c	cost coefficient (unit less)
C_p	specific heat capacity (kJ/kg°C)
CP	heat capacity flow rate (MW/°C)
f	friction factor
h	convective heat transfer coefficient, (kW/m^2.°C)
H	enthalpy (MW)
K	thermal conductivity, (W/m.°C)
j	interest rate (%)
$\dot{m}$	mass flow rate (kg/s)
n	investment return duration (y)
Nu	Nusselt number
OP	operating period (h/y)
Pe	Peclet number
PP	power price (NZD/MWh)
Pr	Prandtl number
Q	heat load / utlity target (MW)
Re	Reynolds number
T	temperature (°C)
T^*	shifted temperature (°C)
T^{**}	double shifted temperature (°C)
U	overall heat transfer coefficient, (kW/m^2.°C)
UP	utility price (NZD/MWh)
W	power target (MW)
X	exergy (MW)

Greek

Δ	difference between two states
ϕ	volume percent of particle, %
μ	viscosity, kg/m.s^2
ρ	density, kg/m^3
$\sum$	summation of parameters

Subscripts

0	reference
bf	base fluid
c	cold
c,ut(i)	cold utility for utility (i)
Cold	cold

cont	contribution
cont,P	contribution, process
cont,PS(i)	contribution, process streams for process i
cont,U	contribution, utility
cont,U(i)	contribution, utility for utility i
cont,US(i)	contribution, utility streams for utility i
d	destruction
ele	electricity
g	gauge
gen	generation
h	hot
h,ut(i)	hot utility for utility (i)
Hot	hot
i	counter
j	utility counter
k	interval counter
m	counter for hot streams
min	minimum
min,P(i)	minimum, process for each process i
min,PP(i)	minimum, process to process for process i
min,PU(i)	minimum, process to utility for process i
n	counter for cold streams
nf	nanofluid
R	range
s	supply
st	step
Sink	sink
Source	source
t	target
x	exergy

Abbreviations

ACC	Annualised Capital Cost
BCC	Balanced Composite Curve
CC	Composite Curves
ChW	chilled water
CTST	Conventional Total Site Targeting
CTS	constant temperature storage
CW	cooling water
EA	Exergy Analysis
ED	exergy destruction
EMAT	Exchanger Minimum Approach Temperature
FT	Feasibility Table
GCC	Grand Composite Curve
HI	Heat Integration
HEN	heat exchanger network
HOL	hot oil loop
HPS	high pressure steam

HR	Heat Recovery
HRL	Heat Recovery Loop
HRN	Heat Recovery Network
HTC	heat transfer coefficient
HTE	heat transfer enhancement
HTHW	high temperature hot water
HW	hot water
ISCC	Interplant Shifted Composite Curves
LIES	locally integrated energy sectors
LPS	low pressure steam
LTHW	low temperature hot water
MINLP	mixed integer non-linear programming
MILP	mixed integer linear programming
MP	Mathematical Programming
MPS	medium pressure steam
MSDS	Material Safety Data Sheet
MWCNT	multi-wall carbon nanotube
NF	nanofluid
PA	Pinch Analysis
PDM	Pinch design method
PHE	Plate Heat Exchanger
PI	Process Integration
PUM	Process Utility Matrix
PT	Problem Table
PTA	Problem Table Algorithm
SUGCC	Site Utility Grand Composite Curve
SWG	Shaft Work Generation
TAC	Total Annualised Cost
TS	Total Site
TSHI	Total Site Heat Integration
TSHR	Total Site Heat Recovery
TSM	Time Slice Model
TSP	Total Site Profile
TS-PTA	Total Site Problem Table Algorithm
TSST	Total Site Sensitivity Table
TW	tempered water
UC	Utility Cost
UEN	Utility Exchanger Network
UTSI	Unified Total Site Integration
UTST	Unified Total Site Targeting
VHPS	very high pressure steam
VTS	variable temperature storage

Chapter One

Introduction

1.1 Background

The process industries used 30 % of global energy consumption with an annual growth expectation of 2.1 % for process heat and 2.6 % for electricity in 2015 (International Energy Agency, 2016). Energy-intensive processes, such as oil and gas refineries, chemical and petrochemicals, cement, iron and steel, and pulp and paper plants, as well as large non-energy-intensive processes, such as textile and food and beverage industries, currently account for 89 % of total industrial heat consumption. Despite increasing energy demands, depleting fossil fuel reserves, pressure to reduce Greenhouse Gas emissions, and increasing energy prices, energy in the form of low-grade heat is still not fully utilised. Globally, 87 % of energy inputs in 2015 from oil, natural gas, coal, nuclear, and renewables converted into heat and electricity, powered the various sectors of economies, such as transport, building and small industries (International Energy Agency, 2016).

New Zealand's economy is highly dependent on agriculture-related industries such as meat processing, dairy factories, and pulp and paper processes which normally operate in the low temperature range (<120°C). Therefore, to continue New Zealand’s strong presence and competitiveness in world food and forest products trade markets and compete with economies of developing countries like China, reducing production costs while supplying high quality products is important. For this reason, more attention to the optimisation and targeting of energy consumption of the processing of primary products is of extraordinary importance.

In New Zealand it is estimated that total industrial heat demand is approximately 27 % of total national primary energy use. Food, meat, dairy and beverage processing plants are the largest energy users in the New Zealand economy. Other significant energy users include oil and gas refining, chemical manufacturing, pulp and paper and wood processing. Figure 1-1 shows process heat energy use from

manufacturing in New Zealand derived from coal, natural gas, wood, and geothermal.

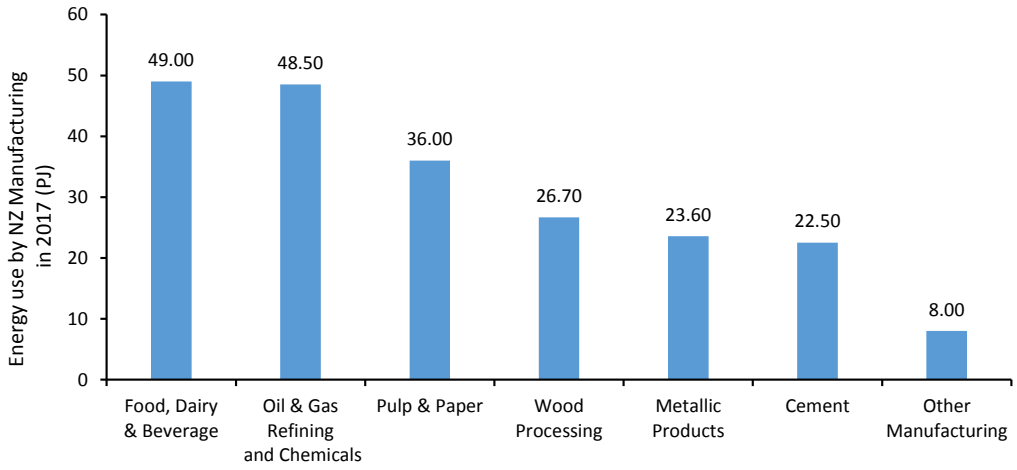

Figure 1-1: Estimated process heat use for industrial sector of New Zealand based on 2016 data (Atkins, 2017).

Industrial energy efficiency can be vastly improved (30 – 50 %) by applying the engineering concepts of Process Integration (PI) for green field and retrofit design (Klemeš, 2013). Process Integration is a holistic approach to process design and optimisation that looks at how a collection of processes or systems are best integrated. Process Integration methods, which include Pinch Analysis (PA), primarily aim to reduce energy and resource usage and emissions in industrial plants and has been successfully applied across many industries. It achieves this by providing a framework for systematic and rigorous systems analysis to understand intrinsic thermodynamic requirements of industrial production systems with a special emphasis on the efficient use of energy and water, and the minimisation of environmental impacts (Klemeš, 2013). More specifically, Heat Integration (HI) techniques, such as PA, have been developed to:

i. determine targets for hot and cold utility use;
ii. provide insight about the process utility needs; and
iii. design effective heat exchanger networks and utility systems for maximum energy recovery, and efficient supply of that utility.

Figure 1-2 represents energy flows in a typical process plant. Process heat demand of the plant is satisfied by different levels of pressure (and temperature) in a cogeneration system. Fire heaters can satisfy high temperature heating demands

in the site. Also, the refrigeration system satisfies the site's low temperature cooling demands; cogeneration system is used to satisfy site's power demand and balanced by power imports and/or exports to/from the site. The residual heat from the site's process and utility systems can be rejected to the ambient air and cooling water system (Oluleye et al., 2016).

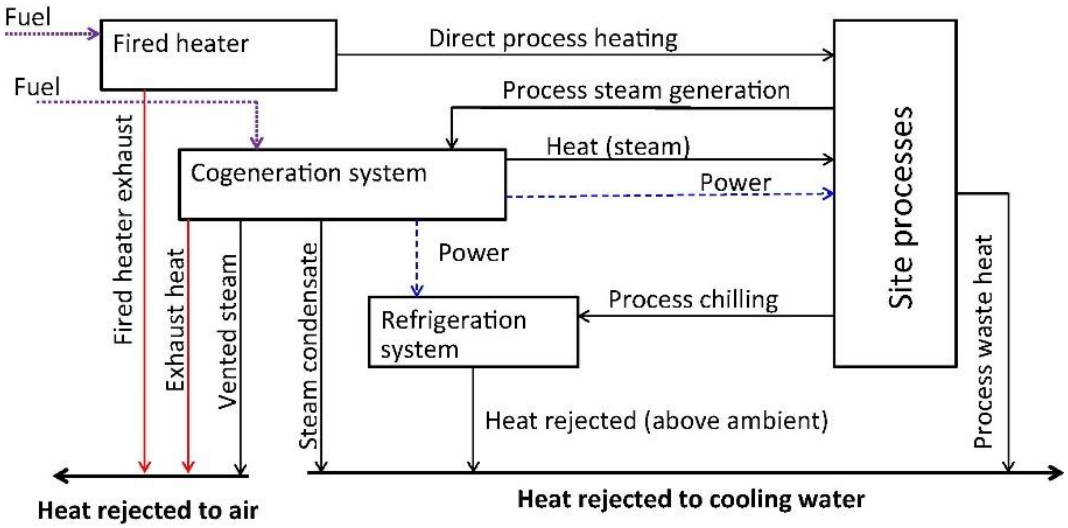

Figure 1-2: Energy flows in a typical process plant (Oluleye et al., 2016).

Dhole and Linnhoff (1993) introduced the concept of a Total Site (TS), which is a cluster of zones, plants and processes co-located on a single site that are served by a common utility system. The idea of Total Site Heat Integration (TSHI) is to recover heat through the TS utility system indirectly. As a result, additional energy efficiency gains have been realised in the traditional high temperature chemical process industry (e.g. oil and gas refineries). The TS concept provides more energy saving perspectives for each individual plant and the overall cluster. To date, TSHI has been successfully applied to clusters of high temperature plants, such as oil and gas refineries, petrochemical plants, power plants and steel making factories, which are typically operated continuously. However, these conventional techniques face additional challenges when applied to processes such as meat and dairy processes, pulp and paper, and recently bioenergy processes that operate and generate waste heat at much lower temperatures (<120°C). Many of these processes tend to be operated in a semi- and non-continuous manner and to transfer heat from one part of the site to another part requires the use of isothermal and non-isothermal utilities. These types of processes are common in

New Zealand and developing a modified TSHI method that can handle these difficulties is important for the New Zealand processing industry.

1.2 Thesis Aim

The aim of this research is to develop improved and unified methods for TSHI targeting, optimisation and network design for industrial sites to span the full range of processing temperatures and thermal utility types. The extended methodology will be demonstrated and explained by being applied to three industrial case studies, which include:

i. a Kraft Pulp Mill plant (including combined heat and power system, evaporators, and two hot water utility loops);
ii. a large Dairy factory (including utility and dryer exhaust integration, evaporators, chilled water system and hot water utility loop); and
iii. a Petrochemical Complex producing a wide range of chemical and petrochemical products.

To achieve the overall aim, first, a robust and improved energy targeting procedure for site-wide heat integration via indirect heat transfer between different plants will be established. This new method must apply to processes with both isothermal and non-isothermal utilities. Utility levels (including number of and temperature/pressure levels) will be considered and a systematic identification and selection criteria for the selection of the optimal utilities in TS will be established. The second aim of the thesis is to develop a unique method for optimal selection of utility temperatures and number of utility mains. This new optimisation method must be able to be applied to both isothermal and non-isothermal utilities and to existing energy targeting methods and the new targeting method presented in this thesis. Finally the third aim is to develop a new Heat Exchanger Network (HEN) design method that will be able to synthesis and design Heat Exchanger Networks based on the new developed targeting method. A key output of the research will be a software spreadsheet tool using the developed methodology that can model the performance and economic viability of each low-high temperature process and whole TS industrial cluster.

1.3 Thesis Outline

Chapter 2 thoroughly reviews the key literature and advances in the areas of PI, PA, and TSHI that are most relevant to the thesis aim. It examines the current state of the art for TSHI targeting methods. It highlights that there is a potential for heat recovery of low-grade waste heat. However, there is a noticeable deficiency in the literature connecting low temperature and high temperature TS methodologies. In this thesis, low temperature processes refer to the processes that operate below 120 °C. The shortcoming is that heat recovery opportunities between high and low temperature plants are not fully exploited because of the lack of methods to evaluate the potential heat recovery (i.e. targeting) and design of the heat recovery system, including the definition of utility levels and temperatures, and design of the Heat Exchanger Network (HEN).

Chapter 3 presents a brief overview of the thesis structure. Challenges of the conventional TSHI methods for targeting, optimisation and HEN design for non-isothermal utilities is laid out. Key research questions of this thesis are also raised in Chapter 3. In the second half of the chapter, three industrial case studies: a Kraft Pulp Mill Plant in Sweden, a large Dairy Factory in New Zealand, and a European Petrochemical Complex, which are studied in this thesis are introduced. This chapter also demonstrates an overview of an Excel^{TM} spreadsheet software tool that has been developed to target industrial plants including individual processes and a TS. The subsequent four chapters present the details of the method and results of the method as applied to the three industrial case studies.

Chapter 4 presents a new TSHI targeting methodology that calculates more achievable and realistic TSHI targets for sites that use isothermal and/or non-isothermal utilities compared to Conventional Total Site Targeting (CTST) methods. The new method is called the Unified Total Site Targeting (UTST) method. Critical differences and improvements between the new UTST method and CTST methods are highlighted in this chapter. The new method has been applied to the three case studies to evaluate its merits compared to the CTST methods.

Chapter 5 develops a new utility temperature selection and optimisation method for TSHI. It highlights the importance of correctly selecting the optimal utility temperatures of the optimisable utilities and the impact these temperatures have on heat recovery targets and Total Annualised Cost (TAC) set by TSHI. The chapter introduces a systematic procedure base on Mathematical Programming (MP) techniques such as derivative based analysis, thermodynamic concepts such as exergy destruction, and economic metrics such as utility cost. Total Annualised Cost is examined as the main objective function in the optimisation procedure. The new utility temperature selection and optimisation method has wider appeal than just USTS method, the new method is applicable for all types of TSHI methods. The evolution of the Excel™ spreadsheet software tool has been completed based on optimisation procedure in this chapter.

Chapter 6 focuses on HEN synthesis and design in TS. It compares Utility Exchanger Networks (UEN) that are strictly designed to achieve the targets for two TSHI methods. Practical UEN structures are synthesised and compared for Kraft Pulp Mill case study. It highlights the importance of series and parallel matches in the UEN; and how these matches may create a dependency on two or more separate processes, where operational and control issues may occur, higher piping costs may be imposed, and utility target temperatures may not be achieved in the consecutive processes if one or more processes were to be out of service. In this chapter, TS targets have been calculated using the developed software tool and networks have been designed with the help of Supertaget™ for both the CTST and UTST methods.

Chapter 7 discusses further developments on TSHI area. The first half of Chapter 7 introduces the influence of a new assisted heat transfer method on the TS. It presents a new method for calculating assisted heat transfer and shaft work targets for an example TS problem. Results have been examined to discover how heat recovery pocket spans Pinch Region to increase TS heat recovery and its effect on shaft work generation.

The second half of this chapter highlights the implementation of nanofluids as a Heat Transfer Enhancement (HTE) technique in PI. As a case study, the effect of replacing water with various nanofluids as the heat transfer medium in an

industrial Heat Recovery Loop (HRL) is modelled. Selection of different nanofluids and implementation of the selected nanofluid in the HRL system of another large dairy factory in New Zealand has been studied, as a case study.

Chapter 8 summarises the major findings of the research and provides recommendations for areas of future work.

Chapter Two

Literature Review

2.1 Introduction

The literature relevant to the thesis aim broadly falls into the closely related categories of Process Integration (PI) and Total Site Heat Integration (TSHI) as shown in Figure 2-1. The PI research field is enormous and, as a result, the scope of this literature review chapter is limited to those areas of research that are most relevant to the thesis aim. In the first section, a comprehensive definition of PI is presented. PI is divided into two categories, Heat Integration (HI) and Mass Integration (MI), where each section can be studied using Pinch Analysis (PA) and Mathematical Programming (MP) techniques. Subsequently, based on the thesis aim, development of PA and MP for HI have been reviewed. TSHI provides the opportunity of inter-plant HI for a cluster of processes. Both PA and MP can be applied on TSHI studies. The goal is to design a Heat Exchanger Network (HEN) based on TSHI to economically transfer energy between several plants using centralised utility system.

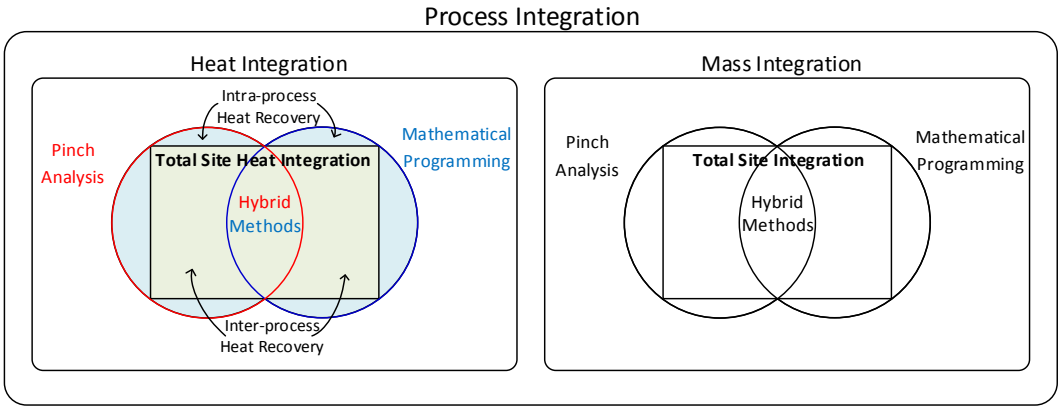

Figure 2-1: A general overview of PI in the literature.

In the TSHI section, development of the method, including existing methods and Heat Recovery Loop (HRL) method – as a special case, optimisation, and HEN synthesis and design, have been reviewed. Finally, the opportunity of using Heat Transfer Enhancement (HTE) techniques as an additional tool to improve Heat Recovery (HR) will be reviewed.

2.2 What is Process Integration?

PI covers a wide range of applications and includes a family of systematic methodologies for integrating and combining whole processes or several parts of processes to reduce the consumption of resources, such as energy and mass, and/or harmful emissions into the environment (Klemeš et al., 2013). PI started mainly as PA, also known as Pinch Technology, based on HI motivated by the world energy crisis of the early 1970s.

The most popular definition of PI has been adopted by the International Energy Agency (Gundersen, 2000) which is:

'Systematic and general methods for designing integrated production systems ranging from individual processes to Total Sites, with special emphasis on the efficient use of energy and reducing environmental effects.'

El-Halwagi (1997) has presented another general conceptual definition for PI, by his definition:

'Process Integration as a holistic approach to process design and operation that emphasises the unity of the process.'

PI has a key role in addressing energy efficiency and waste heat utilisation/recovery in the process industries. There are three approaches to PI: i) graphical methods including PA; ii) MP methods; and iii) hybrid approaches (Klemeš and Kravanja, 2013). Application of PI techniques to a wide variety of industries has helped realise meaningful increases in energy efficiency through the improved process- and Total Site-level integration (Klemeš, 2013).

HI has been extensively used in the process industries (such as oil and gas refining, chemical, petrochemical, pulp and paper, food and beverage, and steel making) and power generation plants over the last 40 years (Klemeš and Kravanja, 2013). HI provides systematic design and optimisation procedures for energy recovery using Heat Exchanger Network (HEN). Numerous definitions have been defined for HI, which always refers to the combination of steady state, semi-continuous or batch processes and process streams to achieve Heat Recovery (HR) via a heat exchanger.

Since the first foundation of PI in the 1970s and 1980s, many challenges and analogous extensions have been considered. Examples of the variety of research directions over the recent eight years are:

- Combined mass and energy integration in process design (Gassner and Maréchal, 2010)
- Material and resource conservation networks (Foo, 2013)
- Simultaneous targeting and design of HEN (Wan Alwi and Manan, 2010)
- Application of Exergy Analysis as a PI technique (Tarighaleslami et al., 2011).
- Study on property-based resource conservation network (Saw et al., 2011)
- Carbon Emissions Pinch Analysis (CEPA) for emissions reduction within the electricity sector (Atkins et al., 2010a).
- Reduction of air pollution and harmful emissions in large industries (Sinaki et al., 2011).
- Improving energy recovery through soft data optimisation (T. G. Walmsley et al., 2013).
- TSHI incorporating the water sensible heat (Liew et al., 2014c).
- Heat recovery and thermo-economic optimisation of dairy plants (T. G. Walmsley et al., 2015a).
- TSHI with district heating (Liew et al., 2013b) and cooling (Liew et al., 2016).
- Design and integration of evaporation systems including vapour recompression (T.G. Walmsley, 2016).
- Process modification of Total Site (TS) for capital cost reduction (Chew et al., 2015a).

PI concepts, methods and applications have been well explained in several books such as “Chemical Process Design and Integration” by Smith (2005), “Pinch Analysis and Process Integration” by Kemp (2007), and recently the “Handbook of Process Integration: Minimisation of Energy and Water Use, Waste and Emissions” by Klemeš (2013).

2.3 Development of Pinch Analysis: a Graphical Tool for PI

PA is an elegant insight and graphical technique for HI targeting and HEN design (Linnhoff and Hindmarsh, 1983). It has been well-utilised in the process industry

as a tool to maximise energy saving and HR and reducing overall energy demand and emissions within individual process units (Hackl and Harvey, 2013a).

In the early 1970s, the first work was performed by Hohmann (1971) in his PhD thesis at the University of Southern California, USA. He introduced thermodynamic-based reasoning for evaluating the minimum energy requirements of a HEN synthesis problem through application of a Feasibility Table (FT). His results were not extensively published beyond his thesis with the exception of only one conference presentation (Hohmann and Lockhart, 1976).

Two other research groups have developed concepts of HI, based on PA, building on concepts from Hohmann's PhD thesis. First, in the UK, Linnhoff and Flower presented a two-part paper in synthesis of HEN, Systematic generation of energy optimal networks (Linnhoff and Flower, 1978) and Evolutionary generation of networks with various criteria of optimality (Flower and Linnhoff, 1978), followed up by the Linnhoff's PhD thesis (Linnhoff, 1979). The Problem Table Algorithm (PTA) was introduced by Linnhoff while at ETH Zurich (Linnhoff, 1972). During remaining years of the 1970s, Linnhoff in his PhD thesis at the University of Leeds determined the potential of HI by using thermodynamic second law analysis in the context of chemical process design, (Linnhoff, 1979).

The second group was from Japan, at the Chiyoda Chemical Engineering & Construction Co., Ltd. Tsurumi, Yokohama. They developed HEN synthesis based on definition and construction of Composite Curves (CC) (Umeda et al., 1978), introduced optimum water reallocation in a refinery (Takama et al., 1980), and constructed the Temperature-Enthalpy (T-H) diagram for heat integrated system synthesis (Itoh et al., 1986).

Figure 2-2 presents a schematic CC of a process and the Pinch point (Klemeš et al., 2010). Based on the fact that heat can only be transferred from higher to lower temperatures HR is restricted by the shape of the CCs and reduction of an external heating utility is accompanied by a comparable reduction in cold utility demand (Linnhoff and Flower, 1978). HR between hot and cold streams is restricted by the shape of the CCs. The point that presents the smallest minimum approach temperature or ΔT_{min} (vertical distance between hot and cold CCs) represents a bottleneck for HR and is referred to as the Heat Recovery Pinch. Inputting a range

of ΔT_{min} enables a determination of a near-optimal trade-off between capital (investment) and operating (energy) costs.

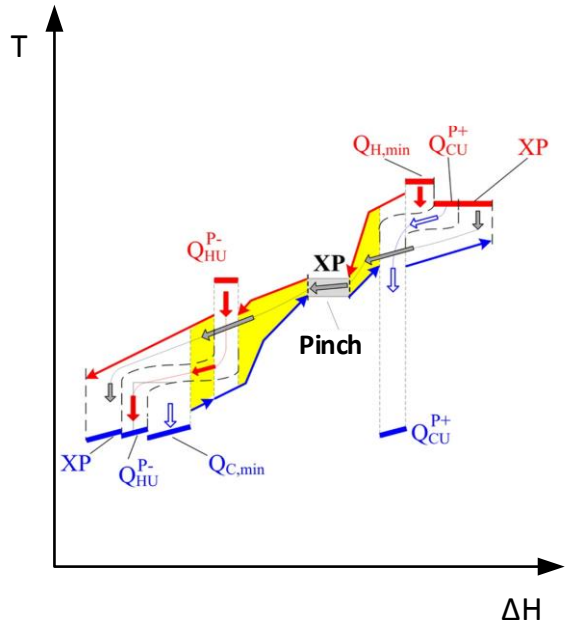

Figure 2-2: A schematic of CCs and Pinch implications (Klemeš et al., 2010)

A set of design and performance targets for HENs as the Pinch Design Method (PDM) were introduced by Linnhoff and Hindmarsh (1983), followed by extensions to the original PA method, such as targeting minimum total area (Colberg and Morari, 1990), targeting heat exchanger shells (Ahmad and Smith, 1989), targeting pressure drop (Polley et al., 1990), stream specific minimum approach temperatures (Shenoy, 1995), and application to retrofits (Ciric and Floudas, 1989). In general, the Pinch concept may be applied to any system that may be characterised by supply and demand profiles in terms of quantity and quality. Applications of PA beyond HI include hydrogen networks (Towler et al., 1996), reducing wastewater effluent as well as fresh water in process plants based on PA (Wang and Smith, 1994), Mass Integration of water networks (Foo, 2009), mass exchange networks (El-Halwagi, 2006), carbon constrained energy planning (Foo et al., 2008b), and energy investment constrained energy planning for electricity sectors (M. R. W. Walmsley et al., 2014a) and transport sectors (M. R. W. Walmsley et al., 2015). Other developed applications of PA include utility system optimisation (Shenoy et al., 1998), distillation columns (Bandyopadhyay, 2007), fired heater integrated networks (Varghese and Bandyopadhyay, 2007), batch

process integration (Majozi, 2005), and semi-continues process integration (Atkins et al., 2010b).

PA method is well explained in detail in the Chemical Process: Design and Integration "Chemical Process: Design and Integration" book by Smith (2005) and "Pinch Analysis and Process Integration" by Kemp (2007). A food industry overview of HI is presented in the "Handbook of Water and Energy Management in Food Processing" (Klemeš et al., 2008).

In conclusion, the important strength of the PA approach to PI is the targeting stage where sound performance targets are determined prior to the design stage. To be of greatest value, targets should be achievable and realistic to properly provide critical guidance in the design stage for the engineer regarding the performance limitations and inherent compromises within a system.

2.4 Mathematical Programming Concept of PI

Mathematical Programming (MP) in PI typically solves network superstructures to find feasible and optimal designs. Early stages of MP techniques' development started at late 1980s and early 1090s in parallel to PA development (Papoulias and Grossmann, 1983). MP deals mainly with HI, simultaneous optimisation and HI, and synthesis or retrofit of HEN. Reduction in utility consumption is not the only advantages of using MP simultaneous approaches, such techniques can lead to reducing raw material intake (Lang et al., 1988). MP combines algorithmic methods with fundamental design concepts (Biegler et al., 1997). It is capable of optimising both single- and multi-objective problems including HEN retrofit (Furman and Sahinidis, 2002).

MP offers many advantages and a number of disadvantages over other approaches. Main capabilities of MP are optimality, feasibility, and integrality of the produced solutions. In this approach, a solution can be optimised with respect to a single objective optimisation or multi-objective optimisation. By applying MP, an appropriate trade-off between capital and operating costs, revenue, and a range of environmental footprints can be established (Klemeš et al., 2010).

Disadvantages of the MP approach can be summarised as difficulties in problem formulation. Also, direct impact and adjustment of the solution at the critical

design decision points are not always quite crystal clear. This makes PA, as a graphical method, vital for the industry to provide increased efficiency and industrial acceptance at initial steps. Another important issue with MP approach is the MP base solutions are usually locally optimal while industrial plants within extremely competitive economies require the best possible globally optimal solution (Klemeš et al., 2010).

A very good in-depth review of major applications of MP techniques in the synthesis and planning of sustainable processes is presented by Grossmann and Guillén-Gosálbez (2010). Detailed application of MP methods in optimisation of TSHI systems is presented in Section 2.5.5.

2.5 Total Site Heat Integration – TSHI

One of the most important developments of PI is TSHI, also known as Total Site Analysis (TSA), Total Site Integration (TSI), or Site-Wide Integration. TSHI combines hot and cold utility requirements of each individual process to allow for better HI. Figure 2-3 illustrates the general concept of TSHI in an industrial cluster of process plants, including continuous, semi-, and non-continuous processes operating in high and/or low temperatures. The cluster employs a centralised utility system with a variety of isothermal and non-isothermal utilities which are used and generated within the system.

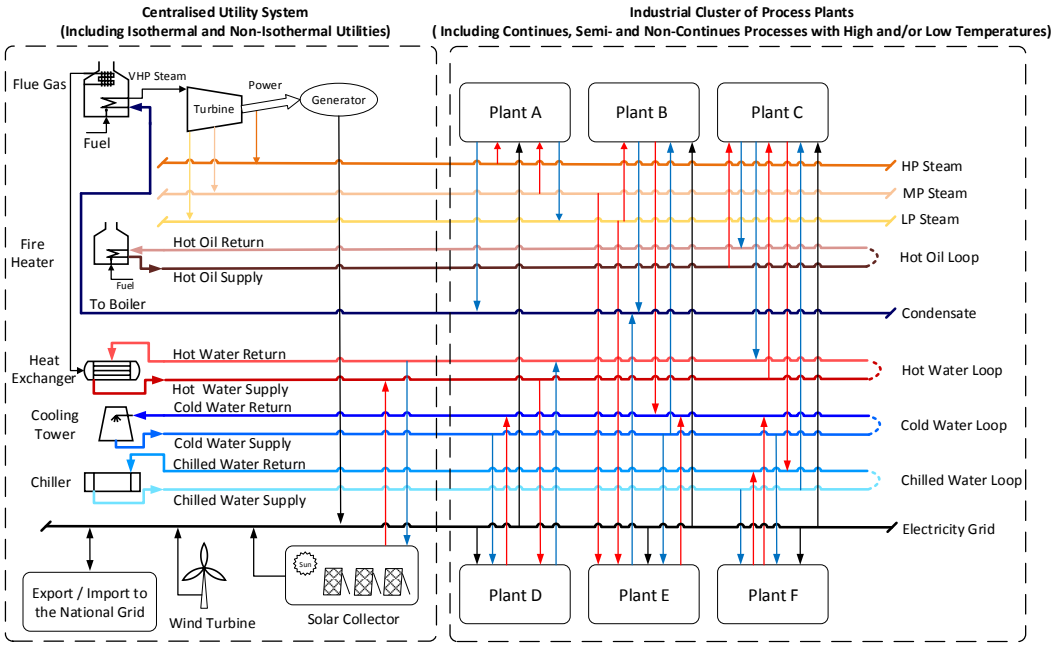

Figure 2-3: General view of a TSHI system.

The intermediate fluid that is used in indirect HI method is referred as a subset of hot or cold utility. Utilities can be classified into two groups: isothermal utilities and non-isothermal utilities. In isothermal utilities, utility temperature is assumed to be constant while transferring heat during generation and consumption in processes. For non-isothermal utilities, significant temperature change normally occurs during transferring heat through the plant. As Figure 2-3 shows, the central utility system generates the required heat using both renewable and non-renewable energy sources.

2.5.1 Direct versus Indirect TSHI

Two basic methods to recover heat between multiple plants and processes: direct HR and indirect HR methods (Ahmad and Hui, 1991). The direct method integrates heat between individual processes by using process streams directly. The indirect method integrates heat by applying an intermediate fluid as heat carrier in fluid loops across the plant (Atkins et al., 2012a). Direct HI offers maximum energy benefits in TSHI of the overall plant. In this approach, different processes may be combined and considered as a single large process to provide maximum energy saving through the maximum possible heat transfer across different processes of the plant. In practice, some disadvantages arise from direct HI of a TS, which are:

i. High complexity of HEN with likelihood of multiple streams crossing the physical limit of each plant. Thus, the investment cost increases with increasing piping, number of pumps and compressor units.
ii. Topological complexity may be considered for chemical processes safety hazards due to direct integration of far away streams.
iii. Low operational flexibility and controllability of the overall plant.

Indirect integration, on the other hand, by using an intermediate fluid (such as steam, hot oil, and water) through a central utility system, enables greater advantages of flexibility and process control to be achieved; however, it reduces energy conservation opportunities. Using an intermediate fluid, which helps in transferring heat from one process to the other, by an addition of different minimum approach temperatures will reduce the interval of effective heat transfer between pinches. Comparing to the direct integration, the energy saving

potential reduces and the number of heat exchangers increases. Therefore, the trade-off is between the capital cost of extra heat exchangers and the operating cost of pumping and utility usage seems to be inevitable (Atkins et al., 2012a). The different options of direct and indirect HR for multiple processes/zones are illustrated schematically in Figure 2-4. As it can be seen in Figure 2-4a, b, and e direct HR is occurred while Figure 2-4c and d a utility system is exploited for HR in the TS.

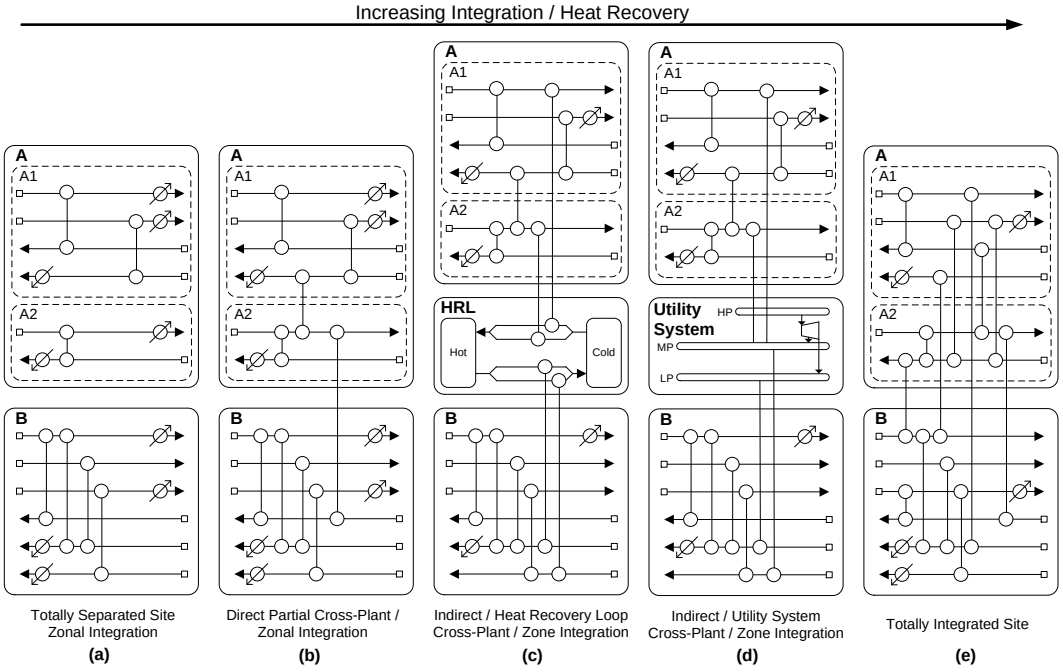

Figure 2-4: Schematic grid diagram of various levels of integration on a site with multiple processes/zones using direct or indirect heat transfer (Atkins et al., 2012a).

Different Pinch Temperature locations of individual processes in the cluster provide the potential for energy conservation through site level integration. Figure 2-5 presents how TSHI concept provides energy saving perspectives for each individual process within a large plant.

Morton and Linnhoff (1984) demonstrated that the overlap of two Grand Composite Curves (GCC) identifies the maximum possible HR between the processes. Ahmad and Hui (1991) extended the concept of indirect and direct integration. Their method prioritises integration of individual processes and zones, which they called areas of integrity (Ahmad and Hui, 1991), before integrating across an entire site using the utility system (Hui and Ahmad, 1994).

Dhole and Linnhoff (1993) explained the use of site source and sink profiles in order to present targets for steam generation and utilisation between processes. Pockets in the GCC indicate the intra-process HR potential and, therefore, they proposed to remove pockets from above and the below Pinch of each GCC (Step 1, Figure 2-5). Then, by shifting portions of GCCs above and the below Pinch, the site source and sink profiles, known as Total Site Profiles (TSP), may be constructed (Step 2). The next step is utility targeting in TS and the construction of Site Utility Composite Curves (SUCC) (Step 4). SUCC has two separate parts: Utility Generation Curve and Utility Consumption Curve. By pinching these two curves, minimum heating and cooling requirement of the TS can be determined. Finally, the Site Utility Grand Composite Curve (SUGCC) can be plotted based on SUCC to estimate Shaft Work Generation (SWG) potential across the TS (Step 5 added by Raissi (1994)). Shortly after its initial development, Klemeš et al. (1997) summarised successful applications of TSHI to an acrylic polymer manufacturing plant, several oil refineries and a tissue paper mill, which all showed utility savings between 20 – 30 %. The application of SUGCC has been further extended by Perry et al. (2008) to reduce carbon footprint through the integration of renewable energy sources.

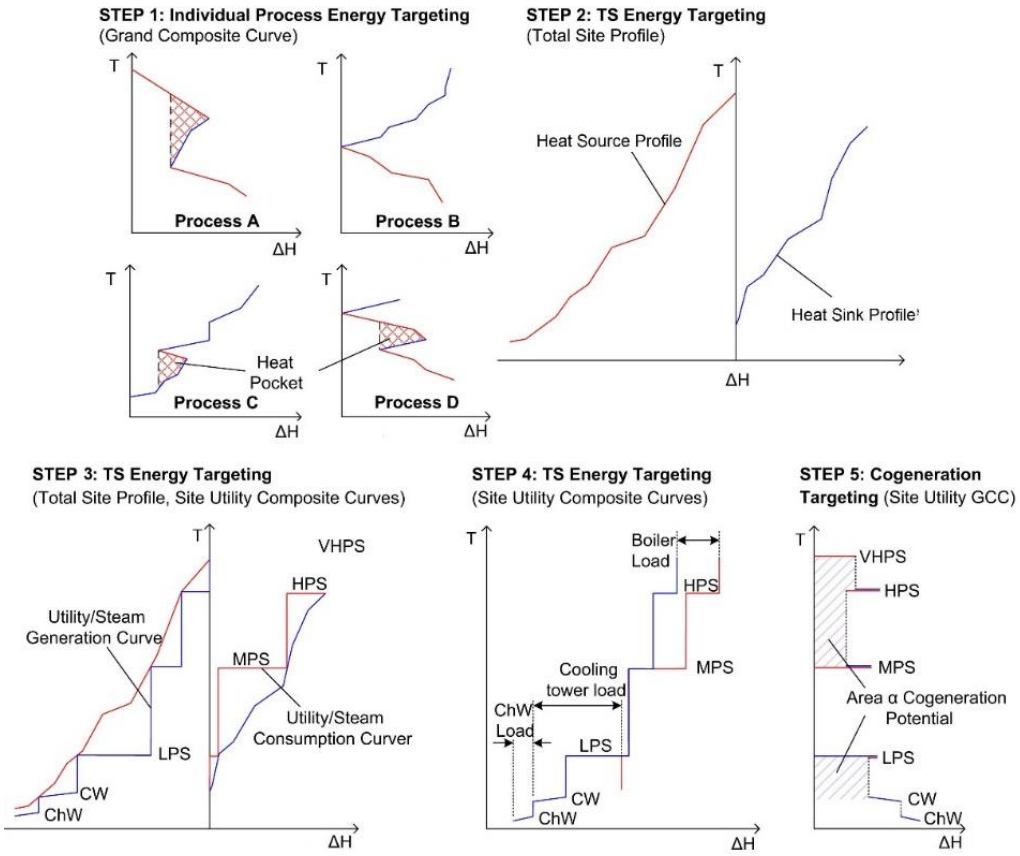

Figure 2-5: PA and initial targeting steps for TSHI, re-created from (Raissi, 1994).

2.5.2 Recent Developments and Applications of TSHI

Inter-process integration through TSHI has recently led to identifying utility savings in slaughter and meat processing by 35 % (Fritzson and Berntsson, 2006), large industrial parks in Japan by 53 % (Matsuda et al., 2009) and Thailand by 28 % (Matsuda et al., 2014), two Chinese petrochemical complexes by 61 % and 76 % (Feng et al., 2011), a Malaysian petrochemical plant by 24.5 % (Liew et al., 2014a), chemical processing clusters by 42 % (Hackl and Harvey, 2015), and Kraft pulp mills by 13 % (Bonhivers et al., 2014).

Notable developments to the TSHI targeting method includes: temperature shifting using process (Varbanov et al., 2012) and stream (Fodor et al., 2012) specific minimum approach temperatures which are known as conventional TSHI methods. Other developments in the area are application of TSHI to Locally Integrated Energy Sectors (LIES) (Perry et al., 2008), heat exchange restrictions (Becker and Maréchal, 2012), integration of solar thermal energy into processes with heat demand (Nemet et al., 2012c), seasonal energy availability (Liew et al., 2013a), centralised utility system planning (Liew et al., 2013b), retrofit investigations in TS (Liew et al., 2014a), process modifications for capital cost reduction (Chew et al., 2015b), minimisation of thermal oil flow rate in hot oil loops (Bade and Bandyopadhyay, 2014), variable energy availability (Liew et al., 2014b), TS utility system targeting (Sun et al., 2015), and TS mass, heat and power integration using process PI and process graph (P-graph) (Ong et al., 2017).

A site-wide HI study on a large industrial cluster performed by several researchers, Matsuda et al. (2009) claimed that even a highly efficient individual plant will further improve its energy efficiency by TSHI. Hackel et al. (2011) showed that by site-wide collaboration it is possible to increase HR and utilisation of excess heat as well as reducing energy cost in a chemical cluster. Another detailed multiple plant study in an industrial zone was performed to present a systematic methodology to target and design waste HR systems considering economic objectives by Stijepovic and Linke (2011).

The principals of plus/minus technique in PA was suggested by Linnhoff and Vredeveld (1984). It suggests that the amount of heat provided by hot streams should be increased (+) or the amount of heat required by cold streams shoul be

decreased (-) above the Pinch. Likewise, below the Pinch, the amount of heat required by cols streams should be increased (+) or the amount of heat required by hot streams should be decreased (-). Similar logic has been suggested for TSHI by Vaideeswaran (2001). He introduced Process Utility Matrix (PUM) to evaluate multiple utility targets in a TSHI system. Later, Nemet et al. (2012a) extended the application of PUM method to evaluate TS changes which accounts for including/excluding of different processes. Chew et al. (2013b) studied process modification potential introducing a two-step algorithm to enhance HR using plus/minus technique in TSHI.

A model for estimating cogeneration potential in a TS based on thermodynamic concepts has been presented by Sorin and Hammache (2005). The concept of extractable power and steam header efficiency to estimate cogeneration potential was presented by Harell (2004) using graphical techniques. An algebraic equivalent of Harell's method, proposed by Mohan and El-Halwagi (2006), was applied to a biomass based cogeneration system. Simplicity and the linearity of the model can be considered as the advantages and difficulty in estimating the header efficiency can be mentioned as major disadvantages of the model. Ghannadzadeh et al. (2012) presented a new shaft work targeting model, which calculates the temperature of steam mains, steam flow rate and shaft power generated by the steam turbines in expansion zones of the SUGCC from bottom to top. They used a simple steam turbine expansion model with a constant isentropic efficiency. They claimed the new method offers more realistic estimates of the TS cogeneration targets than previous models.

Bandyopadhyay et al. (2010) proposed a modification of the Site Grand Composite Curve (SGCC) that incorporates assisted heat transfer based on the theory of Bagajewicz and Rodera (2000). Assisted heat transfer takes into account the pockets of the process GCC, which were not considered by Dhole and Linnhoff (1993). Bandyopadhyay et al. (2010) showed that a modified TSP and SGCC may show increased HR potential. However, the economy of the approach must be explored, as an increased integration using additional steam mains can be costly.

Recently, several researchers have investigated, low grade industrial heat, waste to heat, and renewables (Perry et al., 2008). Varbanov and Klemeš (2011)

investigated the potential of integrating renewables with varying availability. This indicated that significant further energy savings can be achieved. Nemet et al. (2012b) proposed a new methodology for maximising the use of renewables with variable availability. Walmsley et al. (2015b) presented the integration of solar thermal with low temperature industrial site-wide plants. Chew et al. (2013a) analysed the industrial implementation issues of TS, and Atkins et al. (2012b) performed PI on the individual plants at a large dairy factory. Also, Walmsley et al. (2013) applied soft data optimisation industrially on a large dairy factory. Low et al. (2013) studied the opportunities for low-grade HR in UK food processing industry in continuation of the work by Fritzson and Berntsson (2006), who studied inter-process integration through TS to identify substantial savings in slaughter and meat processing. T.G. Walmsley (2016) used hybrid TSPs to assist the design of milk evaporation systems. He showed that integrated vapour recompression can reduce utility use and low grade waste heat.

Seasonal energy availability was studied by Liew et al. (2013a) and later by Bonhivers et al. (2014). Bonhivers et al. (2014) analysed the HEN of Kraft pulp mills and concluded a bridge between cooler and heater is essential to achieve heat savings in an existing HEN. Recently, Liew et al. (2017) reviewed TSHI application for planning and design of the industrial, urban and renewable system. They identified the need for sustainable development of new TSHI approaches for industrial, urban and renewable energy system integration.

2.5.3 Heat Recovery Loop – TSHI for Semi-Continuous Processes

TSHI has primarily focused on high temperature applications where steam can be exploited as an integral part of the utility system to recover heat and efficiently produce power. Since steam is assumed to be isothermal in its generation and consumption as a utility, a TS network is simple to design to achieve the TSHI targets. However, effectively applying conventional TSHI techniques to lower temperature processing applications and sites (i.e. <120 °C) is more challenging. For these sites, TSHI is achieved via a liquid (e.g. hot and cold water) as intermediate fluid in utility systems or a dedicated indirect HR system (M. R. W. Walmsley et al., 2013a). Thermal storage is needed to balance the instantaneous imbalances of the intermediate fluid flow between distinct processes. This system

is called Heat Recovery Loop (HRL), (Rodera and Bagajewicz, 1999). Figure 2-6 presents a schematic of a conventional HRL system.

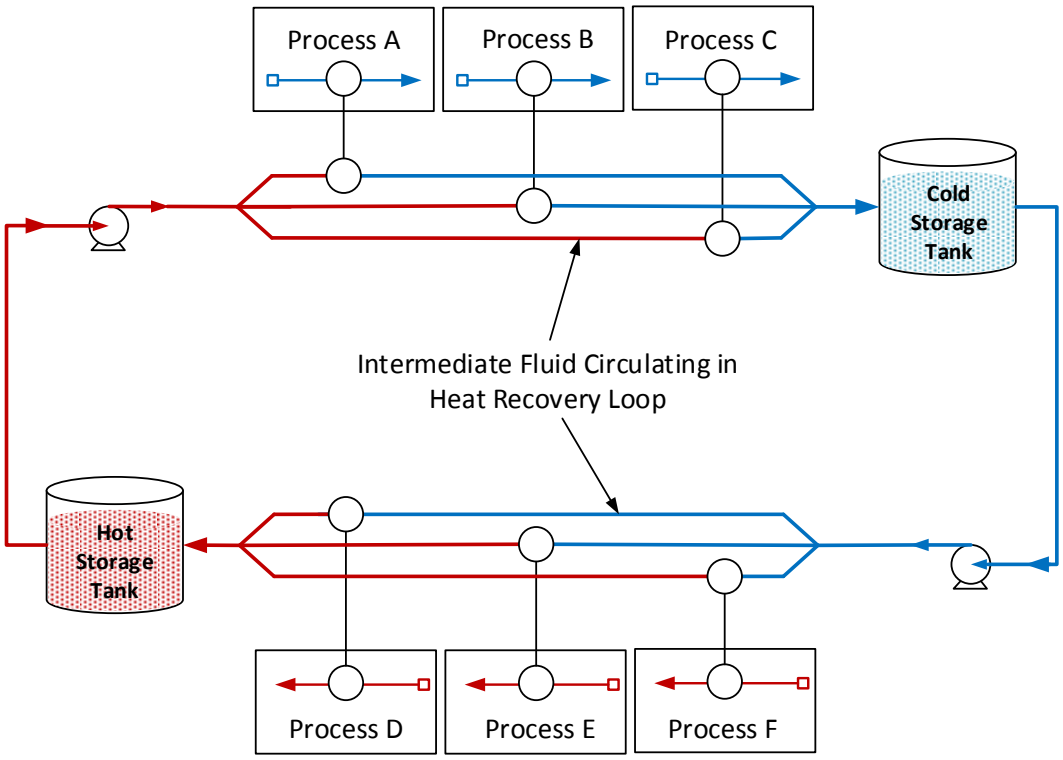

Figure 2-6: A schematic of a conventional HRL system.

Initially, the concept of HRL developed in consequences of batch processes integration. Graphical and MP based targeting and design methods have been developed for TSHI of batch processes. Kemp and MacDonald (1987, 1988) introduced the Time Slice Model (TSM) in order to deal with the non-continuous nature of batch processes and the method was later expanded by Kemp and Deakin (1989). Stoltze et al. (1993) used a hybrid combinatorial optimisation and PA method to target the number of heat storage tanks and their temperatures to maximise inter-process HR savings. Later Stoltze et al. (1995) refined the approach and named it the Permutation Method. The method was further developed by Mikkelsen (1998), who added a post-optimisation stage for fine tuning the system variables; however, the method has proven difficult to apply in practice. The constraint of fixed temperature heat storage as applied in Stoltze et al. (1995) was relaxed by Chen and Ciou (2009) enabling increased HR after applying Mixed Integer Linear Programming (MILP) to find the design with the minimum total cost.

A graphical Pinch based methodology for indirect HR assuming constant temperature- variable mass heat storage was introduced by Krummenacher and Favrat (2001). They developed the concept that a limiting supply temperature, which causes a Heat Storage Pinch and restricts increased HI without the addition of a new storage temperature level and its associated storage, piping, and pumping costs. The method was originally developed for batch processes; however, the principles also apply to semi-continuous processes particularly when multiple plants are integrated on a TS, as Sherrin and Nicol (1995) showed by using a heuristic based method for TSHI of semi-continuous processes using an intermediate closed hot and cold water loop system.

The use of a HRL for site-wide heat integration of low temperature processes was investigated by Atkins et al. (2012b) and later formalised into a comprehensive method by Walmsley et al. (2014a). Other notable studies on various parts of the design, operation and optimisation of HRLs are: new thermal storage design by using a stratified tank (Walmsley et al., 2009), changing of storage temperature for seasonal production changes (Atkins et al., 2010b), utilisation and sizing of thermal storage capacity (Atkins et al., 2012b), area targeting and storage temperature selection for HRL (Walmsley et al., 2012). Further, Walmsley et al. (2013b) have explained the evaluation of heat exchanger sizing methods for improving the area and storage temperature selection in HRLs, and the integration of industrial solar use in HRL (T. G. Walmsley et al., 2015b). Many of the results from these HRL studies culminated in HRL targeting and design method, Chapter 20, in the “Handbook of process integration: Minimisation of energy and water use, waste and emissions” (Klemeš, 2013).

The conventional control system of a HRL measures and compares the outlet temperature of the intermediate loop fluid from each heat exchanger to a common hot or cold temperature set point. The flow rate of the fluid through each heat exchanger is adjusted to achieve the set point temperature. In this approach, hot and cold storage temperatures are held constant over time. This approach is called the Constant Temperature Storage (CTS) approach. Walmsley et al. (2013c) introduced an alternative approach to HRL control, which varys the set point of individual heat exchangers depending on their temperature driving force. This

alternative approach is called Variable Temperature Storage (VTS) due to the mixing of different temperatures entering the tanks. T.G. Walmsley et al. (2014a) have compared the two HRL control approaches to find the VTS system results in a more effective distribution of temperature driving force between heat exchangers. They showed lower average loop flow rates giving reduced pressure drop and pumping requirements, and an increase in average temperature difference between hot and cold storage temperatures, which increases thermal storage density and capacity. Recently, the use of Mixed Integer Non-Linear Programming (MINLP) model with economic objectives to optimise hot water circles has been presented by Chang et al. (2015). Later they extended their work for the application of MINLP model in HRLs (Chang et al., 2016). Another approach is presented by Wang et al. (2015), which offers TS targeting as an initial stage followed by HEN design and area targeting, which is solved using Mixed Integer Non-Liner Programming.

In general, the method of T.G. Walmsley et al. (2014a), as well as previous graphical HRL methods, are overly restrictive on the structure of the HR network, which define the interactions between utility and process streams. The MP methods, such as Wang et.al (2015), lack the same insights as graphical methods and require specialised solves to find the best solution. This demonstrates that improvement may be possible despite the advancements and merits of both the graphical and MP approaches in the area of HRL.

2.5.4 The State-of-The-Art of TSHI Methods

Since TSHI has a strong foundation in PI and has proven as a useful tool for engineers to plan and make strategic decisions regarding energy conservation for entire processing sites, several researchers have been working to extend the method to achieve more meaningful targets, apply more practical constraints on HEN, and increase the range of applications. This section reviews the most notable developments in TSHI targeting and compares the advantages and disadvantages of the various methods to illustrate the gap in the knowledge for covering both isothermal and non-isothermal utility targets in a single procedure. Figure 2-7 presents the six most common TSHI targeting methods in the literature and are discussed in the following sections.

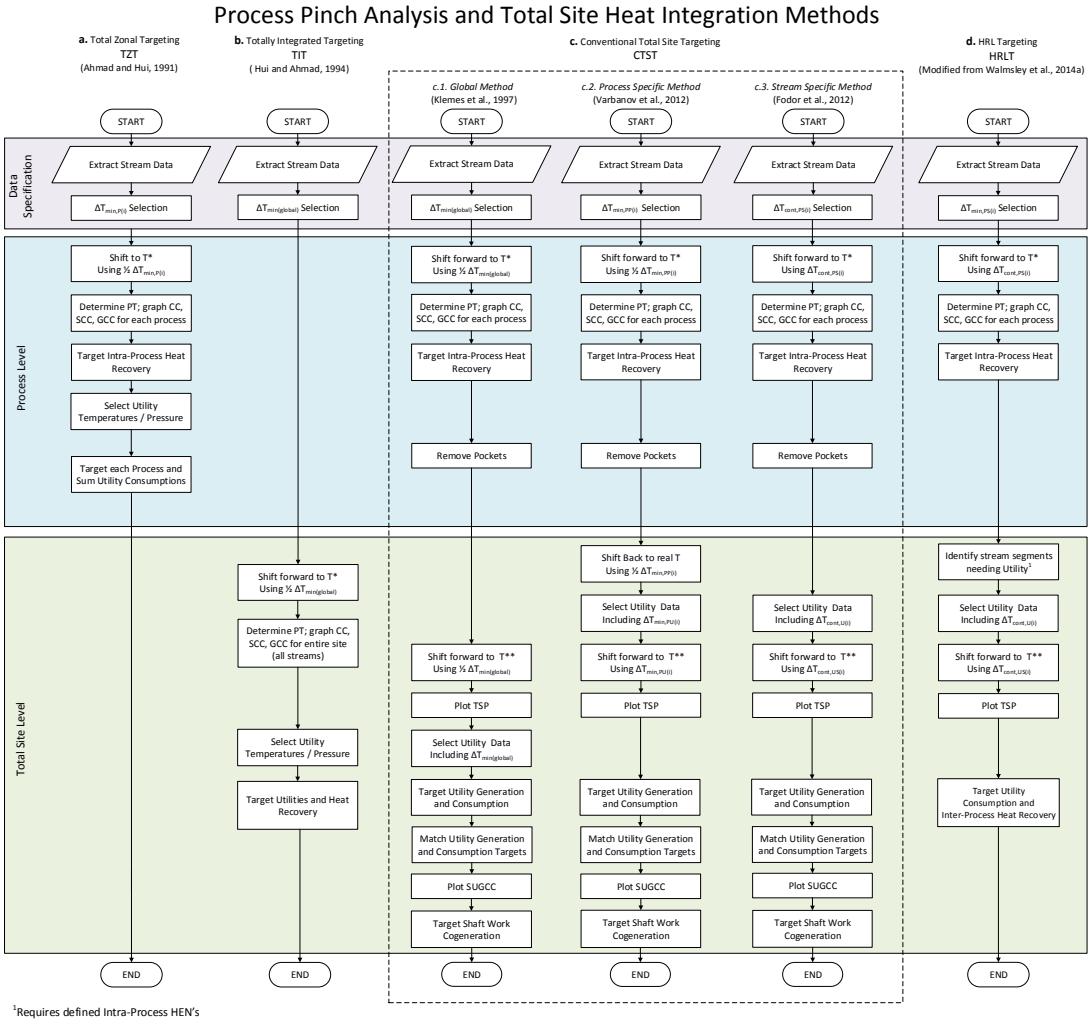

Figure 2-7: Comparison between various PA and TSHI targeting methods.

2.5.4.1 Total Zonal Targeting (TZT) Method

TZT method (Ahmad and Hui, 1991) is based on the very initial concept of PI and PA presented by Linnhoff and Flower (Linnhoff and Flower, 1978). In this method, Figure 2-7a, each process is considered as a single plant and integrated separately. Therefore, each process has separate targets and the final utility requirements, for both hot and cold utilities, and the amount of HR can be obtained by summation of utility requirements and HR of each individual plant. As shown in Figure 2-4a, TZT calculates the lowest HR targets within the TS.

2.5.4.2 Totally Integrated Targeting (TIT) Method

In this approach, Figure 2-7b, different processes are combined and considered as a single process in the plant to provide maximum energy saving with the maximum possible heat transfer across different processes of the plant (Hui and Ahmad,

1994). In practice, the disadvantages of direct HI, as reviewed in Section 2.5.1, devalue the usefulness of this method. In summary, TIT method needs complex networking with many streams potentially crossing the physical limit of each plant, increasing the cost of integration as more pumps and compressors are required. Topological disadvantages and costs may also be considered such as creating safety hazards due to direct integration of far away streams with less overall operational flexibility and controllability of the site, Figure 2-4e.

2.5.4.3 Conventional Total Site Targeting (CTST) Method

CTST method follows the initial idea of TSHI for the traditional high temperature chemical process industry (e.g. oil and gas refineries). However, these conventional techniques (Figure 2-7c) face additional challenges when applied to low temperature and/or non-continuous processes (e.g. dairy processes, pulp and paper plants). Klemeš et al. (1997) introduced a procedure for CTST method, referred to as the Global CTST method. A modification to CTST method was presented by Varbanov et al. (2012), introducing process specific minimum difference temperature method. Later, Fodor et al. (2012) modified CTST method with the definition of stream specific minimum temperature difference method. The schematic of diagram for CTST methods is presented in Figure 2-4d.

2.5.4.3.1 Global CTST Method

This method is well explained in the literature (Kemp, 2007) as the basic TSHI method. Figure 2-7c presents the global CTST method procedure. Figure 2-8 illustrates the method graphically. The first step is data extraction. By using flow sheets, process heating and cooling demands are extracted as stream data for further use to obtain HR targets for each process using PA. The next step is the selection of minimum temperature difference (ΔT_{min}). In general, selection of higher ΔT_{min} gives a higher amount of utility demand but lower capital cost. The opposite is true for low ΔT_{min} values, i.e. low energy cost, high capital cost. Supertargeting, energy targeting and experience are three typical ways of specifying a realistic ΔT_{min} (Kemp, 2007). Next, as it is shown in Figure 2-8, process stream temperatures are shifted by ½ ΔT_{min} to an intermediate temperature scale (T^*) and the Problem Table (PT) and related graphs such as CC, GCC and Site Composite Curve (SCC) are constructed. In the next step, the pockets from the GCC

are removed in the traditional manner and the sources and sinks segments are extracted. Then after a second shift (Figure 2-8a) using ½ ΔT_{min} to the utility temperature scale (T^{**}), the extracted GCC segments are combined to plot site source and sink profiles, i.e. TSP. Then, by using utility temperature and pressure specifications, utility generation and consumption can be targeted from the TSP. Finally, SUGCC is plotted and SWG can be targeted.

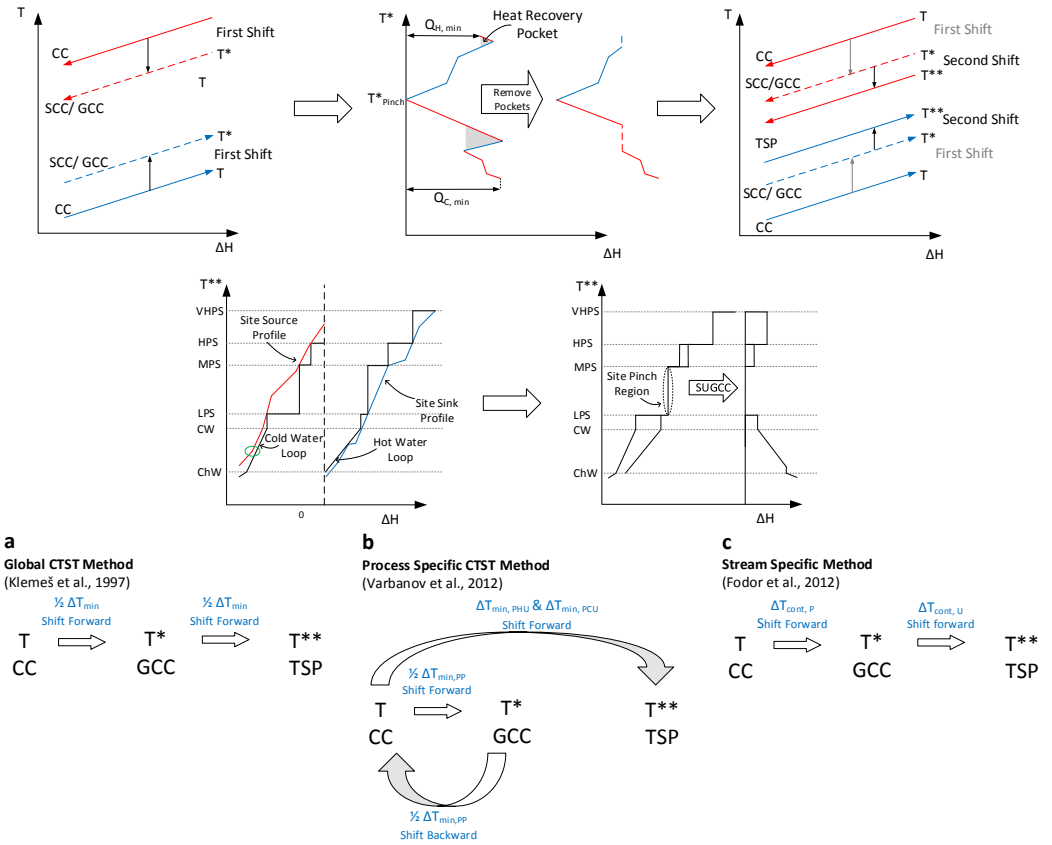

Figure 2-8: General overview of TS steps and temperature shifts in various CTST methods.

2.5.4.3.2 Process Specific CTST Method

This method modifies the global CTST method by employing changes in TSP construction algorithms. It allows separate ΔT_{min} specification for heat exchange within each process and also between each process and each utility (Varbanov et al., 2012). In this method $\Delta T_{min,PP}$ (process to process) for each plant needs to be selected and the first shift is by using ½ $\Delta T_{min,PP}$ (Figure 2-8b). Then the procedure can be continued following global CTST method. Then by using the relevant individual specifications for minimum allowed temperature difference $\Delta T_{min,PU}$ ($\Delta T_{min,PHU}$ for heating utilities and $\Delta T_{min,PCU}$ for cooling utilities) the extracted segments can be shifted forward to the temperature scale of the utilities, T^{**}, as is

shown in Figure 2-7c. Again, the rest of the procedure follows the same procedure of global CTST method (Figure 2-7).

2.5.4.3.3 Stream Specific CTST Method

This method deals with stream-specific ΔT_{min} inside each process by setting different ΔT contribution (ΔT_{cont}) and also using different ΔT_{cont} between the process streams and utility system (Fodor et al., 2012). The method's algorithm is similar to previous methods (Figure 2-7c.3); however, the major differences are: individual streams (both process and utility streams) are assigned a ΔT_{cont} value based on the characteristics of the stream. Then, the first shift is to T^* using ΔT_{cont}. When the pockets are removed, by using the relevant individual specifications for minimum allowed temperature difference $\Delta T_{cont,US}$ the extracted segments can be shifted forward to the temperature scale of the utilities, T^{**}, as is shown in Figure 2-8c. Once again, the rest of the procedure is followed the same procedure of global CTST method (Figure 2-8).

2.5.4.4 Heat Recovery Loop Targeting Method

The HRL method, a dedicated indirect HR system for low temperature processes using non-isothermal utilities (e.g. hot and cold water loops), is a standalone method that can be considered as a special case of conventional TSHI methods, Figure 2-7d. Walmsley et al. (2014a) presented a new method for targeting and design of HRLs using VTS technique. This approach is based on the daily time average CC. They showed that the method has more HR potential in comparison with CTS technique. The significant difference between this method and other conventional TSHI methods is this method requires defined intra-process HEN to be able to select candidate stream segments that need utility at the TS level. As a result, HRL targets depend on the HEN design, while in conventional TSHI methods, the targets may be determined prior to HEN synthesis. Similar to the Stream Specific CTST method, ΔT_{cont} for utility stream matches is used in this method. After TSP construction, utility consumption targets and inter-process HR may be targeted. Figure 2-4c presents the schematic of HEN arrangement in the HRL targeting method.

2.5.4.5 Method Comparison and Discussion

Summarising all above, the major limitation of conventional TSHI methods is the treatment of non-isothermal utilities during the targeting process. In addition, this limitation will influence the HEN synthesis and design based on the conventional method targets. In conventional TSHI methods, non-isothermal utilities are often treated in the same way of isothermal utilities. In the case of an isothermal utility, its temperature does not change while transferring heat during generation and consumption. In TSHI targeting, isothermal utility representation is simplified by showing only the constant temperature segments (i.e. horizontal lines), not considering temperature changes in preheating, superheating or sub-cooling segments. Cooling water utility, at times, may also be considered a pseudo-isothermal utility by assuming a high cooling water flow rate, i.e. minimal temperature change. For a non-isothermal utility, sensible heat is the primary source of heat transfer, which means significant temperature change occurs during its generation and consumption. As a result, upper and lower temperatures are an important consideration for each non-isothermal utility. In low temperature processes (i.e. < 120°C) hot and cold water are considered as non-isothermal utilities, which are shown as diagonal segments on T-H plots, with the slope being inversely proportional to flow rate. Therefore, non-isothermal utility targets obtained using conventional TSHI methods are overly optimistic compared the targets that can be achieved practically. These targets are significantly lower, based on HRL method, than targets that are calculated using conventional methods as HRL method put more constraint on HEN.

In CTST method, non-isothermal utility target temperate can be achieved with fewer constraints, i.e. CTST method inherently allows target temperature to be met using a single heat exchanger or using heat exchanger matches in series and/or parallel configurations from any process in the plant. On the other hand, the HRL method has an additional constraint that the non-isothermal utility target is restricted to be achieved with only one heat exchanger. No constraint on conventional method network design may cause some operational, safety, and control issues while for HRL method intra-process HEN information is required in targeting stage and network constraints are highly restrictive. Detailed

explanation on non-isothermal utility targeting, optimisation, and HEN design challenges are presented in Section 3.2.

Therefore, the gap in the literature is the lack of a TSHI method that calculates realistic and achievable targets for both isothermal and non-isothermal utilities. In this context, the achievable target means one that accounts for feasible HR constraints, and realistic target means one where the target temperature of the utility stream is met with a single process in the TS.

2.5.5 TSHI Optimisation: Number of Utility Mains and Utility Temperatures

In parallel to the development of graphical TS methods, optimisation techniques have been conducted to the TSHI methods to improve utility targets and HEN synthesis and design. Various methods in the literature for optimisation of the number of and temperatures of utility levels for steam (i.e. isothermal) utility systems and new methods based on optimisation of non-isothermal (i.e. hot water or hot oil) utilities are presented. Makwana (1997) introduced R-curve method in his PhD thesis to optimise the existing utility system through top-level analysis. R-Curves provide clear evaluation of the site utility system, which is possible to understand the characteristics and identify energy saving potential of the utility system. Later, Makwana et al. (1998) used the R-curve concept for retrofit and operation management of existing TS. Zhu and Vaideeswaran (2000) proposed a relation between cogeneration efficiency with heat-to-power ratio using the R-curves. Kenney (1984) presented the concept of R-curve in the book “Energy Conservation in the Process Industries” in detail and Kimura and Zhu (2000) applied the method for an industrial energy system followed by Matsuda et al. (2009) who applied the R-curve concept to a Japanese large-scale site. Utilising the industrial R-curve concept in analysing the TS utility systems to improve turbine hardware model was presented by Varbanov et al. (Varbanov et al., 2004).

An accurate shaft-work targeting model based on typical isentropic efficiencies of steam turbines and rules of thumb for targeting the cogeneration potential of a combined heat and power plant was introduced by Mavromatis and Kokossis (1998) known as the Turbine Hardware Model (THM). Later, the application of this

model in an Indian sugar factory was studied to establish cogeneration potential (Raghu Ram and Banerjee, 2003).

The use of MP techniques in TS in order to minimise costs of energy supply was introduced by Marechal and Kalitventzeff (1998). They also developed a method to target TS utility system, which has changes in utility demands of different plants (Marechal and Kalitventzeff, 2003). Several studies have applied MP based methods to optimise the utility temperatures. Shang and Kokossis (2004) proposed a methodology to optimise steam levels under different operational scenarios using a boiler and turbine hardware model. The study developed a transhipment model to represent a TS system and used the location of steam levels, the overall fuel requirement, the cogeneration potential and the cooling utility demand as major decision variables to minimise Utility Cost (UC) by applying a multi-period MILP model. Tarighaleslami et al. (2010) presented an approach for reduce cooling water cost as non-isothermal utility. Later, Hesas et al. (2011) studied the cooling water makeup cost in oil refineries. Prashant and Perry (2012) used a MINLP model to determine the cost optimal location and number of steam levels to meet the process heating and cooling demands. Sun et al. (2014) showed that at the Site Pinch region there is no SWG potential. They also showed that by adding new steam mains within or away from the Site Pinch can significantly improve boiler steam saving, high temperature utility targets (>120 °C), and SWG. Later they proposed a practical approach based on extended site composite curves to provide realistic utility targets (Sun et al., 2015). The method only allows for boiler feedwater preheating, steam superheating in steam generation, steam desuperheating for process heating, and condensate HR from steam consumption. However, the method doesn't take other non-isothermal utilise into account.

Nemet et al. (2013) showed that an appropriate trade-off between investment cost and utility cost may not provide realistic results when only current utility prices are considered during the optimisation of HEN for its whole lifetime. Later, they proposed a new TS optimisation model including the selection of utility pressure levels for intermediate utilities to optimise total cost considering future energy prices (Nemet et al., 2015). The model also included thermal and hydraulic parameters, such as pipeline layout design, pipe design, and insulation thickness

and heat losses, when synthesising the MINLP problem through the trade-off between capital and operating cost. Recently, Song et al. (2017) presented a modified MINLP model with an objective of TAC to determine the final inter-plant HEN configurations.

Another approach to utility temperature optimisation is graphical based methods. Song et al. (2016a) developed a new graphical method called Interplant Shifted Composite Curves (ISCC) to target the maximum HR for indirect HI between two plants without basic changes, such as infrastructure improvements, in the existing HEN. The ISCC method selects streams with the potential to participate in the TS, and determines maximum feasible HR as well as minimises the flow rate of the heat transfer medium. However, the method has not been applied to industrial clusters with different level of utilities. Boldyryev et al. (2014) developed a method to decrease capital cost by minimising heat transfer area for HR on TS using different utility levels. In their method, heat transfer area is reduced by selection of the appropriate temperature of intermediate utilities. Minimum heat transfer area depends on slopes of TSP in each enthalpy interval.

Exergy Analysis (EA) is another PI tool for optimisation of process HI. Parker (1989) introduces a fast and easy algorithm for the energy-capital trade-off in a HEN, but in this method the effect of the capital trade-off on the utility system was not taken into an account. Dhole (1991) combines PA and EA to for a multiple utility optimisation problems. The method showed reducing the exergy destruction (ED) in a HEN will ultimately benefit the power generation in the utility plant. An Exergy Grand Composite Curve was used to minimise the exergy losses in the HEN and can be constructed from the GCC by converting the temperature axis into Carnot factor. A combined PA and EA method is presented by Linnhoff and Dhole (1992) to optimise low temperature processes. They also studied the effect of utility temperature change on ED in TS cogeneration targets (Dhole and Linnhoff, 1993). Klemeš et al. (1997) estimated utility demands by exergy efficiency coefficients based on maximum energy recovery design of the entire process. Tarighaleslami et al. (2009) presented the merits of exergy analysis in the energy optimisation of large chemical plants such as crude oil refineries. Rivero et al. (2004) used exergy and exergo-economic analysis on combined distillation unit of an oil refinery to

achieve additional opportunities for PI. Followed by optimisation of atmospheric distillation unit of a crude oil refinery using exergy profiles (Tarighaleslami et al., 2012). Hackl and Harvey (2013b) used EA in the TS to target shaft work in sub-ambient and cryogenic processes. Exergo-economic and exergo-environmental evaluations of the coupling of a gas-fired steam power plant with a TS utility system were performed by Khoshgoftar Manesh et al. (2014). Karellas et al. (2013) used EA to optimise waste HR systems in the cement industry. The parallel study has been carrying out in the steel industry (Kaşka, 2014). Ghannadzadeh and Sadeqzadeh (2017a) combined Pinch and exergy analysis of an ethylene oxide production process to boost energy efficiency toward environmental sustainability. Later, they used exergy aided PA to enhance energy integration towards environmental sustainability in a chlorine-caustic soda production process (Ghannadzadeh and Sadeqzadeh, 2017b). Farhat et al. (2015) combined EA and classical HR optimisation via HENs in TS to increase HR between plants. However, they did not consider optimisation regarding UC.

2.5.6 Total Site Heat Exchanger Network Design and Retrofit

The aim of the HEN synthesis and design is to recover heat from the process by matching hot process streams and cold process streams to minimise the economic objective. After HR between hot and cold streams, hot and cold utility are imported to supply any energy requirement for HEN. Early HEN design based on PA method was proposed by Tjoe and Linnhoff (1986) to provide retrofit targets for utility consumption, and heat transfer area. However, in this method, the obtained area targets cannot reflect a complete area distribution within the HEN. The method was extended by Polly et al. (1990) to take into account pressure drop constraints. Later, Zhu and Nie (2002) considered pressure drop for HEN grassroot design. In their method, the pressure drop is considered at both targeting and design stages in a systematic manner. Subsequent research was conducted to overcome Pinch design method limitations.

Shokoya and Kotjabasakis (1991) proposed a technique to integrate the area distribution of the existing HEN into the targeting stage. This technique proposed more realistic area targets than the technique proposed by Tjoe and Linnhoff (1986). Cost matrix method for HEN retrofit was introduced by Carlsson et al.

(1993). They considered heat transfer area cost, equipment and pumping costs, and physical distance between the pair of streams. In addition, to minimise HEN's heat transfer area Exchanger Minimum Approach Temperature (EMAT) has been defined which is a degree of freedom that can enable reductions in the number of heat exchangers needed for the HEN to achieve the process targets. In general EMAT is equal or lower than global minimum approach temperature which shows the minimum acceptable distance between CCs. This concept was comprehensively reviewed by Shenoy (1995). Later, Akbarnia et al. (2009) presented a new approach in PA considering piping costs in total cost targeting for HEN. A correlation of piping costs for individual streams was presented that includes factors such as pipe size, pressure rating, and construction material, i.e. heat exchanger cost plus piping cost, and consequently total cost. Raei and Tarighaleslami (2011) used area efficiency coefficient to improve HEN area and capital cost. Jin et al. (2008) combined PA and exergo-economic analysis determining optimal minimum approach temperature for HEN synthesis. In this method, using a subsection integral on Balanced Composite Curves (BCC) exergy consumption of heat transfer in HENs is calculated.

Various MP and modelling techniques such as MILP have been applied to improve and optimise the scheduling and HEN design in the batch process by Lee and Reklaitis (1995). Ciric and Flouds (1989) proposed a systematic two-stage approach for the retrofit design of HENs. In the first stage, ΔT_{min} is selected and calculations for minimum utility cost are made. In the second stage, all possible heat exchange matches are considered. To do this a MILP models is required. Asante and Zhu (1997) introduced a two-stage hybrid methodology for retrofit of HENs. The method is based on identifying structural limitations to the HR of the existing HEN and modifying these limitations. Foo et al. (2008a) developed a minimum unit targeting method for batch HEN design. The method is an evolution of batch mass exchange network. Smith et al. (2010) presented a methodology for HEN retrofit, which is applicable to complex industrial revamps, considering existing networks and constraining the number of modifications. The method modified the network Pinch approach (Asante and Zhu, 1997) to be applicable in HEN design in which the thermal properties of streams are temperature-

dependent. The modified method combines structural modifications and cost optimisation in a single step to avoid missing cost-effective design solutions.

The synthesis problem of optimal HENs using multiple utilities was synthesised by Ponce-Ortega et al. (2010). They developed a MINLP based on a stage-wise superstructure that contains all possible matches between hot and cold streams in every stage. Unlike previous MP approaches, in this model, exchanges of process streams with utilities are allowed in each stage of the superstructure to determine the optimal location of hot and cold utilities. The model is able to handle forbidden and restricted matches as well as isothermal and non-isothermal process streams.

In the past decades, the synthesis and design of HEN have been well studied and applied to several practical industrial cases. For further HR and energy utilisation improvement of TS, integration between HEN and its associated energy system (i.e. centralised utility system) have been considered in different cases such as integration of HEN with Organic Rankine Cycle (Chen et al., 2014), absorption cycle (Lira-Barragán et al., 2014), trigeneration systems (Hipólito-Valencia et al., 2014), and thermal membrane distillation systems (González-Bravo et al., 2015).

The utility system is the heart of any industrial site energy system. In recent years, the synthesis and optimisation of the HEN as the utility system have been considered by many researchers (Klemeš et al., 2013). Liew et al. (2013b) proposed an improved Total Site Sensitivity Table (TSST) to determine the optimal size of a utility generation system to be able to design backup generators and piping system. Na et al. (2015) developed a modified superstructure containing a utility substage considering multiple utilities. In their method, utility main locations are considered to be fixed according to temperature and series connections between utilities to improve the model size and convergence. Liew et al. (2014c) proposed an extended Total Site Problem Table Algorithm (TS-PTA) to target the minimum utility requirement in a steam system that considers water sensible heat. Sun et al. (2015) presented a graphical approach based on extended SCC to provide a realistic TS utility targeting method accounting for boiler feedwater preheating, and steam superheating and desuperheating. Followed by Luo et al. (2016) who presented a simultaneous synthesis of the utility system and HEN incorporating

steam condensate and boiler feedwater. In their method, TS HEN is composed of several interlinked sub-HENs. They have formulated the links between sub-HENs and utility system.

A graphical method was proposed by Wang et al. (2014) to determine energy target of inter-plant heat integration with three different indirect connection patterns (parallel, split, and series) considering Site Pinch region. They showed that the parallel pattern connection will always recover more heat, but require more complex networks and higher investment costs. When the heat quality requirements of two heat sinks are similar, the split connection pattern achieves a better energy-capital trade-off. Series connection pattern is more attractive when the heat quality requirement of two heat sinks are very different as it offers shorter pipeline requirement.

Song et al. (2016b) presented a new strategy to select streams for inter-plant HR to achieve maximum possible HR via indirect HI. Using this technique, the existing HEN remains unchanged but the number of the participated streams may be reduced. The technique has only been applied to a two plant problem. They extended their work introducing ISCCs to select participant plants and hot/cold streams for inter-plant HI among three plants, which will be able to reduce the number of participant streams before integration, while keeping energy targets unchanged (Song et al., 2016a).

Zhang et al. (2016) presented a MINLP model for simultaneous HEN design for HI using hot direct discharges/feeds between process plants. Recently, Song et al. (2017) presented a modified MINLP model with an objective of TAC to determine the final inter-plant HEN configurations.

As mentioned above, many studies have been conducted on HEN synthesis and design in the past decades; however, these methods are based on using one of the CTST methods. None of the mentioned HEN design methods have considered network synthesis incorporating both isothermal and non-isothermal utilities using non-isothermal utility constraints in the network design. However, there is still a gap in literature to present UEN synthesis based on TSHI techniques for utility systems that use non-isothermal utilities, such as water. Recently, attempts

have been made to improve HR in the HEN by using heat transfer enhancement techniques.

2.6 Heat Transfer Enhancement

Different concepts and methods have been proposed to minimise energy use in process plants ranging from HR systems for individual processes to TSHI. In individual processes, various techniques have been applied to increase heat transfer rates in heat exchangers. These methods are known as Heat Transfer Enhancement (HTE). Generally speaking, HTE techniques are divided into two main groups: active techniques and passive techniques. In the active techniques, an external force is required, such as surface vibration, electrical or magnetic field, or acoustic move on fluid. Passive techniques, on the other hand, require no external forces. Rather, passive techniques increase heat transfer by changing the surface geometry or by adding some additives to the fluids (Huminic and Huminic, 2012). Active techniques due to their additional energy requirements are less often considered in PI methods, while passive techniques are common in PI literature.

The HTE procedure for HEN retrofit has been suggested by Zhu et al. (2000). His method is based on accounting for HTE effects in the application of PA techniques. Pan et al. (2011) performed HTE tests for commercial shell and tube heat exchangers using turbulators for intensified tube side heat transfer. They continued their work by presenting MILP based iterative method to retrofit design HENs (Pan et al., 2012). Optimisation of large scale HEN with different intensified heat transfer is their latest HTE study in PI area (Pan et al., 2013). Using HTE in PI has many benefits, and the three most popular ones are stated as:

i. Enhanced heat exchangers require a less heat transfer area for a given heat duty, this is due to higher heat transfer coefficients.
ii. For a given heat exchanger, heat transfer capacity can be increased without any change in the physical size or area of the exchanger.
iii. Enhanced heat exchangers can achieve higher overall heat transfer coefficients with the same or lower fluid velocities. This may lead to lower friction, which means a reduction in the pumping requirements.

These techniques, such as inserting turbulators in tubes and using helical baffles in shells (Jafari Nasr and Shafeghat, 2008), are useful for shell and tube heat exchangers, which are a common heat exchanger type in chemical process industries. Jafari Nasr et al. (2015) also presented combinations between different HTE techniques to achieve higher heat transfer rates. However, other techniques are presented for HTE of other heat exchanger types such as CFD analysis in plate-fin heat exchangers (Khoshvaght-Aliabadi et al., 2014). Wang et al. (2012) studied the application of intensified heat transfer as HTE technique for retrofit of HEN. Recently, Akpomiemie and Smith (2016) proposed HEN retrofit with HTE based on an area ratio approach for a HEN containing shell and tube heat exchangers. Later, they considered pressure drop with HTE in HEN retrofit (Akpomiemie and Smith, 2017).

For many decades, adding solid micron-sized particles to conventional fluids for HTE has been considered due to their high thermal conductivity (Shekarian et al., 2014). However, in practice, operational problems, such as fouling, sedimentation and increased pressure drop, occur by using these additives which dissuades industry from applying this type of HTE technique. Recent progress in nanomaterials technology has made it conceivable to overcome these problems by producing particles at a nano-scale. Compared to micron-sized particles, nanoparticles are engineered to have relatively larger surface area, high mobility, less particle momentum, and higher suspension stability. Suspension of nanoparticles in a fluid create a new category of fluids called nanofluids. Nanofluids are a class of fluids with a suspension of nano-sized particles, which aims to enhance a fluid's heat and mass transfer performance (Daungthongsuk and Wongwises, 2007). Water, ethylene glycol, transformer and turbine oil, and liquid paraffin are usually used as the base fluid, while metals and metal oxides, such as Cu, CuO, Al_2O_3, SiO_2, TiO_2, as well as non-metallic particles, such as Multi-Wall Carbon Nanotubes (MWCNT). The sizes of the nanoparticles are typically <100 nm.

Peyghambarzadeh et al. (2011) showed that using a nanofluid can increase the heat transfer coefficient of car radiators by up to 40 %. Later he showed the overall heat transfer coefficient increased with the application of dilute nanofluids in the

car radiator (Peyghambarzadeh et al., 2013). This research group demonstrated that using 0.4 vol. % CuO/water nanofluid can increase the overall heat transfer coefficient by up to 8 % in car radiators (Naraki et al., 2013). Wu et al. (Wu et al., 2016) presented the thermal performance of MWCNT/water nanofluids in helical heat exchangers. Tohidi et al. (2015) showed the combination of chaotic advection and nanofluids flow in helically coiled tubes offers higher heat transfer coefficient. Pantzali et al. (2009) studied the efficiency of CuO/Water nanofluid with 4 vol. % of CuO nanoparticles as coolants in commercial plate heat exchangers. Tabari and Heris (2015) studied heat transfer coefficient of a milk pasteurisation plate heat exchanger using MWCNT/water nanofluid, and the effect of hybrid MWCNT/water and Al_2O_3/water nanofluid mixture in plate heat exchangers has been studied by Huang et al. (2016). Raei et al. (2017) showed adding 0.15 vol. % concentration γ-Al_2O_3 nanoparticles to the water can increase the heat transfer coefficient up to 23 % in double tube heat exchangers. Recently, Shekarian et al. (2016) developed a new set of equations combining Rapid Design Algorithm (RDA) (Polley et al., 1991), and both twisted tape tube inserts and Al_2O_3/water nanofluid as HTE techniques to design shell and tube heat exchangers. The results show that using turbulators individually and in a hybrid format with nanofluid can be effected on design parameters of a typical heat exchanger by reducing the required heat transfer area up to 10 %. Each of these studies was at the laboratory scale, meaning the implementation of nanofluids in large scale industrial applications is not reported yet. Furthermore, the application of nanofluids, in combination with an integrated process's utility system has not be investigated.

2.7 Conclusions

Total Site Heat Integration is an effective method for design of large scale utility systems that serve large chemical processes, such as refineries, petrochemicals or even lower temperature chemical and process plants. TSHI of different chemical plants might confront batch, semi-continuous or continuous plants which are clustered into one large site. TSHI offers direct and indirect heat integration through a process or plant. The direct HI can achieve more energy saving; however, it is unlikely due to practical operation problems between several processes in the plant. On the other hand, indirect HI with a central utility system offers greater

advantages of process control, flexibility and optimum heat exchangers network design, and has a lower energy recovery target compared to direct integration. Conventional TSHI methods mainly focus on targeting, optimisation, and HEN synthesis and design of high temperature processes that inherently use isothermal utilities. Other special TSHI methods such as HRL method that targets utility and HR for low temperature processes using non-isothermal utilities, put more constraint on the HEN, i.e. effectively applying TSHI techniques to processing applications and sites that required non-isothermal utilities is complex and economically challenging. Therefore, a lack of a unified method that could be able to target and optimise number of utility main and temperature of both isothermal and non-isothermal utilities and be able to offer practical network design is obvious.

Chapter Three

Overview of New Total Site Heat Integration Method Development in the Thesis

3.1 Introduction

Total Site Heat Integration (TSHI) analysis provides a rigorous engineering method for setting energy conservation targets for large multi-plant industrial processing facilities. The purpose of this chapter is to provide an overview of the TSHI methods developed, outlines the major steps and method that are reported in this thesis. TSHI consists of three different stages, as shown in Figure 3-1: i) TSHI targeting methods; ii) utility system optimisation; and iii) heat exchanger network synthesis and design.

Figure 3-1 shows the overview of the TSHI stages and method that are developed in this thesis. At the first stage, a new TSHI targeting method will be proposed. To be of greatest value to the engineer, TSHI targets need to be realistic and achievable in practice. As mentioned before, in this thesis, an achievable target means one that accounts for feasible HR constraints, and a realistic target means one where the target temperature of the utility stream is met within a single process in the cluster. Published studies have shown that the Conventional Total Site Targeting (CTST) methods determine meaningful energy targets for high temperature (>120 °C) processing sites, which primarily use steam utility. However, for low temperature (<120 °C) processing sites that mostly use hot water, a non-isothermal utility, the conventional methods often set overly optimistic targets. This is because these methods allow the utility target temperatures to be achieved using series process-utility heat exchanger matches that could be located in different processes. For many cases, the required network design that achieves the TSHI target is highly likely to be uneconomic and impractical, especially for non-continuous processing sites. Therefore, this thesis aims to develop a new TSHI methodology to overcome the conventional TSHI methods' targeting and practical shortcomings.

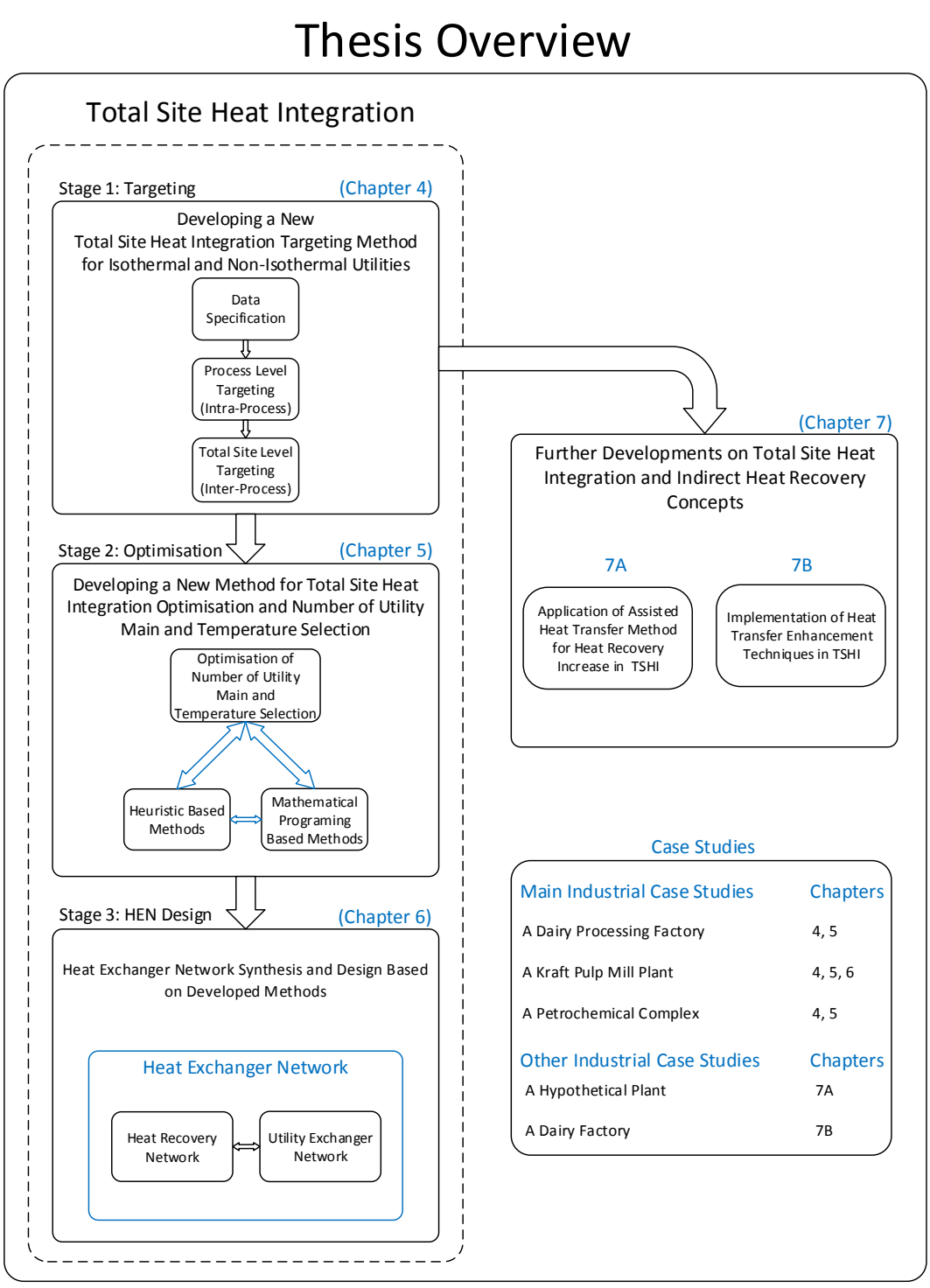

Figure 3-1: Overview of TSHI stages and methods presented in the thesis.

The second stage will be an expansion of the optimisation of the developed new TSHI targeting method as well as optimal utility main and temperature selection. Selection of the number of utility mains and the associated temperatures are an important degree of freedom for the maximisation of TSHI. These can be done using heuristic-based methods and MP based methods in conjunction with heuristics.

In the third and last stage in TSHI, evolutionary heat exchanger network and utility exchanger network will be synthesised based on heat integration targets from the new method. As found in Chapter 2, limited research has been conducted on HEN design including HRN and UEN synthesis in TS, except the special case of using dedicated indirect HR systems (M. R. W. Walmsley et al., 2013a) called HRL, where the network pattern and structure is fixed.

Finally, other developments of TSHI such as assisted heat transfer method in TSHI and the implementation of HTE techniques in TS will be discussed in Chapter 7. Assisted heat transfer method provides a new opportunity to increase HR and SWG targets in TSHI. It will be discussed how maximum assisted TSHI can be targeted by comparing each HR pockets to the SUGCC using background /foreground analysis. In the second half of Chapter 7, the application of the nanofluids as a heat transfer medium in utility systems will be studied to achieve higher HR and lower area targets in TS.

3.2 The Challenge of TSHI for Non-Isothermal Utilities

TSHI faces several targeting, optimisation, and HEN synthesis and design challenges when non-isothermal utilities are considered as a part of the central utility system in plants.

3.2.1 Challenges Faced in TSHI Targeting Stage for Non-Isothermal Utilities

One of the limitations of the conventional TSHI is the treatment of non-isothermal utilities during the targeting process. In these methods, non-isothermal utilities are often treated in the same way as isothermal utilities where the utility supply temperature is the primary constraint. An isothermal utility's temperature remains constant when the utility supplies different processes in a cluster of industrial plants. For non-isothermal utilities that are being consumed and generated (i.e. TSHR), the utility target temperature may be an additional fixed constraint. Pinching non-isothermal utilities against the TSP presents an economic challenge in designing the utility network.

Few TSHI studies have focused on targeting processes and sites that primarily require non-isothermal utilities; nor have they investigated the possibility of

replacing isothermal utilities (e.g. steam) with non-isothermal (e.g. hot oil) to increase HR. A contributing factor for this gap is the lack of a TSHI method that calculates realistic and achievable targets considering both isothermal and non-isothermal utilities. Figure 3-2 presents a simple illustration of the problems faced in applying conventional TSHI and HRL targeting methods to a multi-process site that requires non-isothermal utilities.

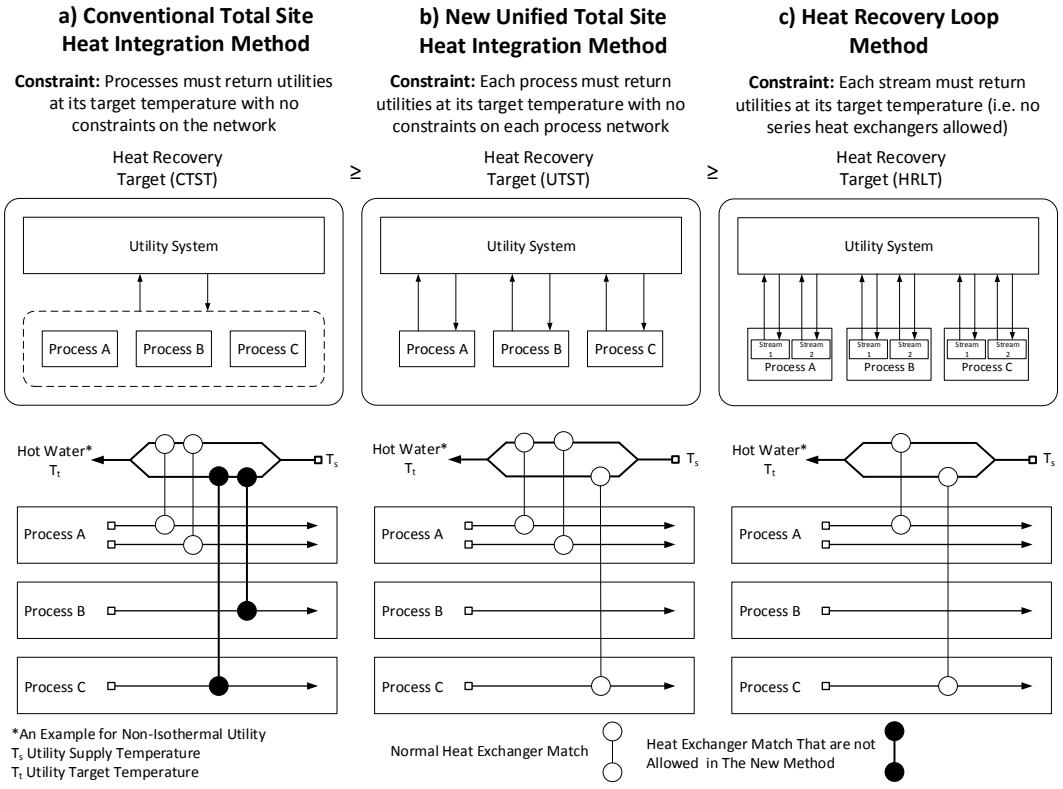

Figure 3-2: Comparison of the frameworks and constraints for a) the conventional TSHI method; b) the new Unified TSHI concept; and c) the HRL method, including example hypothetical utility network designs.

In each of the three methods shown in Figure 3-2 (including the new method), the non-isothermal hot water loop is supplied at its supply temperature and must return to its target temperature. The target temperature for non-isothermal utilities can be achieved a number of ways, but is constrained depending on the targeting method. Conventional TSHI inherently allows the target temperature to be met using a single heat exchanger or using heat exchanger matches in series and/or parallel configurations from any process as illustrated in Figure 3-2a. In some cases, a series set of heat exchangers may be critical to achieving the TS targets. On the other hand, the HRL method as a special case of conventional TSHI methods, has an additional constraint that the utility target temperature must be

achieved with only one heat exchangers as in Figure 3-2c (i.e. it excludes heat exchangers in series). The new method allows heat exchangers in parallel and series to achieve the utility target temperature, if and only if the heat exchangers in series are from the same process as shown in Figure 3-2b.

The targets produced using conventional TSHI for non-isothermal utilities are therefore overly optimistic because it allows the target temperature to be achieved using series matches that could (in theory) be from different processes, which is highly likely to be uneconomic and impractical.

3.2.2 Challenges Faced in TSHI Optimisation and Utility Temperature Selection for Non-Isothermal Utilities

TSHI methods face several challenges that must be recognised in optimisation procedures. One of the challenges with optimisation of TSHI methods is the compounding effect of multiple optimisation variables. Slight changes in utility temperature in TSHI can impact on the heat exchanger unit target, causing a discontinuity in the capital and total cost curves. It can be difficult to distinguish between the weights of each variable on optimisation objectives. For example, focusing solely on total cost as an optimisation objective obscures the fundamental trade-off between capital and operating costs.

Another challenge refers to hydraulic issues. In sites with large-utility systems, an optimisation method may drive non-isothermal utility to low temperature difference causing unacceptably high utility flow rate, pressure drop, and pumping requirements.

Utility selection can be considered as another challenge, especially for the sites that operate in the range of 80 – 120 °C. Water as non-isothermal utility is the cheapest and the most available option in many processes. However, in temperatures close to 100 °C or above, water is likely to convert into the vapour phase; therefore, it must be pressurised to stay in the liquid phase which may impose an extra cost to the utility system. Oil has a wide applicable temperature range, but lower thermal capacity with higher viscosity that increases hydraulic isuues and requires more electrical power, also it uncertain safety and hazard issues for sites such as pharmaceutical and food processing plants.

Another challenge with the optimisation of TS plants is the selection of number of utility mains. An increase in the number of utility mains is likely to improve HR while there is a trade-off between investment and utility costs as the piping work is always one of the major capital costs.

Utility temperature selection also has direct effect on utility cost and fuel consumption. The appropriate utility temperature may increase HR and decrease the amount of utility production requirement while it may also affect the number of required utility mains.

3.2.3 Challenges Faced in TSHI Heat Exchanger Network Synthesis and Design for Non-Isothermal Utilities

Even though utility-process matches are important in targeting stage to calculate achievable and realistic targets, these matches are of great importance in operation of the industrial plants. Conventional TSHI methods' HEN synthesis and design creates a dependency on two separate and distinct processes and one of the original rationales for TS was to achieve HR between individual processes without having these types of dependencies. These dependencies can cause major operation issues especially in clusters containing non-continuous processes. For example, in Figure 3-2a the hot water target temperature on the lower split is achieved by two heat exchangers in series, the first match in Process B and the second from Process C. If there was disturbance in the stream matched from Process B, for example, due to its non-continuous nature, the target temperature would not be achieved by the match from Process C alone. As a result, additional cold utility, such as refrigeration, is consumed to ensure achievement of the target temperature (because this temperature is also its supply temperature as the hot water is regenerated by process streams). If no additional utility is consumed and the water utility is returned to the process for regeneration at a higher temperature than its target, it puts at risk process streams not reaching their target temperature, especially in situations where the exchanger is a utility pinch. As a result, in practice, these types of matches would ordinarily be considered impractical as the operational risk and control complexity outweigh the benefits.

To overcome this HEN synthesis problem in TSHI, Walmsley et al. (2013a) presented a method for dealing with HI between continuous and non-continuous processes that operate at lower temperatures (ambient to ~120 °C), such as food and dairy industries, using a dedicated indirect HR system, which is often referred to as a HRL. In this method, all the heat exchangers from HEN connected to the HRL are considered as parallel to each other, as a pre-defined network structure. Figure 3-2c illustrates the general framework of how the HRL method allows a dedicated hot water or hot oil system (e.g. a utility sub-system) to interact with individual streams. Such a framework has additional constraints that lower the inter-process HR target and requires information about process heat exchanger network designs prior to targeting inter-process heat integration.

3.3 Key Research Questions

Key engineering research questions include: i) How to calculate realistic and achievable targets for TSHI using isothermal and non-isothermal utilities through application of PA tools such as the Problem Table (PT), Composite Curve (CC), Grand Composite Curve (GCC), Total Site Problem Table (TS-PT), Total Site Profile (TSP), Site Utility Grand Composite Curve (SUGCC)? ii) How to select the cost optimal utility temperature and mains for both isothermal and non-isothermal utilities in the TS? iii) What are the limitations of the CTST methods and how these limits affect TS targeting constraints and utility-process heat exchanger matches in the HEN design? These engineering research questions represent the gap in the knowledge as well as a hurdle to the efficient use of generated process heat within the TS.

3.4 Introduction to Industrial Case Studies

The scope of the thesis includes investigation of three industrial case studies using the new and conventional TSHI targeting, optimisation, and design methods.

3.4.1 Kraft Pulp Mill

Södra Cell Värö Kraft Pulp Mill also known as a Sulphate Pulp Mill in southern Sweden (Bood and Nilsson, 2013) has been chosen as a first case study and represent intermediate temperature processes. This plant was the first paper pulp factory in the world to be transformed to totally chlorine free bleaching of the

pulp. The plant has a production capacity of 425,000 Air Dry ton pulp annually within 10 different processes (including 7 miscellaneous streams which are considered as an individual process together) with a total of 64 streams available for TS integration. Kraft Pulp Mill plant can be considered with both high and low temperature processes. The stream data for each individual existing process in the Södra Cell Värö Kraft Pulp Mill plant taken from Bood and Nilsson (2013) are presented in Table 3-1, where T_s is supply temperature and T_t is target temperature of process streams.

Table 3-1: Stream data table for existing processes in the Kraft Pulp Mill case study.

Process	Stream	T_s (°C)	T_t (°C)	CP (kW/°C)
Bleaching	Cooling of BB2 to AWP white wash	82.7	77.8	941.43
	Cooling of BB4	83.2	71.5	787.69
	Gas cooling after srep 4	99.7	90.1	30.52
	Heating of KLR to filter 2&3	81.2	83.3	139.52
	Heating of water to filter 4	1.9	46.5	321.46
	HW to diluter screw feeder	1.9	65.0	280.98
	Steam demand	148.4	148.5	97,480.00
	Steam demand Step 2	184.8	184.9	14,980.00
	Steam demand Step 4	184.8	184.9	30,520.00
Causticizing	Cooling of green liquor	97.1	87.6	244.42
	HW Heating	148.4	148.5	8,650.00
	HW to lime washer	1.9	70.0	13.80
	Mist condenser	84.1	68.4	404.65
Digestion	Blowing Steam Condenser	103.3	103.2	165,850.00
	Cooling od Acc.0	80.0	74.3	1,059.82
	Cooling of hot liquor	165.4	146.5	94.60
	Heating of white liquor	90.8	108.1	103.35
	HW production	70.6	80.0	237.77
	Steam demand	184.8	184.9	202,000.00
	Steam demand	148.4	148.5	34,700.00
	Turpentine Condenser	90.1	50.5	28.28
Evaporator	Steam demand for evaporator	148.4	148.5	517,930.00
	Surface condenser	66.3	66.2	393,950.00
District Heating	Cooling of V1	76.8	53.6	825.26
	District heating demand saw mill	105.4	111.9	635.08
	District heating to tomato farm	37.7	50.0	57.15
	Office facilities heating	65.0	75.0	20.00
	R7D facilities heating	49.2	54.7	7.64
	Steam demand saw mill	148.4	148.5	36,760.00
Miscellaneous 1	Cooling of BSB to bio cleaning	65.0	36.0	130.86
Miscellaneous 2	Cooling of V1 to bio cleaning	53.6	36.0	819.72
Miscellaneous 3	Heating demand, hot air to bark drier	8.3	88.3	91.49
Miscellaneous 4	Leakage steam	99.6	99.5	7,180.00
Miscellaneous 5	Steam demand, chemical plant	148.4	148.5	11,060.00
Miscellaneous 6	Turbine cooling	40.2	40.1	5,810.00

Process	Stream	T_s (°C)	T_t (°C)	CP (kW/°C)
Miscellaneous 7	VKT production	1.9	20.0	186.08
Paper Room	Air cooling from air drier, Step 1	104.0	59.0	79.98
	Air cooling from air drier, Step 2	59.0	50.0	996.33
	Flash Steam condenser	129.1	129.0	13,950.00
	Flash steam condenser	120.2	120.1	28,080.00
	Heating of air to air drier	36.8	122.7	115.04
	Heating of air to cyclone drier	4.3	148.3	76.01
	Heating of paper room facilities	3.0	34.9	15.64
	Heating of paper room facilities	3.0	36.8	61.36
	HW to BSB-tank	52.0	70.0	156.00
	Steam demand, air drier	148.4	148.5	216,900.00
	Steam demand, Wire Steam Box	148.4	148.5	28,760.00
	WW demand in tank	2.7	52.1	156.48
	WW to back water tank	1.9	45.0	79.33
Stripper	Cooling of KLR	117.8	84.4	352.51
	Heating of KLB	66.8	107.7	153.74
	Heating of KLS	63.8	102.9	140.31
	Steam demand MeOH column	148.4	148.5	8,050.00
	Steam demand stripper	148.4	148.5	30,070.00
Recovery Boiler	Feed pre-heating	83.0	106.2	426.03
	Flue gas cooling	204.5	133.2	138.63
	Heating of VKT to feed water	16.1	17.0	148.89
	Steam demand feed water tank	148.4	148.5	131,270.00
	Steam demand recovery boiler	148.8	148.9	117,670.00
	Steam demand recovery boiler	148.4	148.5	63,520.00
	Steam demand, feed pre-heating	184.8	184.9	43,350.00
Wash	Back water (Liquor tank 2 to AWP1)	87.0	78.0	500.67
	Filtrate tank diffuser to COP1	87.0	82.0	213.60
	Thin liquor cooling to blow tank	67.9	38.3	138.18

3.4.2 Large Dairy Processing Factory

The second industrial case study is a large dairy processing factory in New Zealand, which represents low temperature processes (< 120°C). In peak production periods, about 14 million litres of milk are processed daily at this plant that main products are whole, skim and butter milk powders; Cheddar, Colby, Egmont and Mozzarella cheese; and butter. The factory has 19 different processes with 79 available streams for TSHI. Most of the processes in TS are semi-continuous processes. The stream data for each individual existing process in the case study TS is presented in Table 3-2.

Table 3-2: Stream data table for existing processes in the Dairy Factory case study.

Process	Stream	T_s (°C)	T_t (°C)	CP (kW/°C)
AMF Process	AMF	65.0	43.0	0.26
	AMF Buttermilk	15.0	10.0	0.77
	Cream	62.0	75.0	1.24
	Oil 2	80.0	95.0	0.26
	Rec. fat	12.0	55.0	3.36
Butter Process	Buttermilk	12.0	6.0	17.81
	Cream	73.0	85.0	31.19
	Flav. Cream C	10.0	12.0	31.19
	Flav. Cream H	22.0	10.0	31.19
	Flavourtech	180.0	30.0	7.06
Casein Process	COW water C 1	70.0	83.0	9.28
	COW water C 2	35.0	30.0	9.28
	Wash water	45.0	25.0	10.71
	Whey1	74.0	80.0	20.95
	Whey2	47.0	9.0	20.95
Casein Whey Process	UF perm 1	44.0	75.0	61.85
	UF perm 2	59.0	75.0	61.85
	WPC Conc.	10.0	6.0	1.97
Cheese Process	Milk 1	95.0	6.0	2.71
	Milk 2	31.0	95.0	2.71
	Mozz cheese 1	65.0	35.0	6.51
	Mozz cheese 2	32.0	65.0	6.51
	Whey 1	31.0	38.0	260.68
	Whey 2	31.0	36.0	220.75
	Whey cream	56.0	14.0	2.10
	Whey separation	70.0	76.0	178.60
Cheese & Whey UF Process	Cheese milk 1	59.0	75.0	118.60
	Cheese milk 2	10.0	15.0	118.60
	Skim milk 1	59.0	75.0	50.98
	Skim milk 2	10.0	10.0	50.98
Cheese Whey Process	Cheese whey	40.0	10.0	153.08
	HiFat	12.0	10.0	12.77
	HiFat conc.	14.0	8.0	1.91
	LoFat	12.0	10.1	9.00
	LoFat conc.	14.0	8.0	1.63
Evaporator & Dryer Process	Condensate	40.9	25.0	2.44
	Condenser	41.0	40.9	5,490.00
	WPC feed C	53.0	43.0	5.32
	WPC feed H	43.0	65.0	5.32
Milk Powder & Lactose Process	COW water	55.0	10.0	4.64
	Lactose C	70.0	86.0	12.83
	Lactose H	25.0	10.0	12.83
	Retentate	10.0	8.0	2.13
	Skim milk	10.0	8.0	7.25

Process	Stream	T_s (°C)	T_t (°C)	CP (kW/°C)
Milk separation & casein Process	Cream	15.0	9.0	24.73
	Raw milk	40.0	45.0	307.20
	Skim milk	15.0	8.0	276.48
	Standard skim	53.0	65.0	67.97
	Standard skim	10.0	15.0	67.97
Milk separation & casein Process	Evap. Cond.	40.0	10.0	16.06
	Retentate	13.0	8.0	13.96
	Skim milk	20.0	10.0	50.98
	UF perm	16.0	35.0	44.12
Milk UF & CIP Process	DF water	30.0	10.0	0.84
	Permeate	12.0	7.0	26.75
	Retentate	12.0	7.0	9.22
P1 MPC Process	Concentrate 1	45.0	70.0	4.69
	Condensate 2	49.0	20.0	4.66
	Condenser	50.0	49.9	5,520.00
	Retentate	65.0	80.0	8.50
P1 permeate Process	Conc. Perm C	68.0	84.0	29.74
	Conc. Perm H	12.0	10.0	35.02
	Condensate	50.9	20.0	17.41
	Condenser	51.0	50.9	16,800.00
	Evap. Perm	15.0	7.0	12.78
	UF perm	10.5	13.0	70.04
P2 Process	Concentrate	54.0	60.0	5.86
	Condenser	56.0	55.9	12,500.00
P3 Process	Concentrate	65.0	78.0	10.33
P4 Process	Concentrate	56.0	65.0	17.56
	Retentate	64.0	79.0	59.10
P5 Process	Concentrate	51.0	75.0	14.67
	COW water	25.0	25.1	47.84
	Milk	82.0	95.0	59.21
RO/Lactose evaporators Process	Conc perm 2	44.0	58.0	26.09
	Condenser	41.0	40.9	13,620.00
	Dirty condensate	50.0	25.0	8.01
	UF perm	12.0	32.0	97.36

3.4.3 Petrochemical Complex

The last case study represents a Petrochemical Complex with a cluster of high temperature processes that is a located in Europe. Petrochemical complexes operate continuously with higher processing temperatures than Kraft mills and dairy factories. The Petrochemical Complex has 8 individual plants and a total 60 hot and cold streams available for TSHI. In this thesis, very low temperature and cryogenic processes of the plant are not considered in the TS. The available

individual plants and the streams of the Petrochemical Complex to be studied as TS case study are presented in Table 3-3.

Table 3-3: Stream data table for existing processes in the Petrochemical Complex study.

Process	Stream	T_s (°C)	T_t (°C)	CP (kW/°C)
Unit A	C1	177.3	213.4	92.00
	H1	45.4	32.2	2.92
Unit B	C1	113.0	309.0	52.91
	C2	73.4	309.0	39.93
	C3	43.5	143.0	9.65
	H1	296.5	144.4	102.72
	H2	154.0	45.0	34.56
Unit C	C1	143.0	350.0	81.99
	C2	183.0	188.0	154.00
	C3	115.0	131.0	138.00
	C4	260.0	361.0	92.53
	H1	318.0	236.0	21.44
	H2	288.0	194.0	45.88
	H3	203.0	119.0	17.42
	H4	112.0	34.0	21.62
	H5	169.0	101.0	14.06
	H6	173.0	36.0	4.04
	H7	105.0	45.0	104.95
	H8	45.0	28.0	11.06
	H9	128.0	54.0	0.90
	H10	128.0	38.0	5.81
	H11	37.0	33.0	6.86
	H12	269.0	257.0	16.14
	H13	276.0	85.0	5.37
	H14	129.0	88.0	39.45
Unit D	C1	192.0	212.0	60.72
	C2	71.0	212.0	1.40
	C3	50.0	151.0	7.68
	H1	228.0	210.0	77.12
	H2	210.0	92.0	32.18
Unit E	C1	235.0	273.0	87.90
	C2	243.0	260.0	60.44
	H1	82.0	31.0	10.29
	H2	113.0	46.0	51.68
	H3	46.0	41.0	0.11
	H4	46.0	30.0	4.78

Process	Stream	T_s (°C)	T_t (°C)	CP (kW/°C)
Unit F	C1	257.8	259.0	79.35
	C2	69.0	275.9	8.66
	C3	255.1	257.3	815.40
	C4	292.5	293.7	138.73
	H1	91.4	65.6	77.49
	H2	91.4	53.9	12.35
	H3	270.1	222.7	34.05
	H4	175.4	45.3	23.97
	H5	233.4	61.5	7.13
	H6	274.1	58.9	0.60
Unit G	C1	134.0	252.0	11.71
	C2	299.0	321.0	81.15
	H1	220.0	126.0	26.45
	H2	233.0	224.0	14.17
	H3	218.0	171.0	10.14
	H4	282.0	187.0	9.86
	H5	187.0	126.0	6.30
	H6	329.0	77.0	2.20
	H7	229.0	92.0	6.32
	H8	111.0	62.0	36.71
Unit H	C1	88.0	210.0	9.78
	H1	211.0	129.0	9.72
	H2	129.0	80.0	1.15
	H4	131.0	93.0	3.84

3.5 Overview of Total Site Integration (UTSI) Software Tool

An Excel™ spreadsheet software tool called Unified Total Site Integration (UTSI) software has been developed step by step during this research to be able to calculate both conventional and new TSHI targeting and optimisation methods. The outputs of the UTSI software will be presented as the results of each developed method in Chapters 4, 5, 6, and 7. In this section, a general overview of the UTSI software is presented.

As is shown in Figure 3-3, the stream data can be added into the software indicating process and stream name. Supply and target temperatures of each stream are required. Either mass flow rate and specific heat (heat capacity flow rate) or heat load should be defined. In addition, estimated stream heat transfer coefficient (HTC) and ΔT_{cont} for each stream can be specified at this stage.

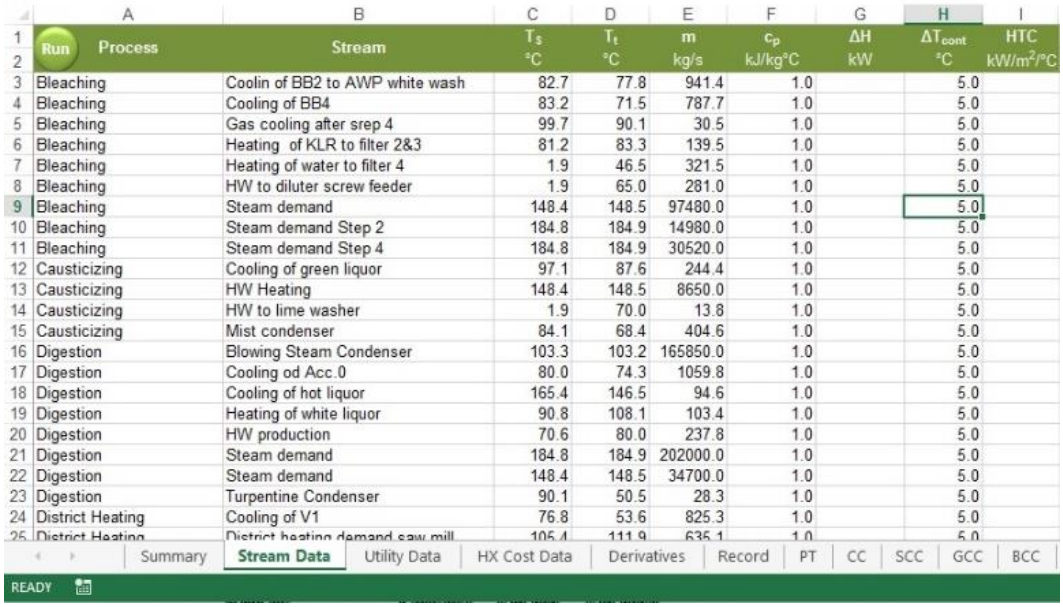

Run	Process	Stream	T_s °C	T_t °C	m kg/s	c_p kJ/kg°C	ΔH kW	ΔT_{cont} °C	HTC kW/m²/°C
	Bleaching	Coolin of BB2 to AWP white wash	82.7	77.8	941.4	1.0		5.0	
	Bleaching	Cooling of BB4	83.2	71.5	787.7	1.0		5.0	
	Bleaching	Gas cooling after srep 4	99.7	90.1	30.5	1.0		5.0	
	Bleaching	Heating of KLR to filter 2&3	81.2	83.3	139.5	1.0		5.0	
	Bleaching	Heating of water to filter 4	1.9	46.5	321.5	1.0		5.0	
	Bleaching	HW to diluter screw feeder	1.9	65.0	281.0	1.0		5.0	
	Bleaching	Steam demand	148.4	148.5	97480.0	1.0		5.0	
	Bleaching	Steam demand Step 2	184.8	184.9	14980.0	1.0		5.0	
	Bleaching	Steam demand Step 4	184.8	184.9	30520.0	1.0		5.0	
	Causticizing	Cooling of green liquor	97.1	87.6	244.4	1.0		5.0	
	Causticizing	HW Heating	148.4	148.5	8650.0	1.0		5.0	
	Causticizing	HW to lime washer	1.9	70.0	13.8	1.0		5.0	
	Causticizing	Mist condenser	84.1	68.4	404.6	1.0		5.0	
	Digestion	Blowing Steam Condenser	103.3	103.2	165850.0	1.0		5.0	
	Digestion	Cooling od Acc.0	80.0	74.3	1059.8	1.0		5.0	
	Digestion	Cooling of hot liquor	165.4	146.5	94.6	1.0		5.0	
	Digestion	Heating of white liquor	90.8	108.1	103.4	1.0		5.0	
	Digestion	HW production	70.6	80.0	237.8	1.0		5.0	
	Digestion	Steam demand	184.8	184.9	202000.0	1.0		5.0	
	Digestion	Steam demand	148.4	148.5	34700.0	1.0		5.0	
	Digestion	Turpentine Condenser	90.1	50.5	28.3	1.0		5.0	
	District Heating	Cooling of V1	76.8	53.6	825.3	1.0		5.0	
	District Heating	District heating demand saw mill	105.4	111.9	635.1	1.0		5.0	

Figure 3-3: Stream data sheet of the UTSI software tool.

Figure Figure 3-4 shows Utility Data sheet in UTSI software tool. Utility type, supply and target temperatures, ΔT_{cont}, utility unit cost, and heat transfer coefficient are inputted in this sheet. Also, the availability of the utility for optimisation through variation of utility supply/target temperatures can be selected.

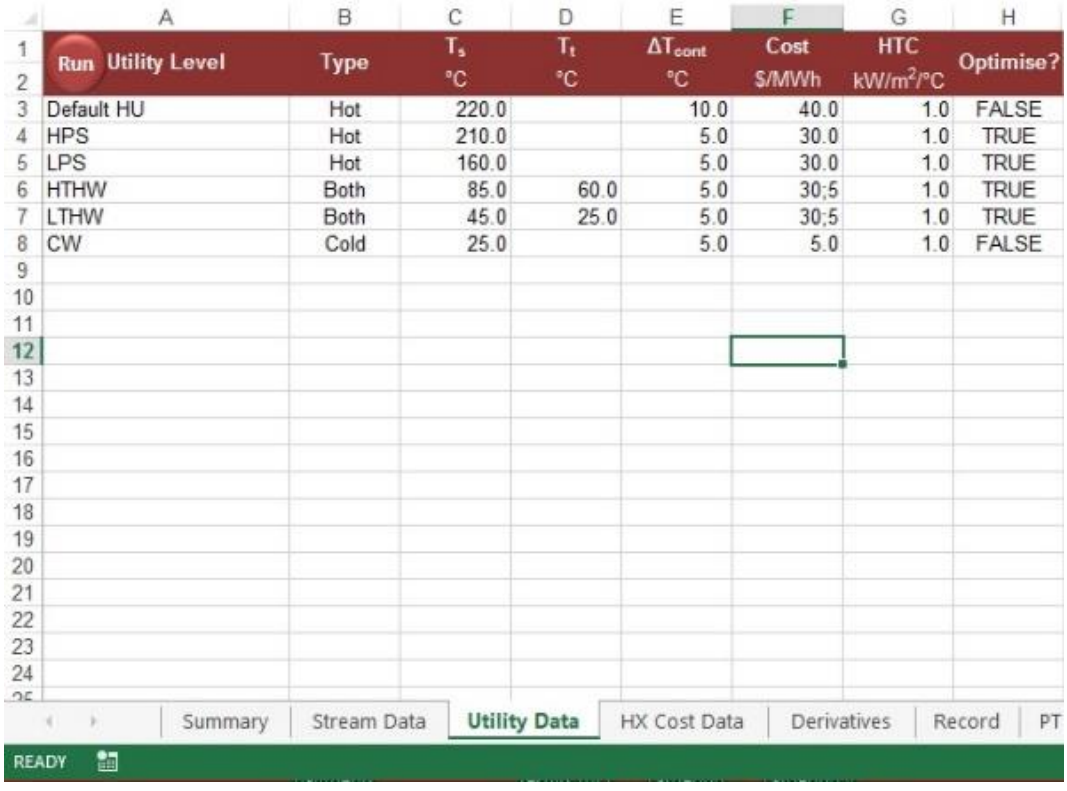

Run	Utility Level	Type	T_s °C	T_t °C	ΔT_{cont} °C	Cost $/MWh	HTC kW/m²/°C	Optimise?
	Default HU	Hot	220.0		10.0	40.0	1.0	FALSE
	HPS	Hot	210.0		5.0	30.0	1.0	TRUE
	LPS	Hot	160.0		5.0	30.0	1.0	TRUE
	HTHW	Both	85.0	60.0	5.0	30;5	1.0	TRUE
	LTHW	Both	45.0	25.0	5.0	30;5	1.0	TRUE
	CW	Cold	25.0		5.0	5.0	1.0	FALSE

Figure 3-4: Utility data sheet of the UTSI software tool.

Capital cost parameters including investment return duration, interest rate, and operating period of the plant can be defined in HX Cost Data sheet (Figure 3-5).

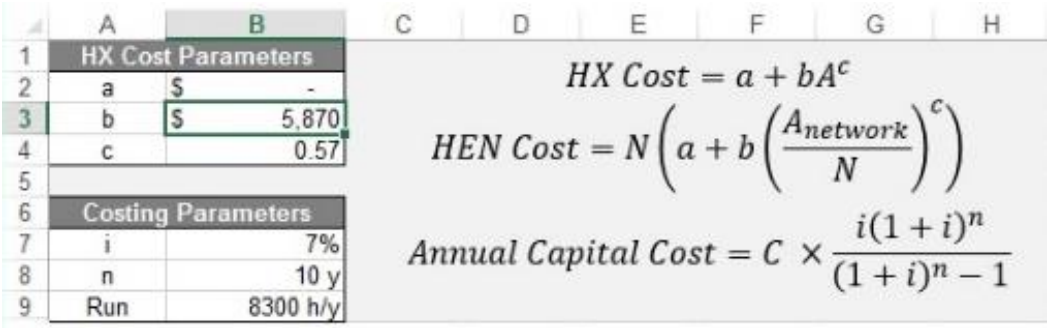

	A	B
1	HX Cost Parameters	
2	a	$ -
3	b	$ 5,870
4	c	0.57
5		
6	Costing Parameters	
7	i	7%
8	n	10 y
9	Run	8300 h/y

$$HX\ Cost = a + bA^c$$

$$HEN\ Cost = N\left(a + b\left(\frac{A_{network}}{N}\right)^c\right)$$

$$Annual\ Capital\ Cost = C \times \frac{i(1+i)^n}{(1+i)^n - 1}$$

Figure 3-5: Heat exchanger data sheet of the UTSI software tool.

In the Settings window, a variety of menus and options for different purposes may be selected as shown in Figure 3-6. The UTSI software calculates HR and utility targets individually for each process and for the TS. The tool also optionally calculates SWG, exergy targets, UC and TAC as well as the Problem Table. It plots CC, BCC, GCCs with and without HR pockets, assisted heat integration graphs, TSP, and SUGCC. Summary sheet shows the results summary.

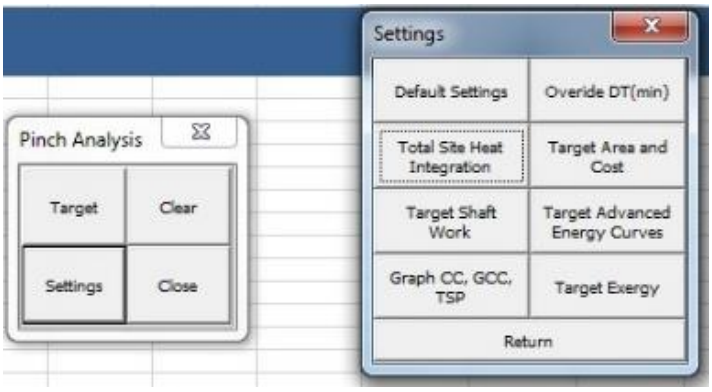

Figure 3-6: Setting window and Summary sheet of the UTSI software tool.

Chapter Four

Unified TSHI Targeting Method[1]

4.1 Introduction

Application of TSHI methodologies helps set targets for maximum energy recovery via heat exchanger and utility network. In conventional TSHI, there are no network synthesis constraints (besides thermodynamics) for heat exchanger matches between process and utility streams. This problem was recently recognised by Sun et al. (2015). As the boiler feed water (non-isothermal utility) pinched against the TSP, they recognised that the heat may need to be transferred from multiple processes and that the network, although thermodynamically feasible, might be too complex in practice (Sun et al., 2015). Conventional TSHI allows process-utility heat exchanger matches in series from any process for the utility to reach its target temperature and then returned to the central utility system (Figure 3-2a). As a result, conventional TSHI targets for non-isothermal utilities can be overly optimistic. The HRL method, on the other hand predefines the network structure by having all HRL heat exchangers in parallel to one another (even within a process). Such a tight constraint for the network lowers the inter-plant HR target and often overlooks opportunities to increase energy efficiency (Atkins et al., 2012a). The gap in the knowledge is, therefore, the lack of an appropriate TSHI method that realistically targets both isothermal and non-isothermal utility consumption.

The aim of this chapter is to introduce an improved TSHI method that calculates more realistic and achievable targets for non-isothermal utilities. The new method is referred as the Unified Total Site Targeting Method (UTST). The non-isothermal utilities in this methodology include hot water system for low temperature processes (e.g. food and beverage processing) and intermediate temperature

[1] The majority of this Chapter formed the basis of a full journal article cited as (Tarighaleslami et al., 2017a) published in Energy:

Tarighaleslami, A.H., Walmsley, T.G., Atkins, M.J., Walmsley, M.R.W., Liew, P.Y., Neale, J.R., 2017, A Unified Total Site Heat Integration targeting method for isothermal and non-isothermal utilities. *Energy* 119, 10–25. doi:10.1016/j.energy.2016.12.071

processes (e.g. pulp and paper processing), as well as hot oil system in high temperature processes (e.g. oil refineries). The new method modified the Conventional TSHI Targeting methods, which normally produces different TS targets for cases when non-isothermal utilities are used in the TS system. Targeting results from the new unified method are compared to the conventional TSHI method using the three case studies that were introduced in Section 3.4. The effects of assumptions inherent in both methods that generate targets for TS integration are illustrated and discussed.

4.2 Methods

4.2.1 A New Unified Total Site Heat Integration Targeting Method

This section explains the procedure of the new Unified Total Site Targeting method. The procedure has three Stages: Data Specification, Process level, and Total Site level. Figure 4-1 illustrates the Unified Total Site Targeting method procedure using a flow diagram and Illustrative graphs.

4.2.1.1 Stage 1 – Data Specification

Step 1, Extract Stream Data: Following conventional methodologies, the parameters of process streams are defined using general process data sets (e.g. process flow sheets).

Step 2, Select ΔT_{min} Contribution (ΔT_{cont}): In this method, due to covering wide range of processes, a stream specific ΔT_{min} contribution is used. The minimum temperature difference between process streams in each process ($\Delta T_{cont,PS(i)}$) is $\Delta T_{cont,P1} + \Delta T_{cont,P2}$. The selection of stream specific ΔT_{cont} should consider the thermo-physical properties of the stream and the energy-capital trade-off through Supertargeting. For example, some process streams may be gases or viscous liquids which have poor heat transfer coefficient, or may be prone to fouling on heat exchanger surfaces. For such cases, the overall heat transfer coefficient of a heat exchanger will be low; therefore, the corresponding heat transfer area will be high. As a result, a relatively high ΔT_{cont} should be selected.

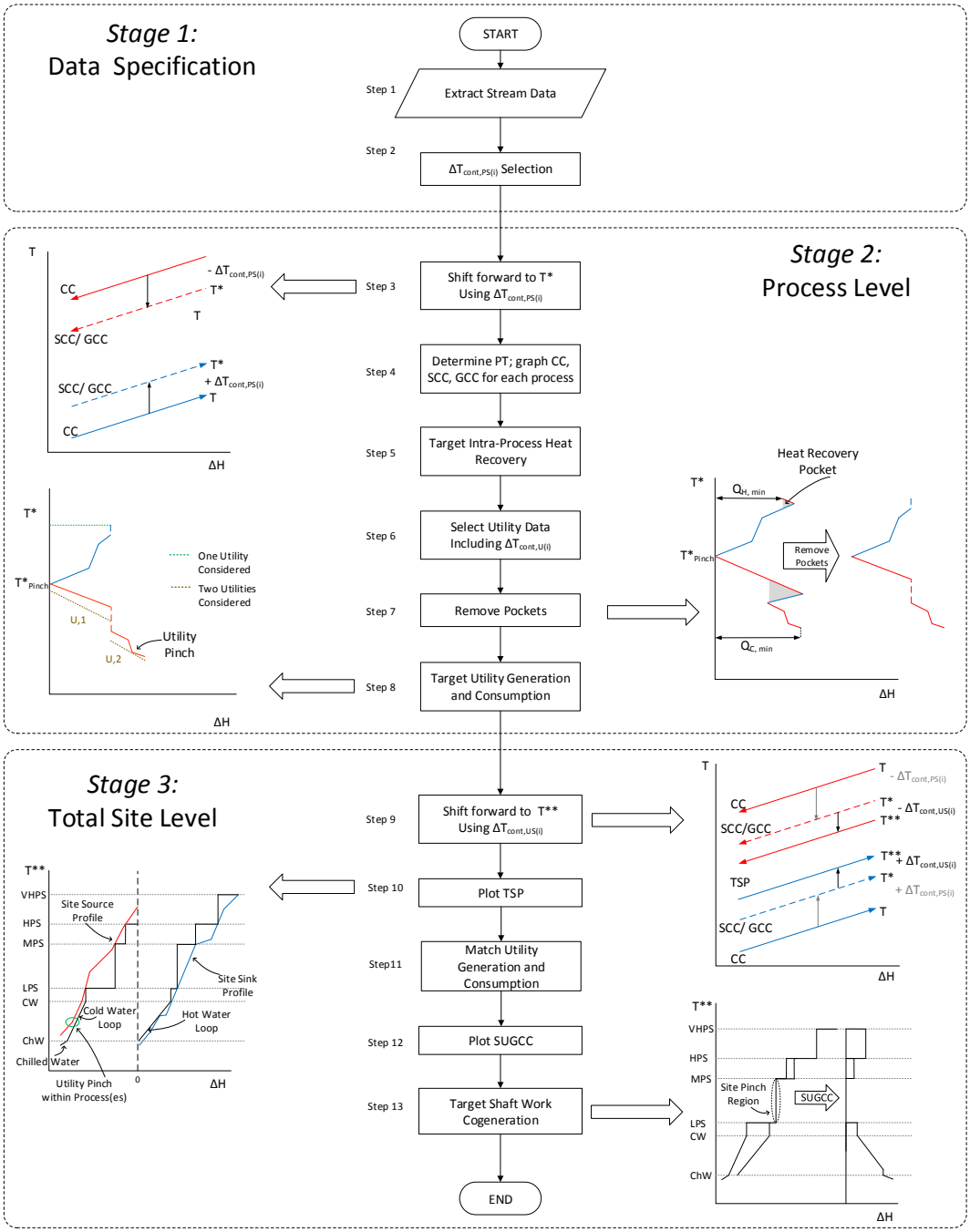

Figure 4-1: Unified Total Site Targeting (UTST) procedure.

4.2.1.2 Stage 2 – Process Level Targeting

Step 3, Shift stream temperatures forward to intermediate temperatures (T^*)

For each process, supply and target temperatures of hot (source) and cold (sink) streams are shifted using individual process stream ΔT_{cont} to the intermediate temperature scale, T^*, according to Equation 4-1,

$$T^* = \begin{cases} T - \Delta T_{cont,P(m)} & \in \text{ Sources} \\ T + \Delta T_{cont,P(n)} & \in \text{ Sinks} \end{cases} \quad (4\text{-}1)$$

Where $\Delta T_{cont,P(m)}$ and $\Delta T_{cont,P(n)}$ are minimum allowed temperature contribution for process individual hot and cold streams.

Step 4, Determine Problem Table (PT), Composite Curve (CC), and GCC for each process: Problem Table can be calculated to determine the Pinch Temperature, CC, SCC and GCC graphs for each individual process.

Step 5, Target intra-process heat recovery: HR targets for the selected ΔT_{cont} values from the CC are obtained for each process. Results include the overall minimum hot and cold utility targets for each process.

Step 6, Select utilities including temperatures and pressures: Selection of the utility temperatures/pressure levels affects inter-process HR targets at the TS level. After targeting TSHR, these temperatures may be re-selected (and optimised) to increase inter-process HR targets. In selection of utilities, the idea of soft and hard (fixed) utility target temperatures should be considered. In this step, the minimum temperature difference for each utility ($\Delta T_{cont,US(i)}$) is selected using a similar procedure explained in Step 2. The equivalent ΔT_{min} between process and utility streams is $\Delta T_{cont,P1} + \Delta T_{cont,U1}$.

Step 7, Remove pockets: Following the CTST method, pockets which represent opportunities for intra-process HR, are removed from GCC and heat source and heat sink segments are extracted from GCC for all processes. Therefore, only the net utility demands of the various processes are considered at the TS level.

Step 8, Target individual process utility generation and consumption: Targeting the utility generation and consumption in the intra-process targeting stage is an important feature of the new method in targeting non-isothermal utility use where the supply and target temperatures of the utility may be important TSHR constraints. This step is an important difference and improvement from the previous work of Liew et al. (2012).

Table 4-1 shows the general framework for the numerical analysis technique of the utility targeting method. The first column of the framework consists of the shifted temperature levels of the both process streams and utilities, arranged in descending order of temperature. The inclusion of shifted utility temperatures in the PT formulation is a small but important modification, which allows for the start

and end temperature of each utility to be contained in the PT temperature column. Following the conventional PT method columns 2 to 6 are determined. Column 6 represents the feasible process heat load cascade and columns 7 and 8 help determine the heat capacity flow rate corresponding to each utility (only two utilities shown).

The minimum heat capacity flow rate (CP) value in columns 7 and 8 is the required heat capacity flow rate of each utility, as indicated in the final entry of columns 7 and 8. It is noted that if the utility system contains more utilities then more columns can be added to Table 4-1. Columns for each utility are ordered from the lowest to highest quality utility (hottest cold utility to the coldest cold utility for below the Pinch and coldest hot utility to the hottest hot utility for above the Pinch). Where supply and target temperatures for two utilities overlap, the calculation in the respective utility CP columns (columns 7 and 8) will also overlap. Table 4-1 demonstrates the procedure for below the Pinch; however, following the same logic starting from process Pinch Temperature, the table can be calculated for above the Pinch.

Table 4-1: General framework for the algebraic technique of the targeting method. Example specific to using cold utilities below the Pinch.

1 Shifted Temperatures T^*_k	2 Interval	3 ΔT ΔT_k	4 Net CP $CP_{net,k}$	5 Interval ΔH ΔH_k	6 Feasible ΔH $\sum \Delta H_k$	7 CP for Utility j $CP_{(U,j)k}$	8 CP for Utility j+1 $CP_{(U,j)k+1}$
T^*_1	Pinch				$\sum \Delta H_1 = 0$		
	1	ΔT_1	$CP_{net,1}$	ΔH_1			
T^*_2					$\sum \Delta H_2$	$CP_{(U,1)2}$	
	2	ΔT_2	$CP_{net,2}$	ΔH_2			
T^*_3					$\sum \Delta H_3$	$CP_{(U,1)3}$	
	3	ΔT_3	$CP_{net,3}$	ΔH_3			
T^*_4					$\sum \Delta H_4$	$CP_{(U,1)4}$	$CP_{(U,1)4}$
	4	ΔT_4	$CP_{net,4}$	ΔH_4			
T^*_5					$\sum \Delta H_5$		$CP_{(U,2)5}$
.	.	.	.	.	.	.	.
.	.	.	.	.	.	.	.
.	.	.	.	.	.	.	.
T^*_{k-1}					$\sum \Delta H_{k-1}$		$CP_{(U,2)k-1}$
	k	ΔT_k	$CP_{net,k}$	ΔH_k			
T^*_k					$\sum \Delta H_k$		$CP_{(U,j)k}$
						$Min(CP_{(U,j)k})$	$Min(CP_{(U,j)k})$

To determine the heat capacity flow rate of each utility (i.e. columns 7 and 8), Equation 4-2 is applied to non-isothermal utilities. Equation 4-2 was derived graphically by finding the equation that determines the maximum CP of a utility based on the utilities target temperature and each shifted temperature interval, for which the utility may be applied. The minimum of these calculated CP values is the maximum feasible utility CP, which does not violate the Pinch constraint.

$$CP_{(U,j)k} = \frac{\min\left\{\sum \Delta H_1, \sum \Delta H_2, \ldots, \sum \Delta H_k\right\} - \sum\left(Q_{U,1}, Q_{U,2}, \ldots, Q_{U,j-1}\right)}{\left|T^*_{t(U,j)} - T^*_k\right|} \qquad (4\text{-}2)$$

Equation 4-2 only applies to the following conditions:

$$\sum \Delta H_k > \sum\left(Q_{U,1}, Q_{U,2}, \ldots, Q_{U,j-1}\right)$$
$$T^*_{s(U,j)} \leq T^*_k < T^*_{t(U,j)} \quad \in \text{ Cold Utility} \qquad (4\text{-}3)$$
$$T^*_{s(U,j)} \geq T^*_k > T^*_{t(U,j)} \quad \in \text{ Hot Utility}$$

Where Q, ΔH and CP are respectively the heat load of each utility, enthalpy change of each temperature interval and heat capacity flow rate, and T^*_t and T^*_s represent shifted utility target temperature and shifted supply temperature respectively. Subscripts *U, j* and *k* represent a number of utility and interval number.

Figure 4-2 illustrates how Equation 4-2 can be derived from a GCC of a single process. Three non-isothermal utilities U,1, U,2, and U,3 are used to supply cooling to below the pinch on the GCC that contains two HR pockets. The supply temperature of the coldest cold utility and target temperature of the hottest cold utility are constraints. In addition GCC kinks are extra constraints required to calculate the CP for each utility. ΔH represents the total amount of external cooling enthalpy required. The CP of the individual utility is calculated by dividing the enthalpy required by the change is temperature (i.e. difference between the utility supply and target temperatures).

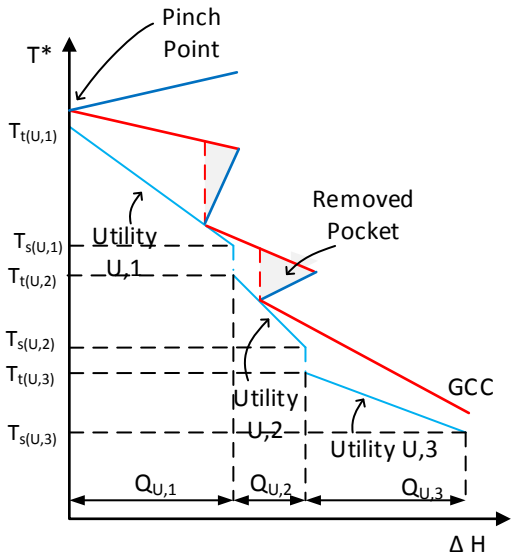

Figure 4-2: Graphical approach for equation 4-2.

Utility target temperatures can be divided into two categories, fixed (hard) temperatures and soft temperatures. Soft utility target temperatures, in this context, refer to target temperatures that are non-essential to be achieved. Soft temperatures may be changed by varying utility heat capacity flow rates. Hard utility temperatures refer to temperature constraints that should be met. Where a non-isothermal utility will the both consumed and generated in TSHI, the utility supply and target temperatures become important constraints. The optimal temperature selection for each non-isothermal utility will be presented in future work.

4.2.1.3 Stage 3 – Total Site Level Targeting

Step 9, Shift intermediate temperatures (T^*) forward to the utility temperature scale (T^{**}): For each individual stream in each individual process, shift the extracted GCC segments to the utility temperature scale (T^{**}) using the corresponding utility $\Delta T_{cont,}$ Equation 4-4.

$$T^{**} = \begin{cases} T^* - \Delta T_{cont,U(m)} & \in \text{ Sources} \\ T^* + \Delta T_{cont,U(n)} & \in \text{ Sinks} \end{cases} \qquad (4\text{-}4)$$

Where $\Delta T_{cont,U(m)}$ and $\Delta T_{cont,U(n)}$ are minimum allowed temperature contribution for specific heating and cooling utilities.

Step 10, Construct Total Site Profile (TSP): Following the conventional method, apply the TS-PT method to composite extracted heat source segments (from Step 9) into a Site Source Profile and heat sink segments into a Site Sink Profile.

Although the new method does not use the TSP to target utility, the TSP plot with process level utility targets remains a useful diagram because it can provide additional information to the designer about the problem. Where a utility does not pinch against the TSP, it is an indication that one or more of the process GCCs constrain the use of that utility. If this such a gap occur, the utility targets for the new and conventional TSHI will be different.

Step 11, Match Utility Generation and Consumption: Utility targets from each process GCC are summed to determine gross and net TS utility targets. The total utility targets may be plotted on the TSP graph representing the Site Utility Composite Curves.

Step 12, Construct Site Utility Grand Composite Curve: Following the conventional methods, Site Utility Grand Composite Curve (SUGCC) can be constructed to obtain the TS Pinch Temperature region, the excess and deficit of each utility, and targets for power generation and shaft work potential from the TS utility system.

Step 13, Target Shaft Work Cogeneration: Using the net utility requirements on the SUGCC a target for shaft work generation may be calculated using a turbine model or thermodynamically based on an isentropic expansion efficiency.

4.2.2 A Comparison Between Conventional and Unified Total Site Heat Integration Targeting Methods

Figure 4-3 presents the targeting procedures of three conventional TSHI targeting methods as well as the new unified TSHI targeting method. The considered conventional methods are: (1) global method (Klemeš et al., 1997), (2) process specific method (Varbanov et al., 2012), and (3) stream specific method (Fodor et al., 2012).

Klemeš et al. (1997) followed previous the TSHI method of Dhole and Linnhoff (1993) by basing targets on a global minimum temperature difference, $\Delta T_{min(global)}$ (Figure 4-3a.1). This method, as with many others, focused on exploiting the steam

utility system to recover heat and produce power for large multi-plant high temperature processing site (e.g. oil refineries). Since steam is normally considered isothermal in its generation and consumption as a high temperature utility, the design of a TS network, which achieves TSHI targets, is fairly simple.

Later, Varbanov et al. (2012) presented a process-specific minimum temperature difference technique, as shown in Figure 4-3a.2. This method employed changes in TSP construction algorithms by allowing separate ΔT_{min} specification for process-to-process heat exchange and also process-to-utility heat exchange. The method added a degree of freedom to assign different ΔT_{min} specifications for each process and utility, which resulted in improved targeting. A third sub-set of conventional TSHI methods is presented by Fodor et al. (2012). This method applies stream and utility specific minimum temperature contribution (ΔT_{cont}), which is presented as Figure 4-3a.3. The targeting procedure is similar to previous methods, i.e. global and process specific methods; however, there are significant changes in HR targets and cogeneration potential. The stream and utility specific ΔT_{cont} method provides an even greater number of degrees of freedom to the designer, which can be used to improve the TSHI targets if such detailed data is available. The new method follows from Fodor et al. (2012) in using stream and utility specific ΔT_{cont} as the basis of the procedure.

A critical difference between the new method (Figure 4-3b) and the conventional methods is the level at which utility targeting is performed. The conventional methods (Figure 4-3a) use the TSP, i.e. TS level, to determine the quantity needed of each specified utility. Whereas the new method uses individual process GCCs, i.e. process level, to target utility use, before transferring these targets to the TS level and looking for heat integration within the utility system (Figure 4-1). This subtle change allows the engineer to know more about how each utility interacts with individual processes. In the new method, the utility system is constrained to supply utilities to and return utilities from each process at specified temperatures. With respect to non-isothermal utilities, this means sequential utility-process matches are allowed within a process to meet fixed utility supply and target temperatures. Sequential utility-process matches are disallowed between processes, as is inherently acceptable within the conventional TSHI method. This

is an important advantage for application of the new method to non-continuous processes or for clusters which contain one or more seasonal processes.

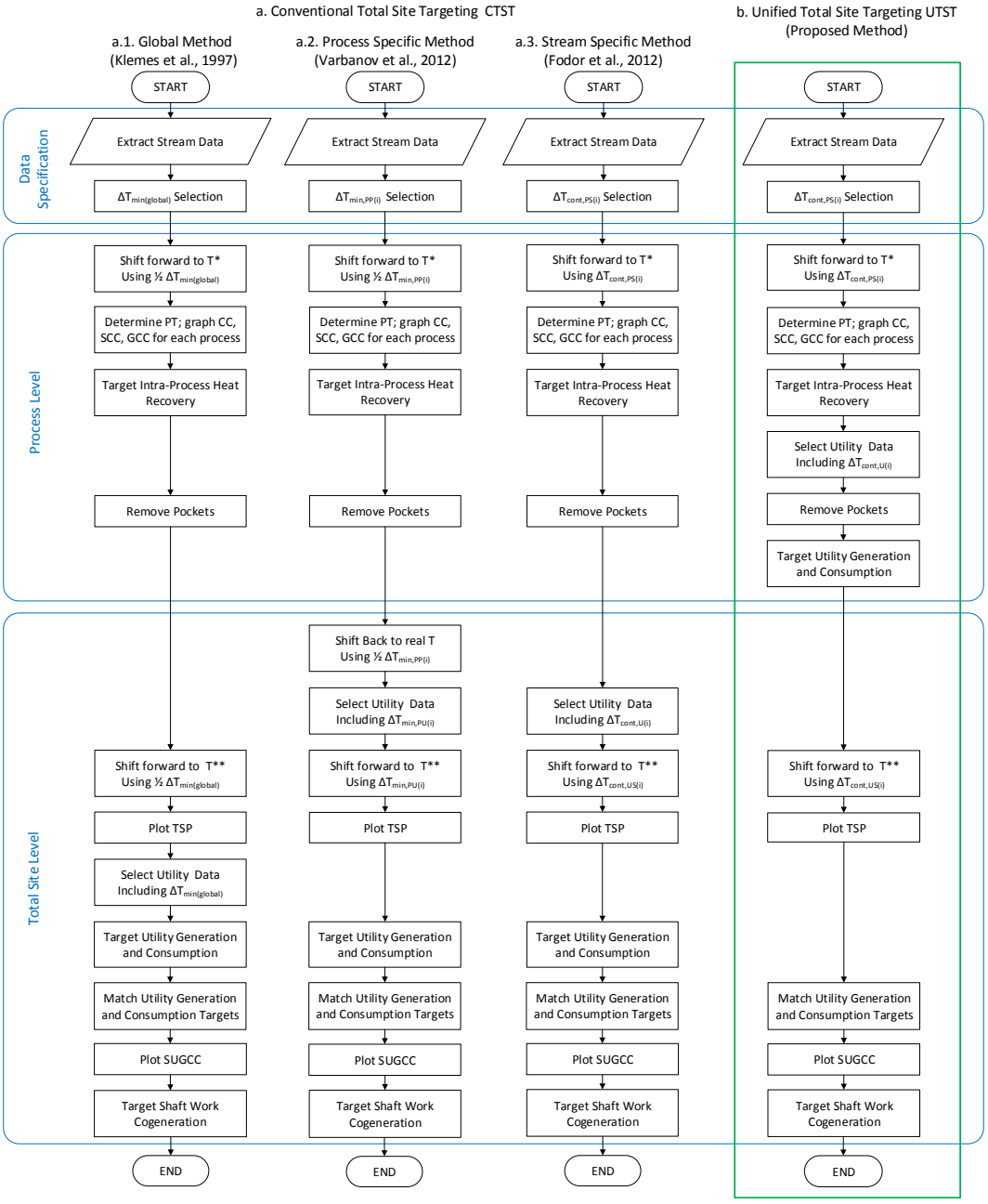

Figure 4-3: Comparison between various Conventional and Unified TSHI targeting methods.

4.3 Application of TSHI Methods to Industrial Case Studies

This section examines three case studies to demonstrate the merits of the new TS targeting method for both high and low temperature processes, which require isothermal and non-isothermal utilities, compared to the conventional TS method, CTST. These case studies contain a variety of continuous and non-continuous processes. The CTST and the UTST methods have been implemented into an

Excel™ spreadsheet software tool called Unified Total Site Integration (UTSI) software for application to the three case studies.

4.3.1 Case Study I: Södra Cell Värö Kraft Pulp Mill

This case study addresses the merits of UTST method for targeting a non-continuous Kraft Mill that spans a wide temperature range where two utility hot water systems are useful for TSHR. The case study is based on the Södra Cell Värö Kraft Pulp Mill plant as explained in Section 3.4.1. Minimum temperature difference and individual minimum contribution temperatures are from the same as used by Bood and Nilsson (2013). Several utility streams including HPS, LPS, HTHW and LTHW systems are assumed in this study to cover the required temperature ranges in TSHI as shown in Table 4-2. Where T_{Hot} is hot temperature and T_{Cold} is cold temperature, and P_R is pressure range of each utility. Power generation has been considered in this case study. The Very High Pressure Steam (VHPS) which enters to the turbine is taken at 450 °C and 90 bar_g. Shaft work targets are based on the UGCC in conjunction with the Medina-Flores and Picón-Núñez turbine model (2010). GCCs for each individual process within TS are presented in Appendix A.

Table 4-2: Required utilities for Kraft Pulp Mill case study.

Utility Name	Utility Type	T_{Cold} (°C)	T_{Hot} (°C)	P_R (bar_g)
High Pressure Steam (HPS)	Hot	209.9	210.0	15
Low Pressure Steam (LPS)	Hot	159.9	160.0	9
High Temperature Hot Water (HTHW)	Both	60.0	85.0	
Low Temperature Hot Water (LTHW)	Both	25.0	45.0	
Cooling Water (CW)	Cold	25.0	*	

*Soft utility temperature

TS targets are presented in Figure 4-4 for both CTST and UTST methods. Dashed lines present the CTST method while solid lines present the UTST method. As illustrated in Figure 4-4 both methods require the same amount of HPS of 27.7 MW. The LPS demand of UTST is only 0.16 MW higher than CTST method.

Both methods target the same amount of HTHW utility consumption. However, the HTHW generation target reduces from 39.4 MW for CTST to 26.7 MW for UTST. The LTHW utility consumption target for CTST method is only 0.13 MW higher than UTST method targets. However, the LTHW generation target is 74.2 MW for the

UTST versus 76.5 MW for the CTST method. The split between HTHW and LTHW in the UTST shows the method tends to require higher quality utilities. The UTST method has 3.0 MW lower shaft Work generation compared to UTST method which rejects 15 MW heat to CW system. TSHR in the UTST method is 0.2 MW lower than the CTST due to the pinched consumption of HTHW and LTHW (Figure 4-5). As demonstrated, the UTST method is able to effectively target dual non-isothermal (hot water) utility systems. Table 4-3 provides a detailed comparison of gross and net utility consumption and generation targets for both CTST and UTST methods for this case study. Gross targets in CTST method refers to targets shown on TSP while net targets represent the actual targets from SUGCC. As such, gross targets in UTST method refers to the summation of targets achieved in each process individually, while net targets are what the utility system must deliver from boilers and thermal generation process. The optimal selection of the number and temperatures of utilities for the UTST method will be presented in Chapter 5.

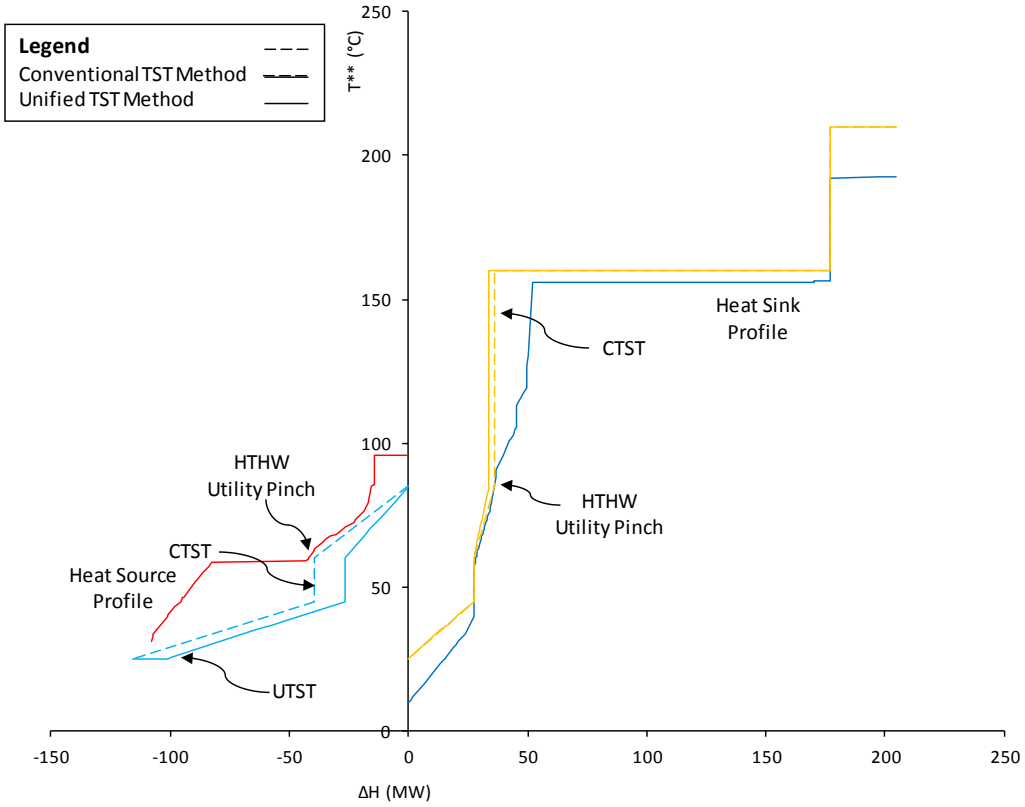

Figure 4-4: Total Site Targets for both CTST and UTST methods in Kraft Pulp Mill.

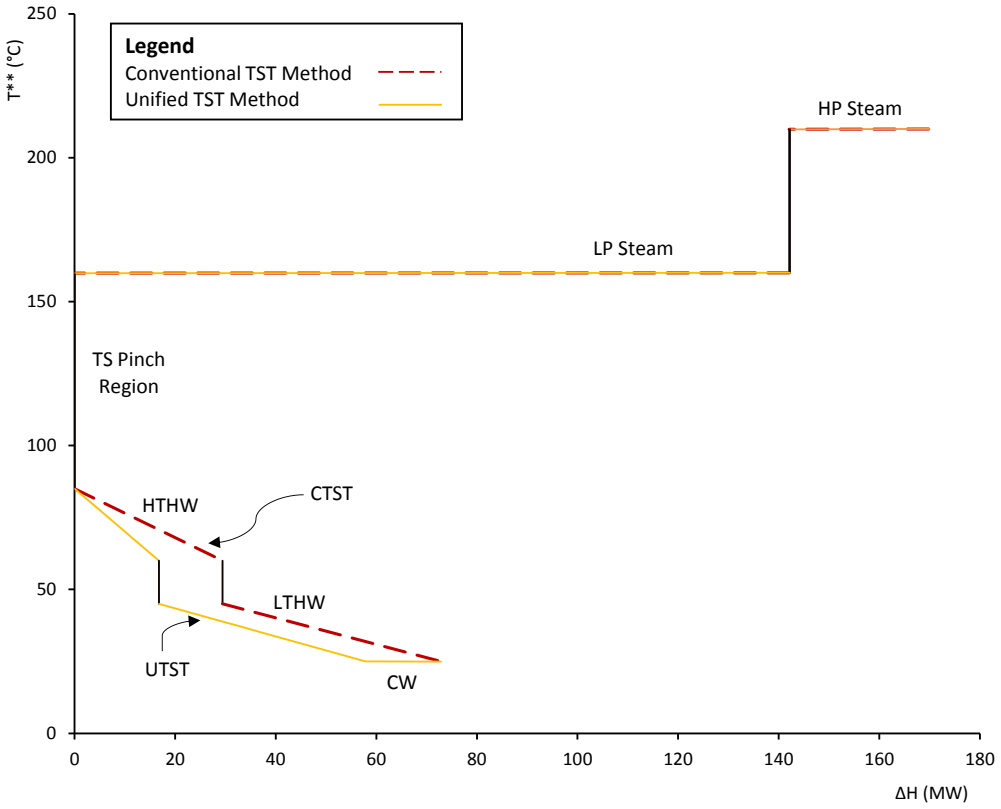

Figure 4-5: SUGCC for both CTST and UTST methods in Kraft Pulp Mill.

Table 4-3: Process level SWG, HR, and utility targets, and a comparison of SWG, HR, and utility targets for two TSHI methods for the Kraft Pulp Mill.

Process Level and Total Site Targets											
Process / Targeting Method	ΣQ_{Hot}	ΣQ_{Cold}	ΣQ_{HR}	SWG	Hot Utility Consumption[1]				Cold Utility Consumption[2]		
					HPS	LPS	HTHW	LTHW	HTHW	LTHW	CW
	MW	MW	MW	MW	MW	MW	MW	MW	MW	MW	MW
Bleaching	32.5	0.0	14.1	9.8	4.6	9.8	0.0	18.2	0.0	0.0	0.0
Causticizing	0.9	7.7	0.9	0.0	0.0	0.9	0.0	0.0	5.3	2.4	0.0
Digestion	23.4	21.3	4.3	2.7	20.2	3.2	0.0	0.0	20.7	0.6	0.0
District Heating	8.0	18.4	0.8	1.3	0.0	8.0	0.0	0.0	0.0	18.4	0.0
Evaporator	51.8	39.4	0.0	11.3	0.0	51.8	0.0	0.0	0.0	39.4	0.0
Miscellaneous 1	0.0	3.8	0.0	0.0	0.0	0.0	0.0	0.0	0.0	3.8	0.0
Miscellaneous 2	0.0	14.4	0.0	0.0	0.0	0.0	0.0	0.0	0.0	0.0	14.4
Miscellaneous 3	7.3	0.0	0.0	1.7	0.0	1.2	3.7	2.4	0.0	0.0	0.0
Miscellaneous 4	0.0	0.7	0.0	0.0	0.0	0.0	0.0	0.0	0.7	0.0	0.0
Miscellaneous 5	1.1	0.0	0.0	0.0	0.0	1.1	0.0	0.0	0.0	0.0	0.0
Miscellaneous 6	0.0	0.6	0.0	0.0	0.0	0.0	0.0	0.0	0.0	0.0	0.6
Miscellaneous 7	3.4	0.0	0.0	0.8	0.0	0.0	0.0	3.4	0.0	0.0	0.0
Paper Room	45.2	0.0	16.8	10.8	0.0	29.9	6.2	9.1	0.0	0.0	0.0
Recovery Boiler	35.7	0.0	9.9	7.5	3.0	32.6	0.1	0.0	0.0	0.0	0.0
Stripper	3.8	0.0	11.8	0.3	0.0	3.8	0.0	0.0	0.0	0.0	0.0
Wash	0.0	9.7	0.0	0.0	0.0	0.0	0.0	0.0	0.0	9.7	0.0
CTST (Gross)	213.0	115.9	58.6	49.3	27.7	142.1	10.0	33.2	39.4	76.5	0.0
CTST (Net)	169.8	72.7	101.8	37.0	27.7	142.1	0.0	0.0	29.4	43.3	0.0
UTST (Gross)	213.1	116.0	58.6	46.3	27.7	142.2	10.0	33.1	26.7	74.2	15.0
UTST (Net)	170.0	72.9	101.6	37.0	27.7	142.2	0.0	0.0	16.8	41.1	15.0

[1]Cold utility generation

[2]Hot utility generation

4.3.2 Case Study II: New Zealand Dairy Processing Factory

The second case study illustrates the advantages of the UTST method for targeting of primarily low temperature processes. The case study is based on a large New Zealand dairy factory as explained in Section 3.4.2. Five different utilities are used in the case study to cover the required temperature ranges, as presented in Table 4-4. GCCs for each individual process within TS are presented in Appendix A.

Table 4-4: Required utilities for Dairy Factory case study.

Utility Name	Utility Type	T_{Cold}(°C)	T_{Hot} (°C)	P_R (bar_g)
Low Pressure Steam (LPS)	Hot	179.9	180.0	10
High Temperature Hot Water (HTHW)	Hot	64.0*	84.0	
Low Temperature Hot Water (LTHW)	Both	25.0	45.0	
Cooling Water (CW)	Cold	24.0	25.0*	
Chilled Water (ChW)	Cold	0.0	2.0*	

*Soft utility temperature

Figure 4-6 presents the TSPs and targets for both the CTST method, in dashed lines, and UTST method, in solid lines, for the dairy case study. A ΔT_{cont} of 2.5 °C for each stream, which is equivalent to $\Delta T_{min(global)}$ = 5 °C, was assumed for the illustration. As can be seen, LPS demand increases from 1.1 MW in the CTST method to 2.3 MW in the UTST method. HTHW demand slightly decreases from 13.7 MW in the CTST method to 13.6 MW in UTST method. For this case study, Utility Pinches on the TSP that occur in the Conventional TS method, are not present in the UTST method. For the UTST method, Utility Pinches occur on GCCs at the Process Level in the utility targeting step. Utility Pinches are necessary in TSHI to achieve maximum HR. LTHW consumption significantly decreases from 3.3 MW for CTST to 2.0 MW for UTST. On the other hand, LTHW generation decreases from 7.5 MW for CTST to 4.7 MW for UTST. CW targets substantially decreases from 2.9 MW for CTST to 0.2 MW. ChW consumption targets, 7.5 MW, are the same in both methods.

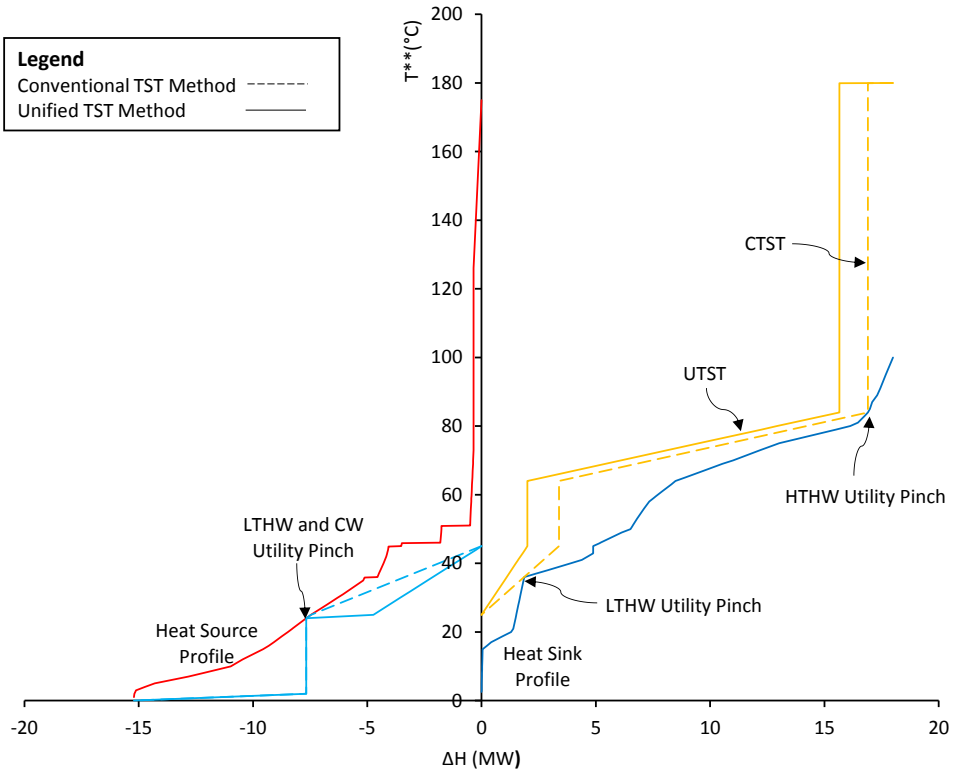

Figure 4-6: Total Site Targets for both CTST and UTST methods in Dairy Factory.

Figure 4-7 plots the Site Utility Grand Composite Curves for both the CTST method, in dashed lines, and the UTST method, in solid lines.

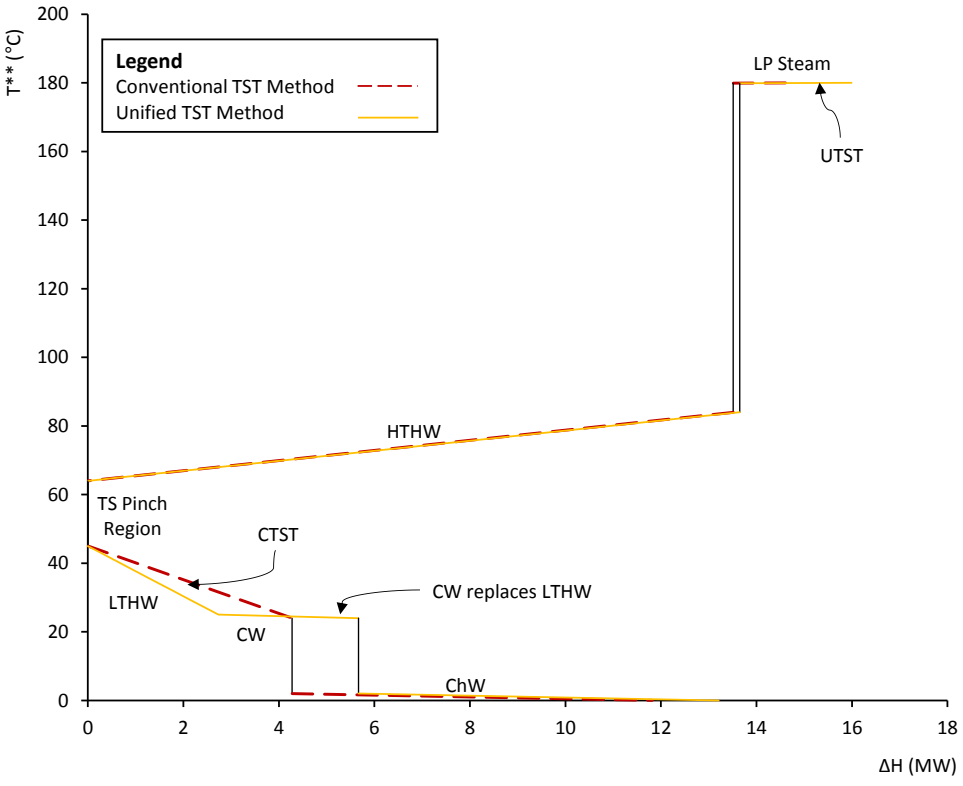

Figure 4-7: SUGCC for both CTST and UTST methods in Dairy Factory.

For this case study, both methods result in the same Site Pinch Region. However, quantity of utilities are different, which impacts on the HR and power generation opportunities related to each method. In Figure 4-7, a difference of 1.3 MW in HR between the methods is seen, where CTST consumes total 14.6 MW of hot utility and 11.9 MW of cold utility versus 16.0 MW of hot utility and 13.3 MW of cold utility in the UTST method. This difference is due to the consumption and generation targets for the LTHW. The more conservative targets for the LTHW system in the UTST method result from the increased constraints around how the non-isothermal utility interacts with the various processes. This constraints cause Utility Pinches to occur within individual processes, rather than on the TSP. Table 4-5 presents a comprehensive comparison of gross and net utility consumption and generation targets for both CTST and UTST methods for the dairy processing factory case study.

Table 4-5: Process level HR and utility targets, and a comparison of HR and utility targets for two TSHI methods for the Dairy Factory.

Process Level and Total Site Targets									
Process / Targeting Method	ΣQ_{Hot}	ΣQ_{Cold}	ΣQ_{HR}	Hot Utility Consumption[1]			Cold Utility Consumption[2]		
				LPS	HTHW	LTHW	LTHW	CW	ChW
	MW	MW	MW	MW	MW	MW	MW	MW	MW
AMF	0.2	0.0	0.0	0.0	0.1	0.1	0.0	0.0	0.0
Butter	0.0	1.1	0.4	0.0	0.0	0.0	0.7	0.0	0.4
Casein	0.2	1.1	0.0	0.2	0.0	0.0	0.0	0.6	0.5
Casein whey	2.9	0.0	0.0	0.0	2.9	0.0	0.0	0.0	0.0
Cheese	4.0	0.1	0.4	0.0	4.0	0.0	0.0	0.0	0.1
Cheese & Whey UF	3.3	0.0	0.0	0.0	2.7	0.6	0.0	0.0	0.0
Cheese whey	0.0	4.7	0.0	0.0	0.0	0.0	0.0	1.7	3.0
Evap/dryer	0.1	0.6	0.0	0.0	0.1	0.0	0.0	0.6	0.0
Milk powder & lactose	0.2	0.4	0.0	0.2	0.0	0.0	0.1	0.0	0.3
Milk sep & casein	2.7	2.1	0.0	0.0	2.4	0.3	0.0	0.0	2.1
Milk UF	0.5	0.8	0.3	0.0	0.0	0.5	0.0	0.0	0.8
Milk UF & CIP	0.0	0.2	0.0	0.0	0.0	0.0	0.0	0.0	0.2
P1 MPC	0.2	0.7	0.0	0.0	0.2	0.0	0.6	0.0	0.0
P1 permeate	0.5	2.2	0.2	0.5	0.0	0.0	2.0	0.0	0.2
P2	0.0	1.3	0.0	0.0	0.0	0.0	1.3	0.0	0.0
P3	0.1	0.0	0.0	0.1	0.0	0.0	0.0	0.0	0.0
P4	1.0	0.0	0.0	0.5	0.6	0.0	0.0	0.0	0.0
P5	1.1	0.0	0.0	0.8	0.4	0.0	0.0	0.0	0.0
RO/Lactose evaps	0.8	0.0	1.6	0.0	0.4	0.4	0.0	0.0	0.0
CTST (Gross)	17.9	15.2	2.9	1.1	13.6	3.3	7.5	0.2	7.5
CTST (Net)	14.7	11.9	6.2	1.1	13.6	0.0	4.2	0.2	7.5
UTST (Gross)	17.9	15.2	2.9	2.3	13.7	2.0	4.7	2.9	7.5
UTST (Net)	16.0	13.3	4.9	2.3	13.7	0.0	2.8	2.9	7.5

[1]Cold utility generation
[2]Hot utility generation

4.3.3 Case Study III: Petrochemical Complex

The third case study is a Petrochemical Complex serviced by a common utility system. Petrochemical Complexes operate continuously with generally higher processing temperatures than Kraft mills and dairy factories and therefore require high pressure steam and very little hot water. This case study addresses the application of the UTST method to higher temperature processes. The case study has been explained in detail in Section 3.4.3. Eight different utilities are used to cover the required temperature ranges as shown in Table 4-6. GCCs for each individual process within TS are presented in Appendix A.

Table 4-6: Required utilities for Petrochemical Complex case study.

Utility Name	Utility Type	T_{Cold} (°C)	T_{Hot} (°C)	P_R (bar_g)
Hot Oil Loop (HOL1)	Hot	365.0*	390.0	
Very High Pressure Steam (VHPS)	Hot	319.9	320	65
High Pressure Steam (HPS)	Hot	249.9	250.0	15
Medium Pressure Steam (MPS)	Hot	189.9	190.0	9
Low Pressure Steam (LPS)	Hot	139.9	140.0	5
Tempered Water (TW)	Cold	60.0	90.0*	
Cooling Water (CW)	Cold	15.0	30.0*	
Chilled Water (ChW)	Cold	8.0	13.0*	

*Soft utility temperature

In both CTST and UTST procedures, a ΔT_{cont} of 10 °C for each stream has been chosen, which is recommended for Petrochemical, Oil and Gas Refineries (Kemp, 2007). The case study has been analysed using both CTST and UTST methods. Figure 4-8 presents the TSP and the utility targets for the UTST method, in solid lines, and for the CTST method, in dashed lines. The UTST method gives very similar utility targets as the CTST method. However, as it can be seen in Figure 4-8 and Figure 4-9, the UTST method presents different non-isothermal utility targets for the TW and CW, which are more likely achievable. The slight utility change in TW and CW of 0.83 MW and 0.8 MW can be observed respectively, while utility targets for HOL, VHPS, HPS, MPS, LPS and ChW are unchanged.

A comprehensive comparison of gross and net utility consumption and generation targets for both CTST and UTST methods for Petrochemical Complex case study is presented in Table 4-7.

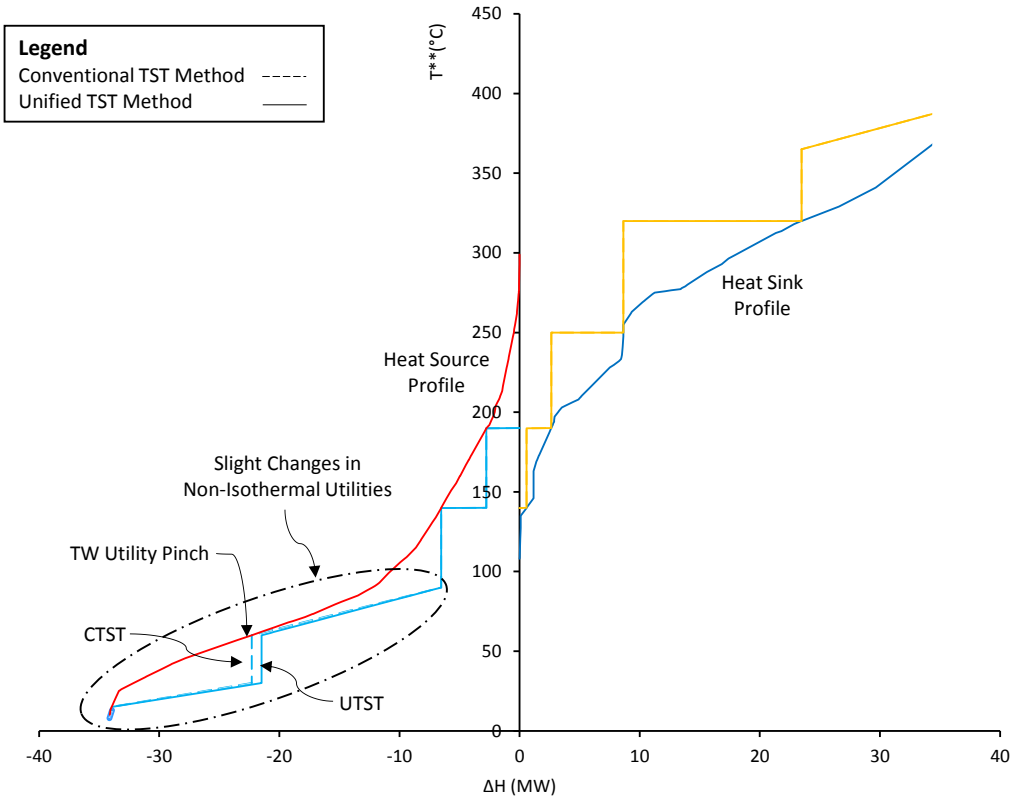

Figure 4-8: Total Site Targets for both CTST and UTST methods in Petrochemical Complex.

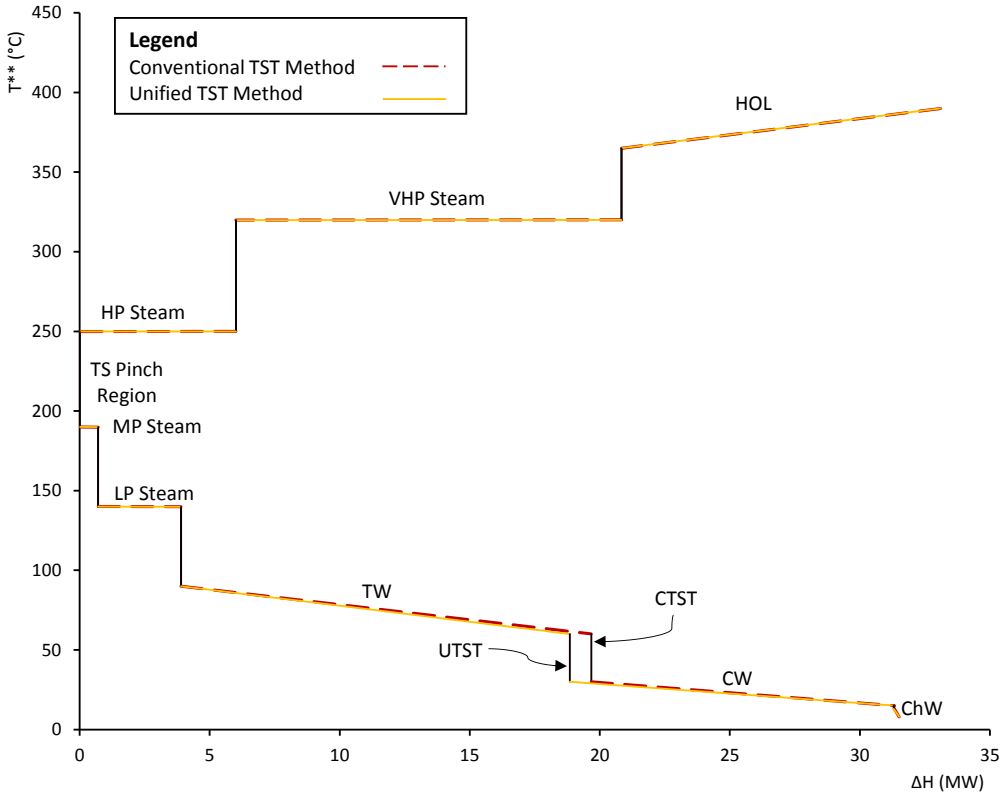

Figure 4-9: SUGCC for both CTST and UTST methods in Petrochemical Complex.

Table 4-7: Process level HR and utility targets, and a comparison of HR and utility targets for two TSHI methods for the Petrochemical Complex.

Process Level and Total Site Targets													
Process / Targeting Method	ΣQ_{Hot}	ΣQ_{Cold}	ΣQ_{HR}	Hot Utility Consumption[1]					Cold Utility Consumption[2]				
				HOL1	VHPS	HPS	MPS	LPS	MPS	LPS	TW	CW	ChW
	MW	MW	MW	MW	MW	MW	MW	MW	MW	MW	MW	MW	MW
Unit A	3.3	0.0	0.0	0.0	0.0	3.3	0.0	0.0	0.0	0.0	0.0	0.0	0.0
Unit B	3.0	1.7	17.7	0.8	2.2	0.0	0.0	0.0	0.3	0.0	0.0	1.4	0.0
Unit C	20.5	11.8	8.8	9.7	5.9	2.3	2.1	0.5	0.0	0.0	6.5	5.2	0.1
Unit D	0.2	3.2	1.9	0.0	0.0	0.2	0.0	0.0	0.4	1.5	1.4	0.0	0.0
Unit E	4.4	4.1	0.0	0.0	4.4	0.0	0.0	0.0	0.0	0.0	1.7	2.3	0.1
Unit F	2.3	7.0	1.6	0.0	2.3	0.0	0.0	0.0	1.3	0.4	2.5	2.8	0.0
Unit G	1.8	6.2	1.4	1.7	0.1	0.0	0.0	0.0	0.8	2.0	2.8	0.7	0.0
Unit H	0.3	0.1	0.9	0.0	0.0	0.2	0.0	0.1	0.0	0.0	0.0	0.1	0.0
CTST (Gross)	35.7	34.1	32.4	12.3	14.8	6.0	2.1	0.6	2.8	3.8	15.8	11.7	0.2
CTST (Net)	33.1	31.5	35.0	12.3	14.8	6.0	0.0	0.0	0.7	3.2	15.8	11.7	0.2
UTST (Gross)	35.7	34.1	32.4	12.3	14.8	6.0	2.1	0.6	2.8	3.8	14.9	12.5	0.2
UTST (Net)	33.1	31.5	35.0	12.3	14.8	6.0	0.0	0.0	0.7	3.2	14.9	12.5	0.2

[1]Cold utility generation
[2]Hot utility generation

In high temperature processes such as oil and gas refineries, petrochemical and metal processing plants using hot oil loops is common for higher temperatures where it is not possible to use excessively high steam pressures. However, the UTST, due to its advantages in targeting non-isothermal utilities with more realistic targets, gives the opportunity to consider hot oil loops as a utility for medium temperature ranges (100 – 300 °C), where steam is normally used. Therefore, an alternate utility design can be investigated for the current case study to include a second hot oil loop (see Figure 4-8). The new hot oil loop (HOL2) has a supply temperature of 210 °C and a target temperature of 160°C. It replaces the MPS and LPS to the new hot oil loop. Figure 4-10 illustrates the TS targets for the case study applying CTST method without HOL2, in dashed lines, versus alternate design with the new hot oil loop applying UTST method in solid lines. GCCs for each individual process within TS are presented in Appendix A.

The application of the UTST method with the alternate set of utility offers slightly more HR opportunities compared to the CTST method with the original utilities. By analysing both Figure 4-10 and Figure 4-11, UTST increases HR by 1.3 MW, which is 3.7 % increase in inter-process HR, due to the addition of HOL2. For UTST with the alternate utilities, TW and CW increase by 1.1 and 0.6 MW respectively compared to the original case applying the CTST method.

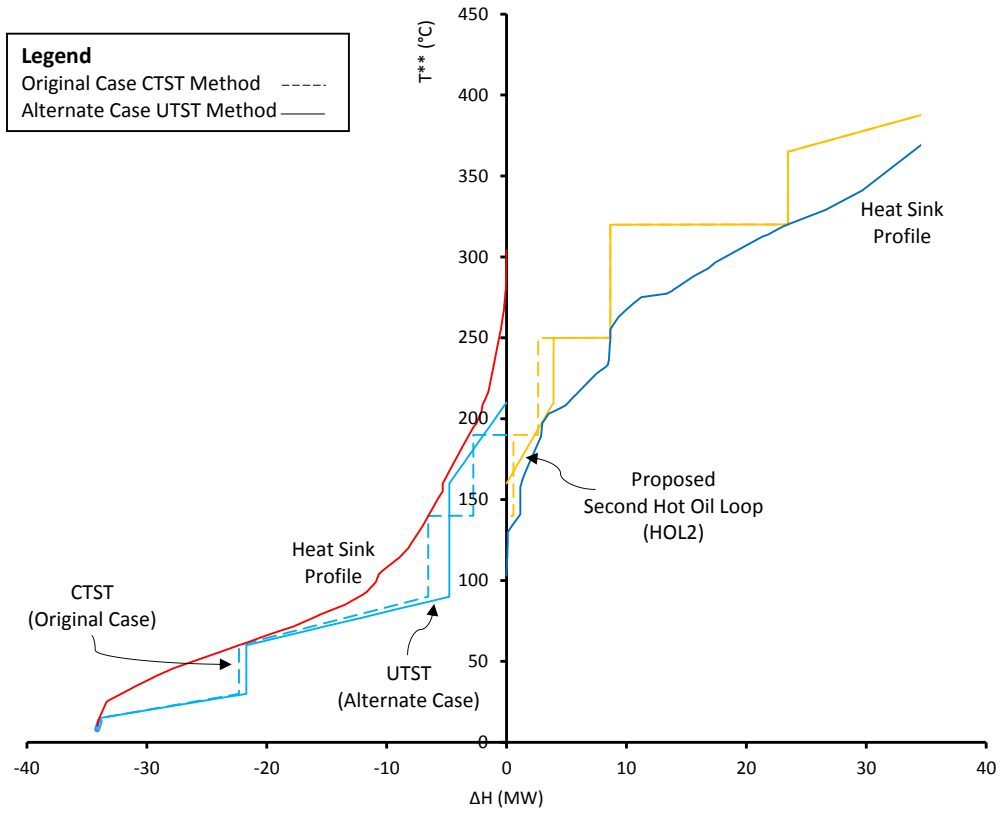

Figure 4-10: Total Site Targets for Petrochemical Complex applying CTST method and alternate case applying UTST method.

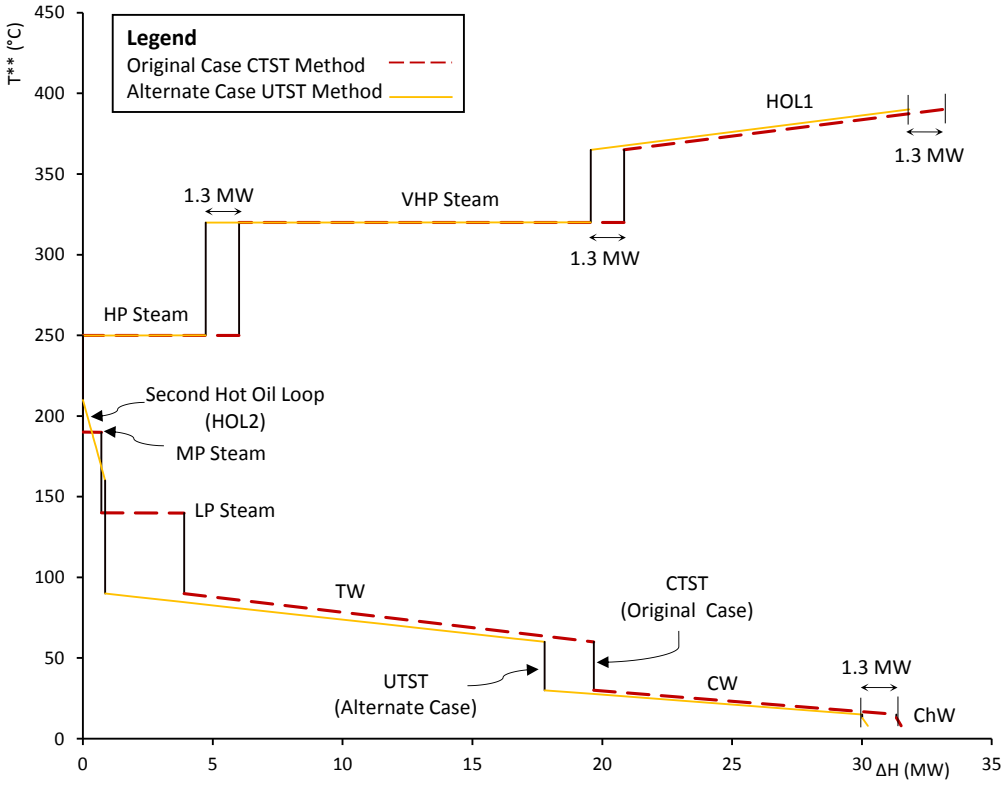

Figure 4-11: SUGCC for Petrochemical Complex applying CTST method and retrofit case applying UTST method.

The advantage of the alternate case is eliminating two utility lines using a non-isothermal utility, which can be effectively targeted using the UTST method. While in this case study high increase in HR is not illustrated, the possibility of substantial increases in HR for other case studies is likely. Detailed information for gross and net utility consumption and generation targets for both TS methods are given in Table 4-8 for alternative utility levels for Petrochemical Complex.

Table 4-8: A comparison of utility targets for two TSHI methods for the Petrochemical Complex with a hot oil loop.

Process Level and Total Site Targets											
Process / Targeting Method	ΣQ_{Hot}	ΣQ_{Cold}	ΣQ_{HR}	Hot Utility Consumption[1]				Cold Utility Consumption[2]			
				HOL1	VHPS	HPS	HOL2	HOL2	TW	CW	ChW
	MW	MW	MW	MW	MW	MW	MW	MW	MW	MW	MW
Unit A	3.3	0.0	0.0	0.0	0.0	3.3	0.0	0.0	0.0	0.0	0.0
Unit B	3.0	1.7	17.7	0.8	2.2	0.0	0.0	0.3	0.0	1.4	0.0
Unit C	20.5	11.8	8.8	9.7	5.9	1.4	3.4	0.0	6.5	5.2	0.1
Unit D	0.2	3.2	1.9	0.0	0.0	0.2	0.0	0.0	3.2	0.0	0.0
Unit E	4.4	4.1	0.0	0.0	4.4	0.0	0.0	0.0	1.7	2.3	0.1
Unit F	2.3	7.0	1.6	0.0	2.3	0.0	0.0	1.3	3.1	2.6	0.0
Unit G	1.8	6.2	1.4	1.7	0.1	0.0	0.0	2.0	3.6	0.7	0.0
Unit H	0.3	0.1	0.9	0.0	0.0	0.2	0.1	0.0	0.0	0.1	0.0
CTST (Gross)	35.7	34.1	32.4	12.3	14.8	4.7	3.9	5.0	17.4	11.7	0.2
CTST (Net)	31.8	30.2	36.3	12.3	14.8	4.7	0.0	1.0	17.4	11.7	0.2
UTST (Gross)	35.7	34.1	32.4	12.3	14.8	5.2	3.5	3.5	18.2	12.2	0.2
UTST (Net)	32.3	30.7	35.8	12.3	14.8	5.2	0.0	0.0	18.2	12.2	0.2

[1]Cold utility generation
[2]Hot utility generation

4.4 Discussion on the Unified Total Site Heat Integration Method

The merits of the new UTST method compared to the conventional method have been illustrated using three case studies, which represent a diverse range of processing types and temperatures.

Five key learnings from the case studies with regards to the conventional and unified methods are:

1. *Targets from the new method suggest that the conventional method often over-estimates TSHI potential for non-isothermal utilities.*

An essential element of the new method is the target incorporates the additional constraint for non-isothermal utilities to reach the target temperature within an individual process. By adding this new constraint, the calculated targets become more achievable and realistic. The over-estimation of TSHI targets for the three case studies from using the conventional method compared to new method are

0.2 % for the Södra Cell Värö Kraft Pulp Mill, 22 % for a New Zealand Dairy Factory, and 0.1 % for Petrochemical Complex.

2. *The new method is equally applicable for high and low temperatures processes, and isothermal and non-isothermal utilities.*

The first case study, the large Dairy Factory, represents low temperature non-continuous processes. The second case study, Kraft Pulp Mill, represents a non-continuous process with a wide range of high to low temperatures. This case study illustrates the similarity of results between the CTST and UTST methods in higher temperature processes and more meaningful targets of UTST method for HR at lower temperatures. In the last case study, non-isothermal utilities at higher temperatures, such as hot oil loops, are common utilities in typical Petrochemical Complexes and Oil refineries. This case study represents the similar outcomes of new method to the Conventional methods in case of traditional continuous high temperature processes.

3. *Utilities Pinches in the new method are best observed at the process GCC level.*

After applying the UTST method steam utility demand increases because by introducing the additional constraints, utility pinches occurred within individual processes at the process level, rather than on the TSP, as is always the case with the conventional method. Also, Utility pinches can be seen for isothermal utilities on the TSP, in additional to the process GCCs. However, in case of non-isothermal utilities, the Pinch may not be visible on the TSP Figure 4-4, Figure 4-6, Figure 4-8 and Figure 4-10).

4. *The new method is advantageous for non-continuous processes.*

An advantage of the UTST method is it only allows utility heat exchangers in series within the same process to achieve a utility's target temperature, as illustrated in Figure 3-2b. As a result, the new method restricts any inter-dependency of utility use between processes, which is important for non-continuous processing clusters that often operate with different schedules and independently.

5. *The use of hot oil in place of steam utility (HPS, MPS and/or LPS) can increase TSHR.*

The third case study on a Petrochemical Complex showed the interesting result of increasing TSHI through replacing MPS and LPS with hot oil. Intuitively, the shape of the individual GCCs will dictate the effectiveness of using hot oil instead of

steam for increasing HR. However, the increase in targeted HR comes at the expense of a poorer heat transfer since the heat transfer coefficient of oil is well below that of condensing/evaporating steam.

4.5 Conclusions

This chapter presented a new TSHI targeting methodology that aims to calculate achievable and realistic TSHI targets for sites that use isothermal and/or non-isothermal utilities. It is called the Unified Total Site Targeting method (UTST). The new method initially targets multiple utility use at the individual process level, as opposed to at the TS level in the conventional method. Non-isothermal utilities are given both fixed supply and target temperatures. This subtle change in procedure ensures a utility is supplied to and returned from each process at the specified temperatures, which translates into setting more achievable and realistic TS energy targets. However, being achievable and realistic does not ensure optimality in terms of energy targets and utility selection. The optimal utility number, utility temperature selection and optimisation of the new TSHI targeting method will be presented in Chapter 5.

Chapter Five

Utility Temperature Selection and Optimisation[1]

5.1 Introduction

The selection of the number of utility levels and the associated temperatures are important degrees of freedom to maximise HR. The earliest optimisation of utility levels based on TSHI was presented by Makwana et al. (1998) for retrofit and operations management of an existing TS and Mavromatis and Kokossis (1998) who presented a model to modify targeting procedure and optimise utility networks for operational variations. Zhu and Vaideeswaran (2000) developed a systematic method for operational optimisation, retrofits, grassroots design, and debottlenecking of TS energy systems.

Since these early studies, researchers have applied both Mathematical Programming (MP) and graphical methods in attempts to optimise the selection of utility pressures and temperatures. The main objective function, minimisation of Total Annualised Cost (TAC), is an acute trade-off between investment (capital cost) and operational (mostly utility) costs. Chapter 2 reviewed the literature on the optimal selection of and identified two primary gaps: i) few studies considered non-isothermal utility temperature selection and optimisation and ii) the simultaneous optimisation of both isothermal and non-isothermal utilities. As an element of a utility optimisation method, exergy may find application but, in the case of utility temperature optimisation beyond turbines, it has not been applied as a tool for utility optimisation. Cost and exergy analysis may also be combined

[1] This Chapter is based on a conference paper in Chemical Engineering Transactions cited as (Tarighaleslami et al., 2016a) and full journal article cited as (Tarighaleslami et al., 2017b) published in Energy:

Tarighaleslami, A.H., Walmsley, T.G., Atkins, M.J., Walmsley, M.R.W., Neale, J.R., 2016. Optimisation of Non-Isothermal Utilities using the Unified Total Site Heat Integration Method. *Chemical Engineering Transactions* 52, 457–462. doi:10.3303/CET1652077

Tarighaleslami, A.H., Walmsley, T.G., Atkins, M.J., Walmsley, M.R.W., Neale, J.R., 2017b. Total Site Heat Integration: Utility selection and optimisation using cost and exergy derivative analysis. *Energy* 141, 949–963. https://doi.org/10.1016/j.energy.2017.09.148

with derivative analysis, as demonstrated by Walmsley et al. (2014b), to create a new method for optimising utility temperature selection.

The aim of this chapter is to investigate the selection of utility temperature (both supply and target) on fuel consumption, power generation, and energy cost with the goal of minimising TAC. Depending on the derivative approach, minimisation of the UC and/or ED targets may be considered as the initial objective functions in the optimisation procedure while TAC is the ultimate objective function. The method is primarily for grassroots design but may also be beneficial for retrofit design studies as an initial step.

5.2 Total Site Utility Temperature Optimisation

In PI techniques, the ultimate objective is to minimise TAC by balancing the trade-off between fuel consumption utility demand and capital investments. The appropriate utility temperature selection can lead to lower UCs using the less expensive utility, increased HR at the TS level, increased cogeneration, and/or decreased refrigeration work consumption. Each utility often has a different unit price. Typically, the lowest temperature cold utility and the highest temperature hot utility have a higher unit price than those with temperatures closer to the Total Site Pinch Temperature range. Another approach for utility optimisation is to maximise the use of less expensive utilities in place of more expensive ones. HR may also be optimised to minimise TAC.

To minimise TAC, those utilities that have the potential to optimise Total Site Heat Recovery (TSHR), power generation/consumption, and fuel consumption must be identified. At the first stage, the designer should recognise whether any utility is optimisable in the TS. An optimisable utility refers to any utility that has the capacity to be generated and consumed within the TS, or a utility that has potential to generate shaft work through a turbine in the utility system. In this context, two categories may be defined for utility target temperatures, i.e. fixed (hard) temperatures and soft temperatures. Soft utility target temperatures refer to target temperatures that are non-essential to be achieved that may be changed by varying utility heat capacity flow rates. With a soft target temperature, it becomes difficult to use a utility for TSHR because as it is generated and consumed, the final temperature of the utility is uncertain. Return utility flows from multiple

processes may then be mixed together resulting in an unknown average temperature. A higher quality utility is needed to heat or cool the return utility flow to the intended supply temperature of the reverse utility (e.g. a hot utility loses heat to become a cold utility). Hard utility target temperatures refer to temperature constraints that must be met. These utility temperatures have an opportunity to be optimised to increase HR.

The TSP in Figure 5-1 can be divided into three different regions. The process heat deficit region sits above the hottest TSP source temperature, which is derived from the Grand Composite Curves (GCC) in each process (or plant) before the TSP is constructed. The process heat surplus region is below the coldest TSP sink temperature and is again derived from the GCCs. The region in between may be in process heat deficit or surplus depending on the balance between utility generation and consumption. Those utilities that occur within this middle region, which may be generated and consumed, are optimisable to maximise TSHR, Utility C and D in Figure 5-1.

When Combined Heat and Power (CHP) generation is exploited, more complex utility options are available. Rejected heat from gas turbines and/or boilers with steam turbines may be used to generate or supply hot utility, e.g. steam. In such systems, the utilities that are in the upper region of Figure 5-1 may provide the potential for SWG through a turbine. These hot utilities can also be considered as optimisable to maximise shaft work, e.g. Utility B. Similarly, for processes which require sub-ambient utility in the lower region of Figure 5-1, the cold utility requires compressors in refrigeration cycles to generate the needed cooling, Utility F. As a result, the appropriate utility temperature selection, which is considered as optimisable, may lead to minimum work consumption.

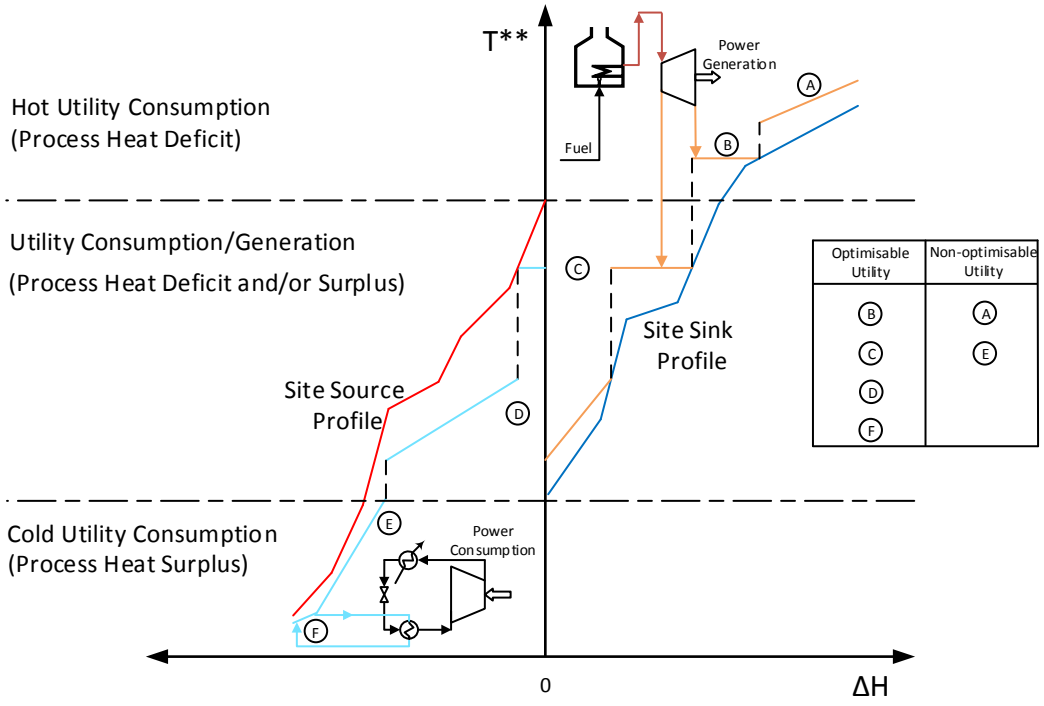

Figure 5-1: Possibility of utility to be optimised in a typical TSP.

In short, any utility that is either connected to a turbine, linked to a refrigeration cycle, or both generated/consumed, is a candidate for temperature optimisation.

UC can be calculated considering hot utility, cold utility, and power generation/consumption prices and targets. Equation 5-1 presents the UC calculation method.

$$UC = \left(\sum \left(UP_{h,ut(i)} \times Q_{h,ut(i)} \right) + \sum \left(UP_{c,ut(i)} \times Q_{c,ut(i)} \right) - \left(PP_{gen} \times W_{gen} \right) \right) \times OP \qquad (5\text{-}1)$$

Where *UP* is utility price, *Q* is utility target, *PP* is power price, *W* is power target, and *OP* is operating period of the plant. Subscripts *h,ut* is hot utility, *c,ut* is cold utility, and *gen* is generation. The final term is an offset but not total power cost.

Total Annualised Cost (TAC) is calculated using UC and Annualised Capital Cost (ACC) as presented in Equation 5-2.

$$TAC = UC + ACC \qquad (5\text{-}2)$$

Where ACC only includes heat exchanger area. Infrastructure costs are not considered in this paper.

5.3 The Role of Exergy Analysis in Utility Temperature Optimisation

To help select utility temperature levels in the TS, exergy and ED may be analysed. Since there is no chemical reaction, separation or mixing in the utility mains, only physical exergy needs consideration (Kotas, 1995).

Exergy is defined as maximum theoretical useful work potential, i.e. shaft work or electrical work, obtainable as two systems interact to equilibrium (Bejan and Tsatsaronis, 1996). Exergy analysis can, therefore, provide insights to process optimisation evaluations. Heat transfer through finite temperature difference always generates entropy and any process that generates entropy always destroys exergy. As a result, ED (X_d) is proportional to the entropy generated (S_{gen}) as in Equation 5-3.

$$X_d = T_0 S_{gen} \geq 0 \tag{5-3}$$

Where T_0 is the reference temperature. As it can be seen ED is a positive quantity for any actual process and becomes zero for a reversible process.

Marmoleji-Correa and Gundersen (2013) summarised a simple method to determine the temperature based physical exergy of a process flow, as shown in Equation 5-4.

$$X = \dot{m} c_p \left[T_0 \left(\frac{T}{T_0} - \ln \frac{T}{T_0} - 1 \right) \right] = \dot{m} c_p T_X \tag{5-4}$$

Exergy can be calculated using Equation 5-4 when the specific heat capacity has been assumed constant with respect to temperature in the range from T to reference T_0. The factor in the square bracket is called exergetic temperature (T_x) and has units of Kelvin. Exergetic temperature is a function of stream temperature in K and the selected zero state temperature, T_0, in K. The reference temperature has been selected as 15 °C, which corresponds to the cooling water temperature. In addition, this temperature can provide the required temperature driving force for cooling down non-isothermal utility systems that are operated near the ambient temperature, e.g. cooling tower system. This equation determines the change in exergy as a process flow heats or cools from its supply to its target temperature.

Figure 5-2 shows the exergy potential of a single heat exchanger where the hot stream as a heat source has an exergy relative to the T_0, and the cold stream as a heat sink has a lower exergy relative to the T_0.

For the ED, it can be said that:

$$X_d = X_{Source} - X_{Sink} \tag{5-5}$$

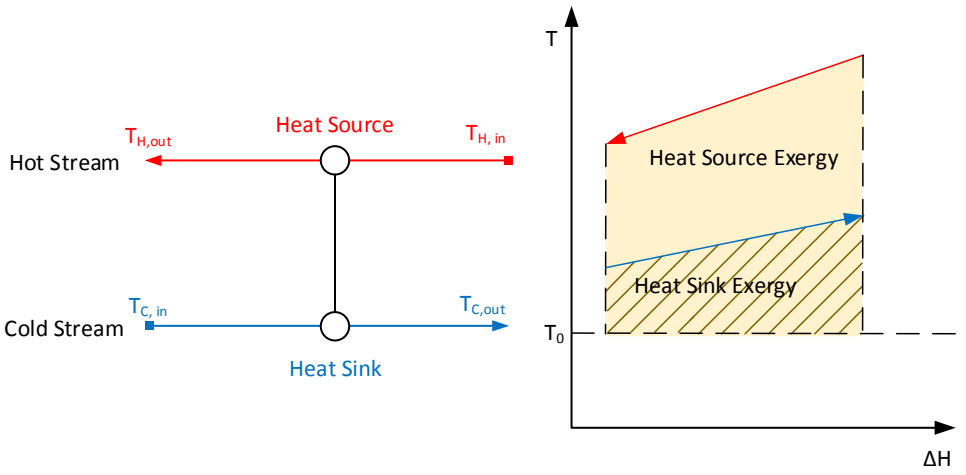

Figure 5-2: Exergy analysis of a single heat exchanger.

The same concept applies to a process plant. Figure 5-3 illustrates utility-process and process-process EDs on a Balanced Composite Curve (BCC). BCCs are particularly useful to demonstrate the effects of multiple utilities, multiple Pinch Temperatures and the driving force in the HEN of a process. Non-isothermal utilities are normally shown as diagonal segments in enthalpy-temperature plots while isothermal utilities are shown as horizontal segments. It is not always easy to distinguish non-isothermal utilities, such as hot water, on a BCC because it often composites with the process streams (Kemp, 2007). However, the BCC is still a useful tool to provide a clear visualisation for ED of heat transfer within a processing system.

In Figure 5-3, three different regions can be recognised: (a) utility source-process sink ED, (b) process source-process sink ED, and (c) process source-utility sink ED. Each of these regions presents exergy transfer and destruction within the process based on the available exergy sources and sinks. As a result, total exergy destruction of the plant can be demonstrated by Equation 5-6.

$$X_d = \sum X_{Source} - \sum X_{Sink} \tag{5-6}$$

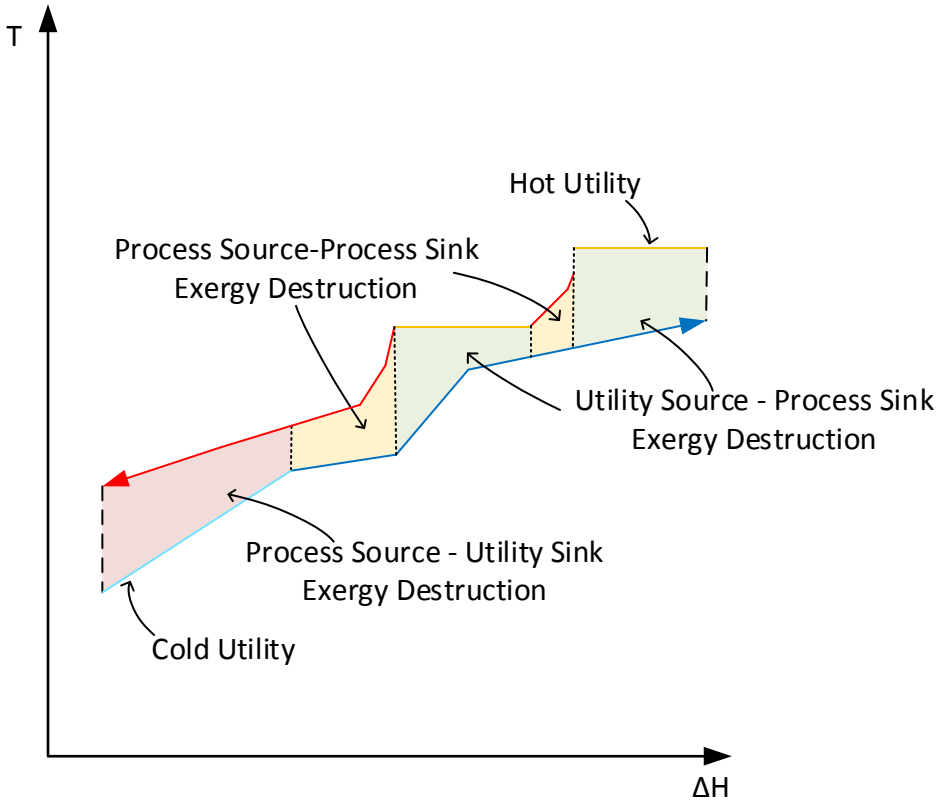

Figure 5-3: Utility-Process and Process-Process ED in a single process BCC.

Figure 5-4 shows how ED applies to a TS Figure 5-4a illustrates the ED region in the TSP. Figure 5-4b shows that by shifting utility temperatures, ED has been increased for small regions on both sides of the TSP while it has decreased for most other regions. In Figure 5-4b, shifted utility temperature levels are illustrated in solid lines and original utility temperature levels from Figure 5-4a are illustrated in dashed lines. In summation, total exergy destruction has been reduced because of the utility temperature change. Equation 5-3 can be applied to analyse TS which determines utility-process ED for entire TS due to heat transfer.

Figure 5-4c shows the work generation potential using the Site Utility Grand Composite Curve (SUGCC). When HR increases (solid utility lines), power generation often decreases. While in the Figure 5-4d, the same concepts of ED reduction apply. Shifting utility temperatures towards the Total Site Pinch region shows an effect on ED resulting in increased HR across the TS and slightly higher power generation for this example. There is a complex trade-off between power generation, HR, and ED that must be considered when analysing the selection of utility temperatures.

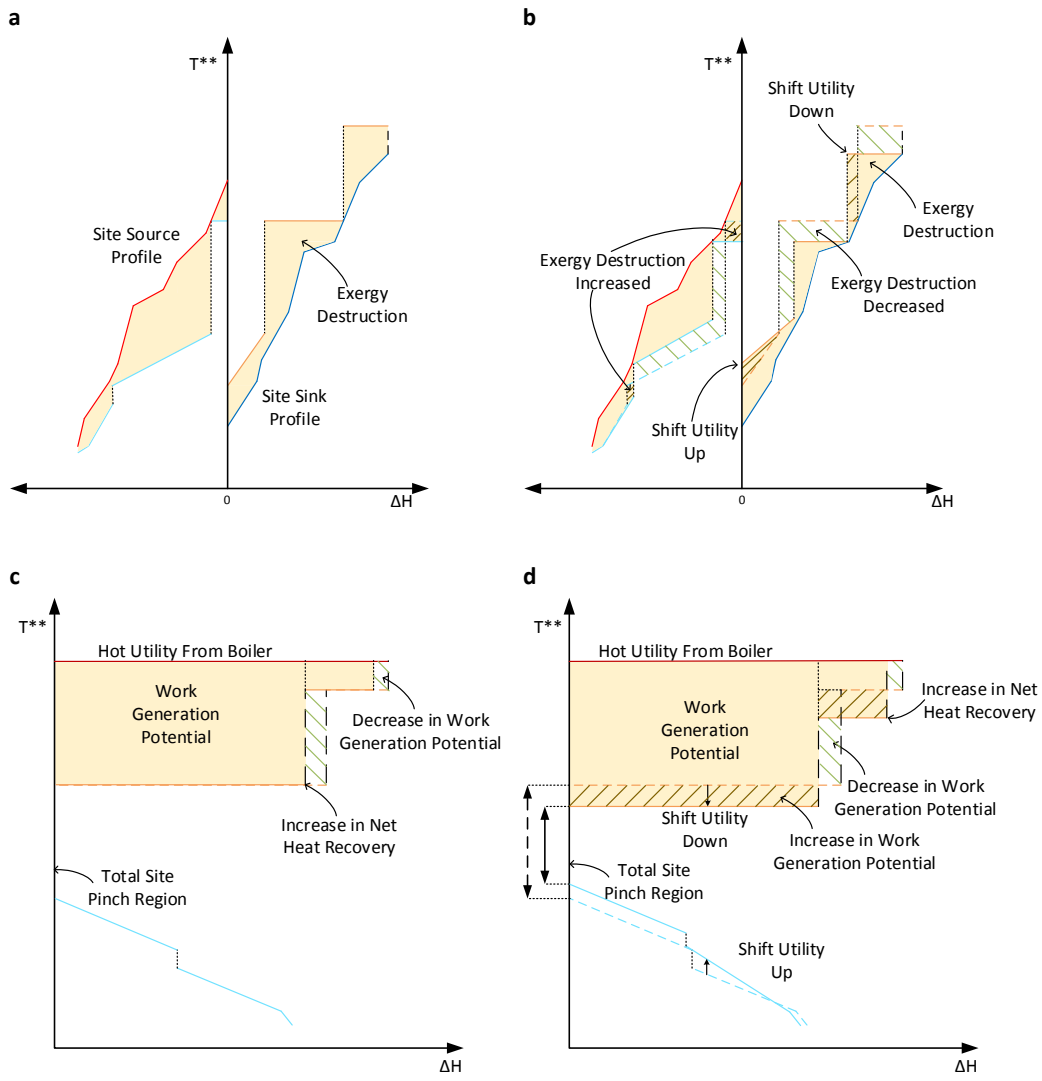

Figure 5-4: a) Total ED in a typical TSP; b) Total exergy destruction as results of utility shifts; c) Typical SUGCC HR and power generation trade-off; d) Complex trade-off between power generation, HR, and ED after utility shifts.

The smaller temperature difference between the hot and cold available utilities in the TS may offer lower ED and a reduction in UCs through improved HR. Improved temperature selection in the TS may provide the opportunity to reduce energy consumption within the TS as the result of a decrease in ED (i.e. shifting utility temperatures towards the Total Site Pinch will cause a reduction in ED). There is a trade-off between hot and cold utility temperature difference in the TS and total heat transfer area, which affects ACC and finally TAC. TAC is normally the final objective function in the optimisation of TS targets. To select utility temperatures, a temperature range may be considered for each required utility.

5.4 Method

5.4.1 Overview

Utility supply and target temperatures can be selected by using the derivative of the objective function. Derivatives provide a direction to change utility temperatures and improve the key TS metrics. Three different approaches are investigated to find the best sequential combination of derivative objective functions in the optimisation procedure.

- Approach 1: Minimise the derivative of the TAC function with respect to temperature, which may be approximated numerically using Equation 5-7.

$$\frac{dTAC}{dT} \cong \frac{TAC(T_i \pm \Delta T) - TAC(T_i)}{\Delta T} \tag{5-7}$$

Where subscript, *i* represents each individual utility temperature for either supply or target temperature (hot or cold sides of the utility) and ΔT is a small change in temperature (step change).

In this approach, the TAC derivative is minimised given the initial utility temperature selection. One of the challenges with this method is that TAC functions are discontinuous functions due to changes in the number of utilities and number of heat exchangers. This means the function contains numerous local minima.

- Approach 2: Minimise the derivative of the UC, then sequentially minimise the derivative of the TAC (UC+TAC). UC derivative may be presented as:

$$\frac{dUC}{dT} \cong \frac{UC(T_i \pm \Delta T) - UC(T_i)}{\Delta T} \tag{5-8}$$

This approach includes a two-step process: first, minimise the derivative of UC iteratively, then, second, minimise the derivative of TAC. But the UC function tends to be more continuous but still can have local minima in the form of flat regions.

- Approach 3: Minimise the derivative of the UC iteratively with the derivative of ED, then sequentially minimise the derivative of the TAC (UC+ED+TAC). Where ED derivative can be presented as:

$$\frac{dX_d}{dT} \cong \frac{X_d(T_i \pm \Delta T) - X_d(T_i)}{\Delta T} \tag{5-9}$$

The third approach, similar to the second approach, includes a two-step process: first, minimise the derivative of UC iteratively and, when constant (flat), minimise the derivative of ED, then, second, minimise the derivative of TAC. It is important to understand that UC functions tend to be continuous with many flat sections where a change in temperature has no impact on UC. In this region, it becomes necessary to apply the derivative of ED as the objective, which is not flat. The logic for initially minimising UC with ED is to help select temperatures that are more likely in the proximity of the global optimum, from which starting point a TAC minima may be located. The TAC local minimum is not guaranteed to be the global optimum It should be noted that to have consistent objective functions in the derivative analysis the exergy in MW was converted to cost per year using an energy conversion factor ($/MWh) based on the energy price and operating period of each case study (Shamsi and Omidkhah, 2012).

5.4.2 Detailed Method and UTSI Software Tool Development

The Excel^{TM} spreadsheet, UTSI software tool, has been extended to include the new utility optimisation procedure. Figure 5-5 presents the detailed utility optimisation procedure. New steps have been added to the TSHI targeting method to complete utility selection and optimisation procedure for any available TSHI method presented in Figure 4-3.

Step 1: Objective function derivatives calculation: A derivative map can be constructed using the framework presented in Table 5-1 for each utility. The first column presents the temperature ranges for hot and cold sides of each utility while optimising utility temperatures. Eight different options can be considered as either hot, cold or both hot and cold sides of the utility may change. The temperature step ΔT_{st} represents the amount of change in the utility temperature for each iteration in the procedure. The smaller temperature step, the less convergence time and the more accurate temperature selection. However, it may be trapped in local optimum as opposed to converging in an overall optimum in the HR function. Therefore, for each of the main objective functions, eight different subset rows have been defined, as it is shown in Table 5-1. In other words, supply and target temperatures of each utility are monitored separately. However,

according to temperature ranges and the nature of the utility, the temperature step may vary.

The next three columns represent one of the objective function derivatives as presented in Section 5.4.1, where subscript *i* represents each individual temperature point at either supply or target temperatures of the utility.

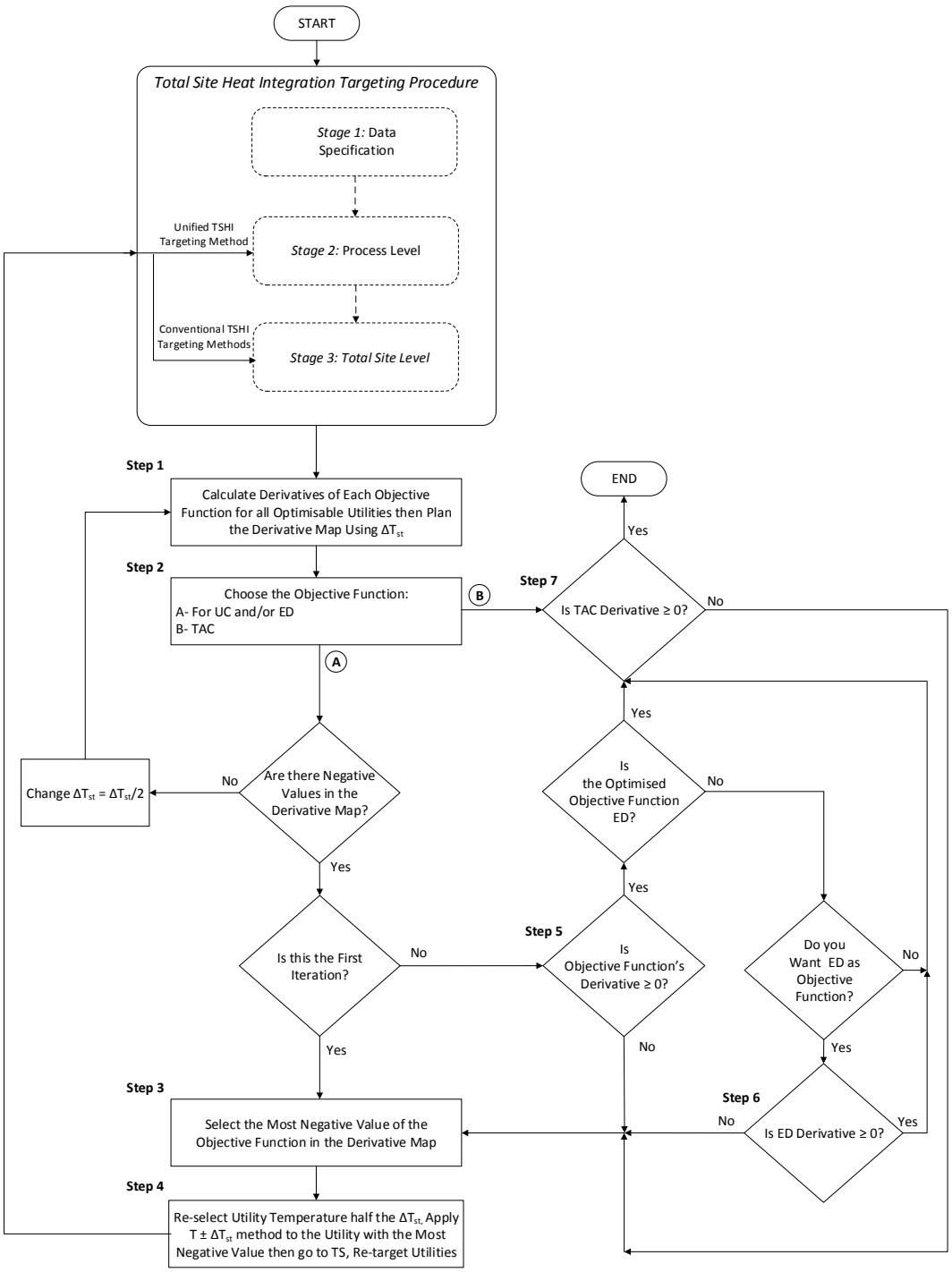

Figure 5-5: Procedure for optimal utility temperature selection of optimisable utilities in TSHI methods.

Table 5-1: A general framework to construct a derivative map for a utility.

Temperature Ranges	Objective Function Derivative		
T_c, T_h (°C)	Utility Cost $\frac{dUC}{dT}$ (NZD/°C)	Exergy Destruction $\frac{dX_d}{dT}$ (kW/°C)	Total Annualised Cost $\frac{dTAC}{dT}$ (NZD/°C)
$T_{c,i}$, $T_{h,i}+\Delta T_{st}$	$\frac{UC(T_{c,j}, T_{h,j}+\Delta T_{st})-UC(T_{c,j}, T_{h,j})}{\Delta T_{st}}$	$\frac{X_d(T_{c,j}, T_{h,j}+\Delta T_{st})-X_d(T_{c,j}, T_{h,j})}{\Delta T_{st}}$	$\frac{TAC(T_{c,j}, T_{h,j}+\Delta T_{st})-TAC(T_{c,j}, T_{h,j})}{\Delta T_{st}}$
$T_{c,i}$, $T_{h,i}-\Delta T_{st}$	$\frac{UC(T_{c,j}, T_{h,j}-\Delta T_{st})-UC(T_{c,j}, T_{h,j})}{\Delta T_{st}}$	$\frac{X_d(T_{c,j}, T_{h,j}-\Delta T_{st})-X_d(T_{c,j}, T_{h,j})}{\Delta T_{st}}$	$\frac{TAC(T_{c,j}, T_{h,j}-\Delta T_{st})-TAC(T_{c,j}, T_{h,j})}{\Delta T_{st}}$
$T_{c,i}+\Delta T_{st}$, $T_{h,i}$	$\frac{UC(T_{c,j}+\Delta T_{st}, T_{h,j})-UC(T_{c,j}, T_{h,j})}{\Delta T_{st}}$	$\frac{X_d(T_{c,j}+\Delta T_{st}, T_{h,j})-X_d(T_{c,j}, T_{h,j})}{\Delta T_{st}}$	$\frac{TAC(T_{c,j}+\Delta T_{st}, T_{h,j})-TAC(T_{c,j}, T_{h,j})}{\Delta T_{st}}$
$T_{c,i}-\Delta T_{st}$, $T_{h,i}$	$\frac{UC(T_{c,j}-\Delta T_{st}, T_{h,j})-UC(T_{c,j}, T_{h,j})}{\Delta T_{st}}$	$\frac{X_d(T_{c,j}-\Delta T_{st}, T_{h,j})-X_d(T_{c,j}, T_{h,j})}{\Delta T_{st}}$	$\frac{TAC(T_{c,j}-\Delta T_{st}, T_{h,j})-TAC(T_{c,j}, T_{h,j})}{\Delta T_{st}}$
$T_{c,i}+\Delta T_{st}$, $T_{h,i}+\Delta T_{st}$	$\frac{UC(T_{c,j}+\Delta T_{st}, T_{h,j}+\Delta T_{st})-UC(T_{c,j}, T_{h,j})}{\Delta T_{st}}$	$\frac{X_d(T_{c,j}+\Delta T_{st}, T_{h,j}+\Delta T_{st})-X_d(T_{c,j}, T_{h,j})}{\Delta T_{st}}$	$\frac{TAC(T_{c,j}+\Delta T_{st}, T_{h,j}+\Delta T_{st})-TAC(T_{c,j}, T_{h,j})}{\Delta T_{st}}$
$T_{c,i}+\Delta T_{st}$, $T_{h,i}-\Delta T_{st}$	$\frac{UC(T_{c,j}+\Delta T_{st}, T_{h,j}-\Delta T_{st})-UC(T_{c,j}, T_{h,j})}{\Delta T_{st}}$	$\frac{X_d(T_{c,j}+\Delta T_{st}, T_{h,j}-\Delta T_{st})-X_d(T_{c,j}, T_{h,j})}{\Delta T_{st}}$	$\frac{TAC(T_{c,j}+\Delta T_{st}, T_{h,j}-\Delta T_{st})-TAC(T_{c,j}, T_{h,j})}{\Delta T_{st}}$
$T_{c,i}-\Delta T_{st}$, $T_{h,i}+\Delta T_{st}$	$\frac{UC(T_{c,j}-\Delta T_{st}, T_{h,j}+\Delta T_{st})-UC(T_{c,j}, T_{h,j})}{\Delta T_{st}}$	$\frac{X_d(T_{c,j}-\Delta T_{st}, T_{h,j}+\Delta T_{st})-X_d(T_{c,j}, T_{h,j})}{\Delta T_{st}}$	$\frac{TAC(T_{c,j}-\Delta T_{st}, T_{h,j}+\Delta T_{st})-TAC(T_{c,j}, T_{h,j})}{\Delta T_{st}}$
$T_{c,i}-\Delta T_{st}$, $T_{h,i}-\Delta T_{st}$	$\frac{UC(T_{c,j}-\Delta T_{st}, T_{h,j}-\Delta T_{st})-UC(T_{c,j}, T_{h,j})}{\Delta T_{st}}$	$\frac{X_d(T_{c,j}-\Delta T_{st}, T_{h,j}-\Delta T_{st})-X_d(T_{c,j}, T_{h,j})}{\Delta T_{st}}$	$\frac{TAC(T_{c,j}-\Delta T_{st}, T_{h,j}-\Delta T_{st})-TAC(T_{c,j}, T_{h,j})}{\Delta T_{st}}$

Step 2: Objective function selection: In this step, initially, the objective function can be selected then in each iteration, the selected objective function (or the objective function which is in the iteration) goes to the related direction A or B in Figure 5-5. This step can lead optimisation procedure for a different combination of objective functions. Two question boxes can lead the procedure back to Step 2 or Step 5 if the iteration is not the first iteration.

Step 3: Selection of appropriate value from the derivative map: The most negative value, i.e. a reduction in cost, utility, or ED, for the objective function is located on the derivative map, which shows the highest potential for improvement, and identifies the utility, its temperature and the direction that it should be changed. The utility corresponding to this value must be selected in this step.

Step 4: Utility temperature re-selection: After identifying the best utility temperature to change, whether utility generation turns to utility consumption or vice versa, ΔT_{st} must be divided by half and the shift backwards or forwards to converge to the optimum; i.e. new ΔT_{st} can be added or subtracted to the utility temperature. After changing the utility temperature, the process is re-targeted according to the TSHI targeting method which is used, and the derivative map is re-calculated. It must be noted that the second derivative is checked in this stage to ensure that the collected points are always moving in the downwards direction to achieve the minimum. This procedure may be repeated unless the result converges. After the first iteration, the optimisation procedure may lead to step 5:

Step 5: Objective function check: The value obtained for the objective function (UC or ED) from the derivative map should be checked. If the value is negative it means there is a potential to improve the objective function by increasing or decreasing its supply/target temperature by ΔT_s. Therefore, the procedure goes back to Step 3; otherwise, it should be checked that if ED is the optimised objective function and/ or if it is targeted that ED be an objective function. The answer may lead the procedure either to Step 6 or Step 7.

Step 6: ED derivative check: In this step, ED is to be checked. The ED negative values represent the potential of further improvement. Therefore, if the corresponding value to the most negative ED value in the other objective function, i.e. UC, is equal to zero or negative, then the utility temperature can be improved.

Step 7: TAC objective function check: This step is similar to step 5 and 6, but this time the value obtained for the TAC column from the derivative map should be checked. The negative value means there is a potential to improve the objective function by increasing or decreasing its supply/target temperature by ΔT_{st}. For negative values go to Step 3, otherwise, there will not be any more potential to improve selected utility temperature, which means all the utility temperatures are optimal.

5.4.2.1 A Brief Comparison to Existing Methods

There are several advantages of this new method compared to the other methods. The exergy analysis is based on exergetic temperatures, which have a linear relationship to exergy flow. Previous TSHI exergy targeting methods were based on converting temperature to Carnot factor and plotting an efficiency-enthalpy diagram. The new method is a derivative based technique that can be programmed while conventional methods are heuristic based (1994), which are difficult to automate. In the specific case of Hui and Ahmed (1994), only some GCC segments are collected for TSHI, which can lead to significantly reduced HR. Hui and Ahmed (1994) also based the pricing of utility on exergy as opposed to actual prices as done in this paper. Furthermore, the UTST method used as part of the optimisation is improved from conventional approaches (Klemeš et al., 1997). Finally, none of the other methods consider non-isothermal utility optimisation within the same procedure as isothermal utilities.

5.5 Utility Temperature Optimisation Results

The case studies have been considered to illustrate the derivative optimisation procedure. Table 5-2 presents TS characteristics of each case study considered for optimisation.

Table 5-2: Total Site characteristics for each case study.

Case study	No. of processes	No. streams available in TS	ΔT_{min} (°C)	Operating Period (h/y)
Kraft Pulp Mill Plant	10	64	10	8,300
Petrochemical Complex	8	60	20	8,600
Dairy Factory	15	79	5	5,500

Capital and energy costs are estimated in New Zealand dollars (NZD). Energy cost for utilities is estimated to be NZD 5 /MWh for cooling utilities, NZD 30 /MWh for heating utilities, NZD 40 /MWh for chilled water (ChW), and NZD 100 /MWh for power generation. To calculate the ACC for all case studies, investment return duration (n) has been set to 10 years with a 7 % interest rate (j). It has been assumed that plate and frame heat exchangers are chiefly required in the dairy factory and shell and tube heat exchangers for the pulp mill and petrochemical case studies. Heat exchanger cost can be calculated based on required heat exchanger area according to Equation 5-10 (Bouman et al., 2004) and cost parameters are taken from Statistic New Zealand Infoshare (2016) data as is shown in Table 5-3. Note that to calculate the total ACC, infrastructure cost such as civil, steel structure, and piping costs are not considered.

$$ACC = \left(a + (b \times A^{c})\right) \times \left(\frac{j \times (1+j)^{n}}{(1+j)^{n} - 1}\right) \tag{5-10}$$

Where A is the heat transfer area in m^2, and a in NZD, b inNZD/m^{2c}, and c are cost coefficients and exponent relating to the heat exchanger type, as given in Table 5-3.

Table 5-3: ACC parameters for Shell and Tube, and Plate and Frame heat exchangers.

Heat Exchanger Type	a	b	c
Shell and Tube	0	5,870	0.57
Plate and Frame	4,265	649	1.00

5.5.1 Case Study I: Södra Cell Värö Kraft Pulp Mill Plant

Södra Cell Värö Kraft Pulp Mill plant in southern Sweden has been chosen as the first case study. The case study has been explained in detail in Section 3.4.1 and Section 4.3.1. All utilities presented in Table 4-2 except cooling water have been considered as an optimisable utility according to the described definition in the method section as it is clear in Table 4-2.

A comparison of utility targets of the base case, in dashed lines, compared to the optimised case in solid lines using original utility temperatures as a starting point are illustrated in Figure 5-6 in TSP and in Figure 5-7 in SUGCC graphs.

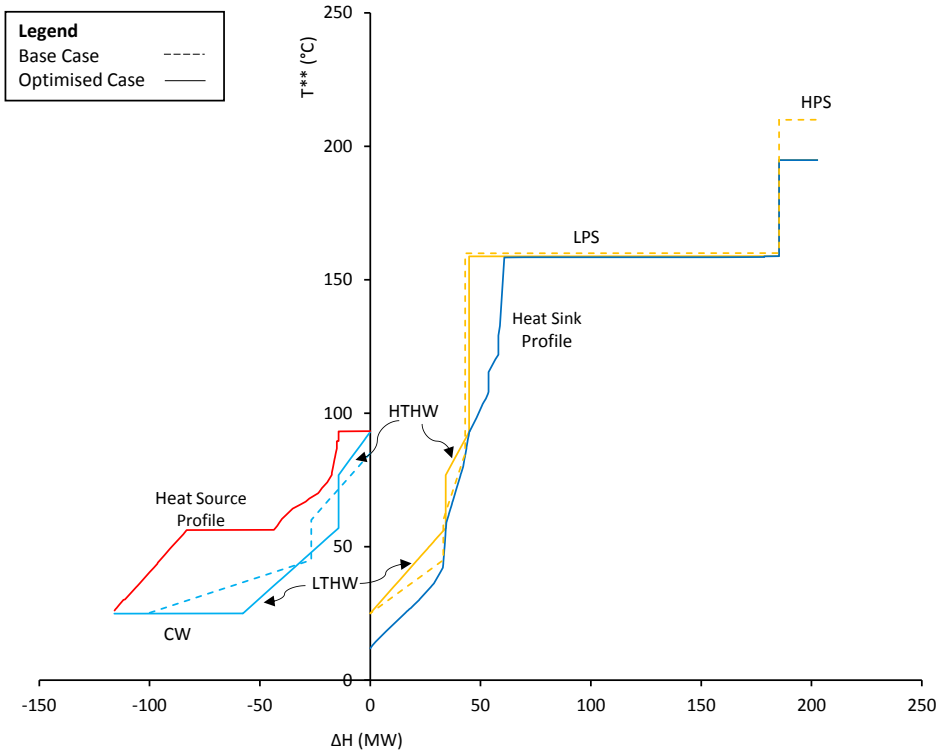

Figure 5-6: Comparison of the base case and optimised case in TSP for Kraft Pulp Mill case study.

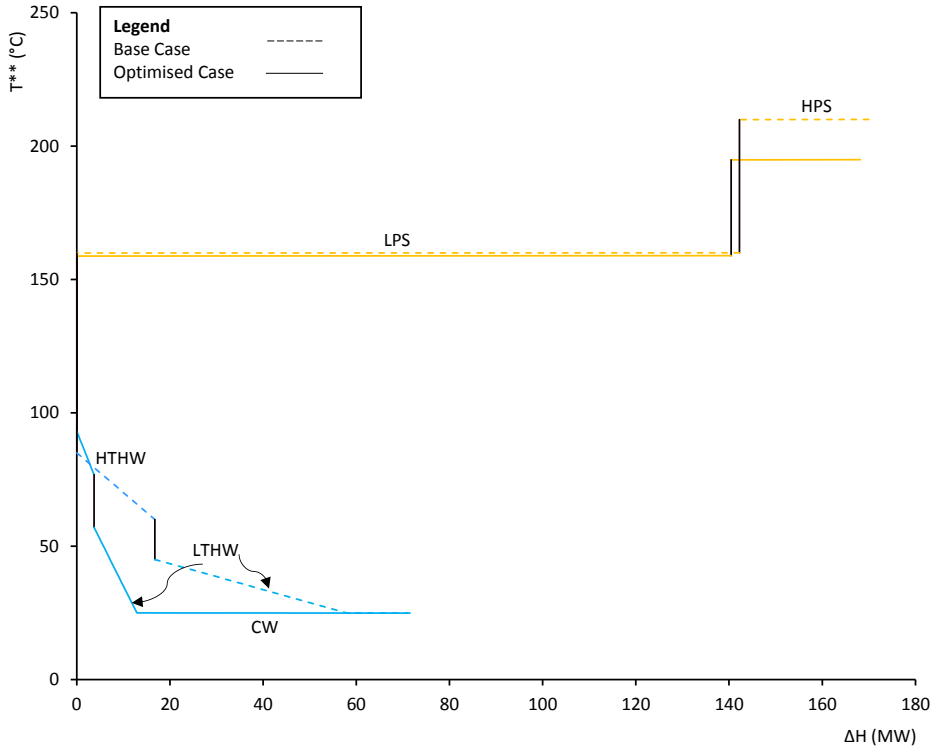

Figure 5-7: Comparison of the base case and optimised case in SUGCC for Kraft Pulp Mill case study.

Targeting has been repeated considering three different approaches. Table 5-4 compares the optimised temperatures obtained by applying optimisation

procedure. Table 5-5 demonstrates targeting results for three different optimisation criteria for the case study. It shows 43.1 MW of TSHR, 37.1 MW of SWG, NZD 14,618,951 /y UC, 77 heat exchanger units, and NZD 16,408,482 /y TAC.

Table 5-4: Optimised utility temperatures comparison for different three criteria in Kraft Pulp Mill case study.

Optimisation Criteria	Isothermal Utility		Non-Isothermal Utility				
	HPS	LPS	HTHW		LTHW		CW
	T_{Hot} (°C)	T_{Hot} (°C)	T_{Hot} (°C)	T_{Cold} (°C)	T_{Hot} (°C)	T_{Cold} (°C)	T_{Cold*} (°C)
Original Utilities	210.0	160.0	85.0	60.0	45.0	25.0	25.0
TAC	194.9	158.9	93.0	76.8	46.0	25.0	25.0
UC+TAC	194.9	158.9	93.0	76.8	46.0	25.0	25.0
UC+ED+TAC	194.9	158.9	93.0	76.8	57.0	25.0	25.0

*T_{Hot} for CW has been considered as soft utility temperature

Table 5-5: Utility targets comparison for different three criteria in Kraft Pulp Mill case study.

Optimisation Criteria	HEU Target #	TSHR Target kW	SWG kW	ED kW	UC NZD/y	TAC NZD/y	Change %
Original Utilities	77	43,061	37,027	19,095	14,618,951	16,408,482	-
TAC	76	44,845	37,384	19,107	13,804,364	15,675,136	-4.47
UC+TAC	76	44,845	37,384	19,107	13,804,364	15,675,136	-4.47
UC+ED+TAC	76	44,845	37,384	20,242	13,804,364	15,669,850	-4.51

The optimised case, UC+ED+TAC criteria, shows a 4.1 % increase in TSHR, 1.0 % increase in SWG, reduction of one heat exchanger unit, and a 4.51 % decrease in TAC compared to other two criteria which have lower TAC reduction. As can be seen in Table 5-5 for all three different cases, SWG and UC are identical. However, ED increases in the third case while TAC has been reduced. This is due to LTHW optimal temperature (57 °C) that increases temperature driving force that led the total required heat transfer area to be decreased while total heat exchangers reduced by one unit. TAC decreases up to 4.5 %.

5.5.2 Case Study II: Petrochemical Complex

This case study demonstrates the advantages of the implementation of the new optimisation method to plants that typically operate at high temperature ranges. The plant is explained in detail in Section 3.4.3 and Section 4.3.3, utilities are presented in Table 4-6. SWG is not considered in this case study.

In this case study MPS and LPS are considered as optimisable utilities. Base case utility targets, in dashed lines, have been compared with optimised targets, in solid lines, using original utility temperatures as a starting point in TSP in Figure 5-8 and in SUGCC in Figure 5-9.

The case study has been targeted and repeated for all three different criteria. The initial utilities used as starting point and the result optimised utilities in each criterion are presented in Table 5-6. Targeting results are presented in Table 5-7. In this case, optimisation based on TAC as an individual objective function has a lower reduction in TAC (-2.52 %) while other two criteria show identical TAC reduction (-3.36 %). This means that when the TS is optimised considering UC as the objective function, the optimal temperatures are used as the starting point for the next optimisation step where TAC is the objective function. The dual optimisation function approach requires fewer iterations and enables an improved target to be achieved. However, in this case, the benefit of including ED in the procedure is negligible since the UC+TAC approach and UC+ED+TAC approach achieve the same final result.

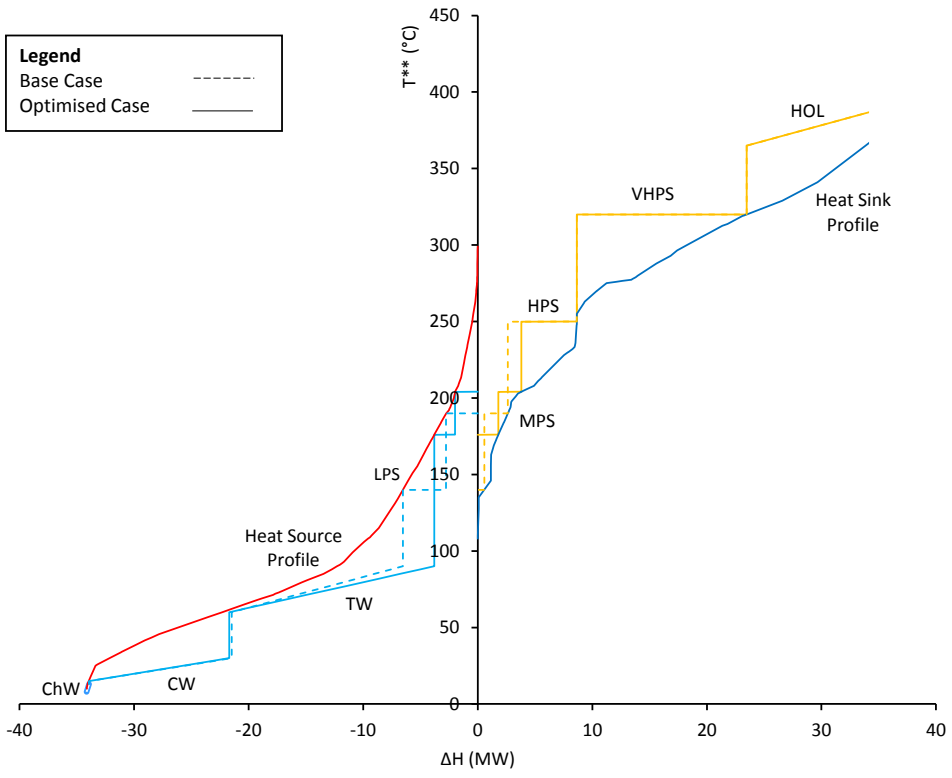

Figure 5-8: Comparison of the base case and optimised case in TSP for Petrochemical Complex case study.

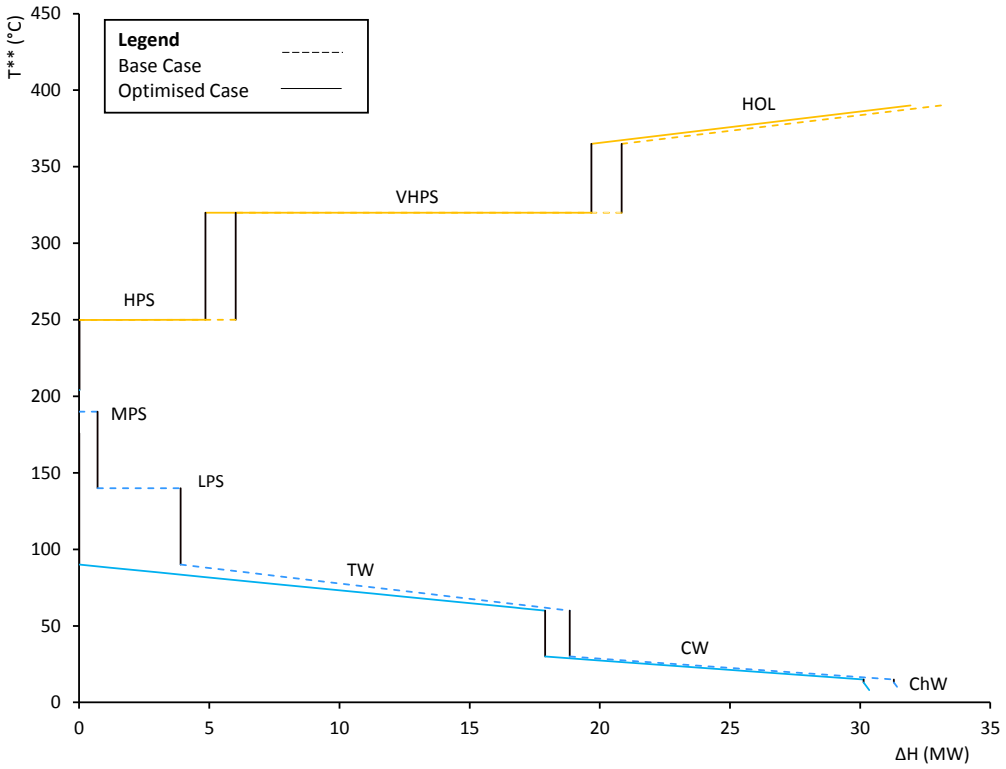

Figure 5-9: Comparison of the base case and optimised case in SUGCC, for Petrochemical Complex case study.

Table 5-6: Optimised utility temperatures comparison for different three criteria in Petrochemical Complex case study.

Optimisation Criteria	Isothermal Utility				Non-Isothermal Utility							
	VHPS	HPS	MPS	LPS	HOL		TW		CW		ChW	
	T_{Hot} (°C)	T_{Hot} (°C)	T_{Hot} (°C)	T_{Hot} (°C)	T_{Hot} (°C)	T_{Cold} (°C)	T_{Hot} (°C)	T_{Cold} (°C)	T_{Hot} (°C)	T_{Cold} (°C)	T_{Hot} (°C)	T_{Cold} (°C)
Original Utilities	320	250	190	140	390	365	90	60	30	15	13	8
TAC	320	250	214	180	390	365	90	60	30	15	13	8
UC+TAC	320	250	204	176	390	365	90	60	30	15	13	8
UC+ED+TAC	320	250	204	176	390	365	90	60	30	15	13	8

Table 5-7: Utility targets comparison for different three criteria in Petrochemical Complex case study.

Optimisation Criteria	HEU Target #	TSHR Target kW	ED kW	UC NZD/y	TAC NZD/y	Change %
Original Utilities	139	2,633	5,759	9,895,506	10,751,421	-
TAC	131	3,488	5,964	9,638,319	10,480,799	-2.52
UC+TAC	134	3,796	5,967	9,545,481	10,390,653	-3.36
UC+ED+TAC	134	3,796	5,967	9,545,481	10,390,653	-3.36

5.5.3 Case study III: New Zealand Dairy Processing Factory

The last case study is the large dairy factory in New Zealand that has been explained in detail in Section 3.4.1 and Section 4.3.3. Table 4-4 presents initial utilities which are used in the plant. All processes in the factory, which is considered as a TS, have recently been investigated and integrated to industry best practice. However, further improvements have been achieved by using the UTST method. In this case study only LTHW has the conditions to be optimisable utility.

Figure 5-10 shows TSP comparison between the Base Case targets using original utility temperatures as a starting point, in dashed lines, and optimised targets in solid lines using the same starting points. As can be seen hot utility targets, utility heat surplus, are identical before and after optimisation but in cold utility side, utility heat deficit, LTHW has been slightly improved.

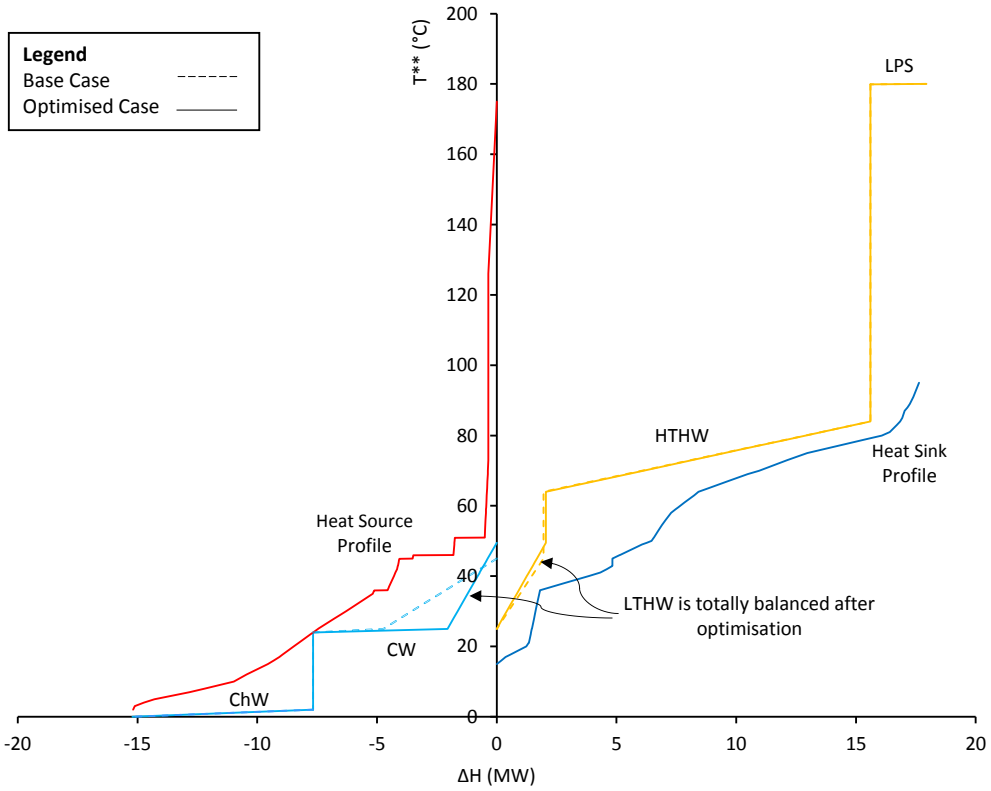

Figure 5-10: Comparison of the base case and optimised case in TSP for Dairy Factory case study.

The similar comparison is illustrated for UGCCs in Figure 5-11 which shows TSHR has been increased about 100 kW.

Surprisingly, Table 5-8 and Table 5-9 show that the optimisation results of all three criteria are identical in this case study. This might be due to a couple of reasons, first, the LTHW is a non-isothermal utility that has only 9.5 % of total heat load in both heat surplus and heat deficit sides of TS which after optimisation is fully balanced. This means the utility has the exact amount of generation and consumption as shown in Figure 5-10. Second, as mentioned above the plant is highly efficient because of recent optimisation planning and also TS targets are now more realistic and accurate based on the UTST method. However, the optimisation targets could still decrease TAC by 0.62 % and increase TSHR by 5.0 % while increasing number of heat exchangers units by one.

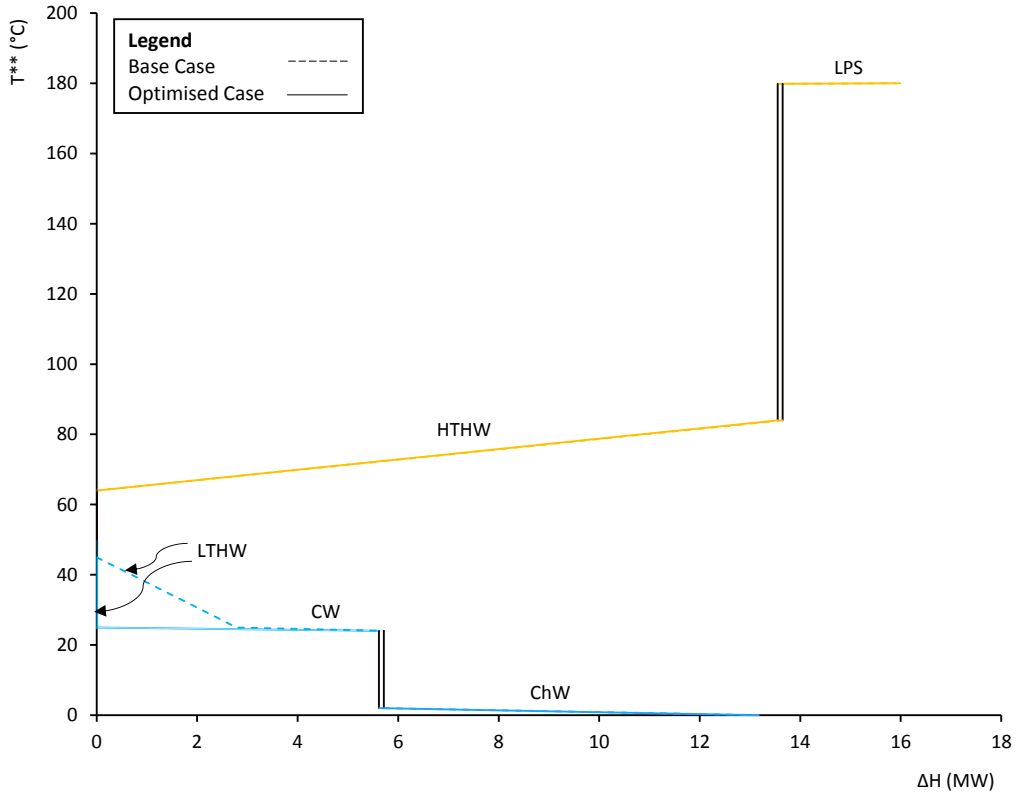

Figure 5-11: Comparison of the base case and optimised case in SUGCC for Dairy Factory case study.

Table 5-8: Optimised utility temperatures comparison for different three criteria in Dairy Factory case study.

Optimisation Criteria	Isothermal Utility	Non-Isothermal Utility						
	LPS	HTHW		LTHW		CW	ChW	
	T_{Hot} (°C)	T_{Hot} (°C)	T_{Cold} (°C)	T_{Hot} (°C)	T_{Cold} (°C)	T_{Cold*} (°C)	T_{Hot} (°C)	T_{Cold} (°C)
Original Utilities	180	84	64	45.5	25	24	2	0
TAC	180	84	64	49.5	25	24	2	0
UC+TAC	180	84	64	49.5	25	24	2	0
UC+ED+ TAC	180	84	64	49.5	25	24	2	0

Table 5-9: Utility targets comparison for different three criteria in Dairy Factory case study.

Optimisation Criteria	HEU Target	TSHR Target	ED	UC	TAC	Change
	#	kW	kW	NZD/y	NZD/y	%
Original Utilities	97	1,952	2,125	4,454,612	4,873,609	-
TAC	98	2,501	2,201	4,435,662	4,843,602	-0.62
UC+TAC	98	2,501	2,203	4,435,662	4,843,602	-0.62
UC+ED+ TAC	98	2,501	2,203	4,435,662	4,843,602	-0.62

5.6 Additional Analysis of the Södra Cell Värö Kraft Pulp Mill

5.6.1 Contours of Utility Temperature Optimisation for Hot Water Loops

For each utility, a range of supply and target temperatures may be chosen and targeted using the UTST method. TS targets including TSHR, SWG, energy cost, and generation and consumption for each utility in the system can also be calculated and recorded using the developed spreadsheet UTSI software tool. The temperature ranges for two hot water utilities in the Kraft Pulp Mill case study were divided into 2.5 °C intervals and the spreadsheet cycled through every logical combination of utility temperatures. In total, the targeting method was repeated 31,200 times to analyse the complete contours of targets for different combinations of utility temperatures. Maps can then be generated to provide additional insights regarding the shape of the various trade-offs.

5.6.1.1 HTHW Utility Hot and Cold Loop Temperature Selection

Figure 5-12 presents TSHR for different ranges of hot and cold temperatures for the HTHW utility, given a LTHW utility of T_{Cold}=30 °C, T_{Hot}= 45 °C, Option A (Figure 5-12a) and T_{Cold}=15 °C, T_{Hot}= 30 °C, Option B (Figure 5-12b).

It can be seen in both LTHW options HR increases for higher T_{Hot} values until it peaks when T_{Hot} is 95 °C, which is a process Pinch in the TS heat source profiles, and then HR decreases. On the other hand, as the result of increase in T_{Cold}, HR increases and remains approximately constant in a region for Option A. However, increases in T_{Cold} shows a decrease for Option B beyond 67.5 °C. When the utility target temperature passes the Site Pinch temperature, utility consumption and generation balance may change. Therefore, due to lack of heat sources the amount of HR will decrease. If the HTHW target temperature is adjusted above the Site Pinch temperature, no cold utility will be generated and the next cold utility (i.e. LTHW in this case) must tolerate all the heat which is rejected to the utility system. The consequence is a significant decrease in amount of HR. Therefore, 95 °C is chosen as the hot temperature for this case study.

Figure 5-13 shows the relation between the net HTHW consumption, HR, SWG, and UC in a range of different cold temperatures. Net utility consumption above the Pinch (i.e. heat source) has been assigned as positive values; below the Pinch (i.e. heat sinks) as negative values. Optimum T_{Cold} might be somewhere in the flat region which is formed as the result of maximum HR. This point represents the maximum HR and the minimum amount of utility cost as well as decrease in SWG. In this region balance between utility generation and consumption should be considered.

Figure 5-13a (option A) shows that HR increases as the T_{Cold} is increased with a constant region between 62.5 to 90 °C. To keep high heat transfer driving force in each utility loop and prevent significant increase in the amount of utility requirement, it is suggested to consider at least a 10 °C temperature difference between T_{Cold} and T_{Hot} in non-isothermal utility loops. Therefore, any temperature between 62.5 to 85 °C could be used for maximum HR; however, by considering temperature driving force and a small HR increase at 75 °C, this temperature will be the chosen as the optimum temperature. For option B (Figure 5-13b) a peak in

HR occurred, with the optimum T_{Cold} range located between 62.5 and 67.5 °C (i.e. constant HR). The HTHW consumption balance changes as T_{Cold} increases, prior to 67.5 °C utility consumption transferred to positive values which means there is no more utility generation and a decrease in HR. Therefore, 67.5 °C is the optimum HTHW cold temperature.

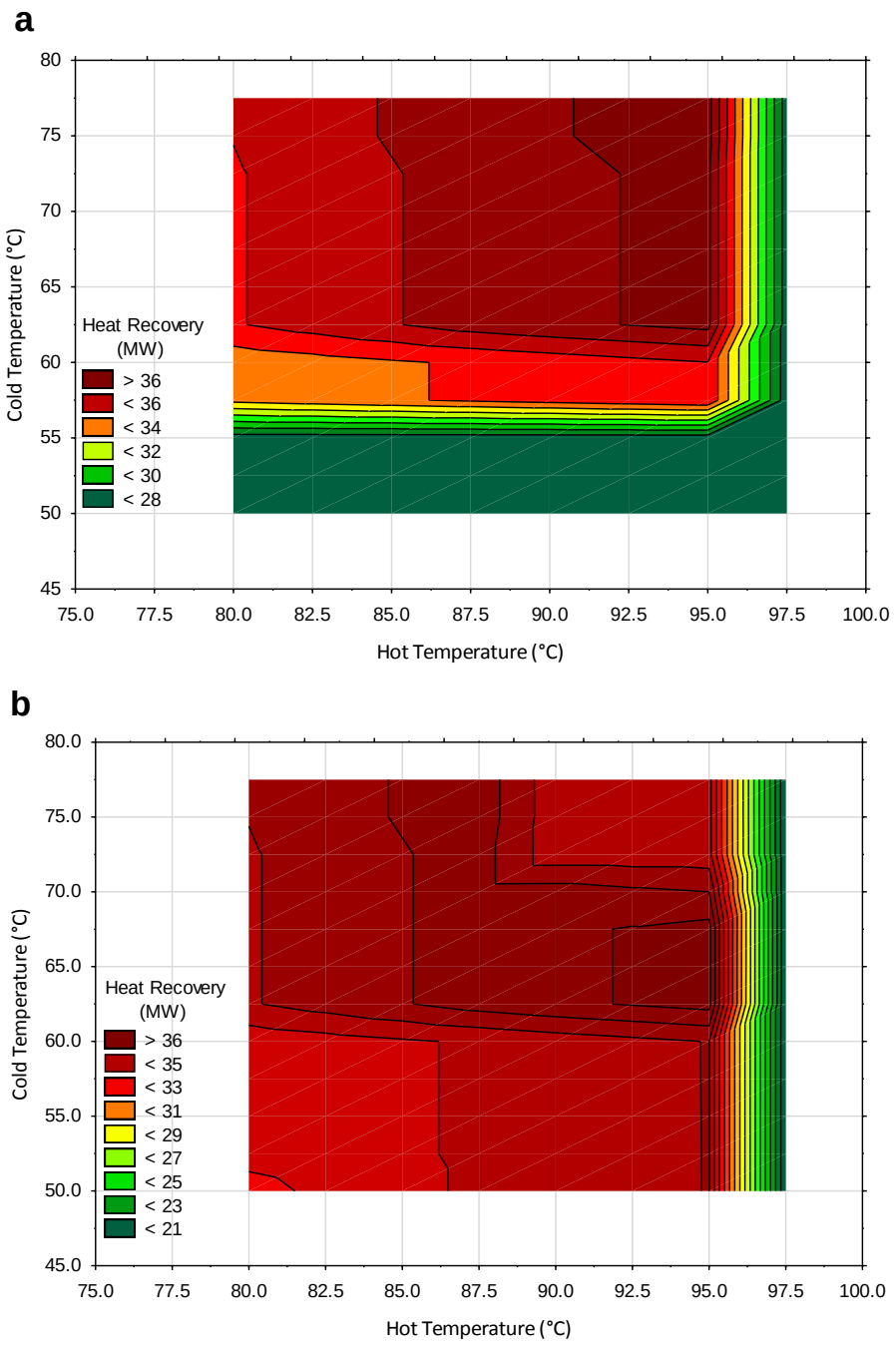

Figure 5-12: HR vs. variation of cold and hot temperatures for HTHW utility loop; a) option A, b) option B.

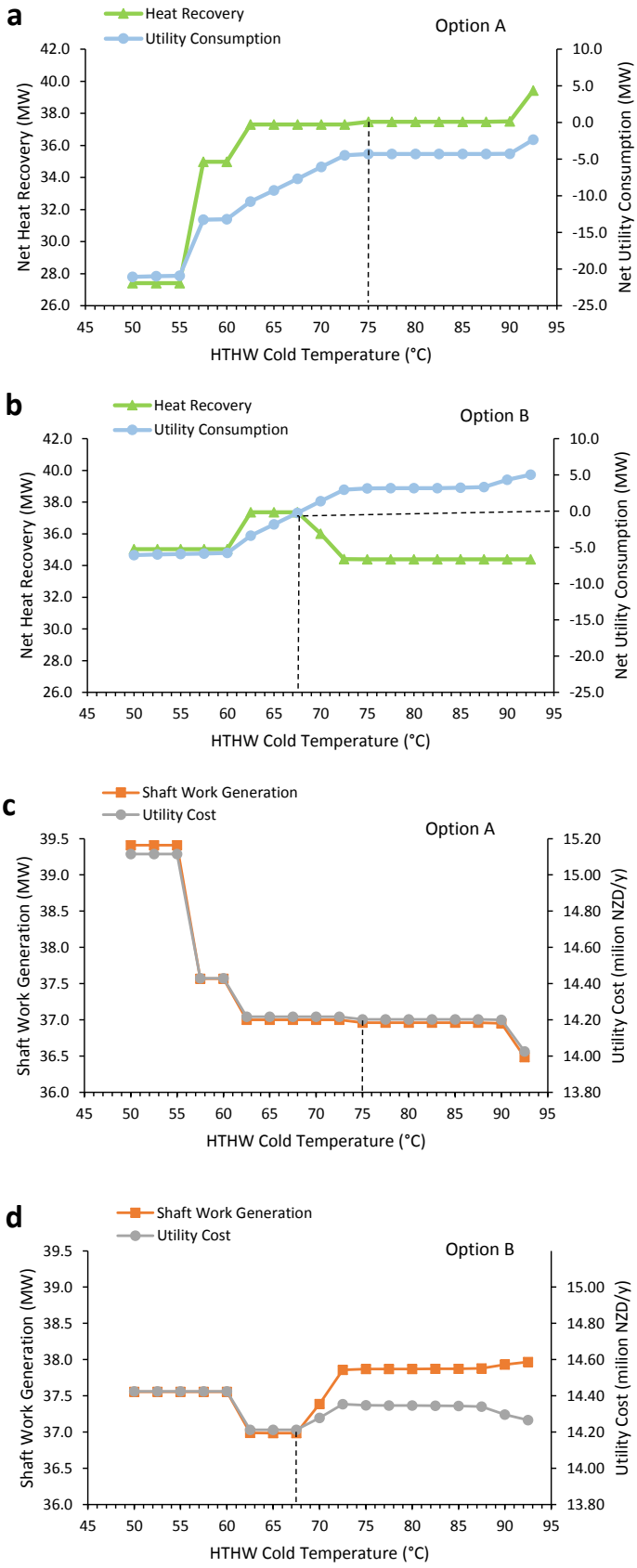

Figure 5-13: HR, HTHW consumption, SWG, and UC vs. cold temperature in Kraft Pulp Mill case study.

Figure 5-13c and Figure 5-13d show that in both cases the region with the highest HR presents the lowest utility cost and shaft work generation potential, which can be interpreted as an acceptable trade-off between shaft work decrease and increased HR. In summary, 75 °C as the cold temperature and 95 °C as the hot temperature have been chosen for the HTHW utility loop.

5.6.1.2 LTHW Utility Hot and Cold Loop Temperature Selection

To set hot and cold temperatures of the last utility loop, which in this case study is LTHW, additional constraints must be considered. Supply temperature of LTHW must be equal or lower than any temperature of process segments in the GCC in each individual process to prevent additional cold utility requirement; thus, T_{Cold} has been set to 30 °C. As shown in Figure 5-14, HR increases and remains approximately constant for T_{Hot} higher than 35 °C. The maximum possible target temperature is 45 °C. Beyond this point, a process Pinch occurs; therefore, additional utility is required. To keep the HR driving force within the highest range and minimise the amount of cold utility, T_{Hot} equal to 45 °C has been chosen as the optimum temperature. At this point, a steady rate of utility cost and shaft work is shown in Figure 5-14. Therefore, 30 °C as the cold temperature and 45 °C as the hot temperature have been chosen for the LTHW utility loop.

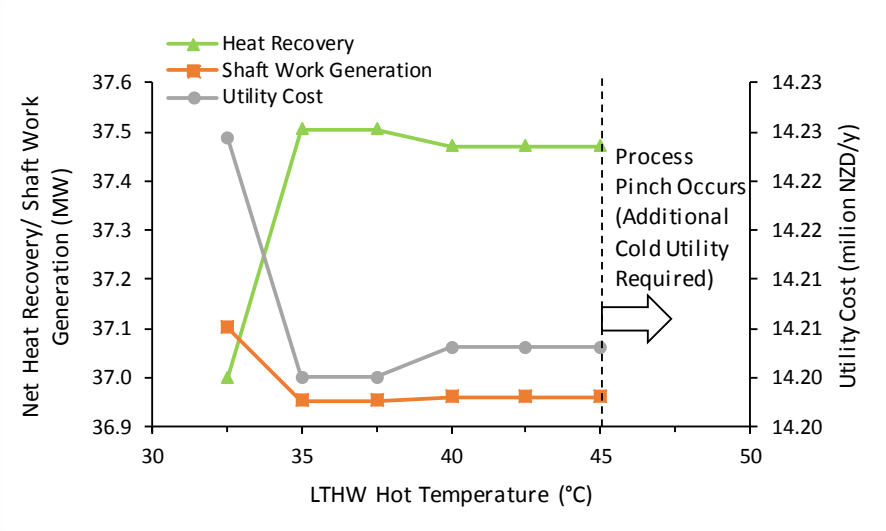

Figure 5-14: Optimum hot temperature selection for LTHW utility loop.

Figure 5-15 shows the initial SUGCC in dashed lines and optimised SUGCC in solid lines. As illustrated in Figure 5-15, by using optimised temperature ranges for HTWH and LTHW utilities, net HR increases up to 3.6 MW with an equal decrease

in LPS requirement. Generally, SWG drops only 0.5 MW compared to 3.6 MW increase in HR. Consequently, total utility savings of NZD 330,000 /y are achieved.

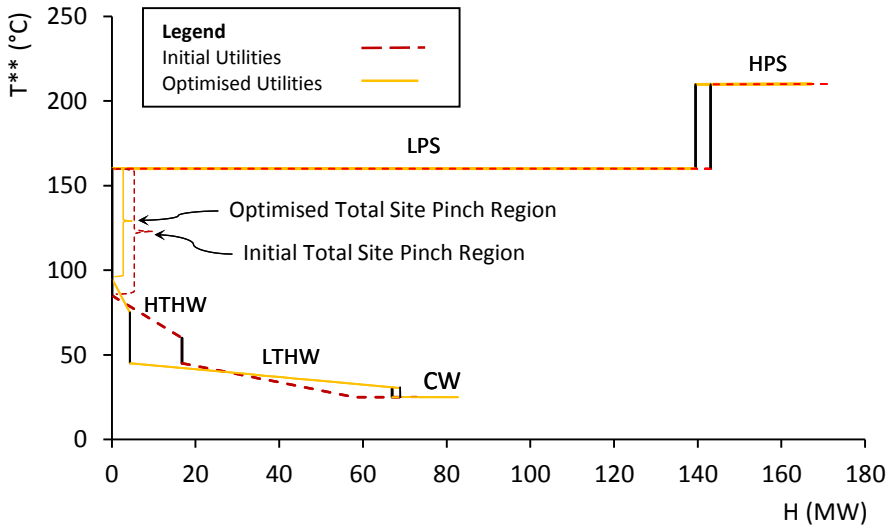

Figure 5-15: Comparison of optimised SUGCC with the base case for the Kraft Pulp Mill case study.

5.6.1.3 Learnings and Heuristics for Non-isothermal Utility Temperature Selection

Understanding gained from this exercise can be summarised into a set of new heuristics that may be able to narrow the search space for the TS utility temperature optimisation problem. Heuristics for supply and target temperature selection of non-isothermal utilities are:

- Constrain the optimisation to allowable utility cold and hot temperature ranges for each utility with consideration for limitations such as pipe pressure ratings, pumping costs, and product quality requirements.
- The optimum combination of utility cold and hot temperatures often occurs for a utility when its net consumption/generation is zero, if this is feasible.
- Increasing a utility's cold or hot temperature, generally shifts the balance of utility use in the direction of generating more cold utility (which is the same as consuming more hot utility). Decreasing a utility's cold or hot temperature has the opposite effect.
- If multiple combinations of cold and hot temperatures for an individual utility are equally optimal, selection of the combination with the greatest temperature difference between the utility supply and target

temperatures will minimise piping and pumping costs and maximise effective thermal storage.

5.6.2 The Effect of the Utility Price on Optimal Utility Temperature Selection

The utility price plays a significant role in the TAC. It may vary site to site and/or location to location. In this section, the effect of the utility price on the optimisation procedure has been studied. The optimisation procedure has been repeated for 5 different hot utility prices (25, 30, 35, 40, and NZD 45 /MWh) in the Kraft Pulp Mill case study. In all cases of different hot utility prices, identical utility optimal temperatures were achieved for all optimisable utilities in the TS as shown in Figure 5-16. This means the optimal utility temperatures are weakly dependent on the utility price for the utility price range that has been studied.

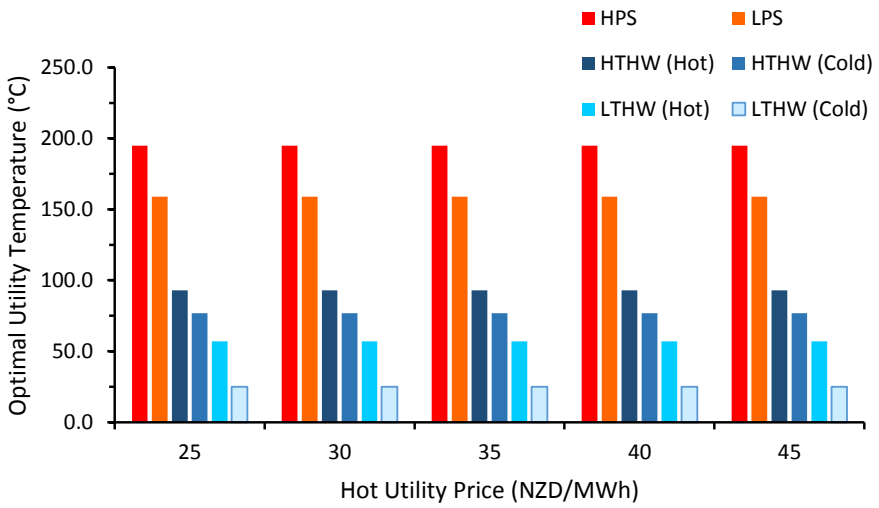

Figure 5-16: The effect of hot utility price on optimal utility temperatures for optimisable utilities in the Kraft Pulp Mill Case study.

Figure 5-17 illustrates the changes of the UC and TAC based on the optimisation results, and the TAC saving in each case with the different hot utility unit price. For each unit price, the optimisation result has been compared to its original unit price based on the case study's targets. As it can be seen in Figure 5-17, by increasing the hot utility price in the plant, the reduction in the UC and TAC may decrease based on the initial results. However, the net annual cost saving increases from NZD 664,574 /y, which is a 7.1 % cost reduction for NZD 25 /MWh to NZD 960,804 /y, which is 2.6 % cost reduction for NZD 45 /MWh.

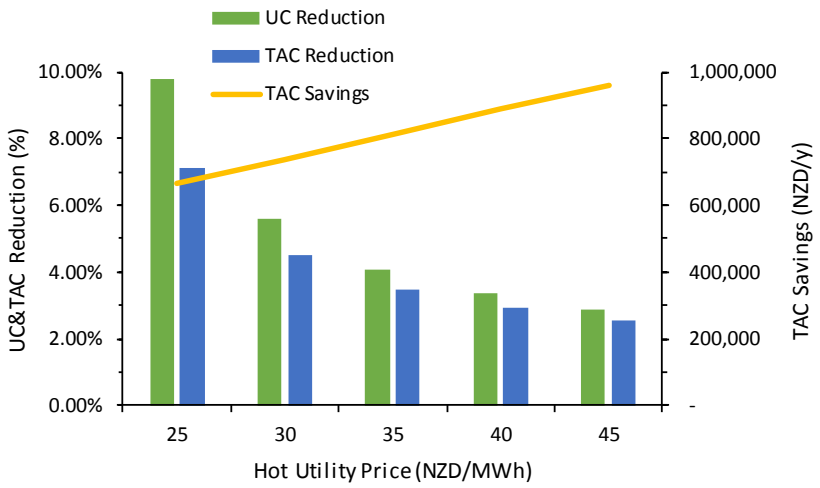

Figure 5-17: Changes in the percentage of UC and TAC reduction, and TAC savings for different hot utility prices in the Kraft Pulp Mill Case study.

5.6.3 The Effect of the Number of Utility Mains on Optimal Utility Temperature Selection

The number of utility mains can greatly affect TSHR, utility and ACCs as well as TAC. In this additional analysis, only four utility mains have been chosen for the Kraft Pulp Mill plant compared to the previous five utility mains to quantify the impact on TAC. HTHW and LTHW have merged together as a single Hot Water (HW) utility. Optimised utility temperatures for the new scenario are presented in Table 5-10.

Table 5-10: New required utility set for Kraft Pulp Mill case study.

Utility	Isothermal Utility		Non-Isothermal Utility		
	HPS	LPS	HW		CW
	T_{Hot} (°C)	T_{Hot} (°C)	T_{Hot} (°C)	T_{Cold} (°C)	T_{Cold*} (°C)
New Utilities	210.0	160.0	75.0	25.0	25.0
New Utility Optimal Temperatures	194.9	158.9	72.3	25.0	25.0

*Soft utility temperature

The new scenario of four utility mains has been targeted with and without optimisation. Results are presented in Table 5-11. After optimisation for the four utility mains case, TAC has decreased by 4.59 %, which offers NZD 773,406 /y of TAC savings. As a percentage, this reduction is not significantly higher than the previous analysis using five utility mains including HTHW and LTHW. In terms of absolute TAC, the optimised four utility mains case is 2.6 % higher than the optimised five utility mains case, NZD 406,031 /y (Table 5-5). In future work, the

TAC trade-off will include other capital costs, such as piping and civil works infrastructure, to correct choose between four or five utility mains.

Table 5-11: Utility targets comparison for four utility mains case and its optimised targets based on UC+ED+TAC criteria in Kraft Pulp Mill case study.

Optimisation Criteria	HEU Target #	TSHR Target kW	SWG kW	ED kW	UC NZD/y	TAC NZD/y	Change %
New Utilities	73	39,135	37,703	23,536	15,198,152	16,849,345	-
UC+ED+TAC	72	39,354	38,705	22,931	14,303,060	16,075,881	-4.59

5.6.4 Sensitivity Analysis of Optimisation Method

A sensitivity analysis has been carried out for the Kraft Pulp Mill case study to determine how parameters such as the temperature starting point and the temperature step size may affect the optimisation procedure and its results. At the first stage, two sets of different starting utility temperatures, Cases 1 and 2 in Table 5-12, have been selected to be applied to the presented procedure. Results have been compared with the optimised results from Section 5.5.1 based on the original utility temperature as a Base Case.

Table 5-12: Optimised utility temperatures comparison for different cases in Kraft Pulp Mill case study.

Start Point Temperatures	Isothermal Utility			Non-Isothermal Utility			
	HPS	LPS	CW	HTHW		LTHW	
	T_{Hot} (°C)	T_{Hot} (°C)	T_{Cold} (°C)	T_{Hot} (°C)	T_{Cold} (°C)	T_{Hot} (°C)	T_{Cold} (°C)
Base Case	210.0	160.0	25.0	85.0	60.0	45.0	25.0
Case 1	230.0	160.0	25.0	90.0	70.0	40.0	25.0
Case 2	210.0	140.0	25.0	90.0	70.0	35.0	25.0
Base Case Optimised	194.9	158.9	25.0	93.0	76.8	57.0	25.0
Case 1 Optimised	194.9	158.9	25.0	93.0	76.8	49.0	25.0
Case 2 Optimised	162.0	138.9	25.0	93.0	76.8	49.0	25.0

Table 5-13 presents the TS targets for the all three optimised cases from Table 5-12. Results converged to similar optimal temperatures for the three cases with a couple of exceptions. The optimised LTHW hot temperature in Case 1 differs from the Base Case, which slightly lowers the TAC target. In Case 2, HPS does not converge to the same temperature as the other cases, which affects its TS target. SWG decreases by 2.7 % and TAC increases by 14 % compared to the Base Case.

Appropriate selection of the initial utility temperatures is important. Utility temperatures may be selected by experience and in conjunction with viewing the TSP where the shape provides valuable information about potential utility mains temperatures. As can be seen in Figure 5-6, the heat sink profile has a flat region around 157 °C and a steep slope in temperature range immediately below 157 °C. If an isothermal utility, i.e. LPS, temperature is chosen below 157 °C, the optimal temperature may not converge above the region's higher boundary. As a result, a logical initial temperature for LPS is >157 °C, as selected in the Base Case.

Table 5-13: Comparison of optimised objective functions with the base case in Kraft Pulp Mill case study.

Start Point Temperatures	TSHR kW	SWG kW	ED kW	UC NZD/y	TAC NZD/y	Change %
Base case	44,845	37,384	20,242	13,804,364	15,669,850	-4.51
Case 1	44,845	37,384	20,196	13,804,364	15,672,299	-4.48
Case 2	44,845	36,399	21,064	16,923,756	18,688,636	13.90

Different step sizes have been considered to study the sensitivity of the presented optimisation procedure. The procedure has been carried out using initial 16 °C step size. It has been repeated for 0.1, 1.0, 8.0, and 24.0 °C. Table 5-14 shows the optimal temperatures for different step sizes. The original temperatures are considered as the utility temperature starting points and targets are repeated for each step size. As it can be seen in Table 5-14, for 8.0 °C and 24.0 °C step size, the same optimal temperature can be achieved. For the 1.0 °C, only cold side of HTHW converged 1.8 °C lower than the optimal case. For the very small step size (0.1 °C) final temperatures did not converge as it may be due to the local optimums of the optimisation function.

Table 5-15 presents TS targets deviation from the initial 16 °C optimal temperature results after optimisation carried out using different step sizes. Only the deviation of the 0.1 °C step size can be taken into an account as it is not converging the optimal utility temperature. It means, it is not easy to adjust utility temperatures by very small amounts due to operational uncertainties such as heat loss and hydraulic difficulties. Therefore, from both Table 5-14 and Table 5-15 it can be said that step size does not have a direct effect on optimisation procedure; however, smaller step sizes may not present accurate results due to unpredicted optimums

in the objective functions. On the other hand, larger step sizes can cover a wide range of the objective function in the mathematical procedure; thus, larger step sizes may present more accurate results.

Table 5-14: Optimised utility temperatures for different step sizes.

Step Size (°C)	Isothermal Utility			Non-Isothermal Utility			
	HPS	LPS	CW	HTHW		LTHW	
	T_{Hot} (°C)	T_{Hot} (°C)	T_{Cold} (°C)	T_{Hot} (°C)	T_{Hot} (°C)	T_{Hot} (°C)	T_{Cold} (°C)
0.1	201.3	158.9	25.0	90.9	60.5	45.0	25.0
1.0	194.9	158.9	25.0	93.0	74.6	57.0	25.0
8.0	194.9	158.9	25.0	93.0	76.9	57.0	25.0
16.0*	194.9	158.9	25.0	93.0	76.9	57.0	25.0
24.0	194.9	158.9	25.0	93.0	76.9	57.0	25.0

*Step applied in initial case study analysis

Table 5-15: Deviation from TS targets for different step sizes compared to initial 16 °C step.

Step Size (°C)	TSHR Deviation %	SWG Deviation %	ED Deviation %	UC Deviation %	TAC Deviation %
0.1	-1.3	0.0	0.0	0.8	0.8
1.0	-0.4	0.1	0.2	0.1	0.1
8.0	0.0	0.0	0.0	0.0	0.0
24.0	0.0	0.0	0.0	0.0	0.0

5.7 Conclusions

This chapter presented a new TSHI utility temperature selection and optimisation method that can optimise both non-isothermal (e.g. hot water) and isothermal (e.g. steam) utilities. The optimisation affects HR, the number of heat exchangers in the Total Site Heat Exchanger Network, heat transfer area, ED, UC, ACC, and TAC. Three optimisation parameters, UC, ED, and TAC have been incorporated into a derivative based optimisation procedure where derivatives are minimised sequentially and iteratively based on the specified approach. The new optimisation procedure has been carried out for three different approaches as the combinations of optimisation parameters based on the created derivative map. The challenge is now to apply these optimal utility temperatures and synthesis a complete HEN that achieves the targets from the UTST method compared with the network that is designed based on the CTST method.

Chapter Six

Heat Exchanger Network Synthesis and Design[1]

6.1 Introduction

After TSHI targets are set, the challenge is then to design a HEN that meets (or nearly meets) the target. As it is shown in Figure 6-1, a HEN for an industrial process may be considered to contain a Heat Recovery Network (HRN) with, process-process heat exchanger matches and a Utility Exchanger Network (UEN), process-utility matches. HRN refers to intra-process HI, which may be targeted, together with utility use, using PI techniques, such as PA. In studies on conventional TSHI (Klemeš et al., 1997), minimal details on the synthesis and design of the UEN are presented. This was likely due to the simplicity of the problem for a steam system where all utility exchangers may be in a parallel arrangement. As discovered in Chapter 2, there is a gap in the literature regarding UEN synthesis based on TSHI techniques for utility systems that use non-isothermal utilities.

The aim of this Chapter is to compare UENs that achieve the TSHI targets of the conventional method and the new unified method. To achieve the aim, UEN synthesis methods are defined for the conventional and Unified TSHI methods such that their targets may be achieved through the design. TSHI targets are based on the global (or process- or stream-specific) minimum approach temperature, ΔT_{min}, concept. However, when it comes to the HEN design phase, a different Exchanger Minimum Approach Temperature (EMAT) may also be set. An EMAT provides a degree of freedom that can enable reductions in the number of heat

[1] This chapter is based on a recent conference paper in Chemical Engineering Transactions cited as (Tarighaleslami et al., 2017c) and full journal article cited as (Tarighaleslami et al., 2018) published in Energy.

Tarighaleslami, A.H., Walmsley, T.G., Atkins, M.J., Walmsley, M.R.W., Neale, J.R., 2017b. A Comparison of Utility Heat Exchanger Network Synthesis for Total Site Heat Integration Methods. Chemical Engineering Transactions 61, 775–780. doi:10.3303/CET1761127

Tarighaleslami, A.H., Walmsley, T.G., Atkins, M.J., Walmsley, M.R.W., Neale, J.R., 2018. Utility Exchanger Network synthesis for Total Site Heat Integration. Energy 153, 1000–1015. https://doi.org/10.1016/j.energy.2018.04.111

exchangers needed for the HEN to achieve the process and/or TS target. As a result, this chapter also investigates the impact of EMAT on HEN design given the stream data with optimised utility temperatures from Chapter 5. The developed TSHI software tool has been used to calculate targets based on both Conventional and Unified TSHI methods. SuperTarget™ by KBC Advanced Technologies (KBC, 2017) has been used to design the networks.

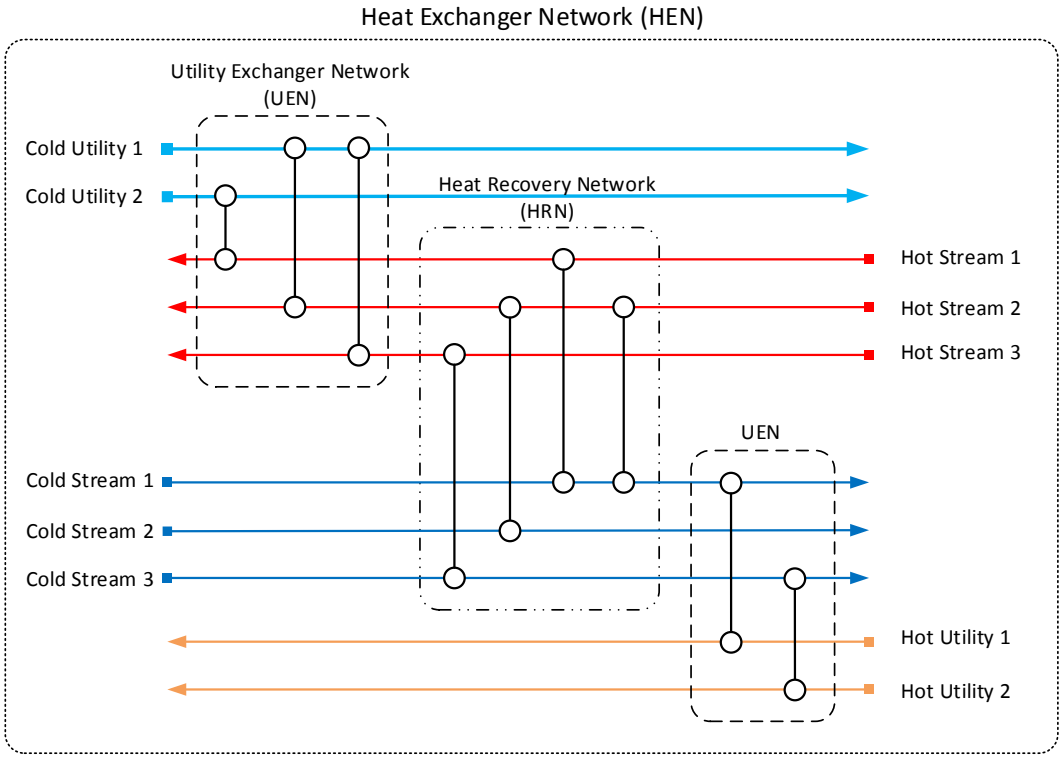

Figure 6-1: A schematic of HEN containing HRN (process-process matches) and UEN (utility-process matches).

6.2 Utility Heat Exchanger Synthesis and Design Method

In this chapter, two methods are applied to perform both HRN and UEN synthesis, with emphasis on the UEN. The methods are only applied to the Södra Cell Värö Kraft Pulp Mill using the optimised utility temperatures from Chapter 5.

The network design methods for the two TSHI methods are given in the next two sections.

6.2.1 Utility Exchanger Network Design Based on the CTST Procedure

To design UEN based on the CTST method the following steps should be applied.

i. Target process HR and utility use;

ii. Design HRN and identify/extract stream segments that need utility for each process;
iii. Target TSHI using the composite of process stream segments that require utility; and,
iv. Design the arrangement of the UEN based on the process stream segments available.

6.2.2 Utility Exchanger Network Design Based on the UTST procedure

To design UEN based on UTST method, as the utilities are targeted in process level, Chapter 4, based on methods constraint TS network design is easier. Therefore, the following steps should be applied.

i. Target process HR and utility use;
ii. Simultaneously design the HRN and UEN for each process assuming a utility may be constrained to be supplied from and returned to the utility system at specified temperatures; and,
iii. Calculate the quantum of TSHR that is achievable based on the balance of sources and sinks for each utility.

Following each of these methods, the automated network design function in SuperTarget™ is applied to generate the HRN and UEN based on the two procedures.

6.3 Utility Heat Exchanger Network Synthesis and Design Results

UEN has been strictly designed based on the CTST and UTST methods. As explained in Chapter 4, CTST methods inherently allow a utility's target temperature to be met using heat exchanger matches in series and/or in a parallel configuration or even by only a single heat exchanger from any process. On the other hand, the new UTST method allows heat exchangers to be in both parallel and series configuration to achieve the utility target temperature, if and only if the heat exchangers in series are from the same process. To demonstrate the merits of the new Unified TSHI method and its target, non-isothermal utility networks for the Kraft Pulp Mill case study (i.e. HTWH and LTHW) are targeted, and HENs designed and analysed.

6.3.1 High Temperature Hot Water Network Design

Figure 6-2 shows a comparison of UEN designs based on the CTST method versus the UTST method for HTHW utility in the Kraft Pulp Mill plant considering EMAT 10 °C. There are four matches in series in each branch for the CTST design (Figure 6-2a). These matches require (before network relaxation) the HTHW utility to be supplied to the Wash process, then piped to Causticizing, subsequently to Miscellaneous 4, and then finally to the Digestion process. The UTST design avoids such matches (Figure 6-2b).

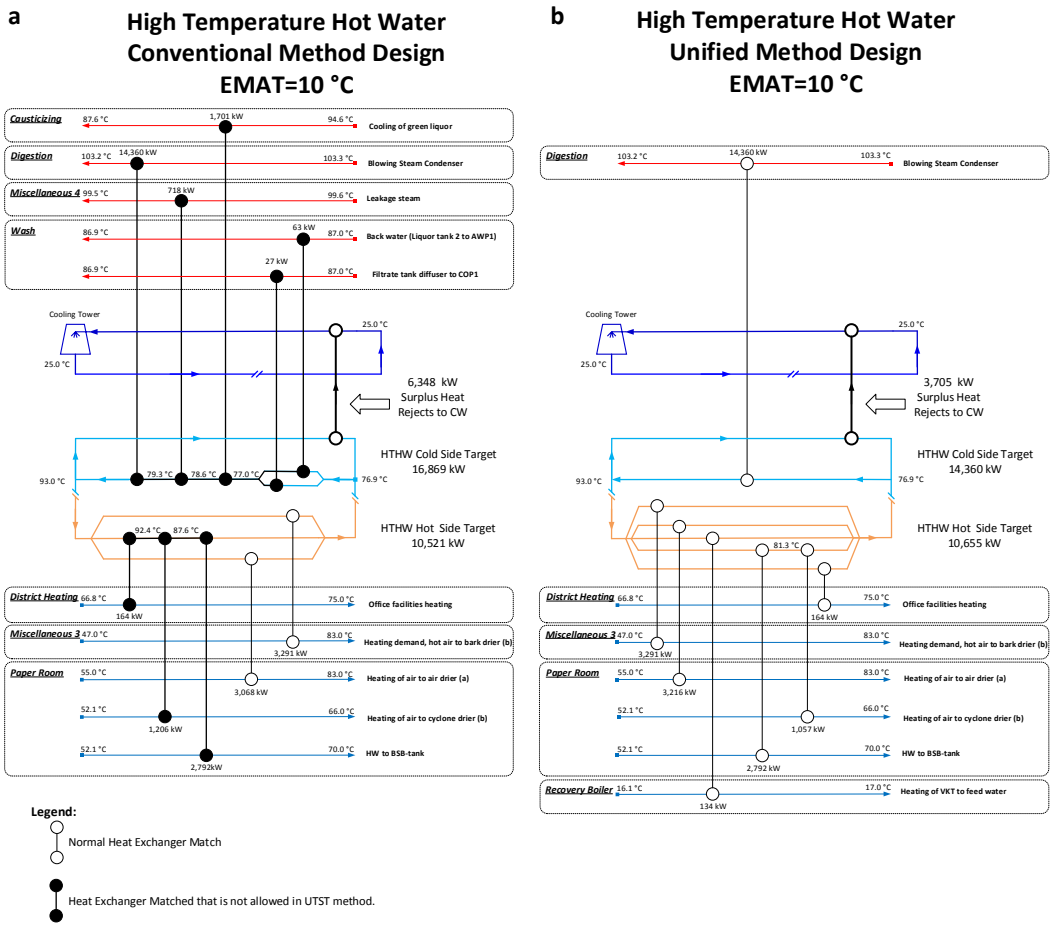

Figure 6-2: HTHW Loop design considering EMAT = 10 °C, for a) Conventional method; b) Unified method.

6.3.2 Low Temperature Hot Water Network Design

Figure 6-3 shows a comparison of UEN designs based on CTST method versus UTST method for LTHW utility of the Kraft Pulp Mill plant considering EMAT 10 °C.

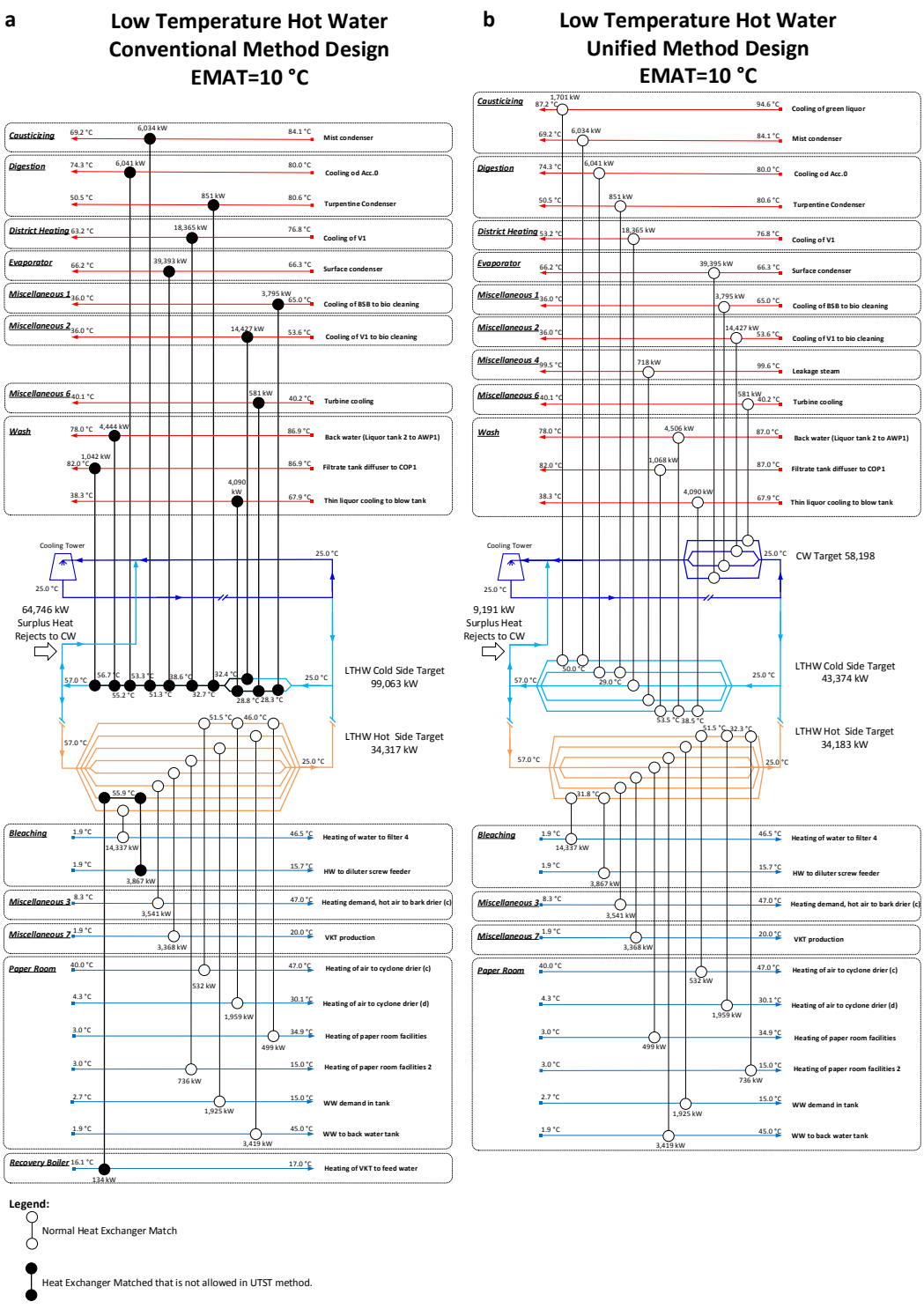

Figure 6-3: LTHW Loop design considering EMAT = 10 °C, for a) Conventional method; b) Unified method.

As shown in Figure 6-3a, all matches on the cold side of the loop are in a series arrangement. This means the LTHW utility is supplied, as an example for the lower branch, to the Miscellaneous 1 process, then passed to the Miscellaneous 6 process, and so on through each of the series matches. Two branches on the hot

side of the loop also contain series matches between different processes. Like the HTHW designs, the UTST design avoids such an arrangement (Figure 6-3b).

6.3.3 HTHTW and LTHW Networks Design Considering EMAT 7.5 °C

Different EMAT may generate different UEN designs because of the structural differences it applies in HEN and as well as in HRN.

The HEN has been redesigned for all processes considering EMAT 7.5 °C for each process. Figure 6-4 shows new UEN design based on EMAT 7.5 °C for HTHW loop. However, there are stil four matches in series for the CTST design (Figure 6-4a) while the UTST design avoids such matches (Figure 6-4b).

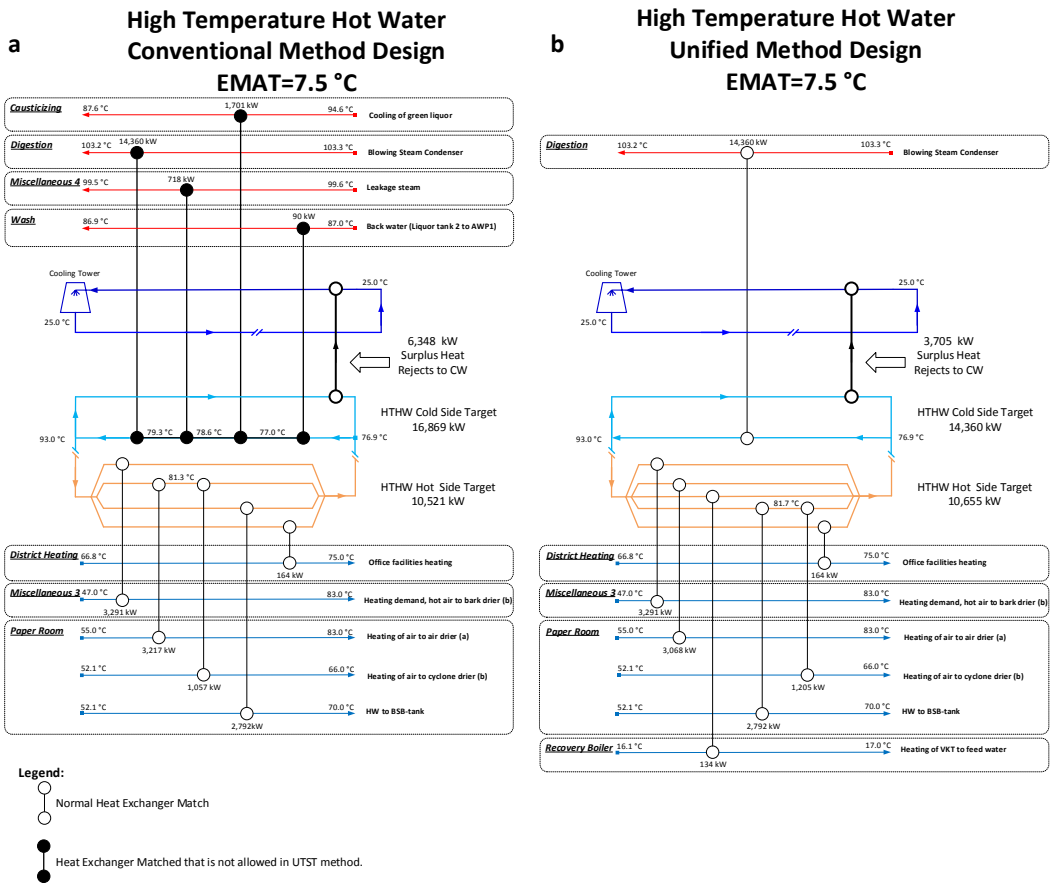

Figure 6-4: HTHW Loop design considering EMAT = 7.5 °C, for a) Conventional method; b) Unified method.

Figure 6-5 shows new UEN design based on EMAT 7.5 °C for the LTHW loop. In this new design, as shown in Figure 6-5a, all matches on the cold side of the loop are in a series arrangement. One branch on the hot side of the loop also contain series matches between different processes. Like the HTHW designs, the UTST design avoids such an arrangement (Figure 6-5b).

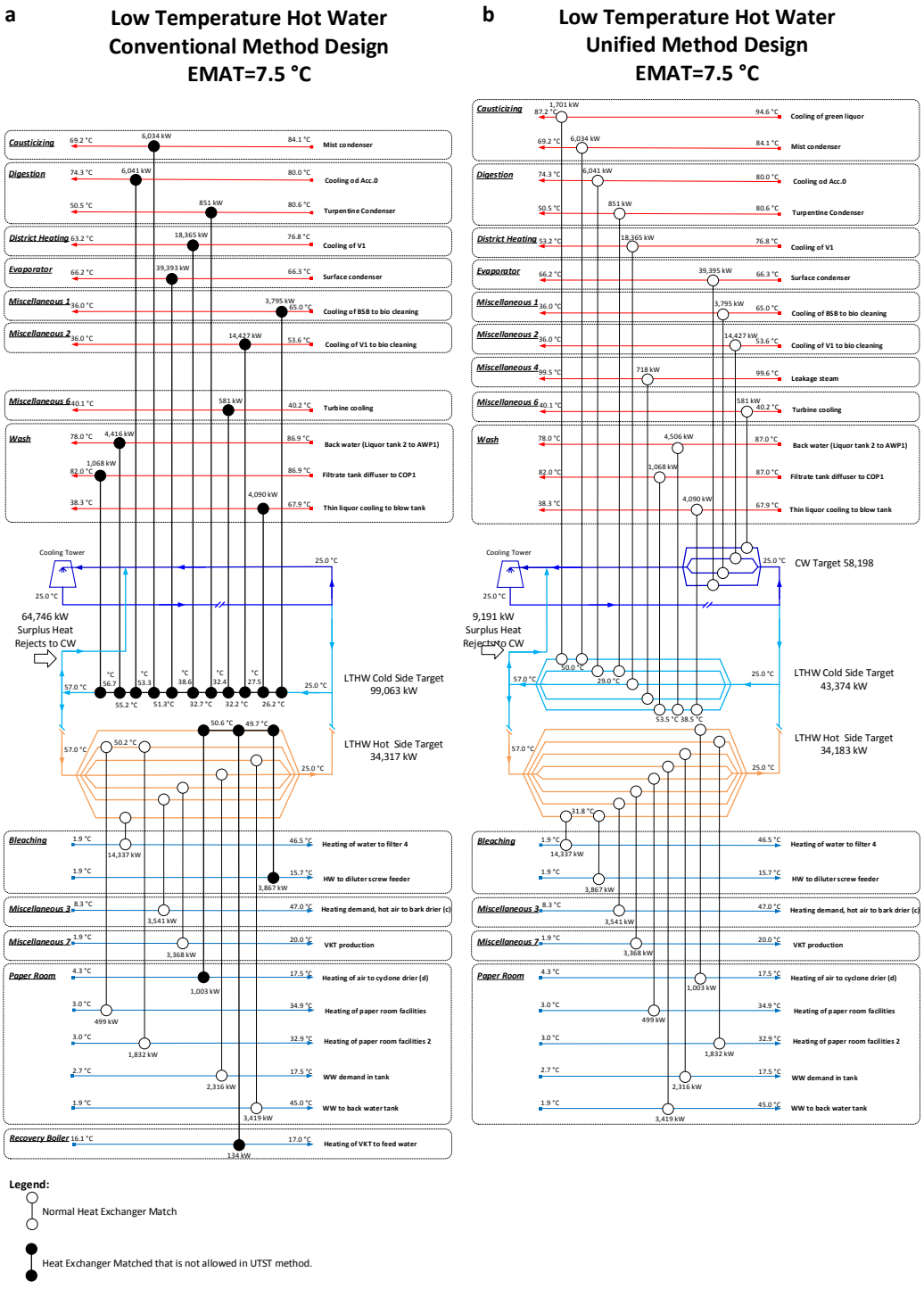

Figure 6-5: LTHW Loop design considering EMAT = 7.5 °C, for a) Conventional method; b) Unified method.

6.4 Discussion

The difference between UEN designs may be considered in four aspects: i) TSHI targeting method differences in design; ii) energy and mass balance of utility loop, iii) HR targets; and iv) structural differences in design.

6.4.1 Impact of TSHI Method on Utility Exchanger Network Design

Different TSHI methods may generate different UEN designs because of the differences in the targeting method and any inherent constraints.

As it can be seen in Figure 6-2a and Figure 6-3a, in both cold and hot sides of HTHW and LTHW loops, series matches are required to achieve the conventional TSHI target. For instance, to achieve the target of hot water generation for the LTHW loop, 11 heat exchangers receiving heat from 8 different processes and zones. To implement such as solution, which is required to achieve the conventional TSHR and utility targets, would be problematic. The pipework required for such a series of matches would be extremely expensive. If one of the processes were to be out of service, it would affect the utility supply temperature to the subsequent process, which may cause operational and/or control issues. It also means the specified target temperature of the utility may not be achieved, potentially propagating process control issues to the hot side of the LTHW system. For this case study, the UEN for the LTHW may be relaxed with no decrease in HR because the sources for the LTHW greatly exceed the sinks. In other cases, such relaxation may not be possible, effectively decreasing the usefulness of the TS target with respect to non-isothermal utility loops.

The unified TSHI method forbids series matches of utility between different processes (Figure 6-2b and Figure 6-3b). This is inherent in the way the TS target is formulated. As a result, the unified method does not use similar series utility matches between processes. Some process-utility matches are therefore different. For example, “Heating of VKT to feed water” stream from Wash process is on LTHW for the conventional TSHI method design and on the HTHW for the unified TSHI method.

6.4.2 Heat and Mass Balancing of Non-Isothermal Utility Loops

Since the case study is a Kraft Pulp Mill plant, the process inherently generates large quantities of low grade heat. As a result, the LTHW and HTHW loops have excess heat, i.e. the source duty is much greater than sink duty. In a final design of UEN, each utility must be balanced in terms of mass and energy for both cold and hot sides. Surplus heat must be rejected to a cooling system, e.g. air-cooled heat

rejection, to maintain a successful operation. The surplus heat may also be considered as a heat source for other uses within another local system such as district heating stream or to the other plants in the cluster. In other cases, a utility loop may have a deficit of heat, which must be provided from higher temperature utilities, e.g. LPS, or directly from the furnace.

As it can be seen in Figure 6-2a, the HTHW loop receives 16.87 MW from process sources on its cold side; however, it only transfers 10.52 MW from the hot side to process sinks. The 6.35 MW surplus heat must be rejected from the utility, e.g. the CW in cooling tower cycle. Similarly, in LTHW loop, the cold side receives 99.06 MW from the process sources and supplies 34.32 MW to process sinks in the UEN design based on the conventional method, Figure 6-3a. The difference, 64.74 MW, must be rejected to the cooling system or to another process. A similar balancing must occur for the UTST method (Figure 6-2b and Figure 6-3b).

A network relaxation approach may be applied to reduce the imbalance between sources and sink connected to a non-isothermal utility. Relaxation may help reduce and eliminate series matches in CTST. In this case, excluded streams may provide surplus heat directly to the cooling system. Another option to transfer heat from the utility loop itself to the cooling system. This heat may be transferred indirectly using a heat exchanger (Figure 6-2) or by directly mixing fluids if the two systems use the same fluid, i.e. water. The advantages of the direct mixing is that the mass balance of the utility loop can be controlled simultaneously with the heat balance of the loop, Figure 6-3. In case of indirect heat transfer from non-isothermal utility loop to the cooling system, utility storage tank will be required.

6.4.3 Utility Targets Before and After HEN Design

After the full HRN and UEN networks are designed, it may not achieve the targets set for the CTST method. Targets assume the HRN is designed such that stream segments that require utility exactly match GCC segments.

GCC is an extreme condition in the network design. Any time there is a temperature difference between utility profiles and process profiles; there is a flexibility that the site does not have to operate at exact minimum approach temperature and exact targets won't necessarily be achieved that match the GCC.

The final split between utilities is affected by the design of the HRN because it determines the actual stream segments left over for use at the TS level and, therefore, how much utility is consumed. The UTST method does not face the same problem because both the HRN and UEN are designed at the process level. If process level targets are achieved, TS targets must also be achieved. Table 6-1 presents a comparison between total cold utility and total hot utility targets as well as heat receive and supply targets for each utility loop before and after network design based on both conventional and unified TS methods.

Table 6-1: Comparison of utility targets before/after UEN design based on CTST and UTST methods.

Targeting Method	Q_{Hot} (MW)	Q_{Cold} (MW)	Heat Supplier Utility				Heat Receiver Utility		
			HPS (MW)	LPS (MW)	HTHW (MW)	LTHW (MW)	HTHW (MW)	LTHW (MW)	CW (MW)
UTST	213.04	115.93	27.74	140.47	10.65	34.18	14.36	43.37	58.20
UTST after Network Design	213.04	115.93	27.74	140.47	10.65	34.18	14.36	43.37	58.20
CTST	213.04	115.93	27.74	140.42	10.55	34.32	17.49	98.44	0.00
CTST after Network Design	213.04	115.93	28.29	139.92	10.52	34.32	16.87	99.06	0.00

6.4.4 Impact of Exchanger Minimum Approach Temperature on Utility Exchanger Network Design

A modification in EMAT causes fundamental changes in HEN's structure, as result, UEN design changes. For example, Figure 6-4a shows that "Filtrate tank diffuser to COP1" stream from Wash process has been eliminated and the heating load has been carried out to process or other utility process matches. Therefore, utility branch and one heat exchanger unit in cold side of the HTHW utility is eliminated compared to the similar case with EMAT 10 °C (Figure 6-2a).

In the hot side of the HTHW new design based on the CTST method, there are no series matches between different processes as a result of a change in EMAT in UEN design. However, this design change has an influence on the UEN design of UTST method (Figure 6-4b where the exchanger heat loads and intermediate stream temperatures differ for the series matches in the new design compared to the initial UEN design (Figure 6-2b).

Similar changes can be seen in both hot and cold sides of the LTHW loop for the new design using EMAT 7.5 °C. In Figure 6-5a, for the cold side of the LTHW loop, utility branch has been eliminated compared to the same case in Figure 6-3a while all 11 heat exchangers placed in the series configuration allowing the utility passes through each process.

Comparison between the hot side of the LTHW utility for both designs (Figure 6-3b and Figure 6-5b) shows the influence if EMAT for both HEN and UEN networks. As it can be seen in Figure 6-3b, there are one series matches in the utility branch that LTHW is supplied to, i.e. Boiler Recovery process and Bleaching process. Other series configuration in this network only supplied utility in one single process, which is allowed based on UTST method constraints. The changes of EMAT impacts on the configuration of the UEN where the unacceptable series matches supplies LTHW utility to the Paper Room process, then passes through Recovery Boiler Recovery Boiler process and finally Bleaching process. In addition, in this design, compared to previous design (Figure 6-3b), "Heating of air to cyclone drier" stream in the Paper Room process has been eliminated therefore 11 heat exchangers in initial designed is reduced to 10 exchangers in the new design.

It is notable that in both designs for both HTHW and LHTW loops, utility and HR targets remain constant as well as the balance of surplus heat that is rejected to the cooling system. Also, the utility and HR targets remain identical before and after UEN design in the Unified TSHI method for both different EMAT designs, while it changes after UEN design in the Conventional TSHI method (as shown in Table 6-1). This supports the proposition made in Chapter 4, that the Unified TSHI method's targets are more achievable than targets calculated using Conventional TSHI methods.

6.5 Conclusions

This chapter presented a comparison of Utility Exchanger Network design between utility and TSHR targets achieved based on the CTST and the UTST methods presented in Chapter 4. UENs were strictly designed to achieve the targets for two TSHI methods. Non-isothermal utilities have been studied for the Kraft Pulp Mill case study, i.e. HTHW and LTHW loops. UEN design has been

repeated using different EMAT to show the impact of the heat exchanger's minimum approach temperature on the HEN design. Also, the utility and HR targets before and after UEN design have been compared for both TSHI targeting methods. Although the new method showed an improved design and practical application, there has been the challenge of how to control non-isothermal utility loops where the target temperatures of both the process and utility flow should be achieved. The design of TSHI for non-isothermal utility loops considering bi-objective control has been identified as an area that requires additional research. The development of effective TS designs including process control are essential to promotion and realisation of TS heat recovery benefits in industry.

In the next chapter, further developments on TSHI including the merits of assisted heat transfer technique for increasing shaft power generation in TS plants and the application of heat transfer enhancement in TSHI will be discussed.

Chapter Seven

Further Developments on Total Site and Indirect Heat Recovery Concepts[1]

7.1 Introduction

In previous chapters, new TSHI targeting, optimisation, and design methods have been developed and applied. The aim of this chapter is to explore new horizons in TSHI using newly developed HTE techniques such as nanotechnology, i.e. nanofluids, and HI concepts that have received limited attention.

In the first half of this chapter, Section 7.2, the concept of assisted heat transfer in TSHI has been studied to develop a new method for an increase in shaft work targets within the TS. Generally, TSHI method prioritises intra-process HI before searching for inter-process HI opportunities via the utility system (Klemeš et al., 1997) and/or dedicated indirect HR systems (T. G. Walmsley et al., 2014a). As mentioned, the TSHI method has five main steps: i) process and stream data specification, ii) process level Pinch Analysis, iii) extraction of excess heating and cooling loads from process GCCs, iv) TSP composition, and v) TS utility consumptions targeting. This section focuses on step iv and, specifically, on the removal internal HR pockets that occur before TSP composition, which may be exploited to assist TSHR and SWG.

[1] This Chapter is based on three publications – two conference papers in Chemical Engineering Transactions cited as (Tarighaleslami et al., 2015) and (Walmsley et al., 2016), and one full journal paper in Applied Thermal Engineering cited as (Tarighaleslami et al., 2016b):

Tarighaleslami, A.H., Walmsley, T.G., Atkins, M.J., Walmsley, M.R.W., Neale, J.R., 2016. Heat Transfer Enhancement for site level indirect heat recovery systems using nanofluids as the intermediate fluid. Applied Thermal Engineering 105, 923–930. doi:10.1016/j.applthermaleng.2016.03.132

Tarighaleslami, A.H., Walmsley, T.G., Walmsley, M.R.W., Atkins, M.J., Neale, J.R., 2015. Heat Transfer Enhancement in Heat Recovery Loops Using Nanofluids as the Intermediate Fluid. Chemical Engineering Transactions 45, 991–996. doi:10.3303/CET1545166

Walmsley, T.G., Atkins, M.J., Tarighaleslami, A.H., Liew, P.Y., 2016. Assisted Heat Transfer and Shaft Work Targets for Increased Total Site Heat Integration. Chemical Engineering Transactions 52, 403–408. doi:10.3303/CET1652068

The second half of the chapter, Section 7.3, presents the implementation of Heat Transfer Enhancement (HTE) techniques in TSHI. As discussed in the literature review, two main groups are considered in HTE; active techniques and passive techniques. Passive techniques have been considered in HI as it offers an increase in HR by changing the geometry in heat exchange equipment. However, recently, the merits of adding nanoparticles as an additive to fluids to increase heat transfer coefficient of the fluid and the rate of heat transfer have been investigated. For instance, substituting coolant fluid with nanofluid in car radiators shows a significant increase in heat transfer rate within the car engine. Therefore, the idea of using nanofluid as heat transfer medium in the utility system of an industrial site has been raised. This section studies the implementation of nanofluid in a site level indirect HR systems.

7.2 Assisted Heat Transfer and Shaft Work Targets for TSHI

Process HR pockets can assist in increasing TSHR. Bagajewicz and Rodera (2000) introduced the idea of assisted heat transfer for directly integrating two processes. Their analysis showed that heat integration between two (or more) processes should chiefly occur between the processes' Pinch Temperatures. However, in some presented cases, maximum HR was only achieved by utilising a process HR pockets, which are normally removed in conventional TSHI (Klemeš et al., 1997), for inter-process integration. For their two process case study, a tabular cascade analysis demonstrated that the Pinch of one plant could exchange heat with a HR pocket of the other process, and thereby increase overall HR. Later, Bandyopadhyay et al. (2010) revisited the idea of assisted heat transfer using a graphical TSHI approach. Their study recommended that GCCs are shifted to the utility temperature scale before segments of HR pockets are removed. Segments of pockets on the right hand side of a new intersection point within the pocket were marked for intra-process HR (i.e. removed), while the left hand segments continued to form part of the TSP. Bandyopadhyay et al. (2010) demonstrated that for one example case the modified TSHI method increased TSHI. However, as will be shown in this paper, such an increase in TSHI is not a generally applicable result.

Process HR pockets can also assist in increasing SWG in TS. Cascading steam from high pressure to the demand using turbines for efficient power production is

commonplace in TSHI (Sun et al., 2013). The concept of assisted shaft work is to utilise a pocket to, first, generate a higher quality steam, e.g. MPS, that is needed by another process and then, second, consume a lower quality steam, e.g. LPS, that is needed by the pocket. As a result, steam is cascaded from high to low pressure, providing an opportunity to assist TS shaft work by integrating with a Combined Heat and Power (CHP) system.

This chapter investigates how assisted heat transfer and assisted shaft work targets can be calculated for increasing TSHI. The conventional TSHI method of Klemeš et al. (1997) and the modified TSHI method of Bandyopadhyay et al. (2010), are compared against the proposed TSHI method, which begins with the conventional TSHI and improves the targets by including assisted heat transfer and shaft work.

7.2.1 Assisted Heat Transfer Theory

The concepts of assisted heat transfer (Figure 7-1) and assisted SWG (Figure 7-2) are illustrated graphically. In conventional TSHI, process HR pockets are preferentially recovered internally to processes. As shown in Figure 7-1 for a two process example using background/foreground analysis, removal of pockets can lower the target amount of TSHR (Bagajewicz and Rodera, 2000).

The maximum amount of assisted heat transfer requires direct integration between the two processes, but this is often uneconomic for large sites. As a result, the steam utility levels may be used as an indirect HR system, as shown in Figure 7-1. Assisted heat transfer targets should, therefore, incorporate the normal TSHI constraint of integrating between processes using the utility system. HR pockets can also be used for assisted shaft work generation (Figure 7-2). Where a pocket spans two steam pressure levels, there is opportunity to generate work. However, the amount of power generation for a single pocket is unlikely to economically warrant its own steam turbine. As a result, such opportunities must also fit into the wider CHP system to be useful.

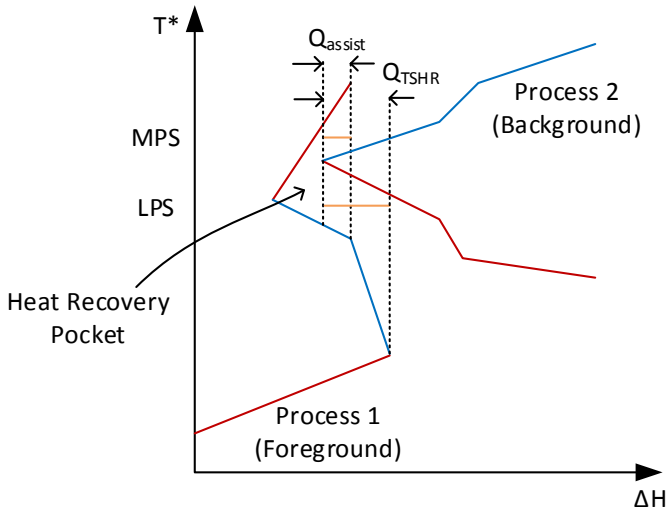

Figure 7-1: The concepts of an assisted heat transfer target for indirect integration of two processes.

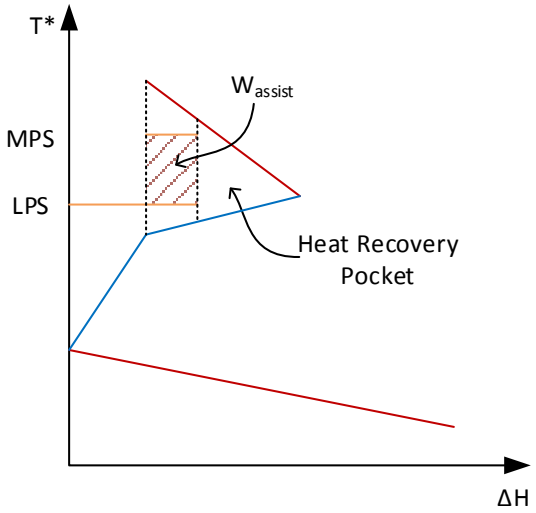

Figure 7-2: The concepts of an assisted shaft work target for a process.

7.2.2 Assisted Heat Transfer Methods

Three methods have been used to determine the TSHI targets for an example TS problem, namely:

i. Conventional TSHI method of Klemeš et al. (1997)

ii. Modified TSHI method with assisted heat transfer of Bandyopadhyay et al. (2010)

iii. Conventional TSHI method with new assisted heat transfer and shaft work targets

The new assisted heat transfer and shaft work targets in Method iii are the important contributions of this chapter. New assisted heat transfer and shaft work targets are determined using a background/foreground analysis of process GCC heat recovery pockets compared to the conventional SUGCC.

7.2.2.1 New Assisted Heat Transfer Target

Where a single HR pocket spans the TS Pinch Region, opportunity arises for assisted heat transfer in TSHI. The maximum assisted heat transfer may be determined by pinching the pocket against the SUGCC, Figure 7-3. Segments of the pocket that overlap the SUGCC should be used to increase TSHI, while non-over lapping segments should be recovered internal to the process.

7.2.2.2 New Assisted Shaft Work Target

Where a single HR pocket spans two utility steam pressure levels (not crossing the Pinch Region), opportunity arises for assisted shaft work in TSHI. As it can be seen in Figure 7-3 ,the maximum assisted shaft work may be determined by pinching the pocket against the steam utilities levels that the pocket spans, on the SUGCC. Segments of the pocket that overlap the two steam levels on the SUGCC should be used to increase TS shaft work, while non-over lapping segments should be recovered internal to the process.

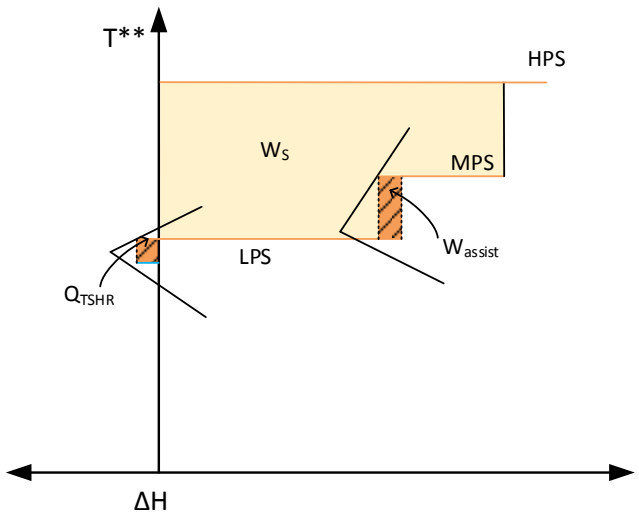

Figure 7-3: The concept of assisted heat recovery and shaft work generation in a SUGGC.

7.2.3 A Total Site Example with Assisted Heat Transfer and Shaft Work

7.2.3.1 Stream and Utility Data

Table 7-1 presents the stream data for four different processes in the example TS problem.

Table 7-1: Steam data for example TS problem.

Process	Stream	Type	T_s (°C)	T_t (°C)	CP (kW/°C)
Process A	A1	Hot	120	60	75
	A2	Hot	150	100	100
	A3	Hot	50	220	35
	A4	Cold	250	230	150
Process B	B1	Hot	200	90	30
	B2	Hot	200	119	230
	B3	Cold	30	200	40
	B4	Cold	130	150	150
Process C	C1	Hot	240	100	10
	C2	Cold	50	250	15
	C3	Cold	40	190	50
	C4	Cold	140	210	100
Process D	D1	Hot	220	170	60
	D2	Cold	80	130	100
	D3	Hot	110	80	75
	D4	Hot	95	70	40

Utilities for the TS include four steam levels are as presented in Table 7-2. The TS problem assumes a process ΔT_{min} of 20 °C and a process-to-utility ΔT_{min} of 10 °C.

Table 7-2: Utility data for example TS problem.

Utility Name	Utility Type	T_s(°C)	T_t (°C)	P_R (bar_g)
Very High Pressure Steam (VHPS)	Hot	282.0	281.9	65
High Pressure Steam (HPS)	Hot	236.0	235.9	30
Medium Pressure Steam (MPS)	Hot	184.0	183.9	10
Low Pressure Steam (LPS)	Hot	144.0	143.9	3
Cooling Water (CW)	Cold	20.0	*	

*Soft utility temperature

7.2.3.2 Process-Level Pinch Analysis

The next step in TS analysis is process level PA. Figure 7-4 presents the GCCs for Processes A, B, C, and D, together with the respective HR (Q_{Rec}), hot utility (Q_{Hot}), and cold utility (Q_{Cold}) targets. Processes A, B, and D each contain HR pockets that may assist TSHR and SWG. The combined intra-process HR is 19,950 kW, combined

hot utility is 18,300 kW, and combined cold utility is 22,130 kW. The Pinch temperatures of the processes are 140 °C for Process A, 190 °C for Process B, Process C is a threshold problem, and 90 °C for Process D.

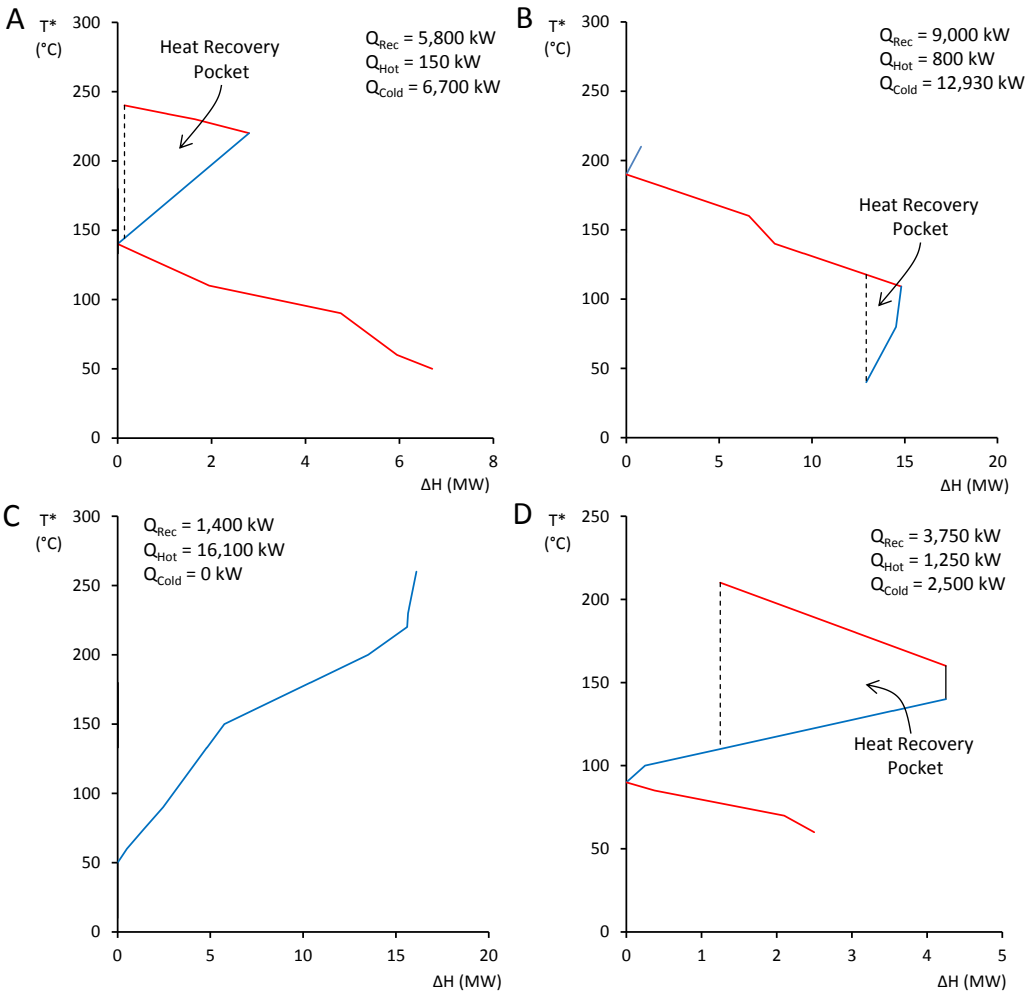

Figure 7-4: GCCs for Processes A, B, C, and D.

7.2.3.3 Conventional Total Site Heat Integration Targets

Process GCCs have been shifted to T^{**}, the utility temperature scale, and composited to form conventional TSPs, as presented in Figure 7-5, using Klemeš et al. (1997) method.

Steam and cooling water utilities may be targeted using the TSP, from which the SUGCC is constructed and a shaft work target is calculated assuming 80 % isentropic efficiency (Figure 7-6). Inter-process HR via the utility is 8,287 kW and the TS shaft work target is 1,062 kW_{ele}. The Pinch Region lies between the MPS and LPS utility levels. The original TSHI method does not include targets for

assisted heat transfer or shaft work, whereas the modified TSHI method of Bandyopadhyay et al. (2010) does.

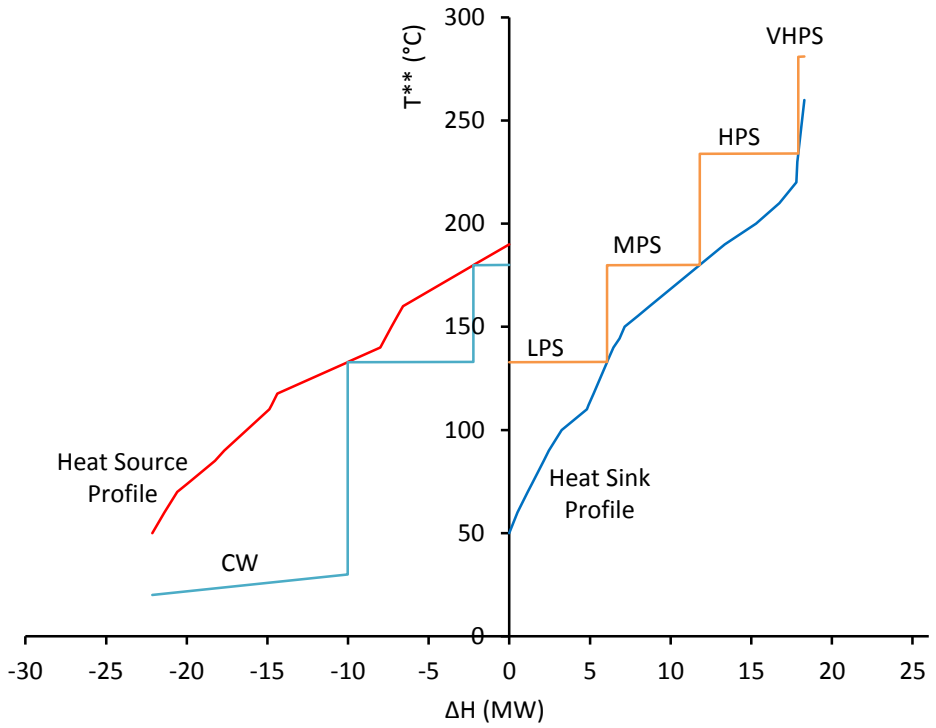

Figure 7-5: TSP of conventional TSHI method for example TS problem.

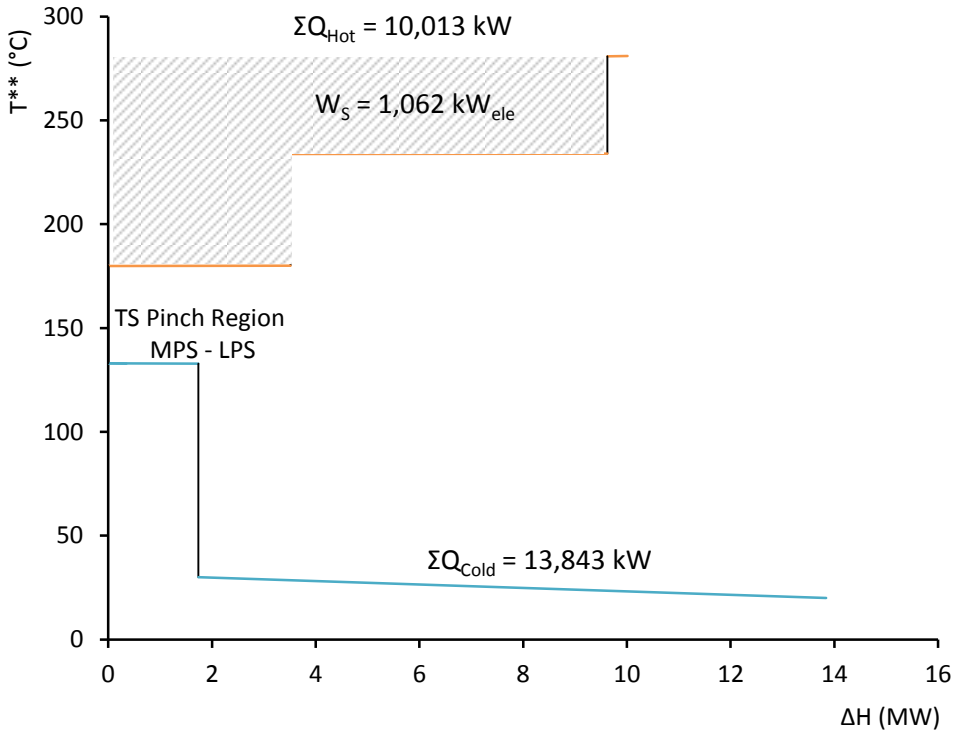

Figure 7-6: SUGCC of conventional TSHI method for example TS problem.

7.2.3.4 Modified Total Site Heat Integration Targets

The method of Bandyopadhyay et al. (2010) may be applied to the same example TS problem. Their modified method carries over segments of most process GCC heat recovery pocket to form part of the TSP, as shown in Figure 7-7.

Modified targets for each utility and the corresponding SUGCC (Figure 7-8) may be determined. As shown in Figure 7-8, the Pinch Region shifts from between MPS-LPS levels in the conventional analysis to between LPS-CW levels. Hot and cold utility targets increase by 154 kW. The shaft work target also increases (69 kW_{ele}), due to the increase in total utility use and the lowering of the Pinch Region, which opens up more potential for power generation. Although the goal of the method of Bandyopadhyay et al. (2010) was to use GCC pockets to assist and increase TSHI, the method is clearly not universally advantageous. For the example TS problem, the modified method is detrimental to TSHI targets. As a result, there is a need to target assisted heat transfers and introduce the idea of assisted shaft work using a new method.

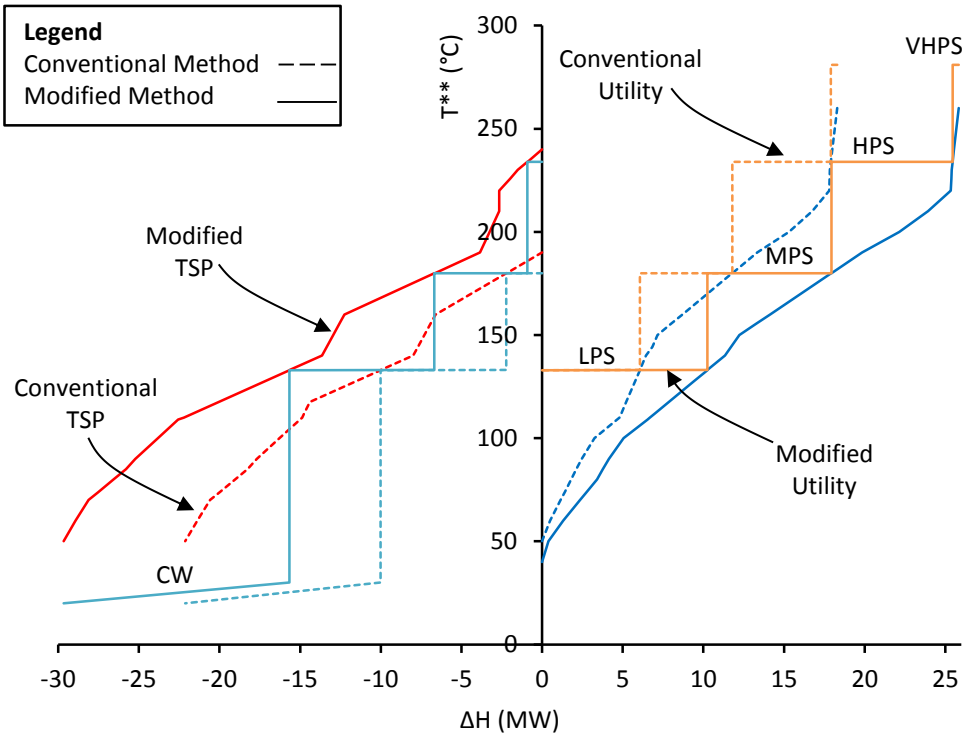

Figure 7-7: Modified TSP for example TS problem using Bandyopadhyay et al. (2010) method.

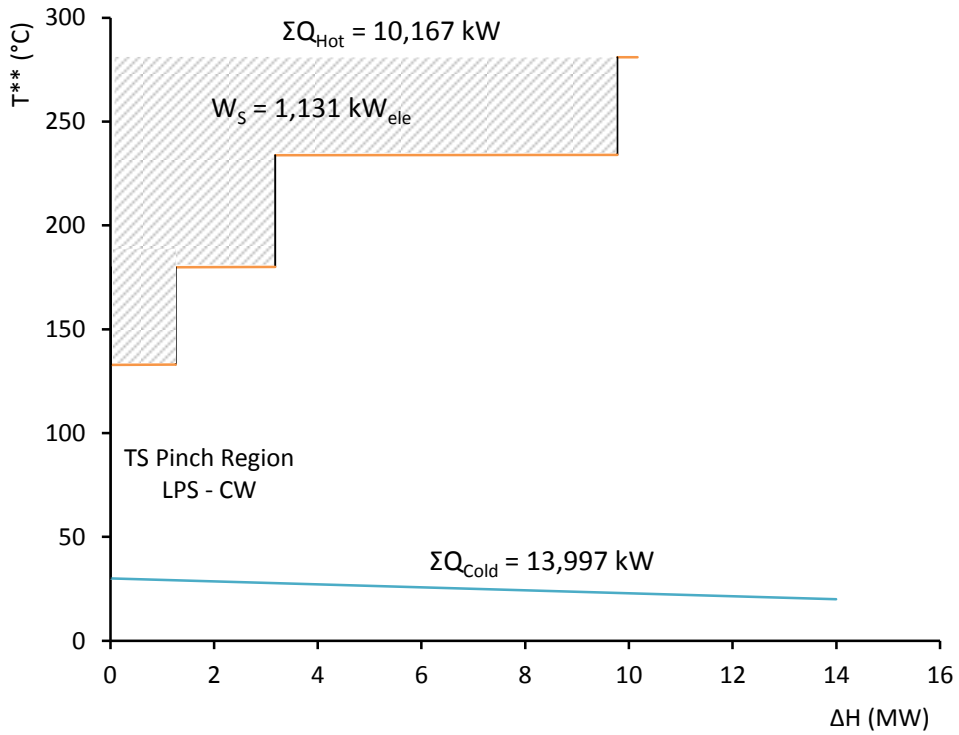

Figure 7-8: Modified SUGCC for example TS problem using Bandyopadhyay et al. (2010) method.

7.2.3.5 New Assisted Heat Transfer and Assisted Shaft Work Targets

The GCC pockets from Processes A, B, and D may be compared with the SUGCC using background/foreground analysis (Figure 7-9b) to identify effective assisted heat integration targets. The pockets have been inversed and positioned to target assisted heat transfer and shafted work, where possible. The segments that are used for assisted integration are then composited into the TSP in Figure 7-9a.

The pocket from Process D spans the Pinch Region MPS-LPS from Figure 7-6, increasing MPS generation by 1,737 kW (above the Pinch) and LPS consumption by 1,737 kW (below the Pinch). As a result, TSHR increases by 1,737 kW, which is a 21% increase in inter-process HR, to total 10,024 kW. The conventional SUGCC has been shifted to the left by 1,737 kW to show the overlap with the pocket from Process D. The segments not overlapping the shifted SUGCC are retained for internal integration within Process D.

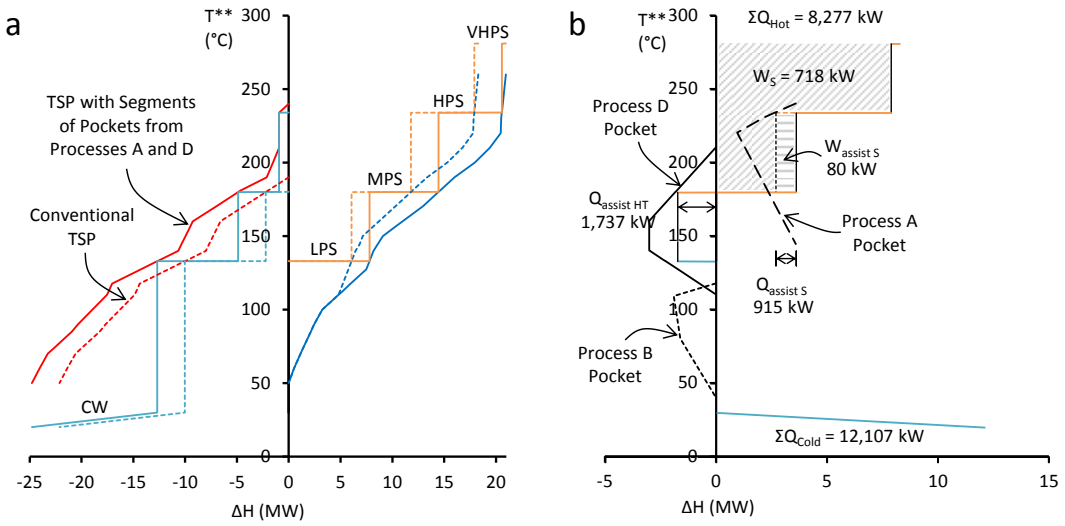

Figure 7-9: a) New TSP including assisting segments of pockets from Process A and D compared to the conventional method; b) Targets for assisted heat transfer and shaft work using the SUGCC and the GCC pockets from Process A, B, and D.

The pocket from Process A sits above the Pinch Region and spans the HPS and MPS levels. This pocket can generate 915 kW of MPS but only needs to the equivalent in LPS. This difference in steam pressure requirements for heating and cooling within the pockets provides the opportunity for assisting shaft work generation. In such cases, MPS generated by the pocket is used to fulfil an MPS demand of another plant, while the demand for LPS by the pocket is satisfied using steam from the LP exit of the turbine. Extracting from the turbine an extra 915 kW of steam at the LPS level instead of the MPS results in assisted shaft work target of 80 kW_{ele}, as indicated by the horizontally shaded area in Figure 7-9b. The remainder of the pocket (i.e. the segments not required for assisted shaft work production) should be internally integrated within Process A. For the given utilities, the pocket from Process B has no potential for assisting TS integration and, therefore, is best left to be internally integrated within Process B.

It is important to note that the total shaft work target is a function of the amount of TSHI and the net consumption of HPS and MPS (and LPS, in other problems). The inclusion of assisted heat transfer from Process D in the TS problem reduces the opportunity for SWG, while the assistance of Process A helps to increase the shaft work target. After including the assisted heat transfer and shaft work targets and the corresponding GCC segments into the TSP and SUGCC, the Pinch Region widens to be between the MPS and CW levels.

Future work needs to be done focusing on developing an improved TSHI method that incorporates targets for assisted heat transfer and SWG.

7.3 Heat Transfer Enhancement of Site Level Indirect Heat Recovery Systems Using Nanofluid

In this section, the benefits of using a nanofluid in a large scale industrial plant is investigated. A step by step procedure for choosing nanoparticles, base fluid, thermo-physical properties and heat transfer correlations is proposed to show how to find the appropriate nanofluid to implement into an existing HRL in a process plant. Various combinations of nanoparticles in water (base fluid) are examined to find which combination returns the best heat coefficient for the same vol. % of nanoparticles added. The selected nanofluid is then modelled as the intermediate fluid in an industrial HRL model.

7.3.1 Method

7.3.1.1 Nanofluid Selection Procedure and Considerations

In this chapter, a systematic method for nanofluid selection and its implementation in process industries is presented. These methods are developed for low temperature (i.e. < 120 °C) processes that are suitable for implementation of nanofluids as the heat transfer media in their utility system. Low temperature processes are normally non-continuous and are operate at lower total heat loads. The method for nanofluid selection for implementing in an industrial system is explained in Figure 7-10.

The first decision is back to the nature of the process and the nanoparticles that are going to be added to the base fluid. For instance, if the process is a pharmaceutical or food and dairy processing, application of some type of nanoparticles might not be allowed. Therefore, technical documents such as MSDS might be useful at this stage. In any fluid heat transfer system, the effect of heat transfer is described by the convective heat transfer coefficient of the fluids, which is a function of a number of thermo-physical properties; the most significant ones are thermal conductivity, density, viscosity, and specific heat.

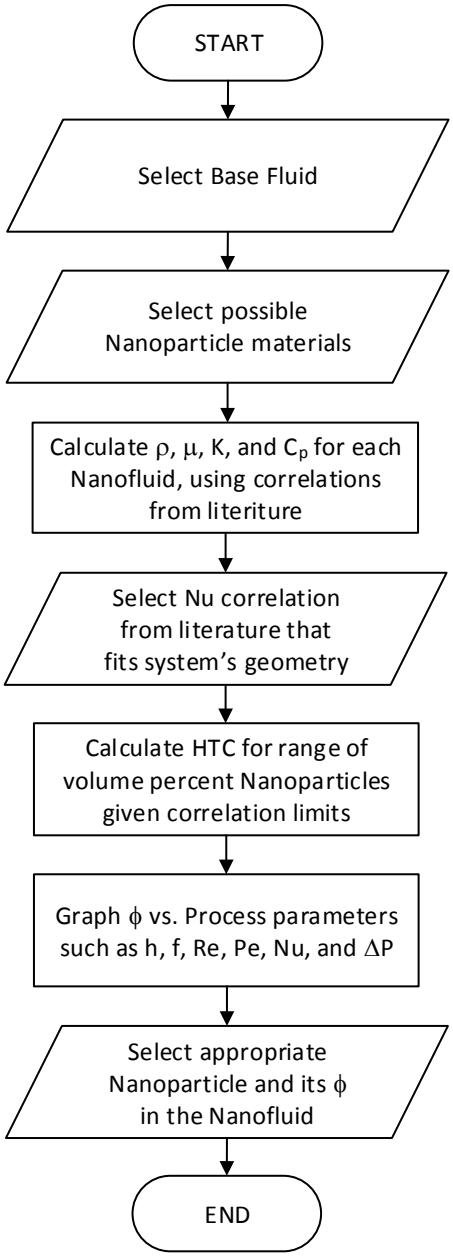

Figure 7-10: Nanofluid selection procedure for an industrial application.

Several experimental correlations are proposed in the literature for nanofluids (Huminic and Huminic, 2012). To match the best one to the system, a designer should consider the geometry of process and heat transfer equipment that the nanofluid will pass through. Following thermo-physical property correlation selection and calculations, appropriate correlations for heat transfer coefficients and pressure drop should be selected for the process. Different heat transfer equipment such as heat exchangers, cooling towers, furnaces etc. might be a constraint in the process. Next step is the calculation of the amount of nanoparticles in nanofluid. To do this, plotting the volume fraction of particles (ϕ) versus a various number of parameters such as convective heat transfer

coefficient, Reynolds number, Nusselt number, friction factor, pressure drop, etc. may give a good insight to the designer for selecting the best nanoparticle/nanofluid and its concentration for the system. Increased convective heat transfer coefficient on one side of the heat exchanger that is matched to the HRL system will affect overall heat transfer coefficient. This increase will show significant impact on heat transfer and duty for individual heat exchangers and, consequently, the HR of the entire system.

7.3.1.2 Heat Recovery Loop Methodology for Total Site Heat Integration

Intermediate fluid in HRLs, which normally is non-isothermal, assists the process to transfer heat from one plant to another. The conventional control system of a HRL measures and compares the outlet temperature of the loop fluid from each heat exchanger to a common hot or cold temperature set point. The flow rate of fluid through each heat exchanger is adjusted to achieve set point temperature. In this approach, hot and cold storage temperatures are constant over time, thus this approach is called the Constant Temperature Storage (CTS) approach. T.G. Walmsley et al. (2015b) introduced an alternative approach to HRL control which is varying the set point of the heat exchangers depending on their temperature driving force. This alternative approach is called Variable Temperature Storage (VTS) due to mixing of different temperatures entering the tanks. Walmsley et al. (2014b) compared the two HRL control approaches to find the VTS system results in more effective distribution of temperature driving force between heat exchangers, lower average loop flow rates giving reduced pressure drop and pumping requirements, and increase in average temperature difference of hot and cold storage temperature, which increases thermal storage density and capacity and continued by T.G. Walmsley (2014a).

The steady state minimum temperature difference (ΔT_{min}) HRL design (M. R. W. Walmsley et al., 2013b), is applied for transient stream data analysis to calculate HR. Four methods to operate and design a HRL have been applied based on methodologies presented by Walmsley et al. (2013c) for the current case study, these are:

i. Conventional design method with CTS control
ii. VTS method of HRL design and operation.

iii. CTS method using selected nanofluid as intermediate fluid in HRL

iv. VTS method using the same selected nanofluid as intermediate fluid in HRL

M.R.W. Walmsley et al. (2013c) show that VTS method provides more HR than CTS method. In this chapter, based on the existing methods, the percent increase in HR for the two HRL design methods using nanofluid as heat transfer media are compared to see if the one benefits more than the other.

7.3.2 Modelling of Nanofluids in an Industrial Heat Recovery Case Study

A large multi-plant dairy factory located in New Zealand, which is different with the previouse case study that studied in thesis, has been chosen as a case study. The factory consists of eight separate semi-continuous processes that share common utility, power, and materials handling services. Plants have been previously investigated and integrated to industry best practice. A HRL was installed as a dedicated indirect HR system to increase inter-plant HI. The existing HRL is using water as the intermediate fluid. Further improvements in HRL performance using HTE are desired. Modifying intermediate fluid (water) to become a nanofluid is therefore investigated.

7.3.2.1 Data Extraction

In this section, process stream data extraction and nanofluid basic data (i.e. nanoparticle and base fluid) extraction are presented.

7.3.2.1.1 Process Streams Data Extraction

Process streams from each individual semi-continuous plant connected to the HRL are presented in Table 7-3, where T_s and T_t are supply and target temperatures, and CP represents time-average heat capacity flow rate. The data is taken from T.G. Walmsley et al. (2015b) where the full transient characteristics of the various streams are presented.

Table 7-3: Extracted process stream data from Dairy Factory.

Stream Name	Utility Type	T_s (°C)	T_t (°C)	CP (kW/°C)
Dryer Exhaust A	Hot	75.0	55.0	139.0
Dryer Exhaust B	Hot	75.0	55.0	73.0
Dryer Exhaust C	Hot	75.0	55.0	44.0
Dryer Exhaust D	Hot	75.0	55.0	28.0
Utility Unit A	Hot	45.0	30.0	8.0
Utility Unit B	Hot	45.0	30.0	8.0
Casein A	Hot	50.0	20.0	22.0
Casein B	Hot	50.0	20.0	32.0
Casein C	Hot	50.0	20.0	32.0
Condenser	Hot	80.0	79.0	351.0
Cheese A	Hot	35.0	20.0	98.0
Cheese B	Hot	35.0	20.0	114.0
Site Hot Water	Cold	16.0	65.0	160.0
Milk Treatment A	Cold	10.0	50.0	104.0
Milk Treatment B	Cold	10.0	50.0	104.0
Milk Treatment C	Cold	11.0	50.0	116.0
Whey A	Cold	12.0	45.0	16.0
Whey B	Cold	14.0	45.0	9.0

7.3.2.1.2 Nanoparticle and Base Fluid Data Extraction

The intermediate fluid which is used in existing HRL is water, as explained before; therefore, water has been chosen as base fluid due to its availability in the system, high heat capacity, non-toxicity and cheap price. A range of nanoparticles have been investigated to find the one that best matches the system. Table 7-4 presents the thermo-physical properties of the base fluid and nanoparticle which are used in this research.

Table 7-4: Thermo-physical properties of nanoparticles and water (base fluid) at 25°C.

Nanoparticle/ Fluid	ρ (kg/m^3)	K (W/m. °C)	C_p (J/kg. °C)	μ (kg/m.s^2)
CuO	6,500.0	20.0	535.6	-
Al_2O_3	3,600.0	36.0	765.0	-
SiO_2	2,200.0	1.4	745.0	-
Cu	8,933.0	401.0	385.0	-
Water	988.2	0.6	4,182.0	0.001

7.3.2.2 Nanofluid Thermo-Physical Property Estimation

The effective thermo-physical properties of the nanofluid can be estimated using classical correlations as usually used for two phase fluid mixtures. For these correlations, nanoparticles are assumed well dispersed within the base fluid and the concentration of the nanoparticles are considered uniform in the system.

Plate Heat Exchangers (PHE) are the most common exchangers in dairy factories. To calculate thermo-physical properties of the nanofluid given the geometry of the system, the following correlations have been chosen for density Equation 7-1, dynamic viscosity Equation 7-2, thermal conductivity Equation 7-3, and heat capacity Equation 7-4, which were used by Khairul et al. (2014).

$$\rho_{nf} = (1-\phi)\rho_{bf} + \phi\rho_{np} \tag{7-1}$$

$$\mu_{nf} = (1+2.5\phi)\mu_{bf} \tag{7-2}$$

$$K_{nf} = (3.761088\phi + 0.017924T + 0.69266)K_{bf} \tag{7-3}$$

$$c_{p,nf} = \frac{(1-\phi)(\rho c_p)_{bf} + \phi(\rho c_p)_{np}}{\rho_{nf}} \tag{7-4}$$

7.3.2.3 Nanofluid convective heat transfer coefficient correlation selection

Considering the system's geometry, i.e. type of heat exchangers, flow regime, hydraulic of system etc., the most suitable correlation should be selected (Kumar et al., 2015). Several experimental and theoretical studies on the convective heat transfer coefficient of nanofluids in PHEs under a turbulent regime have been reported in literature. Khairul et al. (2014) illustrated that the heat transfer coefficient of CuO/Water nanofluid increased by 18 - 27 % compared to water. Their work was very similar to a previous study of the same nanofluid, which presented the following Nusselt number correlation (Pandey and Nema, 2012).

$$Nu = (0.26 + 0.02\phi - 0.0051\phi^2)Pe^{0.27} \qquad 0.5 \le \phi \le 1.5 \tag{7-5}$$

Tiwari et al. (2013) investigated nanofluids made by using Al_2O_3, SiO_2, TiO_2 and CeO_2 nanoparticles. Their investigation showed the heat transfer coefficient of the nanofluid increased with increases in the volume flow rate of the non-nanofluid and nanofluid and with a decrease in the main fluid temperature. They summarised their results using the Equation 7-6.

$$Nu = 0.348\,\mathrm{Re}^{0.663}\,\mathrm{Pr}^{0.33} \qquad 0.5 \le \phi \le 3.0 \qquad (7\text{-}6)$$

Pantzali et al. (Pantzali et al., 2009) developed Equation 7-7 as they studied the efficiency of CuO/Water nanofluid with 4 vol. % of CuO nanoparticles as coolants in commercial PHE. According to their findings, the nature of coolant flow, e.g. turbulent flow, inside the heat exchanger play a significant role in the effectiveness of nanofluids.

$$Nu = 0.247\,\mathrm{Re}^{0.66}\,\mathrm{Pr}^{0.4} \qquad \phi \le 4.0 \qquad (7\text{-}7)$$

7.3.3 Nanofluid Selection and Heat Transfer Coefficient Calculation

CuO/water, Al_2O_3/water, SiO_2/water and Cu/water nanofluids have been initially investigated to find the best nanofluid for use in a HRL system. An Excel™ spreadsheet has been developed in order to calculate thermo-physical properties of nanofluids including their heat transfer coefficient using Equations 7-5, 7-6, and 7-7. To validate developed spreadsheet, Nusselt No. vs. Peclet No. has been plotted in Figure 7-11.

Figure 7-11 is plotted for more point by using similar geometrical and process conditions for lab scale PHE and nanofluid, which has been presented by Khairul et al. (2014), which is compatible with similar graph in their work. To choose appropriate nanofluid, several options of nanofluid and their impact on the heat transfer coefficient have been plotted in Figure 7-12, by using Equations 7-1 to 7-4.

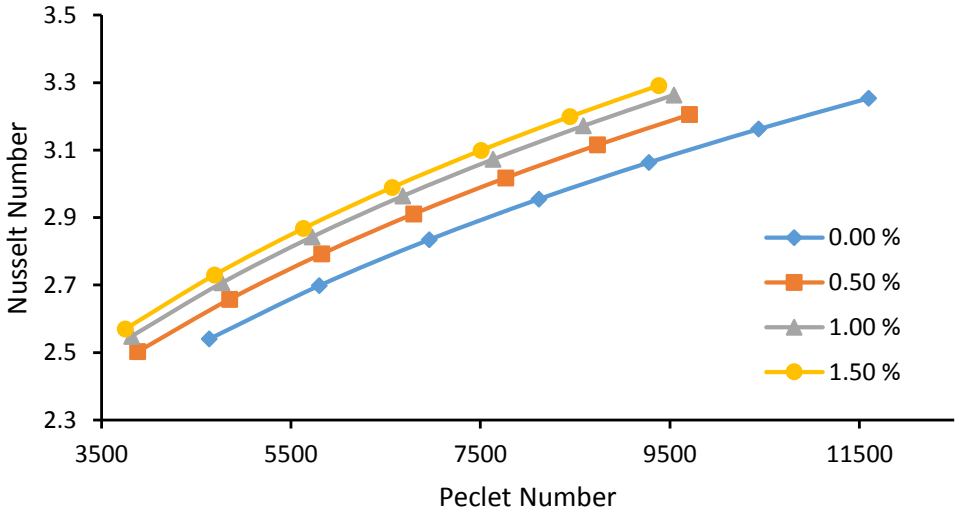

Figure 7-11: Calculated Nu vs. Pe graph for Khairul et al. (2014) experimental data.

The most important part of analysing nanofluid HTE is to find how much different correlations led to increase in heat transfer coefficient when compared to water. Since Equations 7-4 to 7-7 are based on experiments with different geometries and process characterisations (i.e. different heat exchanger size and flow rate), calculated convective heat transfer coefficients using mentioned correlations are not is the same order of magnitude. Therefore, a unified measure as percent increase in convective heat transfer coefficient has been calculated to compare these set of equations.

Figure 7-13 illustrated that according to Equation 7-5 percentage change in heat transfer coefficient increase up to 25 % at 1.5 vol. % in the nanofluid, while Equations 7-6 and 7-7 show a linear increase by increasing of nanoparticle volume percentage in the nanofluid. Thus, achieving the same increase in heat transfer coefficient for Equations 7-6 and 7-7 needs more nanoparticles in nanofluid which may cause higher capital costs and operating cost due to increase in pressure drop. Therefore, as it is shown in Figure 7-13, Equation 7-5 has presented highest increase in heat transfer coefficient in its maximum nanoparticle volume fraction range which is in middle range for Equations 7-6 and 7-7. All above led to select CuO/water nanofluid with 1.5 vol. % of nanoparticle to observe 25 % increase in HRL intermediate fluid convective heat transfer coefficient.

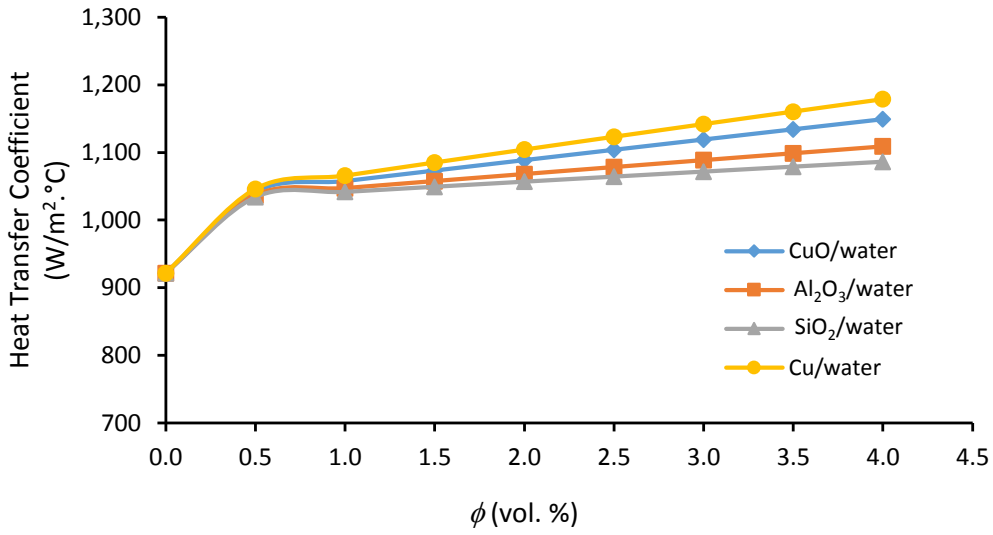

Figure 7-12: Heat transfer coefficient vs. volumetric percentage of CuO/ water, Al_2O_3/water, SiO_2/water and Cu/water nanofluids.

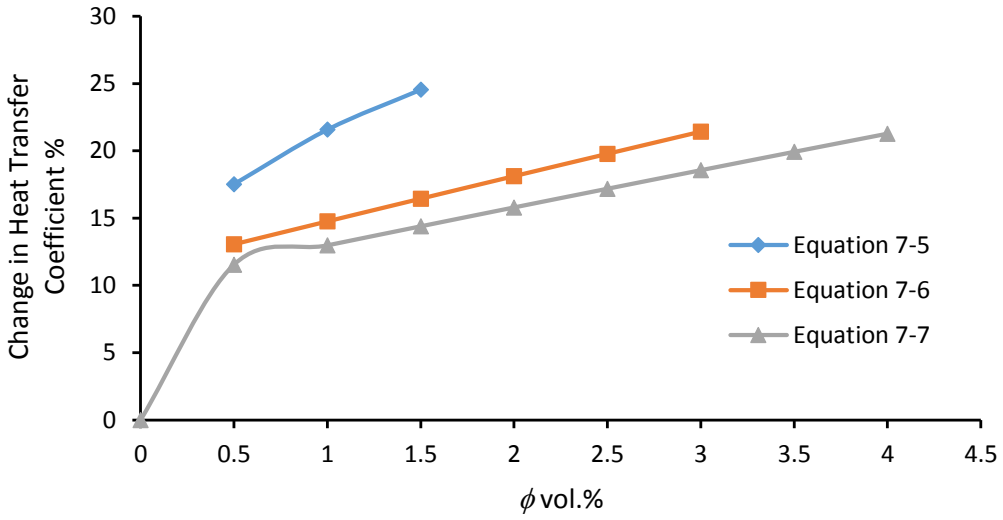

Figure 7-13: Comparison of heat transfer coefficient increase percentage vs. volumetric percentage of CuO/water nanofluid for Equation 7-5, Equation 7-6, and Equation 7-7.

Table 7-5 shows the comparison between thermo-physical properties of the water, as base fluid, and CuO/water, as nanofluid, in HRL. An increase in density, thermal conductivity and viscosity values for the nanofluid as well as decrease in heat capacity is as expected. Adding 1.5 vol. % CuO/water nanofluid is estimated to increase the heat transfer coefficient by 25 % (Equation 7-5), from 4.00 kW/m^2.°C to 5.00 kW/m^2.°C.

Table 7-5: Comparison between thermo-physical properties of the base fluid and nanofluid in HRL.

Nanoparticle/ Fluid	ρ (kg/m^3)	C_p (J/kg.°C)	K (W/m.°C)	μ (kg/m.s^2)	h (kW/m.°C)
Water	1,000.0	4,182.0	0.6000	0.00100	4.00
CuO/Water	1,080.7	3,853.0	0.7382	0.00104	5.00

7.3.4 Results and Discussion

Major process parameters may affect by replacing current intermediate fluid by selected nanofluid (i.e. CuO/water in this case) are investigated to illustrate the advantages and/or disadvantages of such a replacement in existing HRL of the case study.

7.3.4.1 Heat Recovery Potential

The increase of HR as result of applying each design and control procedure is presented in Figure 7-14. HR targets have been calculated for each control

procedure using the developed spreadsheet, then the intermediate fluid properties have been changed in the spreadsheet and HR targets are recalculated. Results of the different cases were compared in the last stage. Results showed that by adding nanofluid to the original intermediate fluid, i.e. water, in both methods show an increase in average HR.

In the CTS method with nanofluid comparing to CTS method without nanofluid, a wide range of variation in increased HR for the process streams on the HRL. The highest increase is in Whey B with 9 % increase and lowest increase is shown in Casein plants, especially Casein B with 5.1 % increase. For hot streams Cheese A* and B*, in case of the CTS method, the hot loop temperature is greater than the stream's supply temperature, and therefore HR is not allowed under the CTS approach. For Dryer Exhaust A, B, C, and D a very small increase is observed, which indicates the air side is the limiting heat transfer coefficient. Also, Utility A and B and Condenser have fixed duties and so increasing the heat transfer coefficient does not impact on HR.

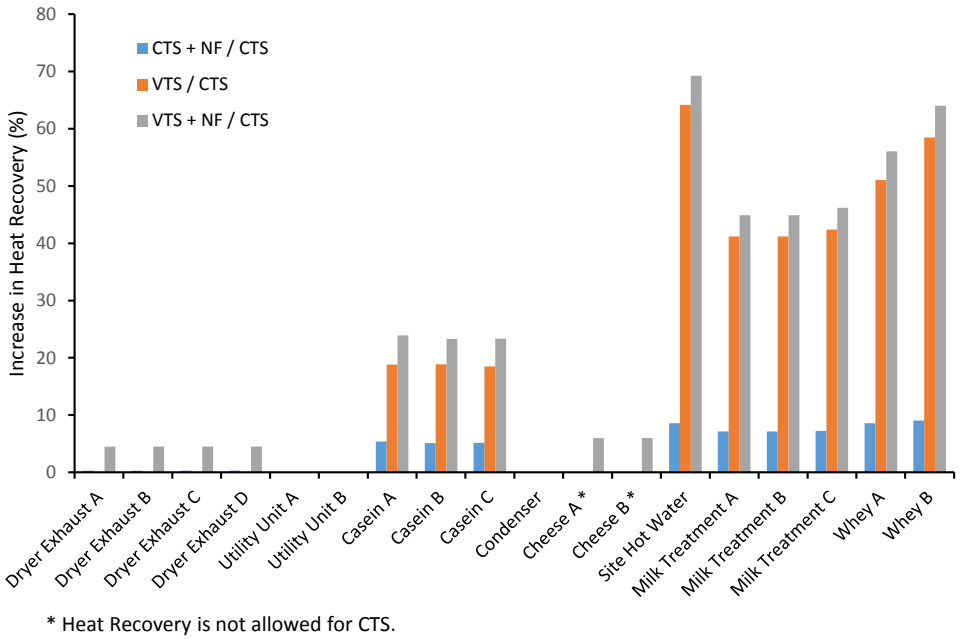

Figure 7-14: HR increase in each process heat exchanger, the comparison between four different methods.

In case of CTS and VTS methods, a significant increase in VTS heat recovery is illustrated in Figure 7-14. This increase is due to the more constraint which are considered in VTS method. Site Hot Water shows the highest increase in HR with 65 % and Whey B and A have second and third high increase with 58 % and 51 %,

respectively. Dryer Exhausts have no change due to same conditions in both methods.

In the case of applying VTS and VTS with nanofluid methods, again a wide range of differences in increase of HR appears. In this case, Cheese A shows highest HR increase with 6 % while Milk Treatment A and B have the lowest increase, 2.6 %. Moreover, it shows a small change in HR for Dryer Exhaust A, B, C, and D and again hot utilities which are condenser, Utility A, and Utility B remain constant due to their fixed duty. Average increase of HR for the entire factory is about 4 % in the case of CTS with nanofluids and 2.5 % in the case of VTS with nanofluids. Liquid-liquid heat exchangers, exclusively, shows 7 % and 4 % increase respectively for CTS and VTS with nanofluids. The differences in the increases in HR between the streams is due to different stream characteristics, flow rates, and heat exchanger types and geometries.

7.3.4.2 Heat Transfer Area

If a nanofluid and its enhanced heat transfer coefficient were applied in the design process to obtain the same duties as the original design without nanofluids, total heat transfer area decreases as given in Table 7-6.

Table 7-6: Comparison of reduction in heat transfer area for different matches.

Match Type	Estimated Reduction in Area (%)
Gas - Liquid	0.3
Vapour - Liquid	7.5
Liquid - Liquid	10.0

Liquid-Liquid matches show a decrease in area of 10 % whereas the decrease in area for gas-liquid matches is negligible as the gas side plays the controlling role in overall heat transfer coefficient of the heat exchanger. Table 7-7 indicates the match type for each individual stream. It can be seen that most of the processes have Liquid-Liquid match. Therefore, average 10 % reduction in capital investment for the HR system and site can be considered.

Table 7-7: Different match types for processes in the case study dairy factory.

Stream Name	Match Type		
	Gas - Liquid	Vapour - Liquid	Liquid - Liquid
Dryer Exhaust A	X		
Dryer Exhaust B	X		
Dryer Exhaust C	X		
Dryer Exhaust D	X		
Utility Unit A			X
Utility Unit B			X
Casein A			X
Casein B			X
Casein C			X
Condenser		X	
Cheese A			X
Cheese B			X
Site Hot Water			X
Milk Treatment A			X
Milk Treatment B			X
Milk Treatment C			X
Whey A			X
Whey B			X

7.3.4.3 Pressure Drop and Friction Factor

Equation 7-8 presents the empirical correlation for friction factor, using experimental data (Pandey and Nema, 2012) for water and nanofluid in a lab scale PHE.

$$f = (2.9 + 5.6\phi - 0.12\phi^2)Pe^{-0.13} \quad (7\text{-}8)$$

CuO/water nanofluid with different particle volume fractions is employed in the friction factor computation. Figure 7-15 illustrates by the lab scale PHE data (Pandey and Nema, 2012), friction factor increased with the increase of nanoparticle concentration in nanofluid. However, it decreases for higher coolant flow rate as 5 L/min nanofluid has lower friction factor than 2 L/min in any concentration of nanofluid.

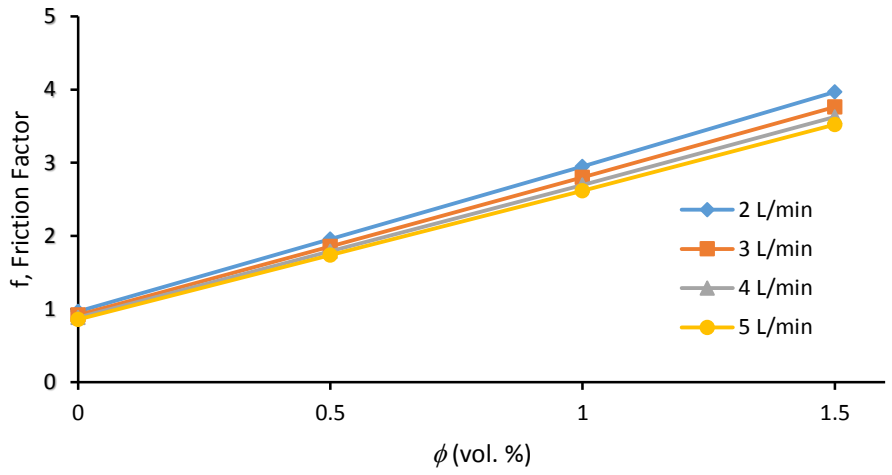

Figure 7-15: Comparison of ϕ vs. f (friction factor) for CuO/water nanofluid in different flow rates in a PHE, data from (Pandey and Nema, 2012).

Pressure drop is a function of a number of parameters such as friction factor, density, viscosity, volumetric flow rate and in addition the geometry of the heat exchanger. In industrial practice, the flow rates are higher than the flowrates studied by Pandey and Nema (2012), and hence the effect of nanoparticles concentration on pressure drop in PHE must be considered more carefully, as pressure drop is known to increase with velocity to almost the square power. In addition, the pressure drop in the pipeline will increase as well. Therefore, a closer study on the amount of total pressure drop in the industrial scale, and a trade-off between the increase in the HR, heat exchange area and pressure drop is highly recommended.

7.4 Conclusions

Assisted heat transfer concept put a step forward to achieve higher HR and SWG targets. Analysis results show that assisted heat transfer increases TSHI only when a process HR pocket spans the TS Pinch Region. The maximum assisted TSHI can be targeted by comparing each HR pocket to the SUGCC using background/foreground analysis. Where HR pockets span two steam pressure levels away from the TS Pinch Region (usually above), the example shows the potential for assisted SWG. In this case, the source segment of the HR pocket generates steam (e.g. MPS), which replaces steam that would otherwise have been extracted from a steam turbine. The sink segment of the HR pocket consumes lower pressure steam (e.g. LPS), which is extracted from the turbine. If

a HR pocket falls outside these two situations (assuming direct inter-process integration is disallowed), the entire pocket should be recovered internal to a process.

Adding 1.5 vol.% CuO to the intermediate fluid of a HRL shows an increase in HR of whole plant. Results show that by applying various HRL design methods accompanied by using nanofluid as an intermediate fluid is desirable way of achieving significant HR without the need for extra heat exchanger area and infrastructure. In the case of air-liquid exchangers, the air side heat transfer coefficient restricts the overall heat transfer coefficient and in utility and condenser streams no changes in HR are observed because they are a fixed duty. Alternative to increasing HR, results show that by using nanofluid as intermediate fluid of HRL total heat exchanger area in the HRL for liquid- liquid heat exchangers decreases significantly.

Chapter Eight

Conclusions and Recommendations for Future Work

8.1 Conclusions

The new improved and unified Total Site Heat Integration (TSHI) targeting method calculates more meaningful and realistic Total Site targets for non-isothermal utilities such as hot and cold water, and hot oil. The new targeting method is demonstrated through three industrial case studies that represent a mix of high temperature and low temperature processes, which use isothermal and non-isothermal utilities. The new method provides the opportunity for the engineer to evaluate different design options, such as replacing a steam main with a hot oil loop, which may simplify the utility network and/or increase overall heat recovery.

A new improved TSHI utility temperature optimisation procedure has been successfully developed and applied to the three industrial case studies. Key parts of this work were the concept of an optimisable utility, the use of derivatives during optimisation and the inclusion of exergy destruction. Results showed that best optimisation procedure minimises the derivative of the Utility Cost iteratively with the derivative of exergy destruction, then sequentially minimises the derivative of the Total Annual Cost. The three case studies achieved Total Annual Cost reductions in the range of 0.6 to 4.6 %. Additional analysis focused on the Kraft Pulp Mill showed significant variations in hot utility price NZD 25 to 40 /MWh has minimal effect on optimal utility temperature selection. Sensitivity analysis for optimisation method shows about 1 % deviation from optimal results. Identical optimal temperatures can be achieved using different starting point temperatures.

Utility Exchanger Network designs for the Kraft Pulp Mill case study reinforce the practical value of the new unified TSHI target method. Results showed practical Utility Exchanger Networks can be designed to meet all heat recovery and utility targets. Further simplification of the network has been achieved by setting an Exchanger Minimum Approach Temperature slightly below the ΔT_{min} from which

targets are calculated. In contrast, Utility Exchanger Network designs based on conventional TSHI methods require, at times, for several process sources or sinks to be matched in a series arrangement to achieve the TSHI target. This impractical design can be resolved through network relaxation but only at the expense of increased utility use. This in turn lessens the value of setting targets for non-isothermal utilities based on the conventional method since the targets are unachievable in practice.

Further developments of TSHI focused on the concepts of assisted heat integration and Heat Transfer Enhancement for Heat Recovery Loops. The study on assisted heat integration showed a 21 % increase in Total Site heat recovery and slightly greater power cogeneration for an example Total Site problem. In general, the study concluded that process Grand Composite Curves with heat recovery pockets that span two or more utility levels are candidates for assisting TSHI. In the second further develop, using nanofluid as an intermediate fluid of a Heat Recovery Loop showed an increase in Total Site heat recovery with individual exchanger duties increasing by up to 9 % for liquid-liquid matches and no effect on air-liquid matches.

8.2 Recommendations for Future Work

Suggestions for future work in TSHI are may be categorized as following.

8.2.1 TSHI Targeting Methods

This thesis addressed the TSHI targeting difficulties for non-isothermal utilities. However, for the industrial sites that contain high temperature and cryogenic processes, such as special chemical or petrochemical processes, a unified targeting procedure needs further improvement to include more emphasis on shaft work. As shown in this thesis, exergy analysis has high capability to be considered in TSHI studies. Therefore, utility targeting of very low temperature processes considering exergy potential of the utilities may be a key part of a solution.

The developed unified method covers heat recovery and utility targeting demand of TS sites; however, operational parameter of processes such as non-isothermal utility storage potential may be studied in the future works.

8.2.2 TSHI Optimisation and Temperature Selection Methods

An appropriate number of utility mains and utility temperature selection can even increase more HR targets in TS plants. Cost and exergy derivative method has been introduced in this thesis. However, more studies can be done on sensitivity to different utility prices since it varies from site to site and, even, process to process. In this thesis, only heat exchanger costs were included in TAC. Due to the inherent estimation difficulty and uncertainty, piping and other capital works piping cost are not included. Future work should include methods to estimate TAC to set targets to optimise utility temperatures and number of utility mains more accurately before design of the TS systems.

Major energy consuming industrial clusters use fossil fuels as main energy supplier in term of process heat within TS. A large portion of the process heat is transferred via utility system; therefore, utility temperature optimisation of such a site may decrease the amount of fossil fuel consumption and reduce emissions. Therefore, from environmental point of view, it may be beneficial consider environmental costs, e.g. Greenhouse Gas emission costs, in the utility temperature optimisation objective function.

Recent developments of implementation of P-graph concept in TSHI may offer better insight for optimisation of TS targeting methods. P-graph may be used to understand the integration of different utility mains in TS plants. The number of required utility mains and utility optimal temperature may be reflected in different P-graph designs. Also, P-graphs may be able to provide an insight to incorporate TS Pinch techniques as safety and environmental indices in the analysis.

8.2.3 HEN Design and Control

Process control is a very important part of plant operability and has direct impacts on the controllability, stability, profitability, product yield, and safety. If process control is not considered until after the HEN is designed, then the process may not be controllable without undoing some of the alterations that made the HEN design optimal. Process control research is often neglected in HI and PA methods, especially with respect to TSHI network design. There may be a significant research room on process control, at least at the HEN synthesis level. Existing process

control methods and insights could be integrated into a TS and its HEN (i.e. UEN) design method to help ensure that any changes on UEN based on the new UTST method does not result in an uncontrollable system.

8.2.4 Application of HTE Techniques in TSHI

Current work is initial steps to this new concept of increasing HI through nanofluid HTE technique. As a suggestion, other base fluids such as ethylene glycol, if there are no compatibility constraints for its use with the process, may be considered. Hybrid nanofluids that achieve higher heat transfer rates may also be studied. Further experimental investigations for determining the thermal and hydraulic performance of nanofluids using a broader range of heat exchanger geometries, operating conditions, and volume percent of nanoparticles in nanofluids is required. Also, a competitive economical study of using nanofluids as intermediate fluid in industrial utility loop with the amount of HR and heat transfer area reduction is vital. This is due to the current nanoparticle production technology that the nanofluid preparation cost in industrial scale may not be economical.

References

Ahmad, S., Hui, D.C.W., 1991. Heat recovery between areas of integrity. Computers & Chemical Engineering 15, 809–832. https://doi.org/10.1016/0098-1354(91)80027-S

Ahmad, S., Smith, R., 1989. Targets and design for minimum number of shells in heat exchanger networks. Chemical Engineering Research and Design 67, 481–494.

Akbarnia, M., Amidpour, M., Shadaram, A., 2009. A new approach in pinch technology considering piping costs in total cost targeting for heat exchanger network. Chemical Engineering Research and Design 87, 357–365. https://doi.org/10.1016/j.cherd.2008.09.001

Akpomiemie, M.O., Smith, R., 2017. Pressure drop considerations with heat transfer enhancement in heat exchanger network retrofit. Applied Thermal Engineering 116, 695–708. https://doi.org/10.1016/j.applthermaleng.2017.01.075

Akpomiemie, M.O., Smith, R., 2016. Retrofit of heat exchanger networks with heat transfer enhancement based on an area ratio approach. Applied Energy 165, 22–35. https://doi.org/10.1016/j.apenergy.2015.11.056

Asante, N.D.K., Zhu, X.X., 1997. An automated and interactive approach for Heat Exchanger Network retrofit. Chemical Engineering Research and Design 75, 349–360. https://doi.org/10.1205/026387697523660

Atkins, M.J., 2017. Process heat use in New Zealand. Personal Communication, Energy Research Centre, University of Waikato.

Atkins, M.J., Morrison, A.S., Walmsley, M.R.W., 2010a. Carbon Emissions Pinch Analysis (CEPA) for emissions reduction in the New Zealand electricity sector. Applied Energy 87, 982–987. https://doi.org/10.1016/j.apenergy.2009.09.002

Atkins, M.J., Walmsley, M.R.W., Neale, J.R., 2012a. Targeting using process integration for large industrial sites operating non-continuously. CHEMECA 2012 Conference, Wellington, New Zealand 574–583.

Atkins, M.J., Walmsley, M.R.W., Neale, J.R., 2012b. Process Integration between individual plants at a large dairy factory by the application of heat recovery loops and transient stream analysis. Journal of Cleaner Production 34, 21–28. https://doi.org/10.1016/j.jclepro.2012.01.026

Atkins, M.J., Walmsley, M.R.W., Neale, J.R., 2010b. The challenge of integrating non-continuous processes – milk powder plant case study. Journal of Cleaner Production 18, 927–934. https://doi.org/10.1016/j.jclepro.2009.12.008

Bade, M.H., Bandyopadhyay, S., 2014. Minimization of thermal oil flow rate for indirect integration of multiple plants. Industrial & Engineering Chemistry Research 53, 13146–13156. https://doi.org/10.1021/ie502059f

Bagajewicz, M., Rodera, H., 2000. Energy savings in the total site heat integration across many plants. Computers & Chemical Engineering 24, 1237–1242. https://doi.org/10.1016/S0098-1354(00)00318-5

Bandyopadhyay, S., 2007. Thermal integration of a distillation column through side-exchangers. Chemical Engineering Research and Design 85, 155–166. https://doi.org/10.1205/cherd06108R1

Bandyopadhyay, S., Varghese, J., Bansal, V., 2010. Targeting for cogeneration potential through total site integration. Applied Thermal Engineering 30, 6–14. https://doi.org/10.1016/j.applthermaleng.2009.03.007

Becker, H., Maréchal, F., 2012. Energy integration of industrial sites with heat exchange restrictions. Computers & Chemical Engineering 37, 104–118. https://doi.org/10.1016/j.compchemeng.2011.09.014

Bejan, A., Tsatsaronis, G., 1996. Thermal Design and Optimization, First. ed. John Wiley & Sons, New York, USA.

Biegler, L.T., Grossmann, I.E., Westerberg, A.W., 1997. Systematic Methods of Chemical Process Design, First. ed. Prentice Hall, Upper Saddle River, N.J.

Boldyryev, S., Varbanov, P.S., Nemet, A., Klemeš, J.J., Kapustenko, P., 2014. Minimum heat transfer area for Total Site heat recovery. Energy Conversion and Management 87, 1093–1097. https://doi.org/10.1016/j.enconman.2014.04.029

Bonhivers, J.C., Svensson, E., Berntsson, T., Stuart, P.R., 2014. Comparison between pinch analysis and bridge analysis to retrofit the heat exchanger network of a kraft pulp mill. Applied Thermal Engineering 70, 369–379. https://doi.org/10.1016/j.applthermaleng.2014.04.052

Bood, J., Nilsson, L., 2013. Energy Analysis of Hemicellulose Extraction at a Softwood Kraft Pulp Mill, Case Study of Södra Cell Värö (MSc Thesis). Chalmers University of Technology, Gothenburg, Sweden.

Bouman, R.W., Jesen, S.B., Wake, M.L., Earl, W.B., 2004. Process capital cost estimation for New Zealand 2004.

Carlsson, A., Franck, P.A., Berntsson, T., 1993. Design better heat exchanger network retrofits. Chemical Engineering Progress 89.

Chang, C., Chen, X., Wang, Y., Feng, X., 2016. An efficient optimization algorithm for waste Heat Integration using a heat recovery loop between two plants. Applied Thermal Engineering 105, 799–806. https://doi.org/10.1016/j.applthermaleng.2016.04.079

Chang, C., Wang, Y., Feng, X., 2015. Indirect heat integration across plants using hot water circles. Chinese Journal of Chemical Engineering 23, 992–997. https://doi.org/10.1016/j.cjche.2015.01.010

Chen, C.-L., Chang, F.-Y., Chao, T.-H., Chen, H.-C., Lee, J.-Y., 2014. Heat-Exchanger Network synthesis involving organic Rankine cycle for waste heat recovery. Ind. Eng. Chem. Res. 53, 16924–16936. https://doi.org/10.1021/ie500301s

Chen, C.-L., Ciou, Y.-J., 2009. Design of indirect heat recovery systems with variable-temperature storage for batch plants. Industrial & Engineering Chemistry Research 48, 4375–4387. https://doi.org/10.1021/ie8013633

Chew, K.H., Klemeš, J.J., Wan Alwi, S.R., Abdul Manan, Z., 2013a. Industrial implementation issues of Total Site Heat Integration. Applied Thermal Engineering 61, 17–25. https://doi.org/10.1016/j.applthermaleng.2013.03.014

Chew, K.H., Klemeš, J.J., Wan Alwi, S.R., Manan, Z.A., 2015a. Process modification of Total Site Heat Integration profile for capital cost reduction. Applied Thermal Engineering 89, 1023–1032. https://doi.org/10.1016/j.applthermaleng.2015.02.064

Chew, K.H., Klemeš, J.J., Wan Alwi, S.R., Manan, Z.A., 2015b. Process modifications to maximise energy savings in total site heat integration. Applied Thermal

Engineering 78, 731–739. https://doi.org/10.1016/j.applthermaleng.2014.04.044

Chew, K.H., Wan Alwi, S.R., Klemeš, J.J., Abdul Manan, Z., 2013b. Process Modification Potentials for Total Site Heat Integration. Chemical Engineering Transactions 35, 175–150. https://doi.org/10.3303/CET1335029

Ciric, A.R., Floudas, C.A., 1989. A retrofit approach for heat exchanger networks. Computers & Chemical Engineering 13, 703–715. https://doi.org/10.1016/0098-1354(89)80008-0

Colberg, R.D., Morari, M., 1990. Area and capital cost targets for heat exchanger network synthesis with constrained matches and unequal heat transfer coefficients. Computers & Chemical Engineering 14, 1–22. https://doi.org/10.1016/0098-1354(90)87002-7

Daungthongsuk, W., Wongwises, S., 2007. A critical review of convective heat transfer of nanofluids. Renewable and Sustainable Energy Reviews 11, 797–817. https://doi.org/10.1016/j.rser.2005.06.005

Dhole, V.R., 1991. Distillation Column Integration and Overall Design of Subambient Plant. (PhD Thesis). University of Manchester Institute of Technology, Manchester, UK.

Dhole, V.R., Linnhoff, B., 1993. Total site targets for fuel, co-generation, emissions, and cooling. Computers & Chemical Engineering 17, Supplement 1, S101–S109. https://doi.org/10.1016/0098-1354(93)80214-8

El-Halwagi, M.M., 2006. Process Integration. Academic Press, San Diego- USA.

El-Halwagi, M.M., 1997. Pollution Prevention Through Process Integration-Systematic Design Tools. Academic Pres, San Diego- USA.

Farhat, A., Zoughaib, A., El Khoury, K., 2015. A new methodology combining total site analysis with exergy analysis. Computers & Chemical Engineering 82, 216–227. https://doi.org/10.1016/j.compchemeng.2015.07.010

Feng, X., Pu, J., Yang, J., Chu, K.H., 2011. Energy recovery in petrochemical complexes through heat integration retrofit analysis. Applied Energy 88, 1965–1982. https://doi.org/10.1016/j.apenergy.2010.12.027

Flower, J.R., Linnhoff, B., 1978. Synthesis of heat exchanger networks: II. Evolutionary generation of networks with various criteria of optimality. AIChE Journal 24, 642–654. https://doi.org/10.1002/aic.690240412

Fodor, Z., Klemeš, J.J., Varbanov, P.S., Walmsley, M.R.W., Atkins, M.J., Walmsley, T.G., 2012. Total Site Targeting with stream specific minimum temperature difference. Chemical Engineering Transactions 29, 409–414. https://doi.org/10.3303/CET1229069

Foo, D.C.Y., 2013. A generalised guideline for process changes for resource conservation networks. Clean Technologies and Environmental Policy 15, 45–53. https://doi.org/10.1007/s10098-012-0475-4

Foo, D.C.Y., 2009. State-of-the-Art review of Pinch Analysis techniques for water network synthesis. Industrial & Engineering Chemistry Research 48, 5125–5159. https://doi.org/10.1021/ie801264c

Foo, D.C.Y., Chew, Y.H., Lee, C.T., 2008a. Minimum units targeting and network evolution for batch heat exchanger network. Applied Thermal Engineering 28, 2089–2099. https://doi.org/10.1016/j.applthermaleng.2008.02.006

Foo, D.C.Y., Tan, R.R., Ng, D.K.S., 2008b. Carbon and footprint-constrained energy planning using cascade analysis technique. Energy 33, 1480–1488. https://doi.org/10.1016/j.energy.2008.03.003

Fritzson, A., Berntsson, T., 2006. Energy efficiency in the slaughter and meat processing industry—opportunities for improvements in future energy markets. Journal of Food Engineering 77, 792–802. https://doi.org/10.1016/j.jfoodeng.2005.08.005

Furman, K.C., Sahinidis, N.V., 2002. A critical review and annotated bibliography for Heat Exchanger Network synthesis in the 20th century. Industrial & Engineering Chemistry Research 41, 2335–2370. https://doi.org/10.1021/ie010389e

Gassner, M., Maréchal, F., 2010. Combined mass and energy integration in process design at the example of membrane-based gas separation systems. Computers & Chemical Engineering 34, 2033–2042. https://doi.org/10.1016/j.compchemeng.2010.06.019

Ghannadzadeh, A., Perry, S., Smith, R., 2012. Cogeneration targeting for site utility systems. Applied Thermal Engineering 43, 60–66. https://doi.org/10.1016/j.applthermaleng.2011.10.006

Ghannadzadeh, A., Sadeqzadeh, M., 2017a. Combined pinch and exergy analysis of an ethylene oxide production process to boost energy efficiency toward environmental sustainability. Clean Technologies and Environmental Policy 1–16. https://doi.org/10.1007/s10098-017-1402-5

Ghannadzadeh, A., Sadeqzadeh, M., 2017b. Exergy aided pinch analysis to enhance energy integration towards environmental sustainability in a chlorine-caustic soda production process. Applied Thermal Engineering 125, 1518–1529. https://doi.org/10.1016/j.applthermaleng.2017.07.052

González-Bravo, R., Elsayed, N.A., Ponce-Ortega, J.M., Nápoles-Rivera, F., El-Halwagi, M.M., 2015. Optimal design of thermal membrane distillation systems with heat integration with process plants. Applied Thermal Engineering 75, 154–166. https://doi.org/10.1016/j.applthermaleng.2014.09.009

Grossmann, I.E., Guillén-Gosálbez, G., 2010. Scope for the application of mathematical programming techniques in the synthesis and planning of sustainable processes. Computers & Chemical Engineering 34, 1365–1376. https://doi.org/10.1016/j.compchemeng.2009.11.012

Gundersen, T., 2000. A Process Integration Primer- Impelementing Agreement on Process Integration. International Energy Agency, SINTEF Energy Research, Trondheim, Norway.

Hackl, R., Andersson, E., Harvey, S., 2011. Targeting for energy efficiency and improved energy collaboration between different companies using total site analysis (TSA). Energy 36, 4609–4615. https://doi.org/10.1016/j.energy.2011.03.023

Hackl, R., Harvey, S., 2015. From heat integration targets toward implementation – A TSA (total site analysis)-based design approach for heat recovery systems in industrial clusters. Energy 90, Part 1, 163–172. https://doi.org/10.1016/j.energy.2015.05.135

Hackl, R., Harvey, S., 2013a. Framework methodology for increased energy efficiency and renewable feedstock integration in industrial clusters.

Applied Energy 112, 1500–1509. https://doi.org/10.1016/j.apenergy.2013.03.083

Hackl, R., Harvey, S., 2013b. Applying exergy and total site analysis for targeting refrigeration shaft power in industrial clusters. Energy 55, 5–14. https://doi.org/10.1016/j.energy.2013.03.029

Harell, D.A., 2004. Resource Conservation and Allocation via Process Integration (PhD thesis). Texas A&M University, Texas, USA.

Hesas, R.H., Tarighaleslami, A.H., Sharifzadeh Baei, M., 2011. An economical comparative study of different methods for decrease cooling towers makeup cost in oil refineries. World Applied Sciences Journal 12, 988–998.

Hipólito-Valencia, B.J., Lira-Barragán, L.F., Ponce-Ortega, J.M., Serna-González, M., El-Halwagi, M.M., 2014. Multiobjective design of interplant trigeneration systems. AIChE Journal 60, 213–236. https://doi.org/10.1002/aic.14292

Hohmann, E.C., 1971. Optimum Networks for Heat Exchange (PhD Thesis). University of Southern California, Los Angeles, USA.

Hohmann, E.C., Lockhart, F., 1976. Optimum heat exchangers network synthesis. In Proceedings of the American Institute of Chemical Engineers., American Institute of Chemical Engineers Atlantic City, NJ:

Huang, D., Wu, Z., Sunden, B., 2016. Effects of hybrid nanofluid mixture in plate heat exchangers. Experimental Thermal and Fluid Science 72, 190–196. https://doi.org/10.1016/j.expthermflusci.2015.11.009

Hui, C.W., Ahmad, S., 1994. Total site heat integration using the utility system. Computers & Chemical Engineering 18, 729–742. https://doi.org/10.1016/0098-1354(93)E0019-6

Huminic, G., Huminic, A., 2012. Application of nanofluids in heat exchangers: A review. Renewable and Sustainable Energy Reviews 16, 5625–5638. https://doi.org/10.1016/j.rser.2012.05.023

International Energy Agency, 2016. World Energy Outlook [WWW Document]. URL https://www.docdroid.net/IOBt86G/world-energy-outlook-2016.pdf.html (accessed 7.5.17).

Itoh, J., Shiroko, K., Umeda, T., 1986. Extensive applications of the T-Q diagram to heat integrated system synthesis. Computers & Chemical Engineering 10, 59–66. https://doi.org/10.1016/0098-1354(86)85046-3

Jafari Nasr, M.R., Shafeghat, A., 2008. Fluid flow analysis and extension of rapid design algorithm for helical baffle heat exchangers. Applied Thermal Engineering 28, 1324–1332. https://doi.org/10.1016/j.applthermaleng.2007.10.021

Jafari Nasr, M.R., Shekarian, E., Tarighaleslami, A.H., Khodaverdi, F., Badini Pourazar, M., 2015. The impact of application of heat transfer enhancement technologies on design of shell and tube heat exchangers. Iranian Chemical Engineering Journal 14, 64–74.

Jin, Z.L., Qiwu, D., Minshan, L., 2008. Heat Exchanger Network synthesis with detailed heat exchanger design. Chemical Engineering & Technology 31, 1046–1050. https://doi.org/10.1002/ceat.200800108

Karellas, S., Leontaritis, A.-D., Panousis, G., Bellos, E., Kakaras, E., 2013. Energetic and exergetic analysis of waste heat recovery systems in the cement industry. Energy 58, 147–156. https://doi.org/10.1016/j.energy.2013.03.097

Kaşka, Ö., 2014. Energy and exergy analysis of an organic Rankine for power generation from waste heat recovery in steel industry. Energy Conversion and Management 77, 108–117. https://doi.org/10.1016/j.enconman.2013.09.026

KBC, 2017. SuperTarget. KBC Advanced Technologies, London, UK.

Kemp, I.C., 2007. Pinch analysis and process integration, 2nd ed. Butterworth-Heinmann, Cambridge, UK.

Kemp, I.C., Deakin, A.W., 1989. The cascade analysis for energy and process integration of batch processes: part 1 and 2. Chemical Engineering Research and Design 67, 495–516.

Kemp, I.C., MacDonald, E.K., 1988. Application of pinch technology to seperation, reatcion and batch processes. IChemE Symposium Series 109, 239–257.

Kemp, I.C., MacDonald, E.K., 1987. Energy and process integration in conteneous and batch processes. IChemE Symposium Series 105, 185–200.

Kenney, W.F., 1984. Energy Conservation in the Process Industries. Academic Pres, Inc., Orlando, USA.

Khairul, M.A., Alim, M.A., Mahbubul, I.M., Saidur, R., Hepbasli, A., Hossain, A., 2014. Heat transfer performance and exergy analyses of a corrugated plate heat exchanger using metal oxide nanofluids. International Communications in Heat and Mass Transfer 50, 8–14. https://doi.org/10.1016/j.icheatmasstransfer.2013.11.006

Khoshgoftar Manesh, M.H., Navid, P., Baghestani, M., Khamis Abadi, S., Rosen, M.A., Blanco, A.M., Amidpour, M., 2014. Exergoeconomic and exergoenvironmental evaluation of the coupling of a gas fired steam power plant with a total site utility system. Energy Conversion and Management 77, 469–483. https://doi.org/10.1016/j.enconman.2013.09.053

Khoshvaght-Aliabadi, M., Hormozi, F., Zamzamian, A., 2014. Effects of geometrical parameters on performance of plate-fin heat exchanger: Vortex-generator as core surface and nanofluid as working media. Applied Thermal Engineering 70, 565–579. https://doi.org/10.1016/j.applthermaleng.2014.04.026

Kimura, H., Zhu, X.X., 2000. R-Curve concept and its application for industrial energy management. Industrial & Engineering Chemistry Research 39, 2315–2335. https://doi.org/10.1021/ie9905916

Klemeš, J.J., 2013. Handbook of process integration: Minimisation of energy and water use, waste and emissions. Woodhead Publishing, Cambridge, UK.

Klemeš, J.J., Dhole, V.R., Raissi, K., Perry, S.J., Puigjaner, L., 1997. Targeting and design methodology for reduction of fuel, power and CO2 on total sites. Applied Thermal Engineering 17, 993–1003. https://doi.org/10.1016/S1359-4311(96)00087-7

Klemeš, J.J., Friedler, F., Bulatov, I., Varbanov, P., 2010. Sustainability in the Process Industry: Integration and Optimization, First. ed. McGraw-Hill Education, New York.

Klemeš, J.J., Kravanja, Z., 2013. Forty years of Heat Integration: Pinch Analysis (PA) and Mathematical Programming (MP). Current Opinion in Chemical Engineering 2, 461–474. https://doi.org/10.1016/j.coche.2013.10.003

Klemeš, J.J., Smith, R., Kim, J.-K., 2008. Handbook of Water and Energy Management in Food Processing, First. ed. Woodhead Publishing Limited, Cambridge, England.

Klemeš, J.J., Varbanov, P.S., Kravanja, Z., 2013. Recent developments in Process Integration. Chemical Engineering Research and Design 91, 2037–2053. https://doi.org/10.1016/j.cherd.2013.08.019

Kotas, T.J., 1995. The Exergy Method of Thermal Plant Analysis. Krieger Pub., Florida, USA.

Krummenacher, P., Favrat, D., 2001. Indirect and Mixed Direct-Indirect Heat Integration of Batch Processes Based on Pinch Analysis. International Journal of Thermodynamics 4, 135–143. https://doi.org/10.5541/ijot.1034000074

Kumar, V., Tiwari, A.K., Ghosh, S.K., 2015. Application of nanofluids in plate heat exchanger: A review. Energy Conversion and Management 105, 1017–1036. https://doi.org/10.1016/j.enconman.2015.08.053

Lang, Y.-D., Biegler, L.T., Grossmann, I.E., 1988. Simultaneous optimization and heat integration with process simulators. Computers & Chemical Engineering 12, 311–327. https://doi.org/10.1016/0098-1354(88)85044-0

Law, R., Harvey, A., Reay, D., 2013. Opportunities for low-grade heat recovery in the UK food processing industry. Applied Thermal Engineering 53, 188–196. https://doi.org/10.1016/j.applthermaleng.2012.03.024

Lee, B., Reklaitis, G.V., 1995. Optimal scheduling of cyclic batch processes for heat integration—I. Basic formulation. Computers & Chemical Engineering 19, 883–905. https://doi.org/10.1016/0098-1354(94)00091-2

Liew, P.Y., Lim, J.S., Wan Alwi, S.R., Abdul Manan, Z., Varbanov, P.S., Klemeš, J.J., 2014a. A retrofit framework for Total Site heat recovery systems. Applied Energy 135, 778–790. https://doi.org/10.1016/j.apenergy.2014.03.090

Liew, P.Y., Theo, W.L., Wan Alwi, S.R., Lim, J.S., Abdul Manan, Z., Klemeš, J.J., Varbanov, P.S., 2017. Total Site Heat Integration planning and design for industrial, urban and renewable systems. Renewable and Sustainable Energy Reviews 68, 964–985. https://doi.org/10.1016/j.rser.2016.05.086

Liew, P.Y., Walmsley, T.G., Wan Alwi, S.R., Abdul Manan, Z., Klemeš, J.J., Varbanov, P.S., 2016. Integrating district cooling systems in Locally Integrated Energy Sectors through Total Site Heat Integration. Applied Energy 184, 1350–1363. https://doi.org/10.1016/j.apenergy.2016.05.078

Liew, P.Y., Wan Alwi, S.R., Klemeš, J.J., Varbanov, P.S., Abdul Manan, Z., 2014b. Algorithmic targeting for Total Site Heat Integration with variable energy supply/demand. Applied Thermal Engineering 70, 1073–1083. https://doi.org/10.1016/j.applthermaleng.2014.03.014

Liew, P.Y., Wan Alwi, S.R., Klemeš, J.J., Varbanov, P.S., Abdul Manan, Z., 2013a. Total Site Heat Integration with Seasonal Energy Availability. Chemical Engineering Transactions 35, 19–24. https://doi.org/10.3303/CET1335003

Liew, P.Y., Wan Alwi, S.R., Lim, J.S., Varbanov, P.S., Klemeš, J.J., Abdul Manan, Z., 2014c. Total Site Heat Integration incorporating the water sensible heat. Journal of Cleaner Production, Emerging industrial processes for water management 77, 94–104. https://doi.org/10.1016/j.jclepro.2013.12.047

Liew, P.Y., Wan Alwi, S.R., Varbanov, P.S., Manan, Z.A., Klemeš, J.J., 2013b. Centralised utility system planning for a Total Site Heat Integration network. Computers & Chemical Engineering, PSE-2012. 57, 104–111. https://doi.org/10.1016/j.compchemeng.2013.02.007

Liew, P.Y., Wan Alwi, S.R., Varbanov, P.S., Manan, Z.A., Klemeš, J.J., 2012. A numerical technique for Total Site sensitivity analysis. Applied Thermal

Engineering 40, 397–408. https://doi.org/10.1016/j.applthermaleng.2012.02.026
Linnhoff, B., 1979. Thermodynamic Analysis in the Design of Process Networks (PhD Thesis). University of Leeds, Leeds, UK.
Linnhoff, B., 1972. Thermodynamic analysis of the cement burning process (Thermodynamische Analyse des Zementbrennprozesses) (Diploma Work). Abteilung IIIa, ETH Zurich.
Linnhoff, B., Dhole, V.R., 1992. Shaftwork targets for low-temperature process design. Chemical Engineering Science 47, 2081–2091. https://doi.org/10.1016/0009-2509(92)80324-6
Linnhoff, B., Flower, J.R., 1978. Synthesis of heat exchanger networks: I. Systematic generation of energy optimal networks. AIChE Journal 24, 633–642. https://doi.org/10.1002/aic.690240411
Linnhoff, B., Hindmarsh, E., 1983. The pinch design method for heat exchanger networks. Chemical Engineering Science 38, 745–763. https://doi.org/10.1016/0009-2509(83)80185-7
Linnhoff, B., Vredeveld, D.R., 1984. Pinch Technology Has Come of Age. Chemical Engineering Progress 80, 33–40.
Lira-Barragán, L.F., Ponce-Ortega, J.M., Serna-González, M., El-Halwagi, M.M., 2014. Optimum heat storage design for solar-driven absorption refrigerators integrated with heat exchanger networks. AIChE Journal 60, 909–930. https://doi.org/10.1002/aic.14308
Luo, X., Huang, X., El-Halwagi, M.M., Ponce-Ortega, J.M., Chen, Y., 2016. Simultaneous synthesis of utility system and heat exchanger network incorporating steam condensate and boiler feedwater. Energy 113, 875–893. https://doi.org/10.1016/j.energy.2016.07.109
Majozi, T., 2005. Wastewater minimisation using central reusable water storage in batch plants. Computers & Chemical Engineering 29, 1631–1646. https://doi.org/10.1016/j.compchemeng.2005.01.003
Makwana, Y., 1997. Systematic Energy Management of Total Sites (PhD thesis). UMIST, Manchester, UK.
Makwana, Y., Smith, R., Zhu, X.X., 1998. A novel approach for retrofit and operations management of existing total sites. Computers & Chemical Engineering 22, Supplement 1, S793–S796. https://doi.org/10.1016/S0098-1354(98)00150-1
Marechal, F., Kalitventzeff, B., 2003. Targeting the integration of multi-period utility systems for site scale process integration. Applied Thermal Engineering 23, 1763–1784. https://doi.org/10.1016/S1359-4311(03)00142-X
Maréchal, F., Kalitventzeff, B., 1998. Energy integration of industrial sites: tools, methodology and application. Applied Thermal Engineering 18, 921–933. https://doi.org/10.1016/S1359-4311(98)00018-0
Marmolejo-Correa, D., Gundersen, T., 2013. New graphical representation of exergy applied to low temperature process design. Industrial & Engineering Chemistry Research 52, 7145–7156. https://doi.org/10.1021/ie302541e
Matsuda, K., Hirochi, Y., Kurosaki, D., Kado, Y., 2014. Application of Area-wide Pinch Technology to a Large Industrial Area in Thailand. Chemical

Engineering Transactions 39, 1027–1032. https://doi.org/10.3303/CET1439172

Matsuda, K., Hirochi, Y., Tatsumi, H., Shire, T., 2009. Applying heat integration total site based pinch technology to a large industrial area in Japan to further improve performance of highly efficient process plants. Energy 34, 1687–1692. https://doi.org/10.1016/j.energy.2009.05.017

Mavromatis, S.P., Kokossis, A.C., 1998. Conceptual optimisation of utility networks for operational variations—I. targets and level optimisation. Chemical Engineering Science 53, 1585–1608. https://doi.org/10.1016/S0009-2509(97)00431-4

Medina-Flores, J.M., Picón-Núñez, M., 2010. Modelling the power production of single and multiple extraction steam turbines. Chemical Engineering Science 65, 2811–2820. https://doi.org/10.1016/j.ces.2010.01.016

Mikkelsen, J., 1998. Thermal-energy storage systems in batch processing (PhD Thesis). Technical University of Denmark, Lyngby, Denmark.

Mohan, T., El-Halwagi, M.M., 2006. An algebraic targeting approach for effective utilization of biomass in combined heat and power systems through process integration. Clean Technologies and Environmental Policy 9, 13–25. https://doi.org/10.1007/s10098-006-0051-x

Morton, R.J., Linnhoff, B., 1984. Individual process improvements in the context of site–wide interactions.

Na, J., Jung, J., Park, C., Han, C., 2015. Simultaneous synthesis of a heat exchanger network with multiple utilities using utility substages. Computers & Chemical Engineering 79, 70–79. https://doi.org/10.1016/j.compchemeng.2015.04.005

Naraki, M., Peyghambarzadeh, S.M., Hashemabadi, S.H., Vermahmoudi, Y., 2013. Parametric study of overall heat transfer coefficient of CuO/water nanofluids in a car radiator. International Journal of Thermal Sciences 66, 82–90. https://doi.org/10.1016/j.ijthermalsci.2012.11.013

Nemet, A., Klemeš, J.J., Kravanja, Z., 2015. Designing a Total Site for an entire lifetime under fluctuating utility prices. Computers & Chemical Engineering, A Tribute to Ignacio E. Grossmann 72, 159–182. https://doi.org/10.1016/j.compchemeng.2014.07.004

Nemet, A., Klemeš, J.J., Kravanja, Z., 2013. Optimising entire lifetime economy of heat exchanger networks. Energy 57, 222–235. https://doi.org/10.1016/j.energy.2013.02.046

Nemet, A., Klemeš, J.J., Varbanov, P.S., Atkins, M.J., Walmsley, M.R.W., 2012a. Total Site Methodology as a Tool for Planning and Strategic Decisions. Chemical Engineering Transactions 29, 115–120. https://doi.org/10.3303/CET1229020

Nemet, A., Klemeš, J.J., Varbanov, P.S., Kravanja, Z., 2012b. Methodology for maximising the use of renewables with variable availability. Energy 44, 29–37. https://doi.org/10.1016/j.energy.2011.12.036

Nemet, A., Kravanja, Z., Klemeš, J.J., 2012c. Integration of solar thermal energy into processes with heat demand. Clean Technologies and Environmental Policy 14, 453–463. https://doi.org/10.1007/s10098-012-0457-6

Oluleye, G., Jobson, M., Smith, R., Perry, S.J., 2016. Evaluating the potential of process sites for waste heat recovery. Applied Energy 161, 627–646. https://doi.org/10.1016/j.apenergy.2015.07.011

Ong, B.H.Y., Walmsley, T.G., Atkins, M.J., Walmsley, M.R.W., 2017. Total site mass, heat and power integration using process integration and process graph. Journal of Cleaner Production 167, 32–43. https://doi.org/10.1016/j.jclepro.2017.08.035

Pan, M., Bulatov, I., Smith, R., 2013. Exploiting tube inserts to intensify heat transfer for the retrofit of Heat Exchanger Networks considering fouling mitigation. Industrial & Engineering Chemistry Research 52, 2925–2943. https://doi.org/10.1021/ie303020m

Pan, M., Bulatov, I., Smith, R., Kim, J.-K., 2012. Novel MILP-based iterative method for the retrofit of heat exchanger networks with intensified heat transfer. Computers & Chemical Engineering 42, 263–276. https://doi.org/10.1016/j.compchemeng.2012.02.002

Pan, M., Bulatov, I., Smith, R., Kim, J.-K., 2011. Novel optimization method for retrofitting heat exchanger networks with intensified heat transfer, in: Computer Aided Chemical Engineering. Elsevier, pp. 1864–1868.

Pandey, S.D., Nema, V.K., 2012. Experimental analysis of heat transfer and friction factor of nanofluid as a coolant in a corrugated plate heat exchanger. Experimental Thermal and Fluid Science 38, 248–256. https://doi.org/10.1016/j.expthermflusci.2011.12.013

Pantzali, M.N., Mouza, A.A., Paras, S.V., 2009. Investigating the efficacy of nanofluids as coolants in plate heat exchangers (PHE). Chemical Engineering Science 64, 3290–3300. https://doi.org/10.1016/j.ces.2009.04.004

Papoulias, S.A., Grossmann, I.E., 1983. A structural optimization approach in process synthesis—III. Computers & Chemical Engineering 7, 723–734. https://doi.org/10.1016/0098-1354(83)85024-8

Parker, S.J., 1989. Supertargeting for Multiple Utilities. (PhD Thesis). University of Manchester Institute of Technology, Manchester, UK.

Perry, S., Klemeš, J.J., Bulatov, I., 2008. Integrating waste and renewable energy to reduce the carbon footprint of locally integrated energy sectors. Energy 33, 1489–1497. https://doi.org/10.1016/j.energy.2008.03.008

Peyghambarzadeh, S.M., Hashemabadi, S.H., Hoseini, S.M., Seifi Jamnani, M., 2011. Experimental study of heat transfer enhancement using water/ethylene glycol based nanofluids as a new coolant for car radiators. International Communications in Heat and Mass Transfer 38, 1283–1290. https://doi.org/10.1016/j.icheatmasstransfer.2011.07.001

Peyghambarzadeh, S.M., Hashemabadi, S.H., Naraki, M., Vermahmoudi, Y., 2013. Experimental study of overall heat transfer coefficient in the application of dilute nanofluids in the car radiator. Applied Thermal Engineering 52, 8–16. https://doi.org/10.1016/j.applthermaleng.2012.11.013

Polley, G.T., Panjeh Shahi, M.H., Picon Nunez, M., 1991. Rapid design algorithms for shell-and-tube and compact heat exchangers. Chemical Engineering Research and Design 69, 435–444.

Polley, G.T., Panjeshahi, M.H., Jegede, F.O., 1990. Pressure drop considerations in the retrofit of heat exchanger networks. Transactions of the Institute of Chemical Engineers 68, 286–295.

Ponce-Ortega, J.M., Serna-González, M., Jiménez-Gutiérrez, A., 2010. Synthesis of Heat Exchanger Networks with optimal placement of multiple utilities. Ind. Eng. Chem. Res. 49, 2849–2856. https://doi.org/10.1021/ie901750a

Prashant, K., Perry, S., 2012. Optimal selection of steam mains in Total Site utility systems. Chemical Engineering Transactions 29, 127–132. https://doi.org/10.3303/CET1229022

Raei, B., Shahraki, F., Jamialahmadi, M., Peyghambarzadeh, S.M., 2017. Experimental study on the heat transfer and flow properties of γ-Al2O3/water nanofluid in a double-tube heat exchanger. Journal of Thermal Analysis and Calorimetry 127, 2561–2575. https://doi.org/10.1007/s10973-016-5868-x

Raei, B., Tarighaleslami, A.H., 2011. A Survey on a Heat Exchangers Network to Decrease Energy Consumption by Using Pinch Technology. Journal of Environmental Science and Engineering 5, 1648–1653. https://doi.org/10.17265/1934-8932/2011.12.011

Raghu Ram, J., Banerjee, R., 2003. Energy and cogeneration targeting for a sugar factory. Applied Thermal Engineering 23, 1567–1575. https://doi.org/10.1016/S1359-4311(03)00101-7

Raissi, K., 1994. Total Site Integration (PhD Thesis). UMIST, Manchester, UK.

Rivero, R., Rendón, C., Gallegos, S., 2004. Exergy and exergoeconomic analysis of a crude oil combined distillation unit. Energy, Efficiency, Costs, Optimization, Simulation and Environmental Impact of Energy Systems 29, 1909–1927. https://doi.org/10.1016/j.energy.2004.03.094

Rodera, H., Bagajewicz, M.J., 1999. Targeting procedures for energy savings by heat integration across plants. AIChE Journal 45, 1721–1742. https://doi.org/10.1002/aic.690450810

Saw, S.Y., Lee, L., Lim, M.H., Foo, D.C.Y., Chew, I.M.L., Tan, R.R., Klemeš, J.J., 2011. An extended graphical targeting technique for direct reuse/recycle in concentration and property-based resource conservation networks. Clean Technologies and Environmental Policy 13, 347–357. https://doi.org/10.1007/s10098-010-0305-5

Shamsi, S., Omidkhah, M.R., 2012. Optimization of Steam Pressure Levels in a Total Site Using a Thermoeconomic Method. Energies 5, 702–717. https://doi.org/10.3390/en5030702

Shang, Z., Kokossis, A., 2004. A transhipment model for the optimisation of steam levels of total site utility system for multiperiod operation. Computers & Chemical Engineering 28, 1673–1688. https://doi.org/10.1016/j.compchemeng.2004.01.010

Shekarian, E., Jafari Nasr, M.R., Tarighaleslami, A.H., Walmsley, T.G., Atkins, M.J., Sahebjamee, N., Alaghehbandan, M., 2016. Impact of Hybrid Heat Transfer Enhancement Techniques in Shell and Tube Heat Exchanger Design. Chemical Engineering Transactions 52, 1159–1164. https://doi.org/10.3303/CET1652194

Shekarian, E., Tarighaleslami, A.H., Khodaverdi, F., 2014. Review of effective parameters on the nanofluid thermal conductivity. Journal of Middle East Applied Science and Technology 6, 776–780.

Shenoy, U.V., 1995. Heat Exchanger Network Synthesis: Processes Optimization by Energy and Resource Analysis. Gulf Publishing Company, Houston, USA.

Shenoy, U.V., Sinha, A., Bandyopadhyay, S., 1998. Multiple utilities targeting for Heat Exchanger Networks. Chemical Engineering Research and Design, Techno-Economic Analysis 76, 259–272. https://doi.org/10.1205/026387698524910

Sherrin, S.C., Nicol, R.S., 1995. Heat integration in semi-continuous food plants using intermediate utility systems. in: CHEMECA, SCI-TECH INFORMATION SERVICES 161–166.

Shokoya, C.G., Kotjabasakis, E., 1991. Retrofit of Heat Exchanger Networks for debottlenecking and energy savings (PhD Thesis). Manchester, Institute of Science and Technology, Manchester, UK.

Sinaki, S.Y., Tarighaleslami, A.H., Jafarigol, F., 2011. Study on external costs of flare gases using Asian development bank method. Chemical Engineering Transactions 25, 39–44. https://doi.org/10.3303/CET1125007

Smith, R., 2005. Chemical Process: Design and Integration. John Wiley and Sons Ltd., Chichester, UK.

Smith, R., Jobson, M., Chen, L., 2010. Recent development in the retrofit of heat exchanger networks. Applied Thermal Engineering 30, 2281–2289. https://doi.org/10.1016/j.applthermaleng.2010.06.006

Song, R., Chang, C., Tang, Q., Wang, Y., Feng, X., El-Halwagi, M.M., 2017. The implementation of inter-plant heat integration among multiple plants. Part II: The mathematical model. Energy 135, 382–393. https://doi.org/10.1016/j.energy.2017.06.136

Song, R., Feng, X., Wang, Y., 2016a. Feasible heat recovery of interplant heat integration between two plants via an intermediate medium analyzed by Interplant Shifted Composite Curves. Applied Thermal Engineering 94, 90–98. https://doi.org/10.1016/j.applthermaleng.2015.10.125

Song, R., Wang, Y., Feng, X., 2016b. Participant plants and streams selection for interplant heat integration among three plants. Chemical Engineering Transactions 52, 547–552. https://doi.org/10.3303/CET1652092

Sorin, M., Hammache, A., 2005. A new thermodynamic model for shaftwork targeting on total sites. Applied Thermal Engineering 25, 961–972. https://doi.org/10.1016/j.applthermaleng.2004.06.021

Statistics NZ, 2016. Infoshare - Select variables - Statistics New Zealand [WWW Document]. URL http://www.stats.govt.nz/infoshare/SelectVariables.aspx?pxID=24d2d4d9-eca5-4988-8fea-c1a353b12e01 (accessed 4.20.17).

Stijepovic, M.Z., Linke, P., 2011. Optimal waste heat recovery and reuse in industrial zones. Energy 36, 4019–4031. https://doi.org/10.1016/j.energy.2011.04.048

Stoltze, S., Lorentzen, B., Petersen, P.M., Qvale, B., 1993. A Simple Technique for Analyzing Waste-Heat Recovery with Heat-Storage in Batch Processes, in: Pilavachi, D.P.A. (Ed.), Energy Efficiency in Process Technology. Springer Netherlands, pp. 1063–1072.

Stoltze, S., Mikkelsen, J., Lorentzen, B., Peterson, P.M., Qvale, B., 1995. Waste-Heat Recovery in Batch Processs Using Heat Storage. Journal of Energy Resources Technology 117, 142–149. https://doi.org/10.1115/1.2835330

Sun, L., Doyle, S., Smith, R., 2015. Heat recovery and power targeting in utility systems. Energy 84, 196–206. https://doi.org/10.1016/j.energy.2015.02.087

Sun, L., Doyle, S., Smith, R., 2014. Graphical cogeneration analysis for site utility systems. Clean Technologies and Environmental Policy 16, 1235–1243. https://doi.org/10.1007/s10098-014-0742-7

Sun, L., Doyle, S., Smith, R., 2013. Cogeneration improvement based on steam cascade analysis. Chemical Engineering Transactions 35, 13–18. https://doi.org/10.3303/CET1335002

Tabari, Z.T., Heris, S.Z., 2015. Heat transfer performance of milk pasteurization plate heat exchangers using MWCNT/Water nanofluid. Journal of Dispersion Science and Technology 36, 196–204. https://doi.org/10.1080/01932691.2014.894917

Takama, N., Kuriyama, T., Shiroko, K., Umeda, T., 1980. Optimal water allocation in a petroleum refinery. Computers & Chemical Engineering 4, 251–258. https://doi.org/10.1016/0098-1354(80)85005-8

Tarighaleslami, A.H., Bozorgian, A., Raei, B., 2009. Application of the exergy analysis in the petroleum refining processes optimization. Presented at the The 1st Territorial Chemistry and Industry Symposium, Damghan, Iran, p. E-1097.

Tarighaleslami, A.H., Hesas, R.H., Omidkhah, M.R., 2010. An approach for water cost of cooling water system in oil refinery. Chemical Engineering Transactions 21, 103–108. https://doi.org/10.3303/CET1021018

Tarighaleslami, A.H., Omidkhah, M.R., Ghannadzadeh, A., Hesas, R.H., 2012. Thermodynamic evaluation of distillation columns using exergy loss profiles: a case study on the crude oil atmospheric distillation column. Clean Technologies and Environmental Policy 14, 381–387. https://doi.org/10.1007/s10098-012-0465-6

Tarighaleslami, A.H., Omidkhah, M.R., Sinaki, S.Y., 2011. An exergy analysis on crude oil atmospheric distillation column. Chemical Engineering Transactions 25, 117–122. https://doi.org/10.3303/CET1125020

Tarighaleslami, A.H., Walmsley, T.G., Atkins, M.J., Walmsley, M.R.W., Liew, P.Y., Neale, J.R., 2017a. A Unified Total Site Heat Integration targeting method for isothermal and non-isothermal utilities. Energy 119, 10–25. https://doi.org/10.1016/j.energy.2016.12.071

Tarighaleslami, A.H., Walmsley, T.G., Atkins, M.J., Walmsley, M.R.W., Neale, J.R., 2018. Utility Exchanger Network synthesis for Total Site Heat Integration. Energy 153, 1000–1015. https://doi.org/10.1016/j.energy.2018.04.111

Tarighaleslami, A.H., Walmsley, T.G., Atkins, M.J., Walmsley, M.R.W., Neale, J.R., 2017b. Total Site Heat Integration: Utility selection and optimisation using cost and exergy derivative analysis. Energy 141, 949–963. https://doi.org/10.1016/j.energy.2017.09.148

Tarighaleslami, A.H., Walmsley, T.G., Atkins, M.J., Walmsley, M.R.W., Neale, J.R., 2017c. A comparison of Utility Heat Exchanger Network synthesis for Total Site Heat Integration methods. Chemical Engineering Transactions 61, 775–780. https://doi.org/10.3303/CET1761127

Tarighaleslami, A.H., Walmsley, T.G., Atkins, M.J., Walmsley, M.R.W., Neale, J.R., 2016a. Optimisation of non-isothermal utilities using the Unified Total Site Heat Integration method. Chemical Engineering Transactions 52, 457–462. https://doi.org/10.3303/CET1652077

Tarighaleslami, A.H., Walmsley, T.G., Atkins, M.J., Walmsley, M.R.W., Neale, J.R., 2016b. Heat Transfer Enhancement for site level indirect heat recovery systems using nanofluids as the intermediate fluid. Applied Thermal Engineering 105, 923–930. https://doi.org/10.1016/j.applthermaleng.2016.03.132

Tarighaleslami, A.H., Walmsley, T.G., Walmsley, M.R.W., Atkins, M.J., Neale, J.R., 2015. Heat Transfer Enhancement in Heat Recovery Loops using nanofluids as the intermediate fluid. Chemical Engineering Transactions 45, 991–996. https://doi.org/10.3303/CET1545166

Tiwari, A.K., Ghosh, P., Sarkar, J., 2013. Heat transfer and pressure drop characteristics of CeO2/water nanofluid in plate heat exchanger. Applied Thermal Engineering 57, 24–32. https://doi.org/10.1016/j.applthermaleng.2013.03.047

Tjoe, T.N., Linnhoff, B., 1986. Using pinch technology for process retrofit. Chemical Engineering 93, 47–60.

Tohidi, A., Ghaffari, H., Nasibi, H., Mujumdar, A.S., 2015. Heat transfer enhancement by combination of chaotic advection and nanofluids flow in helically coiled tube. Applied Thermal Engineering 86, 91–105. https://doi.org/10.1016/j.applthermaleng.2015.04.043

Towler, G.P., Mann, R., Serriere, A.J.-L., Gabaude, C.M.D., 1996. Refinery hydrogen management: cost analysis of Chemically-Integrated Facilities. Industrial & Engineering Chemistry Research 35, 2378–2388. https://doi.org/10.1021/ie950359+

Umeda, T., Ithoh, J., Shiroko, K., 1978. Heat exchanger systems synthesis. Chemical Engineering Progress 74, 70–76.

Vaideeswaran, L., 2001. Site analysis and optimisation accounting for process changes (Ph.D.). The University of Manchester.

Varbanov, P.S., Doyle, S., Smith, R., 2004. Modelling and optimization of utility systems. Chemical Engineering Research and Design 82, 561–578. https://doi.org/10.1205/026387604323142603

Varbanov, P.S., Fodor, Z., Klemeš, J.J., 2012. Total Site targeting with process specific minimum temperature difference (ΔTmin). Energy 44, 20–28. https://doi.org/10.1016/j.energy.2011.12.025

Varbanov, P.S., Klemeš, J.J., 2011. Integration and management of renewables into Total Sites with variable supply and demand. Computers & Chemical Engineering 35, 1815–1826. https://doi.org/10.1016/j.compchemeng.2011.02.009

Varghese, J., Bandyopadhyay, S., 2007. Targeting for Energy Integration of Multiple Fired Heaters. Industrial & Engineering Chemistry Research 46, 5631–5644. https://doi.org/10.1021/ie061619y

Walmsley, M.R.W., Atkins, M.J., Riley, J., 2009. Thermocline management of stratified tanks for heat storage. Chemical Engineering Transactions 18, 231–236. https://doi.org/10.3303/CET0918036

Walmsley, M.R.W., Atkins, M.J., Walmsley, T.G., 2013a. Application of Heat Recovery Loops to Semi-continuous Processes for Process Integration, in: Klemeš, J.J. (Ed.), Handbook of Process Integration (PI), Woodhead Publishing Series in Energy. Woodhead Publishing, Cambridge, UK, pp. 594–629.

Walmsley, M.R.W., Walmsley, T.G., Atkins, M.J., Kamp, P.J.J., Neale, J.R., 2014a. Minimising carbon emissions and energy expended for electricity generation in New Zealand through to 2050. Applied Energy 135, 656–665. https://doi.org/10.1016/j.apenergy.2014.04.048

Walmsley, M.R.W., Walmsley, T.G., Atkins, M.J., Kamp, P.J.J., Neale, J.R., Chand, A., 2015. Carbon Emissions Pinch Analysis for emissions reductions in the

New Zealand transport sector through to 2050. Energy 92, 569–576. https://doi.org/10.1016/j.energy.2015.04.069

Walmsley, M.R.W., Walmsley, T.G., Atkins, M.J., Neale, J.R., 2014b. Options for solar thermal and Heat Recovery Loop hybrid system design. Chemical Engineering Transactions 39, 361–363. https://doi.org/10.3303/CET1439061

Walmsley, M.R.W., Walmsley, T.G., Atkins, M.J., Neale, J.R., 2013b. Methods for improving heat exchanger area distribution and storage temperature selection in heat recovery loops. Energy 55, 15–22. https://doi.org/10.1016/j.energy.2013.02.050

Walmsley, M.R.W., Walmsley, T.G., Atkins, M.J., Neale, J.R., 2013c. Integration of solar heating into Heat Recovery Loops using constant and variable temperature storage. Chemical Engineering Transactions 35, 1183–1188. https://doi.org/10.3303/CET1335197

Walmsley, M.R.W., Walmsley, T.G., Atkins, M.J., Neale, J.R., 2012. Area targeting and storage temperature selection for Heat Recovery Loops. Chemical Engineering Transactions 29, 1219–1224. https://doi.org/10.3303/CET1229204

Walmsley, T.G., 2016. A Total Site Heat Integration design method for integrated evaporation systems including vapour recompression. Journal of Cleaner Production 136, 111–118. https://doi.org/10.1016/j.jclepro.2016.06.044

Walmsley, T.G., Atkins, M.J., Tarighaleslami, A.H., Liew, P.Y., 2016. Assisted heat transfer and shaft work targets for increased Total Site Heat Integration. Chemical Engineering Transactions 52, 403–408. https://doi.org/10.3303/CET1652068

Walmsley, T.G., Walmsley, M.R.W., Atkins, M.J., Neale, J.R., 2014a. Integration of industrial solar and gaseous waste heat into heat recovery loops using constant and variable temperature storage. Energy 75, 53–67. https://doi.org/10.1016/j.energy.2014.01.103

Walmsley, T.G., Walmsley, M.R.W., Atkins, M.J., Neale, J.R., 2013. Improving energy recovery in milk powder production through soft data optimisation. Applied Thermal Engineering 61, 80–87. https://doi.org/10.1016/j.applthermaleng.2013.01.051

Walmsley, T.G., Walmsley, M.R.W., Atkins, M.J., Neale, J.R., Tarighaleslami, A.H., 2015a. Thermo-economic optimisation of industrial milk spray dryer exhaust to inlet air heat recovery. Energy 90, Part 1, 95–104. https://doi.org/10.1016/j.energy.2015.03.102

Walmsley, T.G., Walmsley, M.R.W., Morrison, A.S., Atkins, M.J., Neale, J.R., 2014b. A derivative based method for cost optimal area allocation in heat exchanger networks. Applied Thermal Engineering 70, 1084–1096. https://doi.org/10.1016/j.applthermaleng.2014.03.044

Walmsley, T.G., Walmsley, M.R.W., Tarighaleslami, A.H., Atkins, M.J., Neale, J.R., 2015b. Integration options for solar thermal with low temperature industrial heat recovery loops. Energy 90, Part 1, 113–121. https://doi.org/10.1016/j.energy.2015.05.080

Wan Alwi, S.R., Manan, Z.A., 2010. STEP—A new graphical tool for simultaneous targeting and design of a heat exchanger network. Chemical Engineering Journal 162, 106–121. https://doi.org/10.1016/j.cej.2010.05.009

Wang, Y., Chang, C., Feng, X., 2015. A systematic framework for multi-plants Heat Integration combining Direct and Indirect Heat Integration methods. Energy 90, Part 1, 56–67. https://doi.org/10.1016/j.energy.2015.04.015

Wang, Y., Feng, X., Chu, K.H., 2014. Trade-off between energy and distance related costs for different connection patterns in heat integration across plants. Applied Thermal Engineering 70, 857–866. https://doi.org/10.1016/j.applthermaleng.2014.06.012

Wang, Y., Pan, M., Bulatov, I., Smith, R., Kim, J.-K., 2012. Application of intensified heat transfer for the retrofit of heat exchanger network. Applied Energy 89, 45–59. https://doi.org/10.1016/j.apenergy.2011.03.019

Wang, Y.P., Smith, R., 1994. Wastewater minimisation. Chemical Engineering Science 49, 981–1006. https://doi.org/10.1016/0009-2509(94)80006-5

Wu, Z., Wang, L., Sundén, B., Wadsö, L., 2016. Aqueous carbon nanotube nanofluids and their thermal performance in a helical heat exchanger. Applied Thermal Engineering 96, 364–371. https://doi.org/10.1016/j.applthermaleng.2014.10.096

Zhang, B.J., Li, J., Zhang, Z.L., Wang, K., Chen, Q.L., 2016. Simultaneous design of heat exchanger network for heat integration using hot direct discharges/feeds between process plants. Energy 109, 400–411. https://doi.org/10.1016/j.energy.2016.04.127

Zhu, F.X.X., Vaideeswaran, L., 2000. Recent research development of process integration in analysis and optimisation of energy systems. Applied Thermal Engineering 20, 1381–1392. https://doi.org/10.1016/S1359-4311(00)00013-2

Zhu, X.X., Nie, X.R., 2002. Pressure drop considerations for heat exchanger network grassroots design. Computers & Chemical Engineering 26, 1661–1676. https://doi.org/10.1016/S0098-1354(02)00149-7

Zhu, X.X., Zanfir, M., Klemeš, J.J., 2000. Heat Transfer Enhancement for Heat Exchanger Network retrofit. Heat Transfer Engineering 21, 7–18. https://doi.org/10.1080/014576300270988

Appendix A

Process Level Grand Composite Curves with Utility Targets

Process level Grand Composite Curves (GCC) are presented in this appendix. For each case study, GCCs are constructed and utilities are targeted as the result of the UTSI software tool.

Kraft Pulp Mill Case Study

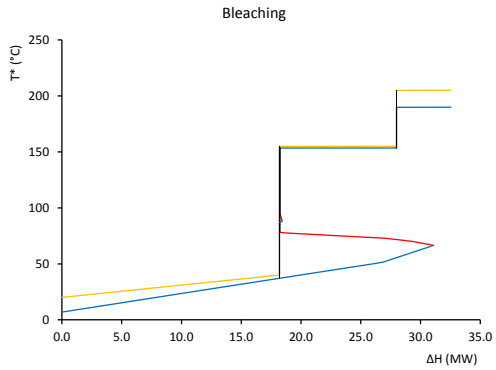

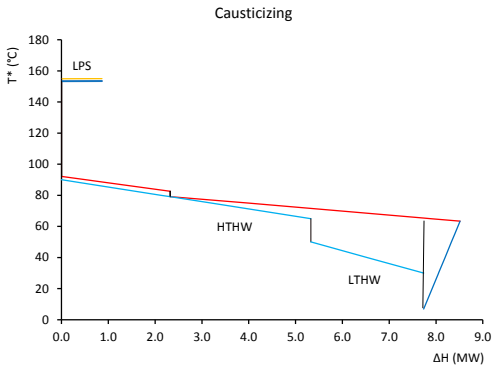

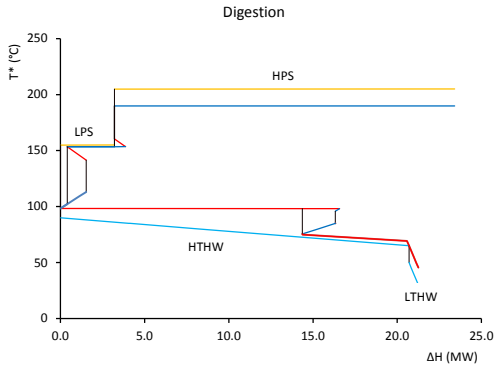

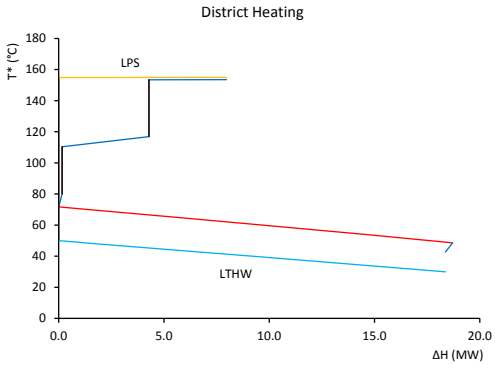

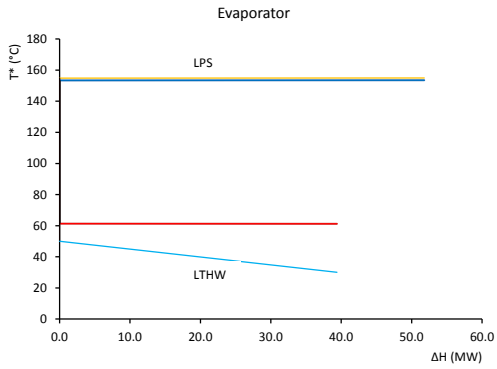

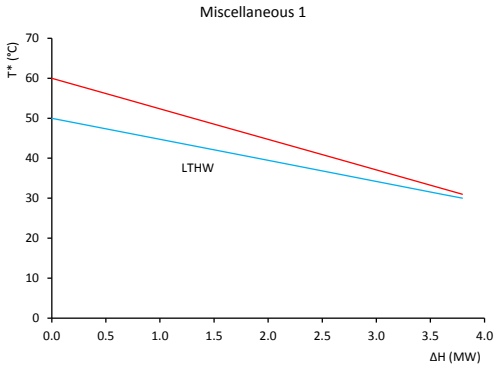

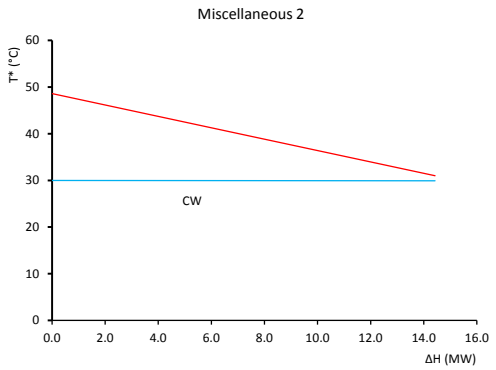

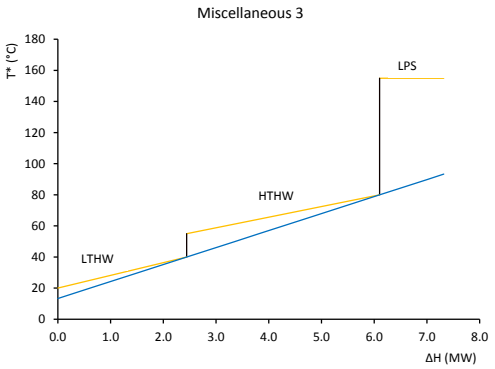

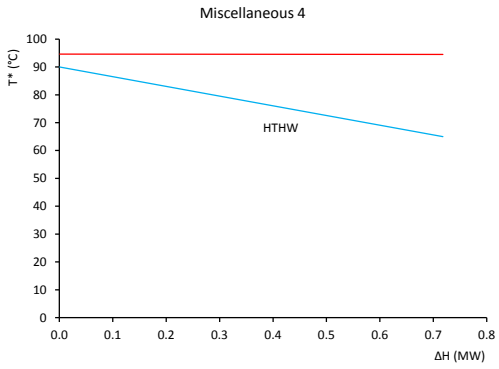
Miscellaneous 4
T* (°C)
HTHW
ΔH (MW)

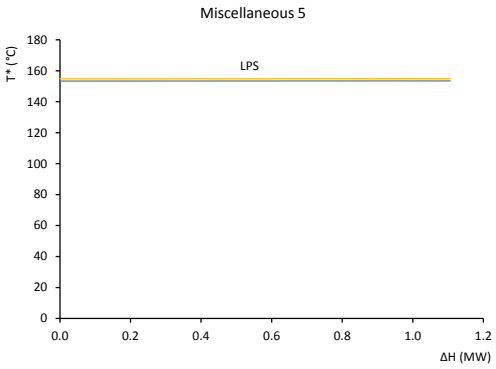
Miscellaneous 5
T* (°C)
LPS
ΔH (MW)

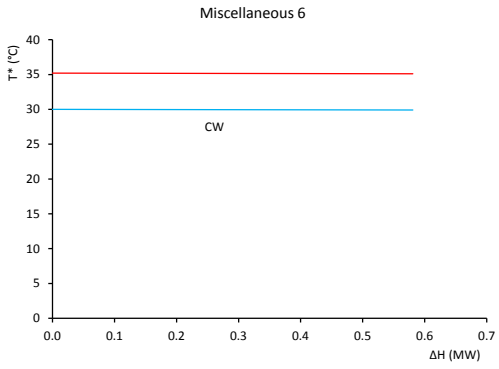
Miscellaneous 6
T* (°C)
CW
ΔH (MW)

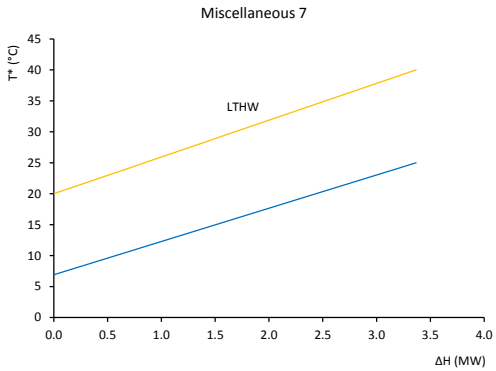
Miscellaneous 7
T* (°C)
LTHW
ΔH (MW)

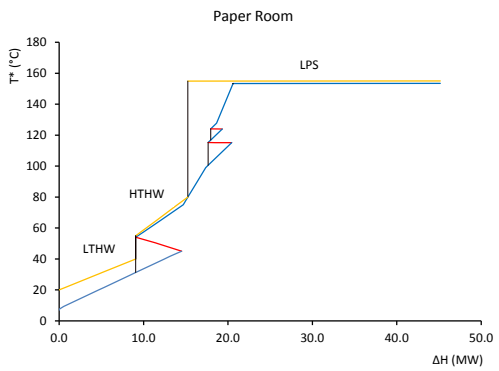
Paper Room
T* (°C)
LPS
HTHW
LTHW
ΔH (MW)

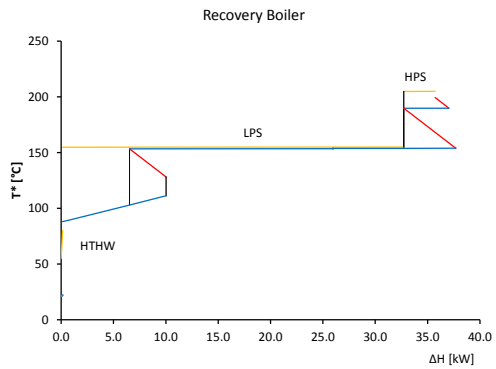
Recovery Boiler
T* [°C]
HPS
LPS
HTHW
ΔH [kW]

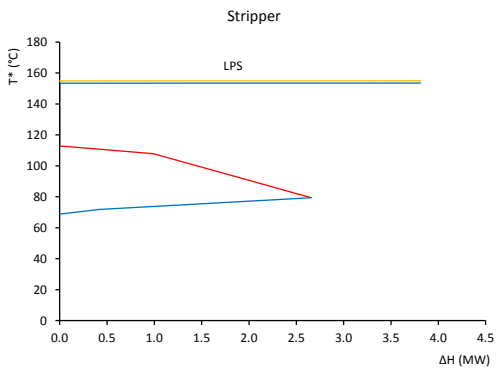
Stripper
T* (°C)
LPS
ΔH (MW)

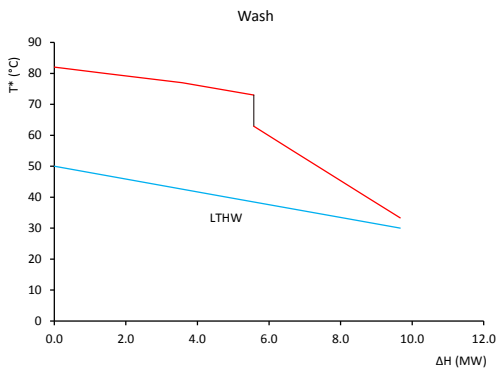
Wash
T* (°C)
LTHW
ΔH (MW)

Dairy Factory Case Study

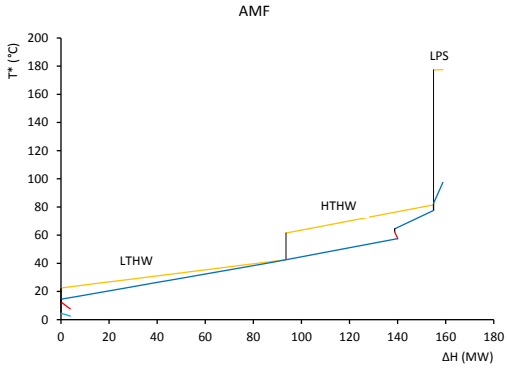

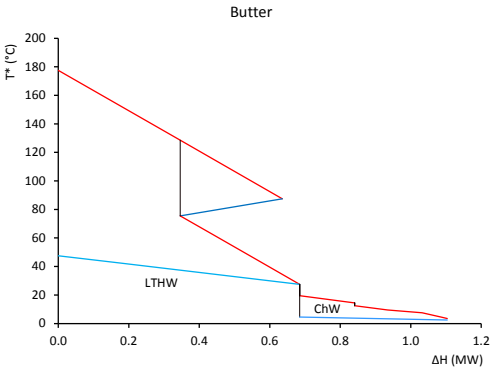

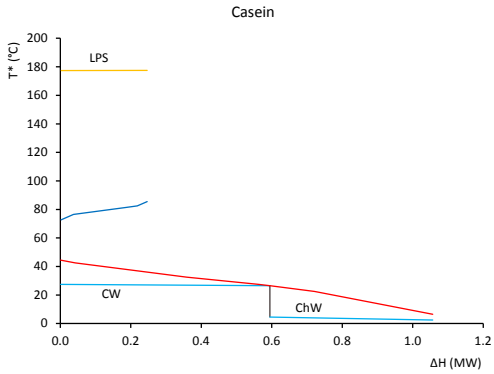

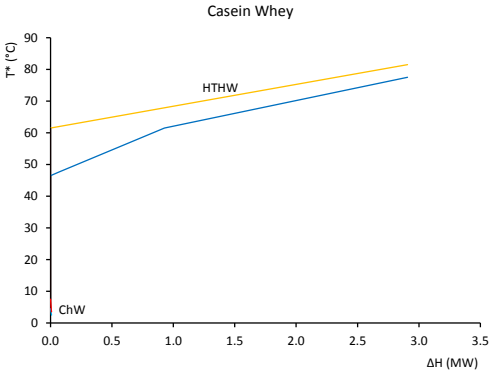

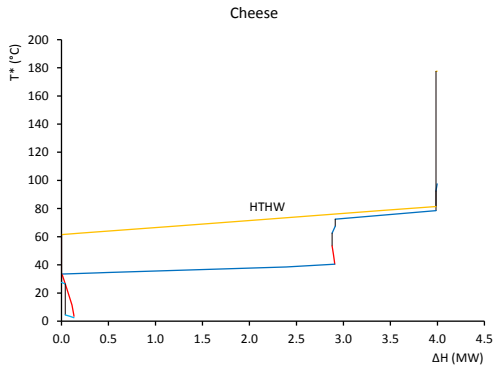

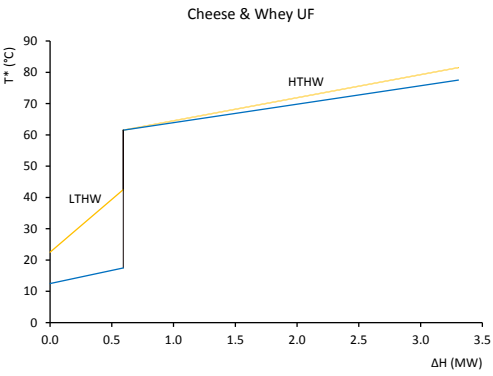

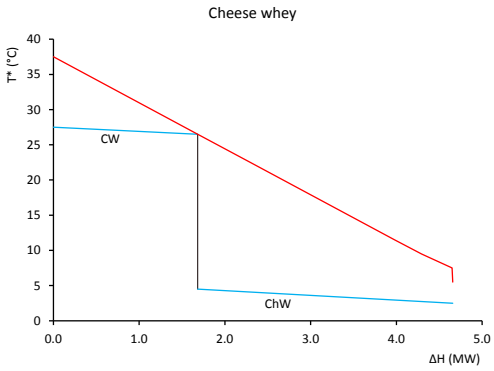

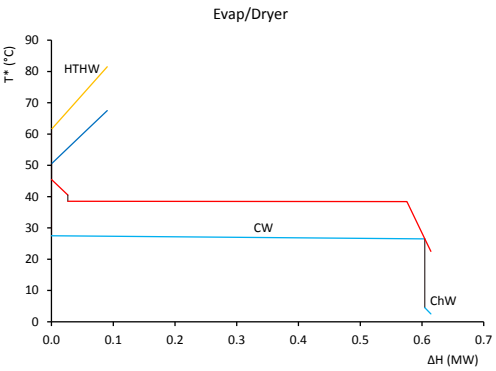

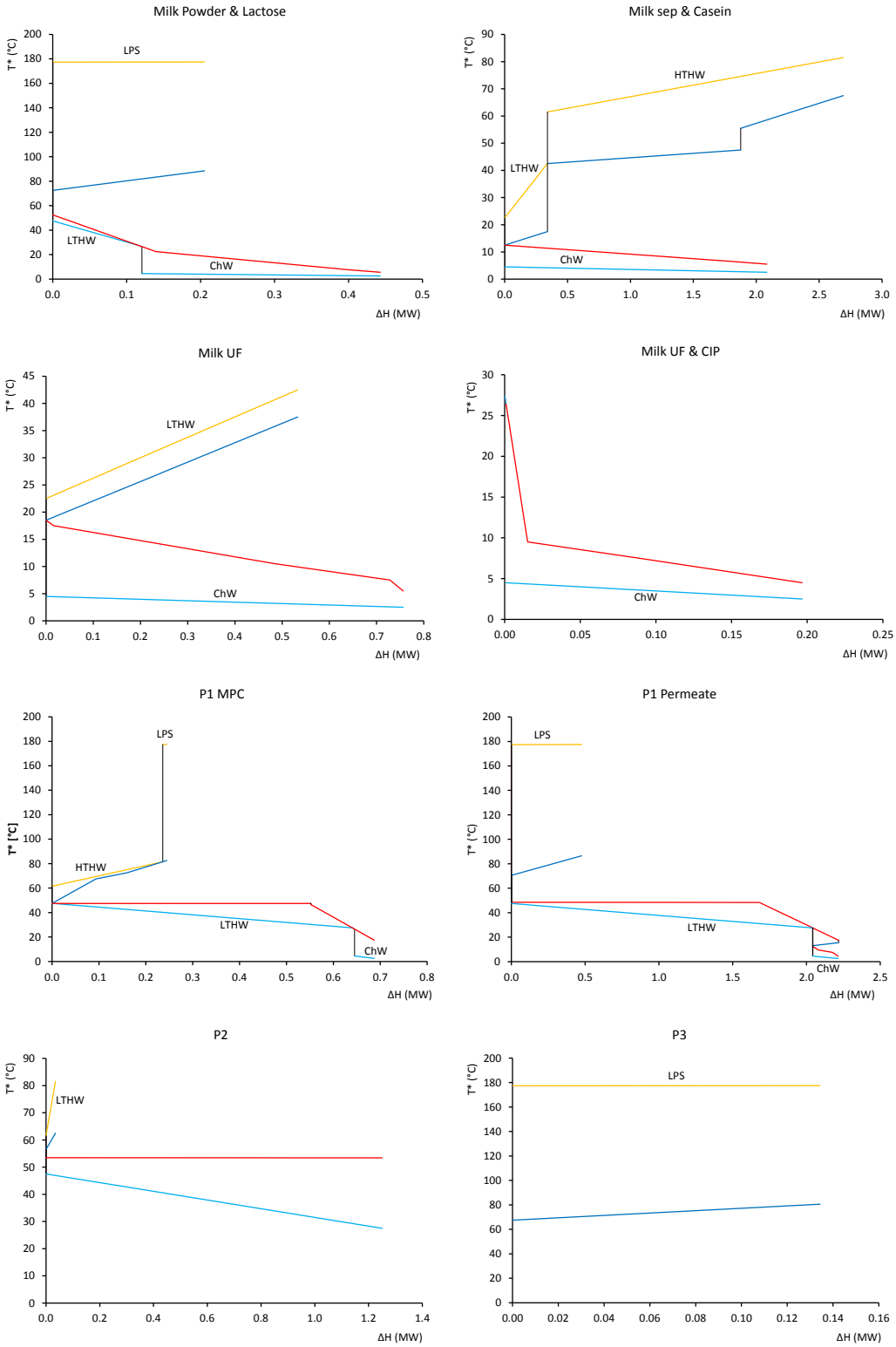
Milk Powder & Lactose
T* (°C)
LPS
LTHW
ChW
ΔH (MW)
Milk sep & Casein
T* (°C)
HTHW
LTHW
ChW
ΔH (MW)
Milk UF
T* (°C)
LTHW
ChW
ΔH (MW)
Milk UF & CIP
T* (°C)
ChW
ΔH (MW)
P1 MPC
T* [°C]
LPS
HTHW
LTHW
ChW
ΔH (MW)
P1 Permeate
T* (°C)
LPS
LTHW
ChW
ΔH (MW)
P2
T* (°C)
LTHW
ΔH (MW)
P3
T* (°C)
LPS
ΔH (MW)

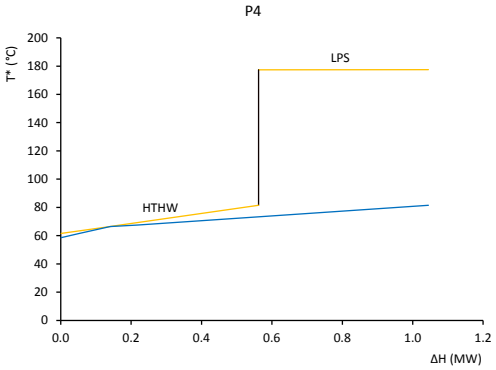
P4
T* (°C)
200
180
160
140
120
100
80
60
40
20
0
LPS
HTHW
0.0
0.2
0.4
0.6
0.8
1.0
1.2
ΔH (MW)

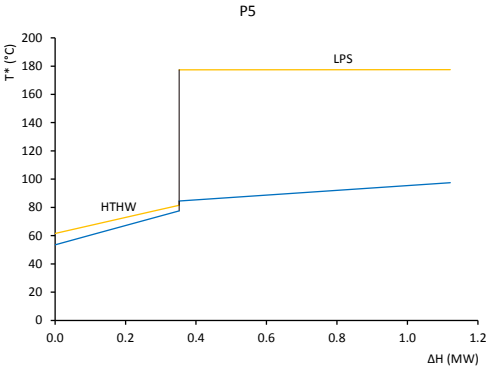
P5
T* (°C)
200
180
160
140
120
100
80
60
40
20
0
LPS
HTHW
0.0
0.2
0.4
0.6
0.8
1.0
1.2
ΔH (MW)

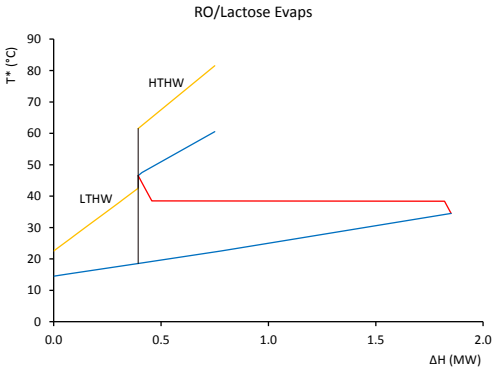
RO/Lactose Evaps
T* (°C)
90
80
70
60
50
40
30
20
10
0
HTHW
LTHW
0.0
0.5
1.0
1.5
2.0
ΔH (MW)

Petrochemical Complex Case Study: Conventional Design

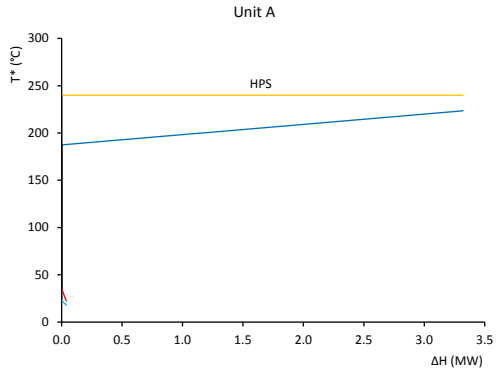

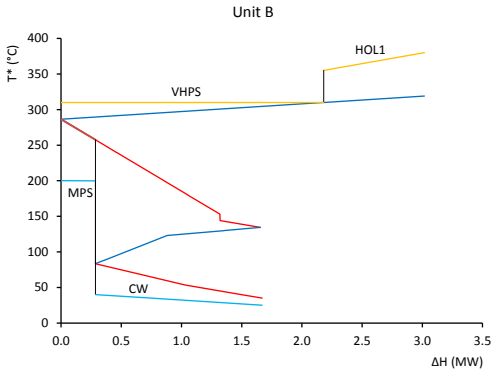

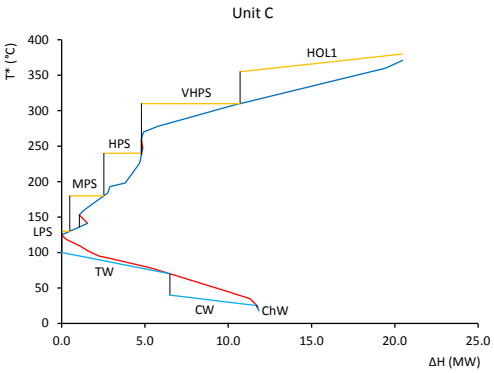

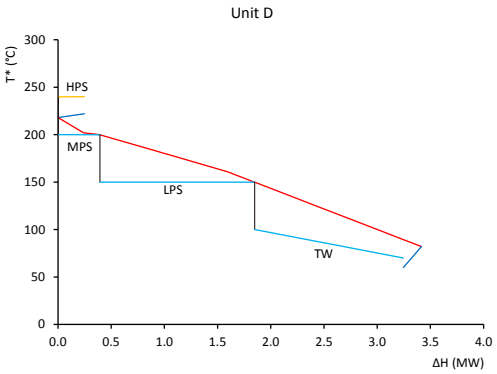

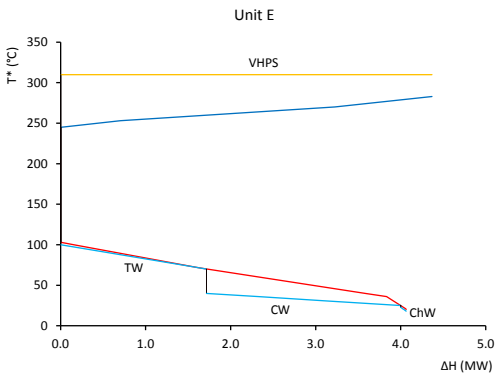

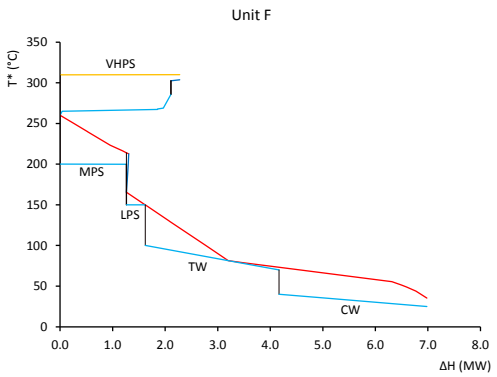

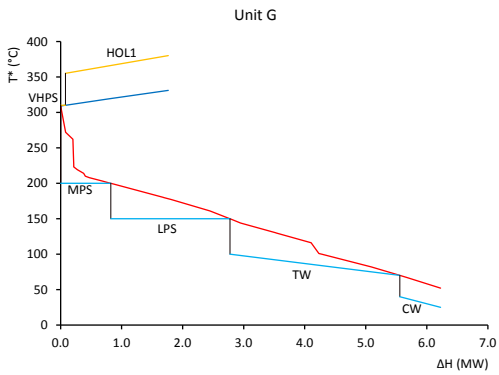

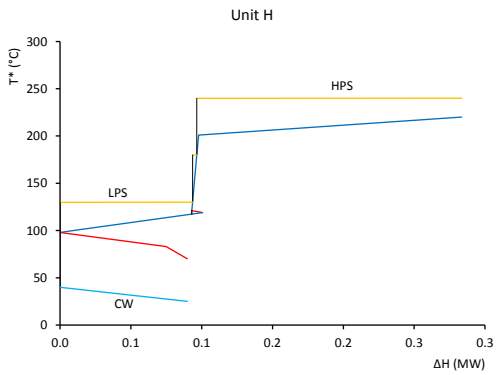

Petrochemical Complex Case Study: Alternative Design

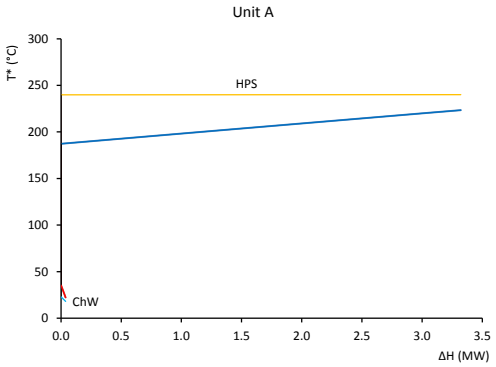

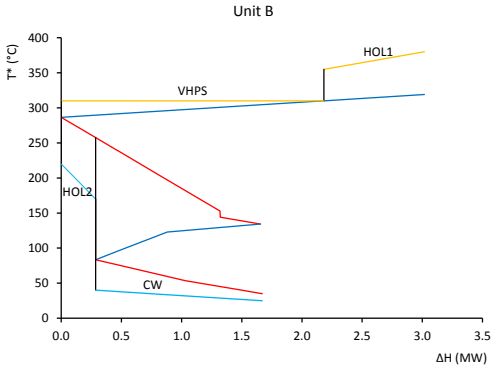

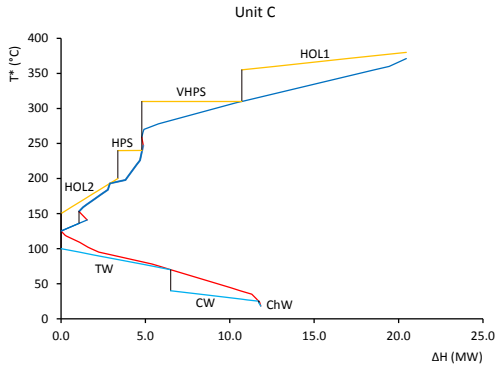

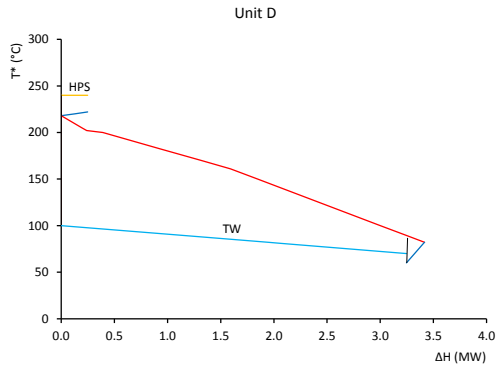

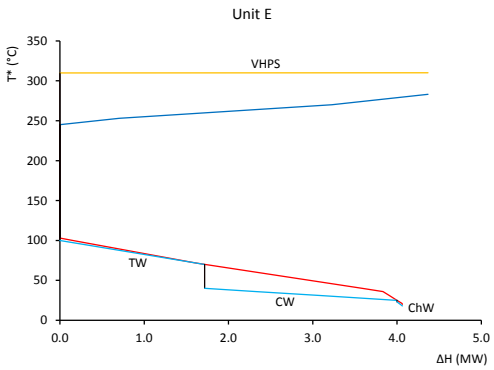

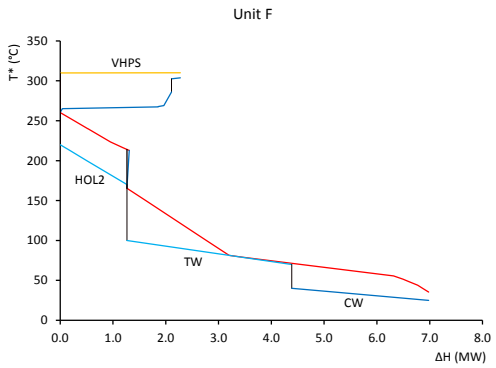

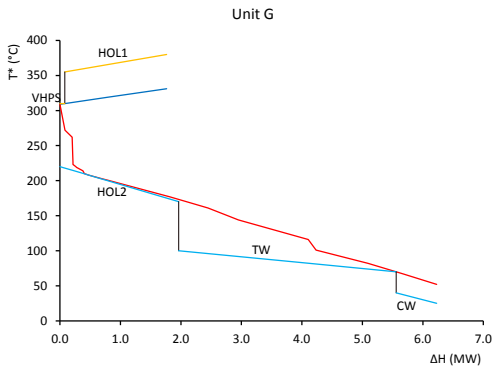

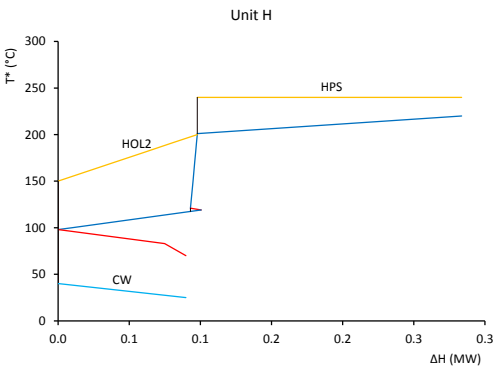

Appendix B

Additional Publications

In parallel to the main objective of the thesis, significant contributions as a co-author have also resulted in three additional journal papers listed below.

1- T. G. Walmsley, M. R. W. Walmsley, **A. H. Tarighaleslami**, M. J. Atkins, J. R. Neale, 2015, Integration options for solar thermal with low temperature industrial heat recovery loops, *Energy*, 90, Part 1, 113–121.

2- T. G. Walmsley, M. R. W. Walmsley, M. J. Atkins, J. R. Neale, **A. H. Tarighaleslami**, 2015, Thermo-economic optimisation of industrial milk spray dryer exhaust to inlet air heat recovery, *Energy*, 90, Part 1, 95–104.

3- E. Shekarian, M. R. Jafari Nasr, **A. H. Tarighaleslami**, T. G. Walmsley, M. J. Atkins, N. Sahebjamee, M. Alaghehbandan, 2016, Impact of Hybrid Heat Transfer Enhancement Techniques in Shell and Tube Heat Exchanger Design, *Chemical Engineering Transactions*, 52, 1159–1164.

Energy 90 (2015) 113–121

Contents lists available at ScienceDirect

Energy

journal homepage: www.elsevier.com/locate/energy

Integration options for solar thermal with low temperature industrial heat recovery loops

Timothy G. Walmsley*, Michael R.W. Walmsley, Amir H. Tarighaleslami, Martin J. Atkins, James R. Neale

University of Waikato, Energy Research Centre, School of Engineering, Hamilton, New Zealand

ARTICLE INFO

Article history:
Received 19 December 2014
Received in revised form
26 May 2015
Accepted 27 May 2015
Available online 18 June 2015

Keywords:
Heat recovery loop
Process integration
Dairy processing
Solar thermal

ABSTRACT

This paper investigates three general methods for integrating industrial solar heating into an HRL (Heat Recovery Loop) using an industrial case study. Integration of solar thermal energy into low temperature pinch processes, like dairy and food and beverage processes, is more economic when combined with an HRL to form a combined inter-plant heat recovery and renewable energy utility system. The combined system shares common infrastructure such as piping, pumping and storage, and improves solar heat utilisation through direct solar boosting of the HRL intermediate fluid's temperature and enthalpy either through parallel or series integration relative to the other sources and sinks in the HRL system. Three options for integrating solar thermal directly into HRLs are dynamically modelled using historical plant data from a large multi-plant dairy case study to demonstrate the hot utility savings potential of the solar-HRL system. For the dairy case study, results show the best location for integrating solar heating into an HRL is in series with the heat sources as the hot fluid returns to the storage tank. This configuration maximises the effectiveness of collecting solar heat as a meaningful replacement of non-renewable process heat.

1. Introduction

Effectively integrating solar heat into industrial processes through generation of low pressure steam and hot water is a subject of growing interest for industry and governments as it is viewed as an important step towards global energy sustainability. Industrial solar thermal process heat generation has tremendous potential for industries that require large amounts of hot water approximately in the 40 °C–80 °C temperature range (i.e. pinch temperature below 40 °C) that are located in countries with long hours and high intensities of sunshine. The types of industries that could benefit most from solar thermal process heat include food, dairy, meat, beverage, textile, agricultural, and low temperature chemical processing.

Identifying the best solar integration point in a process from a technical and economic point of view is a significant challenge, which is enlarged by the current availability of inexpensive fossil fuels in most countries [1]. Low cost implementation of solar process heat in industrial processes requires sharing existing infrastructure including the fluid distribution system (e.g. piping and pumping) and the heat storage system [2]. Existing system may be in the form of a steam and hot water utility system, an indirect HR (heat recovery) system such as an HRL (Heat Recovery Loop) [3], or a combined utility and HR system as proposed in the Total Site (TS) method [4].

Increased inter-process integration through TS has greatly contributed to identifying substantial utility savings in slaughter and meat processing [5], large industrial parks in Japan [6], chemical processing clusters [7], and kraft pulp mills [8]. Hot water loops for indirect heat recovery have been described using a variety of design methods and applications. For example Wang et al. [9] recently developed a new indirect heat recovery superstructure, which was solved using mixed-integer non-linear programming for a two plant system. Rodera and Bagajewicz [10] studied the generic case of inter-process integration on a site with two individual processing plants, which method was later generalised to a site

Abbreviations: CC, Composite Curve; CTS, constant temperature storage; HR, heat recovery; HRL, heat recovery loop; TS, Total Site; VTS, variable temperature storage.

* Corresponding author.
E-mail address: timgw@waikato.ac.nz (T.G. Walmsley).

http://dx.doi.org/10.1016/j.energy.2015.05.080
0360-5442/

Nomenclature

A	area (m^2)
a	coefficient
C	heat capacity flow rate (kW/°C)
G	solar irradiance (kW/m^2)
H	enthalpy (kW)
h	heat transfer film coefficient ($kW/°C/m^2$)
I	solar irradiance (kW/m^2)
m	exponent in Eq. 3
Nu	Nusselt number
NTU	number of (heat) transfer units
n	exponent in Eq. 3
P	temperature effectiveness
Pr	Prandtl number
Q	heat duty (kW)
Re	Reynolds number
T	temperature (°C)
U	overall heat transfer film coefficient ($kW/°C/m^2$)
ΔT	temperature difference
ε	heat exchanger effectiveness
η	efficiency

Subscripts/superscripts

*	shifted
act	actual
amb	ambient
ave	average
dp	design point
L	loop stream
LM	log-mean
max	maximum
min	minimum
p	process stream
s	solar
sp	set point
tar	target

with n processes [11], and applied to four case studies using linear programming [12]. Other studies have applied a graphical approach to design indirect heat recovery systems for batch processes [13] using a time slice model proposed by Kemp and Deakin [14].

The HRL concept is a sub-set of TS integration that use a hot water loop that traditionally has a defined network structure. HRLs are generally applied to indirectly recover and place heat in processing clusters with processing and pinch temperatures below 100 °C [15]. In an HRL system, an intermediate fluid, usually water, is pumped to plants with excess heat in the desired temperature range to recover heat. The fluid is then piped back to a tank, which acts as thermal storage, before being sent to plants that require heating in the same temperature range. The system is closed and the fluid is continuously circulated depending on the heating and cooling requirements of the various processes. Fluid storage acts as a buffer to mass and enthalpy imbalances between the hot and cold sides of the loop and is ideal for improving HR on large multi-process sites with lots of semi-continuous processes in operation. Integration of solar heating with an HRL is advantageous because the two systems can share common infrastructure, and because the solar can be applied to increase both enthalpy and temperature of the intermediate fluid.

Specific to the HRL concept, the benefits of applying solar process heating using an HRL were demonstrated in both a VTS (variable temperature storage) approach and the conventional CTS (constant temperature storage) approach [3]. Methods were developed for maximising the uptake of variable solar heat supply in a low pinch temperature semi-continuous process [15] and for TS Analysis [2]. General aspects of HRL design, thermal storage [16], seasonal operation effects [17] and heat exchanger area optimisation [18] have also been reported. Related studies helpful on solar thermal systems utilizing pressurized hot water storage [19], types of solar collectors and thermal energy storage systems [20], and system performance optimisation and economic analysis [21]. Industrial case studies have also been presented at the 2013 IEA SHC Technology Workshop on Solar Process Heat for Industry for a dairy factory and the brewing industry [22].

The aim of this paper is to investigate how solar as a thermal energy source is best integrated in a low temperature HRL. The New Zealand dairy factory case study from Walmsley et al. [3] is used as the basis of the investigation. The HRL design is based on the VTS method as suggested by Walmsley et al. [3] for maximise the heat recovery to area ratio. Integration of solar thermal in the HRL including scenarios where solar is applied to heat the intermediate fluid in parallel and in series with the other heat sources [23]. The effect of storage volume, coupled with integrated solar is also investigated. The benefits for the various schemes are quantified in terms of increased overall heat savings and reduced cooling utility.

1.1. Options for integration of solar collectors in heat recovery loops

Options for integrating solar collectors into an HRL are presented in Fig. 1 for two tank HRL systems. The variable supply of solar throughout a day/night cycle is integrated within the HRL system without the need for additional storage (Options B, C, & D) unless a third tank is used. The overlap region of the CC (Composite Curves) represents the time-average HR target. As solar is added, heat exchangers in the HRL may be enlarged to maximise the usefulness of solar and to ensure heat transfer on both sides of the loop remain in long term balance.

Option A is the standard two tank HRL without a solar collector. A pinch fixes the temperature of the cold storage temperature (for the case shown), whereas the hot storage temperature can be varied in small range. The slope of the line between these two points represents the inverse of the intermediate fluid's heat capacity flow rate, and the overlapped region is the maximum time-averaged HR.

Option B uses a solar collector in parallel with the HRL heat sources and the hot loop fluid is mixed when returning to the hot storage. Extra flow through the solar collector increases the flow rate of the loop, as illustrated by the lower slope of the loop line, and extends the heat transfer possibilities to a new hot pinch point which is a combination of HR from hot streams (same as Option A) and additional solar which varies from day to night.

Option C uses the solar collector in series as a temperature (and enthalpy) booster of the hot loop fluid before storage. The loop flow rate is unaffected by the addition of the solar collector, and hence the loop line on the CC extends at the same slope until it reaches a hot storage pinch. Depending on the shape of the cold CC a higher solar level may be possible compared to the parallel solar-HRL system (Option B).

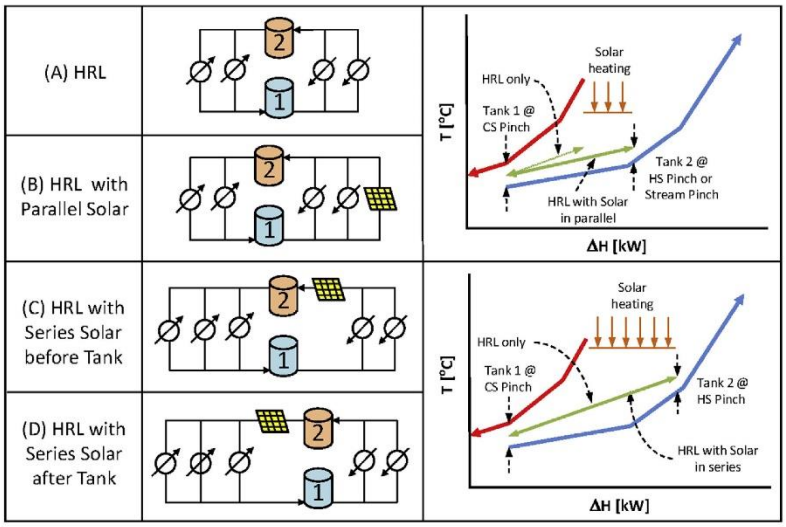

Fig. 1. Solar-HRL system configurations and composite curves for two tank systems.

Option D is similar to Option C except the solar collector is now after the hot storage and fluctuations in solar radiance are not dampened by the thermal storage buffer. The CC remains the same as does the predicted maximum HR and Solar use.

There are many other possible set-ups of a combined solar-HRL system. In general, three-tank HRL and more complicated systems are effectively a combination of Options A, B, C, and D. As a result this paper focused on Options A, B, C, and D.

2. Methods

2.1. Design and operation method for heat recovery loops

The HRL design and operation method applied in this study for a semi-continuous processing site is taken from Walmsley et al. [3], which was originally based on methods from Krummenacher and Favrat [13] and Sadr-Kazemi and Polley [24] for batch processes. Like Total Site Analysis [4], the HRL design methods give preference to zonal and intra-plant heat integration, before looking for opportunities for site-wide integration. Targets for HR and utility use targeting in HRLs are established using a CC approach. These CCs are normally based on time-averaged temperature and flow data and therefore the targets obtained represent the maximum average HR and minimum average utility use. Time average targets for HRLs assume intermediate loop fluid storage is continuously available, which is not always the case in practice. The amount of thermal storage is one barrier to achieving the targets in practice.

The designated control of the HRL also affects heat recovery and utility targets. Conventional control of an HRL is to measure and compare the outlet temperature of the loop fluid from each heat exchanger to a common hot or cold temperature set point. To achieve the set point, the flow rate of the loop fluid through the heat exchanger is adjusted. An important characteristic of this approach is hot and cold storage temperatures are constant over time, i.e. CTS. An alternate approach to HRL control is to vary the set points of the heat exchangers depending on their temperature driving force. This alternate approach is characterised by variable temperature storage, i.e. VTS, tanks due to mixing of different temperatures entering the tanks. Walmsley et al. [3] developed algorithms for targeting and designing conventional CTS and novel VTS based HRLs. Transient HRL performance modelling results of Walmsley et al. [3] demonstrated the benefits of using a VTS compared to the CTS method. As a result this paper applies the VTS method to design and operate an HRL with the addition of solar. The VTS targeting and design algorithm has been implemented in an Excel™ spreadsheet and applied to develop the various designs of combined solar-HRL systems in this work.

2.2. Transient heat recovery loop performance modelling

An Excel™ based spreadsheet tool has also been modified from the work of Walmsley et al. [3] to simulate the transient performance of an HRL integrated with solar thermal according to Options A (no solar), B, C and D. The tool uses the loop temperature control set points and heat exchanger areas targeted from the steady state VTS design method [3] to step-wise calculate the level and temperature of the hot and cold storage tanks. With historical or representative transient stream data, the model may be applied to estimate actual HR for defined volumes of storage. When a stream falls short of its target temperature or storage is unavailable, utility is consumed. In the model, the capacity of the storage tanks and intermediate fluid properties such as density and heat capacity may be specified and the storage tank is assumed to be well-mixed.

In total, the model is required to solve nearly 140,000 counter-current heat exchanger problems for the case study. To simplify the problem, all heat exchangers, regardless of type, are modelled as a counter current heat exchanger. Cross-flow heat exchangers applied to transfer heat to/from gaseous streams from/to liquid streams normally have multiple liquid passes (>6) to produce a near counter flow arrangement [25].

2.2.1. Heat recovery loop control

2.2.1.1. The control system of the HRL is very important. The model incorporates a two level hierarchical control system. For both levels, the intermediate loop flow rate is the manipulated variable. The first level of control aims to achieve an outlet temperature of the loop fluid that is a fixed offset ΔT_{min} from the inlet temperature of the process fluid. As Walmsley et al. [3] explained neither the Log-Mean-Temperature-Difference (ΔT_{LM}) nor the ε-NTU (or P-NTU) method may be applied to solve for the unknown loop flow

rate for this heat exchanger problem. To calculate the flow rate of the loop fluid, a non-standard generalised solution table was iteratively solved using the P-NTU method and Excel™ Solver. Fig. 2 plots the generalised solutions for the HRL heat exchanger performance problem. The temperature effectiveness of the loop fluid, P_L, and the number of transfer units based on the process stream flow rate, NTU_p, maybe calculated from the known data in combination with an estimate of the overall heat transfer coefficient, U. As can be seen of Fig. 2, once these two variables are known, the temperature effectiveness of the process stream, P_p, may be determined, from which the duty of the HRL heat exchanger is calculated together with the loop flow rate through the individual heat exchanger. The model requires a couple of iterations to improve the estimate of U, but it avoids hundreds more iterations that would be needed if a generalised solutions table was not employed.

The second level of control is actioned when the process stream exceeds a hard target temperature according to the first level of the control system. In this case, the loop flow rate is slowed to reduce the duty of the heat exchanger. Since the outlet temperature of the process fluid is set as the target temperature, P_p and NTU_p are both known. Like before, using the generalised solution table (Fig. 2), P_L is found, which is applied to determine the flow rate and return temperature of the loop fluid. The actual $\Delta T_{min,act}$ between the loop fluid's outlet temperature and the process stream's inlet temperature is likely to differ from the target $\Delta T_{min,tar}$. Algebraic manipulation of the definition of P_L leads to identification of simple rules that explain the connection between P_L and ΔT_{min}.

$$P_L = 1 - \frac{\Delta T_{\min}}{|T_{L1} - T_{P1}|} \tag{1}$$

2.3. The above equation implies

$$P_{L,act} > P_{L,tar} \rightarrow \Delta T_{\min,act} < \Delta T_{\min,tar} \tag{2a}$$

$$P_{L,act} = P_{L,tar} \rightarrow \Delta T_{\min,act} = \Delta T_{\min,tar} \tag{2b}$$

$$P_{L,act} < P_{L,tar} \rightarrow \Delta T_{\min,act} > \Delta T_{\min,tar} \tag{2c}$$

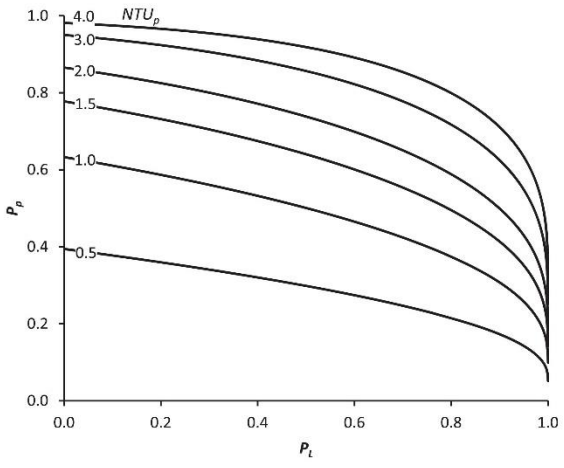

Fig. 2. Heat recovery loop heat exchanger non-dimensional performance.

One of the implications of the above equations and control strategy, for example, is, when the secondary control actions such that a cold process stream meets its target temperature, the resulting cold return temperature of the loop flow may be higher than normal, which warms the cold storage tank. This in turn reduces the potential for heat transfer from the hot side of the HRL.

2.3.1. Accounting for process stream temperature and flow rate fluctuations

Fluctuations in process stream flow rates and temperature, which are characteristic of semi-continuous processes, are successfully accounted for in the spreadsheet model. Heat exchanger areas are designed according to the time-average flow rate of the process stream. When the flow rate of a stream falls below the design point flow rate, U and Q are reduced, and when the flow rate is above, U and Q increase. To account for this in the modelling, individual U values are calculated from the corresponding film coefficients (h) for the process and loop streams, which is proportional to Nusselt number, as a function of Reynolds number (Re) and Prandtl number (Pr). Liquids are assigned a typical design heat transfer film coefficient of 4000 W/°C/m^2; vapours are assigned 2400 W/°C/m^2; and gaseous flows are given 71 W/°C/m^2 [26]. Assuming the fluids have a constant viscosity, density, heat capacity, and Pr number, the ratio of the instantaneous h to the design h_{dp} is related through to the ratio of C through the Reynolds number, where a and n are constants specific to a heat exchanger design,

$$h = a \cdot \mathrm{Re}^n \mathrm{Pr}^m \Rightarrow \frac{h}{h_{dp}} \cong \left(\frac{C}{C_{dp}}\right)^n \tag{3}$$

The spreadsheet model developed for the transient study uses a value of 0.58 for n, which is specific to a plate heat exchanger [27] and is not dissimilar to the range of values for finned tube heat exchangers, 0.52–0.70, calculated from the correlations of Kays and London [25]. The Prandtl number is a function of temperature, which for small changes in temperature may be assumed constant. Design point values are based on the average operating flow rate of a stream.

2.4. Solar collector modelling

Included in the HRL model is solar heating based on recorded data from a local weather station. Solar collector efficiency and duty has been modelled using the design equations and constants given by Atkins et al. [15].

$$Q_s = A_s\left(\eta_0 G - a_1(T_s - T_{amb}) - a_2(T_s - T_{amb})^2\right) \tag{4}$$

Where Q_s is the solar heating duty, η_0 is the optical efficiency (0.764), A_s is the area of the solar collector, G is the solar irradiance, a_1 (1.53 kW/m^2/°C) and a_2 (0.0003 kW/m^2/°C^2) are thermal loss coefficients, T_s is the average temperature of the collector, and T_{amb} is the ambient temperature.

2.5. Dairy factory case study

Integration options for adding solar thermal collectors to an industrial HRL located at a New Zealand multi-plant dairy factory is investigated. The factory consists of eight separate semi-continuous plants that share common utility, power and materials handling services. Plants initially were integrated to industry best practice. Sometime later liquid streams still requiring substantial heating or cooling duties were fitted to an HRL. Further reductions in utility use are being sought through adding sources to the HRL such as

gaseous dryer exhaust HR and solar thermal heating, and adding area to existing heat exchangers. Most of the heat exchangers in the HRL are plate heat exchangers.

For HRL targeting, design and initial optimisation, thermal storage temperatures (T_c, T_h), streams to include in the HRL and heat exchanger areas are sized based on time-average heat capacity flow rates (C) to give a balanced loop according to the methods presented by Walmsley et al. [3]. The minimum approach temperature is fixed at 5 °C, which is a typically economic value for low temperature processes given in the work of Linnhoff [26] and is similar to observations of the authors in the dairy industry, while the amount of additional solar is varied. Solar-HRL configuration Options B, C, and D are considered in the study and are compared to the conventional set-up, Option A, which has no solar heating. The volume of the hot and cold storage tanks is varied between 50 m^3 and 1000 m^3.

2.6. Site stream and solar irradiance data

Average stream data for the New Zealand dairy factory considered is presented in Table 1. In total there are 18 process streams, excluding solar, emerging from four milk powder plants, four other dairy processes, site hot water and air compressor units. Volumetric flow rates were measured by magnetic flow metres and recorded by the company's computer system for a period of two months during peak processing at intervals of 10 min; whereas most temperatures were measured but not logged. As a result historical average temperatures have been used in most cases.

Operating average and daily time average heat capacity flow rates presented in Table 1 are calculated from the historical stream data while temperatures relate to periods when the site/plant is in operation only. The daily time average values include periods when a stream is unavailable throughout a normal day's plant operation due to cleaning and off-product times. Duties based on both heat capacity flow rates are also presented.

The solar collector is assigned a supply temperature of 85 °C when it is placed in parallel to other process steams (Option B). For a ΔT_{min} of 5 °C, it is assumed that solar heating can heat the intermediate fluid up to 80 °C in evacuated tubes. When the solar collector is placed in series (Options C and D), the outlet temperature from the solar collect varies depending on the flow rate through the solar collector, which is determined by the requirements of the HRL process sources and sinks. At times the temperature in the solar collector exceeds 80 °C but has the penalty of greater heat loss, which is an element of Eq. (2). The process stream data for the dairy factory case study is the same as the data used by Walmsley et al. [3]. In their work, further details about instantaneous flow rates and temperatures at 10 min intervals over the considered 2 month period for two of the streams have been presented.

Solar irradiance and ambient temperature data recorded at a nearby weather station has been downloaded from New Zealand's National Climate Database [28]. Solar irradiance data for the entire two months is plotted in Fig. 3 using time of day as the horizontal axis and showing the day average of 0.43 kW/m^2, the day/night average of 0.25 kW/m^2 and the average of the daily peaks of 0.97 kW/m^2.

Table 1
Extracted stream data including the spray dryer exhaust and solar heating sources.

Stream	Type	T_s	T_t	Operating		Time-average	
				C	Q	C	Q
		[°C]	[°C]	[kW/°C]	[kW]	[kW/°C]	[kW]
Dryer exhaust A	HOT	75	55	143	2851	139	2785
Dryer exhaust B	HOT	75	55	75	1497	73	1462
Dryer exhaust C	HOT	75	55	45	898	44	877
Dryer exhaust D	HOT	75	55	29	570	28	557
Utility unit A	HOT	45	30	10	146	8	120
Utility unit B	HOT	45	30	10	146	8	120
Casien A	HOT	50	20	33	999	22	647
Casien B	HOT	50	20	49	1477	32	956
Casien C	HOT	50	20	49	1485	32	962
Condenser	HOT	80	79	993	993	351	351
Cheese A	HOT	35	20	120	1797	98	1470
Cheese B	HOT	35	20	139	2074	114	1691
Solar collector	HOT	85*	–	–	–	–	–
Site hot water (SHW)	COLD	16	65	160	7827	160	7827
Milk treatment A	COLD	10	50	104	4159	104	4159
Milk treatment B	COLD	10	50	104	4159	104	4159
Milk treatment C	COLD	11	50	116	4563	116	4563
Whey A	COLD	12	45	20	663	16	522
Whey B	COLD	14	45	11	340	9	267

3. Results and discussion

3.1. Time-average heat recovery and solar heating targets for combined Solar-HRL system

Targets for minimum hot and cold utility consumption, and maximum HR and solar heating, are obtained from the CCs presented in Fig. 4 for parallel configuration (Option B) with dryer exhaust HR (Fig. 4A) and without dryer exhaust HR (Fig. 4B). The targets for series solar configuration, i.e. Options C and D, are expressed in Fig. 5. Two targets for solar heating are plotted on each of the three CC graphs: maximum solar heating target ($Q_{s,max}$) and a day/night average solar heating target ($Q_{s,ave}$). The maximum solar heating target is only achievable if the system contains an extreme amount of storage to carry over heat from day light hours to night time hours, which is normally highly impractical. The day/night average solar heating target is a smoothed day/night average duty with a peak duty equal to the maximum solar heating target. So long as the sinks are immediately available, all solar heat is meaningfully used for replacing utility.

The solar heating contribution represented by the extended lines on the CCs (Fig. 4A, B and 5), beyond the HRL intermediate fluid line, represent the solar heating potential only. Integrating solar heating into an HRL causes the heating of the sink side of the loop to vary depending on the time of day and level of solar irradiance available for collection. Heating due to solar moves up and down between the normal HRL end point (without solar) to a hot storage pinch point with solar. For parallel configurations, the slope of the HRL line decreases representing an increase in flowrate of the

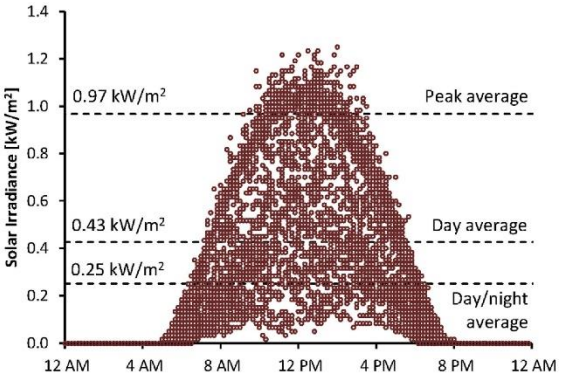

Fig. 3. Solar irradiance recorded by closest weather station the dairy factory [28].

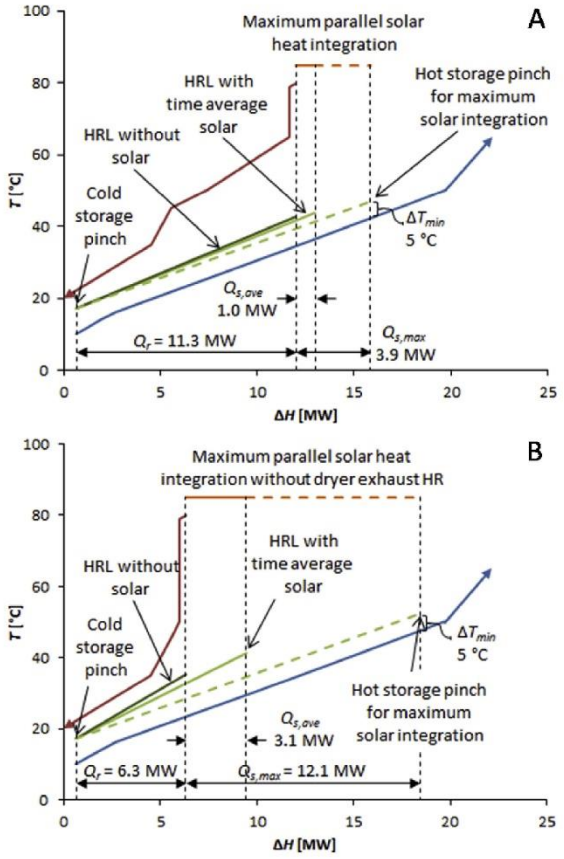

Fig. 4. Composite curves for solar-HRL system with parallel solar collectors, with exhaust heat recovery (A) and without exhaust heat recovery (B).

intermediate fluid. For series configurations, the slope of the HRL line is constant, i.e. constant flow rate, because the total intermediate flow rate is determined by the control of the heat recovery exchangers. The combined intermediate flow then passes through

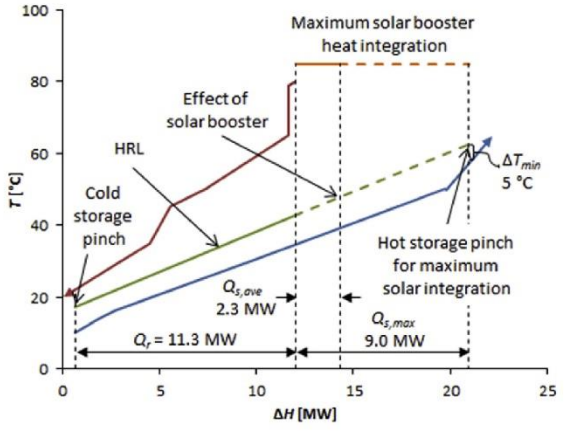

Fig. 5. Composite curves for solar-HRL system with series solar collectors including exhaust heat recovery.

the solar collector. Adding solar heating extends the length of the of the HRL line attracting greater HR and higher hot tank temperatures. Increasing the hot tank temperature also increases the effective thermal storage volume.

When solar heat is available at enthalpy levels that exceed the hot storage pinch point, for example in the middle of the day on a very hot day, the hot storage tank will quickly fill and before long extra cold utility is required to cool excess hot fluid and maintain a balanced loop. To avoid the need for more cooling utility the solar system needs to be designed to produce a maximum enthalpy output that reaches the hot pinch only. Over the course of a 24 h cycle the average heat contribution from the solar will be approximately 25% of this maximum value [3]. This issue can be overcome by substantially increasing the storage of the HRL. Twenty-four hour delivery of solar generated hot water in the HRL would then be possible. However, one would still need backup utility to cover for days with poor sunlight, and therefore such a solution is very expensive and highly unlikely to be economic under current energy prices.

Adding dryer exhaust HR enables HRL performance to increase from 6.3 MW to 11.3 MW as shown in Fig. 4, while reducing the average solar integration from 3.1 MW average to 1.0 MW average. It is apparent from the CCs that dryer exhaust HR which produces intermediate fluid at 60 °C, limits the quantum of solar possible compared to the case without exhaust HR. This is due to the solar return a fluid to the hot tank at a hotter temperature of 80 °C compare to dryer exhaust HR. Switching to a series solar configuration, even with dryer exhaust HR, helps debottleneck the system and enables solar heating to increase to 2.3 MW on average for a combined total of hot utility reduction of 13.6 MW. Note that for parallel solar configuration the solar stream is heated to a maximum of 80 °C, whereas with the series heating solar can exceed 80 °C during the peak solar irradiance levels of a sunny day. Eq. (2) accounts for the higher fluid temperature by increasing its heat loss component [15]. HR levels for the series configuration are identical to the parallel case with dryer exhaust HR at 11.3 MW, but the potential solar heating levels are 2.3 times greater. With more storage and a larger solar collector area, the average output of solar heating can be increased but not without on-going interaction between the CCs and the variable storage temperatures on the loop.

3.2. Transient modelling results for combined Solar-HRL system

3.2.1. Analysis of solar collector area

The results of transient HRL modelling of the three cases using industrial plant data are presented in Fig. 6 for fixed hot and cold storage volumes of 500 m^3. With increasing solar collector area hot utility decreases for each case with series return configuration (Option C) showing the greatest reduction followed by series supply (Option D) and then the parallel configuration (Option B). Similarly the useful solar heating levels were greatest for the series return configuration and lower for the other two cases. The cold utility results are quite interesting. Initially there is minimal difference between the configurations but after about 11,000 m^2 of solar collectors, cold utility begins to rise above the base value of 1.1 MW, first for the parallel configuration and then eventually for the other cases.

The dramatic increase in cold utility for the parallel configuration arises as a consequence of the hot storage pinch that is encountered at lower average solar duties and collector areas. The presence of more collector area drives solar heating to increase the loop heat capacity flow rate to a level that is out of balance with the heat sinks on the cold side of the HRL and the hot storage tank fills to the point where no cold fluid is available for maintaining HRL operation. If the HRL is to stay in operation, cold utility must be

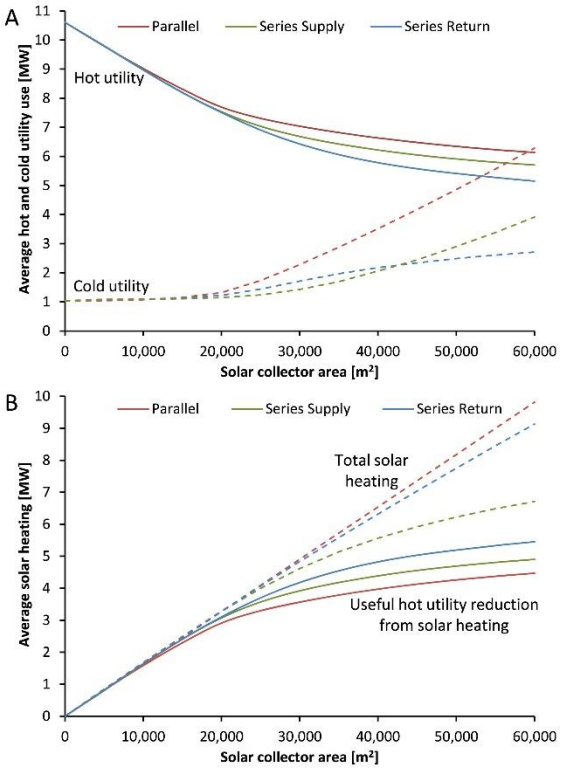

Fig. 6. Solar-HRL system performance with constant hot and cold storage of 500 m^3 including exhaust heat recovery.

consumed to produce cold fluid from the excess hot fluid. Or alternatively, the operation of the HRL may be stopped, which requires more cold utility to be directly applied to some of the process steams. The useful contribution of solar replacement of hot utility still occurs because some of the additional solar enthalpy is above the pinch temperature, leading to a lesser reduction in hot utility. Enthalpy below the pinch temperature must be cooled, which gives rise to the increase in cold utility. Hence the parallel solar configuration is able to exceed the average solar target from the composite, but only at the expense of a cooling penalty. The extra cooling utility required is a complex relationship between solar collector area, solar temperature, availability and variability of source and sink streams, variability of the solar, and the volume of thermal storage.

For series configurations the increase in cold utility happens at slightly greater solar collector areas as predicted by the CC's. With increasing solar collector area the series return and series supply cases have similar cold utility levels up to a solar collector area of 45,000 m^2. For very high solar collector areas, the series supply case has a slightly higher temperature cold tank. The cold storage tank has an average of 18.9 °C for series supply option compared to 16.5 °C for the series return option. This slight difference impacts on the ability of the two options to deliver cooling to hot process streams.

An example of storage tank levels and hot and cold storage temperatures derived from the transient HRL model are presented in Fig. 7. The solar boosting effect arising from the solar can be clearly seen for both configurations. The parallel configuration has smaller temperature fluctuations compared to the series configuration. For the series configuration hot tank temperatures fluctuate from a low of around 39 °C at night to a peak of up to 90 °C in the middle of the day, which is verging on steam generation. In this work, it is assumed the HRL is operated as a closed pressurised water loop. Parallel configuration, on the

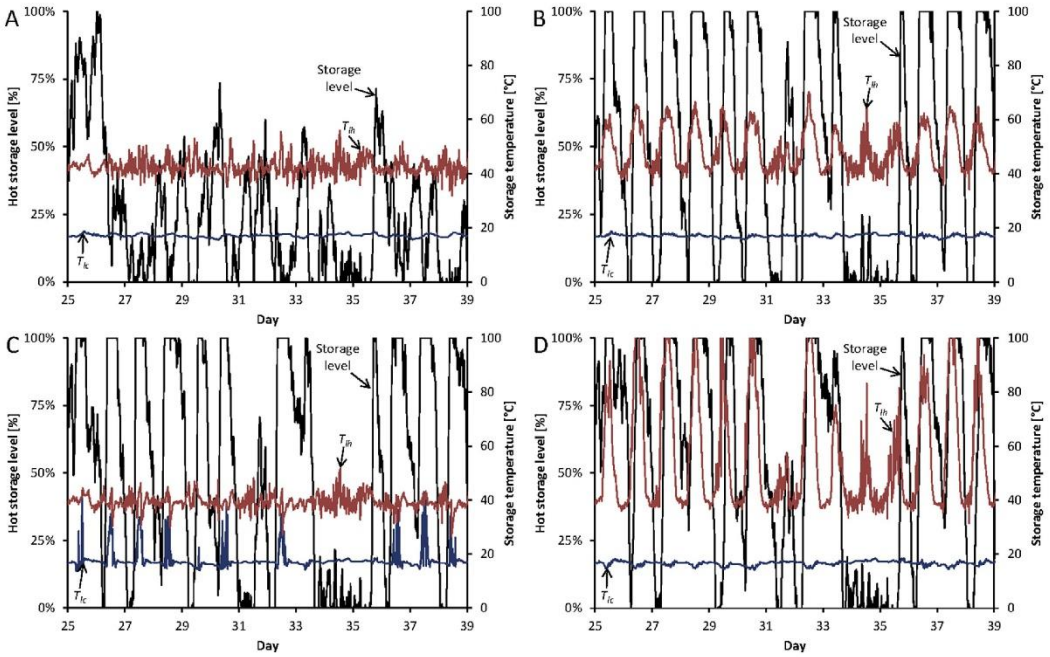

Fig. 7. Hot storage tank levels and hot and cold storage tank temperatures for the case with no solar (A), and cases with solar as a parallel source (B), on the series supply line (C) and on the series return line (D). Tank volume is 500 m^3 and the solar collector is 45,000 m^2 for B, C, and D.

other hand fluctuates with a lower range between 39 °C and 60 °C.

When peak storage temperatures are present, for example in the series configuration case, it is interesting to observe that the cold tank temperature drops into a trough during the peak load period and then returns to normal again. This is caused by the reduction in flow rate on the sink side of the HRL loop to compensate for the higher hot tank temperature, which in turn causes a lower exit temperature as a second of the second level of control as explained previously. Likewise hot tank levels are seen to rise when peak temperatures are present also in response to the reduction in flow to the sink side of the loop.

3.2.2. Analysis of storage capacity

Increasing the hot and cold storage capacity reduces both the hot and cold utility for all three options investigated as shown in Fig. 8A. The reduction in hot utility associated with increasing tank volume to 1000 m^3 is most pronounced for the parallel solar case and the series return case. The series supply case benefits for hot utility reduction are considerably less from increases storage because the solar collector heats fluid leaving the hot fluid tank. On the other hand, the reduction in cold utility resulting from increasing the tank volume is greatest for the series supply case.

Fig. 8B plots the effect of storage volume on total solar heating and useful solar heating as measured by an overall reduction in hot utility use. The total solar heating is independent of storage volume while the usefulness of gaining the solar is improved with increasing storage volume. The difference between the total solar heating maximums (based on fixed solar collector area of 45,000 m^2) for the three cases in Fig. 8B results from solar collector heat loss. The parallel solar case provides the lowest temperature fluid to the solar collector and as result has the lowest average collector temperature and heat loss. The series supply case experiences the highest average collector temperature and therefore has the greatest degree of heat loss.

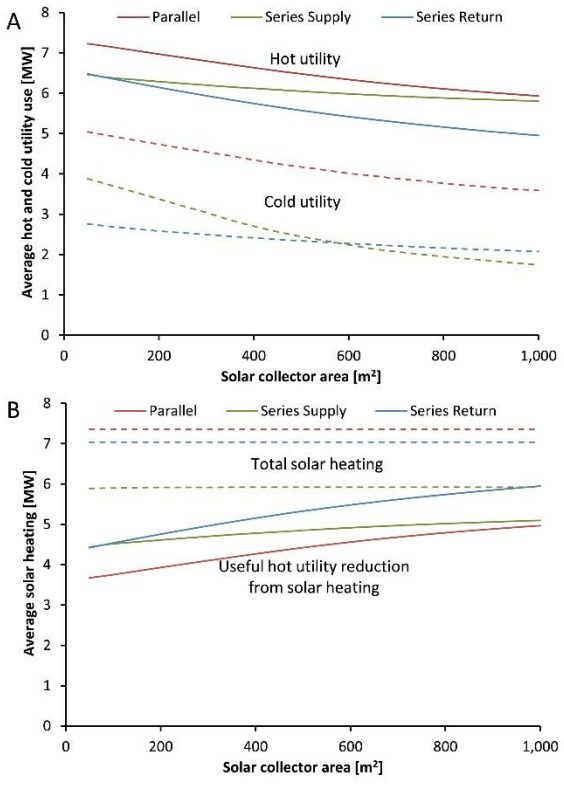

Fig. 8. Solar-HRL system performance with constant solar collector area of 45,000 m^2 including exhaust heat recovery.

The difference between the total solar heating and the useful solar heating curves represents the portion of solar heat that is added below the pinch temperature on average and/or added during periods when solar is not required by the system, i.e. a full hot storage tank. An improved HRL control strategy may be devised in future work to further improve the overall performance of combined solar-HRL systems.

4. Conclusions

Three options for integration of solar thermal into an HRL (Heat Recovery Loop) with variable temperature storage control have been analysed to identify the best performing options given the same solar collector area. For the dairy case study, placing the solar collector in series, relative to other sources in the HRL, increased the time average solar heating target to 2.3 MW from 1.0 MW for the conventional parallel placement of solar. Transient modelling over time of the three solar-HRL options also showed the series configuration to increase HRL performance. Positioning the solar collector in series with other heat sinks on the inflow pipe to heat storage tank consistently produced the highest HRL performance. For this option, the storage tanks acted as a buffer that reduced large swings in temperature, which negatively impacts on heat exchanger performance. Storage volume interacts with the performance of the HRL, with larger volumes being more desirable.

References

[1] Kiraly A, Pahor B, Kravanja Z. Achieving energy self-sufficiency by integrating renewables into companies' supply networks. Energy 2013;55:46–57. http://dx.doi.org/10.1016/j.energy.2013.03.001.

[2] Nemet A, Klemeš JJ, Varbanov PS, Kravanja Z. Methodology for maximising the use of renewables with variable availability. Energy 2012;44:29–37. http://dx.doi.org/10.1016/j.energy.2011.12.036.

[3] Walmsley TG, Walmsley MRW, Atkins MJ, Neale JR. Integration of industrial solar and gaseous waste heat into heat recovery loops using constant and variable temperature storage. Energy 2014;75:53–67. http://dx.doi.org/10.1016/j.energy.2014.01.103.

[4] Klemeš JJ, Dhole VR, Raissi K, Perry SJ, Puigjaner L. Targeting and design methodology for reduction of fuel, power and CO_2 on total sites. Appl Therm Eng 1997;17:993–1003. http://dx.doi.org/10.1016/S1359-4311(96)00087-7.

[5] Fritzson A, Berntsson T. Energy efficiency in the slaughter and meat processing industry—opportunities for improvements in future energy markets. J Food Eng 2006;77:792–802. http://dx.doi.org/10.1016/j.jfoodeng.2005.08.005.

[6] Matsuda K, Hirochi Y, Tatsumi H, Shire T. Applying heat integration total site based pinch technology to a large industrial area in Japan to further improve performance of highly efficient process plants. Energy 2009;34:1687–92.

[7] Hackl R, Andersson E, Harvey S. Targeting for energy efficiency and improved energy collaboration between different companies using total site analysis (TSA). Energy 2011;36:4609–15. http://dx.doi.org/10.1016/j.energy.2011.03.023.

[8] Bonhivers JC, Svensson E, Berntsson T, Stuart PR. Comparison between pinch analysis and bridge analysis to retrofit the heat exchanger network of a kraft pulp mill. Appl Therm Eng 2014;70:369–79. http://dx.doi.org/10.1016/j.applthermaleng.2014.04.052.

[9] Wang Y, Chang C, Feng X. A systematic framework for multi-plants Heat Integration combining Direct and Indirect Heat Integration methods. Energy 2015. http://dx.doi.org/10.1016/j.energy.2015.04.015.

[10] Rodera H, Bagajewicz MJ. Targeting procedures for energy savings by heat integration across plants. AIChE J 1999;45:1721–42.

[11] Bagajewicz M, Rodera H. Energy savings in the total site heat integration across many plants. Comput Chem Eng 2000;24:1237–42. http://dx.doi.org/10.1016/S0098-1354(00)00318-5.

[12] Rodera H, Bagajewicz MJ. Targeting procedures for energy savings in the total site. Lat Am Appl Res 2001;31:477–82.

[13] Krummenacher P, Favrat D. Indirect and mixed direct-indirect heat integration of batch processes based on pinch analysis. Int J Thermodyn 2001;4:135–43.
[14] Kemp IC, Deakin AW. Cascade analysis for energy and process integration of batch processes. Part 1. Calculation of energy targets. Chem Eng Res Des 1989;67:495–509.
[15] Atkins MJ, Walmsley MRW, Morrison AS. Integration of solar thermal for improved energy efficiency in low-temperature-pinch industrial processes. Energy 2010;35:1867–73. http://dx.doi.org/10.1016/j.energy.2009.06.039.
[16] Walmsley MRW, Atkins MJ, Riley J. Thermocline management of stratified tanks for heat storage. Chem Eng Trans 2009;18:231–6.
[17] Atkins MJ, Walmsley MRW, Neale JR. The challenge of integrating non-continuous processes – milk powder plant case study. J Clean Prod 2010;18:927–34. http://dx.doi.org/10.1016/j.jclepro.2009.12.008.
[18] Walmsley MRW, Walmsley TG, Atkins MJ, Neale JR. Methods for improving heat exchanger area distribution and storage temperature selection in heat recovery loops. Energy 2013;55:15–22. http://dx.doi.org/10.1016/j.energy.2013.02.050.
[19] Kulkarni GN, Kedare SB, Bandyopadhyay S. Design of solar thermal systems utilizing pressurized hot water storage for industrial applications. Sol Energy 2008;82:686–99. http://dx.doi.org/10.1016/j.solener.2008.02.011.
[20] Tian Y, Zhao CY. A review of solar collectors and thermal energy storage in solar thermal applications. Appl Energy 2013;104:538–53. http://dx.doi.org/10.1016/j.apenergy.2012.11.051.
[21] Kim Y-D, Thu K, Bhatia HK, Bhatia CS, Ng KC. Thermal analysis and performance optimization of a solar hot water plant with economic evaluation. Sol Energy 2012;86:1378–95. http://dx.doi.org/10.1016/j.solener.2012.01.030.
[22] EUREC. European technology platform on renewable heating & cooling. Eur Technol Platf Renew Heat Cool 2014 (accessed 15/12/2014), www.rhc-platform.org.
[23] Walmsley MRW, Walmsley TG, Atkins MJ, Neale JR. Options for solar thermal and heat recovery loop hybrid system design. Chem Eng Trans 2014;39:361–6.
[24] Sadr-Kazemi N, Polley GT. Design of energy storage systems for batch process plants. Chem Eng Res Des 1996;74:584–96.
[25] Kays WM, London AL. Compact heat exchangers. 3rd ed. Malabar, USA: Krieger Pub. Co.; 1998.
[26] Linnhoff B. Introduction to pinch technology, linnhoff march. 1998. Northwich, UK.
[27] Wang L, Sundén B, Manglik RM. Plate heat exchangers: design, applications and performance. Southampton, UK: WIT Press; 2007.
[28] NIWA. The national climate database. Natl Clim Database 2013. cliflo.niwa.co.nz (accessed 10 11 2013).

Energy 90 (2015) 95–104

Contents lists available at ScienceDirect

Energy

journal homepage: www.elsevier.com/locate/energy

Thermo-economic optimisation of industrial milk spray dryer exhaust to inlet air heat recovery

Timothy G. Walmsley*, Michael R.W. Walmsley, Martin J. Atkins, James R. Neale, Amir H. Tarighaleslami

University of Waikato, Energy Research Centre, School of Engineering, Hamilton, New Zealand

ARTICLE INFO

Article history:
Received 19 December 2014
Received in revised form
5 March 2015
Accepted 7 March 2015
Available online 30 April 2015

Keywords:
Process integration
Heat transfer
Particulate fouling
Spray dryer

ABSTRACT

This study reports a thermo-economic design optimisation of an industrial milk spray dryer liquid coupled loop exhaust heat recovery system. Incorporated into the analysis is the ability to predict the level of milk powder fouling over time and its impacts on heat transfer and pressure drop. Focus is given to a finned round tube, a bare round tube and a bare elliptical tube. Modelling results show that spray exhaust heat recovery is economically viable for the considered industrial case study. Based on the results, the best liquid coupled loop heat exchange system uses a finned tube heat exchanger to recover heat from the exhaust air with a face velocity of 4 m/s and 14 tube rows, which gives a net present value of NZ$2.9 million and an internal rate of return of 71%. The developed thermo-economic assessment method has the ability to cater to site specific needs that affect the utility savings and the capital cost for implementing exhaust heat recovery.

1. Introduction

Spray dryer exhaust heat recovery can typically increase dryer energy efficiency by 10–20 % [1], but it is complicated by the low heat transfer coefficient of air and the presence of powder particulates that may foul the heat exchanger surfaces. Several case studies on spray dryer heat integration for a range of industries from the 1980's, which was subsidised by the UK's energy efficiency demonstration scheme, showed 2–4 years as a typical payback and a steam savings of 10% [1,2]. In general, dryer exhaust heat recovery is applicable to a wide range of other industries. For example, Laurijssen et al. [3] demonstrated that dryer exhaust heat recovery for a conventional multi-cylinder dryer used in the paper industry plays a critical role in lowering thermal energy use by 32%. Han et al. [4] modelled a lignite-fired power station under variable load and proposed to use the hot flue for drying the incoming fuel as a means for heat recovery and boiler efficiency increases in the order of 1–2 %. Tippayawong et al. [5] analysed industrial longan drying practice to show that dryer heat recovery can increase thermal efficiency by 21%.

Increasing energy efficiency in milk spray drying is an important topic for New Zealand because the results of the New Zealand dairy industry heavily impacts the national economy. The installed capacity of milk spray drying in New Zealand reached an estimate of 300 t/h in 2013 with a consumption of around 29 PJ/y of thermal energy. Milk powders supply about 20% of New Zealand's exports. As a consequence, energy efficiency in milk powder production is therefore a prime concern for industry and the New Zealand government as a means of lifting national economic performance. Spray dryer exhaust heat recovery represents a great remaining opportunity for significantly increasing heat recovery in the milk powder production process. In the United States, many milk powder plants have installed exhaust heat recovery systems for pre-heating the inlet air. Besides heat recovery, another benefit for this practice is to minimise inlet dryer air humidity. For these plants, hot air for drying is generated using direct fired natural gas combustion, which combustion reaction increases the air's moisture content. Inlet air pre-heating reduces the fuel consumption, which reduces moisture in the air, which maximises the drying capacity of the air. New Zealand plants, however, favour indirect heating methods of the dryer air using steam or indirect gas fired air heaters. The additional benefit of lower inlet air humidity is not present in the New Zealand case.

The New Zealand dairy industry has been cautious to uptake spray dryer exhaust heat recovery. In the mid-1980's, the Plains Co-

* Corresponding author.
E-mail address: timgw@waikato.ac.nz (T.G. Walmsley).

http://dx.doi.org/10.1016/j.energy.2015.03.102
0360-5442/

Nomenclature

Roman

A	area (m^2)
C	heat capacity flow rate (kW/°C)
C^*	ratio of minimum to maximum heat capacity flow rates for ε-NTU method
c_b	particulate concentration in air flow (kg/kg)
d_p	particle diameter (m)
h	heat transfer film coefficient (kW/°C · m^2)
j	Colburn j factor
NTU	number of transfer units
Nu	Nusselt number
ΔP	pressure drop (Pa or %)
P	temperature effectiveness
Q	heat duty (kW)
R	heat transfer resistance (°C · m^2/kW)
r	radius (μm)
t	time (s)
U	overall heat transfer coefficient (kW/°C · m^2)

Greek

Δ	positive difference between two states
ε	heat exchanger effectiveness
τ	time constant (s)
ϕ	probability

Subscripts/superscripts

c	cold stream
f	fouling
F	frontal
h	hot stream
HX	heat exchanger
i	impact
l	loop
min	minimum
o	overall
p	pass
r	recovery
s	sticking
tot	total
tube	heat exchanger tube
w	wall

Op Dairy Ltd factory installed a glass tube air-to-air exhaust heat recovery system. However, energy surveys of its performance showed that heat recovery levels decreased by as much 40% after 13 h of operation due to milk powder fouling. In 2008, a New Zealand South Island dairy factory built a new state-of-the-art dryer, which was also the world's largest milk dryer at the time, and had plans to install a liquid coupled loop exhaust heat recovery system. The exhaust heat exchanger was built but never installed due to concerns over milk powder fouling causing disruptions to plant production. Since that time an additional twelve milk powder spray dryers have been built in New Zealand all without exhaust heat recovery, which evidences that exhaust heat recovery is not standard industry practice in New Zealand.

Within the field of Process Integration, PA (Pinch Analysis) is an established methodology originally proposed by Linnhoff et al. [6] for targeting heat recovery and utility use for industrial processes using Problem Tables and Composite Curves, and developing cost-effective heat exchanger networks. Recent PA studies on milk powder production have shown that to significantly increase heat recovery, heat is required to be recovered from the exhaust air for either intra-plant [7] or inter-plant heat integration [8]. Selection of soft target temperatures in the milk powder plant such as the final temperature of the exhaust air critically affects the shape of the Grand Composite Curve and the location of the Pinch temperature [9]. The exhaust air temperature of milk spray dryers is typically 65–85 °C. Walmsley et al. [7] showed there is no additional steam savings value in recovering dryer exhaust heat below the temperature range of 50–55 °C based on a minimum approach temperature. Atkins et al. [10] modelled the benefit of spray dryer exhaust heat recovery using a liquid coupled loop heat exchanger system to the overall heat recovery in the milk powder process. However their study was confined to the heat transfer characteristics of the liquid coupled loop heat exchanger system. This study furthers the work of Atkins et al. [10] to look closely at the fouling and cost elements of installing exhaust heat recovery systems in industry.

This paper reports the application of a comprehensive thermo-economic assessment tool for modelling a dryer exhaust-to-inlet air indirect heat recovery system to maximise key economic indicators such as NPV (Net Present Value) and IRR (Internal Rate of Return). The model quantifies the trade-off between heat transfer, pressure drop and fouling in terms of cost so that an optimisation can be performed. Literature correlations for the Colburn j factor and Fanning friction factor f of various heat transfer surfaces from Kays and London [11] form the basis for estimating the overall heat recovery of the system. An estimate of the fouling on the heat exchanger surface based on the milk powder deposition model presented by Walmsley et al. [12] is incorporated into the thermo-economic analysis. The comprehensive model is anticipated to demonstrate whether or not milk spray dryer exhaust heat recovery can be economic for a case study of a New Zealand dairy plant. In the general, the tool developed in this optimisation study has the potential to be applied to any dairy plant.

2. The milk spray dryer exhaust heat recovery system design problem

The design challenge and potential optimisation associated with spray dryer exhaust heat recovery can be expressed diagrammatically as presented in Fig. 1. The up-side down triangle represents the possible exhaust heat exchanger solutions. On the one hand, exhaust heat exchangers with a greater number of tube rows can

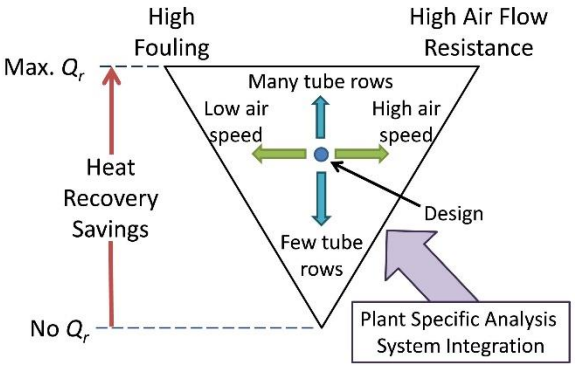

Fig. 1. The exhaust heat exchanger design challenge.

recover more heat (Q_r) but this increases both pressure drop and fouling. Fewer tube rows recover less heat with lower fouling and pressure drop. The air face velocity on the heat exchanger is also important and may be manipulated by changing the duct dimensions. High air velocities reduce fouling and improve heat transfer but also increase pressure drop. Lower air velocities have the opposite effect. Finding the right balance between heat recovery, fouling, and pressure drop is chiefly governed by the number of tube rows of the heat exchanger, the face velocity and the geometry of the heat exchanger surface. These parameters are important degrees of freedom that may be manipulated to maximise the economic benefit of an exhaust heat recovery project.

3. Development of a comprehensive thermo-economic dryer exhaust heat recovery model

3.1. Heat transfer and friction factor modelling for liquid coupled loop heat exchanger systems

3.1.1. Heat exchanger system inputs

The exhaust-inlet liquid coupled loop heat recovery model is set-up to allow user-defined inputs for the design and modelling parameters of the heat recovery system. Fig. 2 is a screenshot from the spreadsheet of the key design parameter inputs. Dimensions of the heat exchangers are calculated based on air mass flow rate in conjunction with the heat exchanger face velocity for the height and width, and the number of tube rows for the depth. The model uses a height to width ratio of 1:1, i.e. square face, which is typically of spray dryer exhaust roof ducts. There is the option of inputting a specific loop flow rate or allowing the tool to calculate the optimum loop flow rate. In Fig. 2, the tube type number refers to a particular tube geometry and arrangement. Each tube geometry and arrangement has been assigned a number and a new tube type maybe selected via a drop down menu.

3.1.2. Governing heat transfer equations based on effectiveness

The concept of a LCHE (liquid coupled loop heat exchanger) for indirect heat transfer is presented in Fig. 3. This indirect heat exchange system consists of two heat exchangers coupled using an intermediate loop fluid [13]. The loop fluid transports heat from the source stream to the sink stream. LCHE systems are most applicable to situations where source and sink streams are physically distant as is the case with spray dryer exhaust heat recovery for New Zealand dairy plants.

The model uses the effectiveness-NTU approach to solve the LCHE system from Kays and London [11]. The governing overall effectiveness (ε_0) relationship for the performance of LCHE systems is

$$\frac{1}{\varepsilon_0} = \frac{C_{\min,o}/C_{\min,c}}{\varepsilon_c} + \frac{C_{\min,o}/C_{\min,h}}{\varepsilon_h} + \frac{C_{\min,o}}{C_l} \quad (1)$$

Each heat exchanger has the option to contain multiple liquid fluid passes to produce a near counter flow heat exchanger arrangement for enhanced heat transfer but at the expense of pumping power. Kays and London provide the following relationship (Eq. (2)) for determining the effectiveness of a multi-pass heat exchanger unit based on n number of passes and an effectiveness of a pass, ε_p, defined by the applicable ε-NTU relationship, which is the unmixed–unmixed cross-flow relationship for this situation. The unmixed–unmixed cross-flow correlation is selected because there is minimal transverse mixing on both the air and water sides within a pass of a finned tube heat exchanger.

$$\varepsilon = \frac{\left(\frac{1-\varepsilon_p C^*}{1-\varepsilon_p}\right)^n - 1}{\left(\frac{1-\varepsilon_p C^*}{1-\varepsilon_p}\right)^n - C^*} \quad (2)$$

The model contains an iterative calculation system so that once the heat exchanger outlet temperatures are known, the air and water properties update, which impacts the inputs to the model, and the system re-solves until the solution converges. Convergence in the solution was based on the changes in the temperatures being less than 0.1 °C. Air properties are called using Excel™ functions from the commercial add-in package @Air (www.techwareeng.com). Water properties are called from built-in spreadsheet functions powered by the open source XSteam tables (www.x-eng.com), which are based on IAPWS IF97 steam and water properties.

Once the model finds a solution, the quality of the solution is checked. The model checks to ensure the temperatures in and out of the heat exchangers are thermodynamically feasible, i.e. no temperature cross, and the duties of the two heat exchangers are the same. The model ensures the number of passes is valid for the number of tube rows. To further clarify, the model assumes that there is an equal number of tube rows per pass. Warning messages appear in the spreadsheet results and are recorded when heat transfer and/or friction factor correlation limits are exceeded.

3.1.3. Heat transfer and pressure drop heat exchanger surface characteristics

Heat transfer and friction factor correlations have been formulated using the tabulated data presented in Kays and London [11] for staggered finned tube banks, bare tube banks and plain plate surfaces, and the data in Walmsley et al. [14] for bare circular and elliptical tube geometries. A power law based equation provided sufficiently good correlation for the data of most tube types and arrangements from Kays and London [11]. Correlations for bare and finned tubes and plain plate air–water geometries are built into the spreadsheet. Table 1 provides the essential heat exchanger surface design variables such as tube diameter, tube/plate arrangements, etc.

In practice, the average heat transfer coefficient varies from row-to-row in a finned tube heat exchanger [11]. Literature correlations applied in the spreadsheet are corrected for the row effect such that the reported Nusselt number or j factor correlations are based on a heat exchanger with infinite rows. There are two methods to account for the row-effect on the heat transfer coefficient: (1) adjust the heat transfer coefficient and (2) use row specific ε-NTU relationships. The approach taken in this work is that of

User Defined Design Parameters

	Exh. HX	Inlet HX	
Air Mass Flow Rate	76	56	kg/s
Temperature In	75.0	15.0	°C
Abs Humidity	50.0	10.0	g/kg
Face Velocity	4.0	4.0	m/s
Tube Type	19	6	
Tube Rows	10	6	
Number of Passes	10	6	
Loop Flow Rate	Optimum		kg/s

Fig. 2. Screenshot from the spreadsheet model showing heat exchanger user defined parameters.

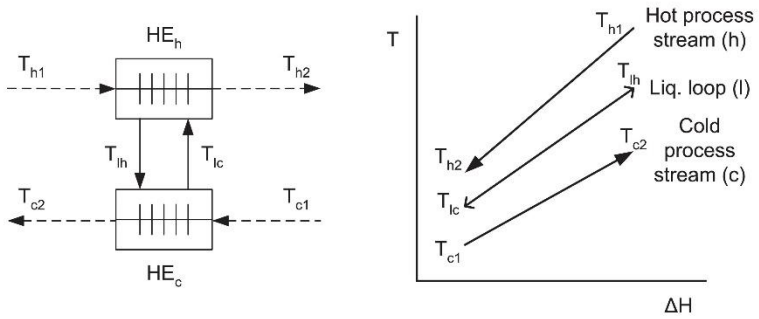

Fig. 3. Liquid couple loop heat exchanger system.

applying the row specific ε-NTU relationships from ESDU (Engineering Science Data Unit) 86018 cited by Wang et al. [15]. This approach is taken because the row specific ε-NTU relationships are less affected by the tube and fin geometry.

3.1.4. Liquid couple loop heat exchanger system optimisation

Holmberg [16] derived the optimum loop heat capacity flow rate assuming counter-flow heat exchanger arrangement,

$$C_l = \frac{(UA)_h + (UA)_c}{\frac{(UA)_h}{C_h} + \frac{(UA)_c}{C_c}} \quad (3)$$

where U is overall heat transfer coefficient and A is heat exchanger area, C is the heat capacity flow rate and subscripts h refers to the hot fluid, c refers to the cold fluid and l refers to the loop fluid.

When $(UA)_h >> (UA)_c$, then C_l in Eq. (3) approaches C_h. The reverse is also true; when $(UA)_c >> (UA)_h$, then C_l approaches C_c. Thus, the optimum C_l always falls somewhere between C_h and C_c. Using a simple spreadsheet, a preliminary investigation into the applicability of Eq. (3) to non-counter-flowheat exchanger arrangements, including the unmixed–unmixed cross-flow arrangement, has been undertaken. The investigation looked at cases where the LCHE system involved two heat exchangers with the same arrangement and varied the UA values for the heat exchangers across a wide range. Preliminary checks using Excel™ Solver showed that Eq. (3) is sufficiently accurate to predict the optimum loop flow rate to achieve a heat transfer within 0.1% of the maximum possible.

The approach applied in the spreadsheet tool to optimise a LCHE system is, first, to select areas for the exhaust and inlet air heat

Table 1
Heat exchanger geometry information. Key for heat exchanger surface codes: C – circular (round); E – elliptical; B – bare; F – finned; KL – Kays and London [11]; W – Walmsley et al. [14].

Source	Tube type (code)	D_o mm	D_i mm	X tube/plate mm	$d_{h,air}$ mm	σ_{air} m²/m²	α m²/m³	S_T mm	S_L mm	Fin pitch fins/m	x_{fin} mm	d_{fin} mm	Φ m²/m²
Bare tube – staggered arrangement													
KL	CB-1.5:1.25-3/8	9.5	6.2	1.7	7.6	0.333	175	14.3	11.9				
W	CB-1.5:1.25 (CFD)	20.0	16.7	1.7	15.9	0.333	84	30.0	25.0				
W	CB-2:1 (CFD)	20.0	16.7	1.7	25.5	0.500	79	40.0	20.0				
W	EB-1.5:1.25 (CFD)	30.8	27.5	1.7	15.9	0.333	84	30.0	38.5				
W	EB-2:1 (CFD)	25.9	22.6	1.7	25.5	0.500	79	40.0	30.8				
Circular finned tube – staggered arrangement													
KL	CF-7.34	9.7	7.2	1.2	4.8	0.538	459	24.8	20.3	289	0.460	23.4	0.892
KL	CF-8.72	9.7	7.2	1.2	3.9	0.524	535	24.8	20.3	343	0.460	23.4	0.910
KL	CF-8.72c	10.7	8.2	1.2	4.4	0.494	446	24.8	20.3	343	0.480	23.4	0.876
KL	CF-7.0-5/8J	16.4	13.1	1.7	6.7	0.449	269	31.3	34.3	276	0.250	28.5	0.830
KL	CF-8.7-5/8J (A)	16.4	13.1	1.7	5.5	0.443	324	31.3	34.3	343	0.250	28.5	0.862
KL	CF-8.7-5/8J (B)	16.4	13.1	1.7	11.7	0.628	216	46.9	34.3	343	0.250	28.5	0.862
KL	CF-9.05-3/4J (A)	19.7	16.4	1.7	5.1	0.455	354	39.5	44.5	356	0.305	37.2	0.917
KL	CF-9.05-3/4J (B)	19.7	16.4	1.7	8.2	0.572	279	50.3	44.5	356	0.305	37.2	0.917
KL	CF-9.05-3/4J (C)	19.7	16.4	1.7	13.6	0.688	203	69.2	44.5	356	0.305	37.2	0.917
KL	CF-9.05-3/4J (D)	19.7	16.4	1.7	4.8	0.537	443	69.2	20.3	356	0.305	37.2	0.917
KL	CF-9.05-3/4J (E)	19.7	16.4	1.7	6.4	0.572	354	50.3	34.9	356	0.305	37.2	0.917
KL	CF-8.8–1.0J (A)	26.0	22.7	1.7	5.9	0.439	299	49.8	52.4	346	0.305	44.1	0.825
KL	CF-8.8–1.0J (B)	26.0	22.7	1.7	13.2	0.642	191	78.2	52.4	346	0.305	44.1	0.825
Plain plate													
KL	2.0 T			0.3	14.5		250	19.1	304.8	79	0.813		0.606
KL	3.01 T			0.3	10.8		323	19.1	304.8	119	0.813		0.706
KL	3.97 T			0.3	8.6		392	19.1	304.8	156	0.813		0.766
KL	5.3 S			0.3	6.1		617	11.9	304.8	209	0.152		0.719
KL	6.2 B			0.3	5.5		669	10.3	304.8	244	0.254		0.728
KL	9.03 SB			0.3	4.6		801	6.4	304.8	356	0.203		0.888
KL	11.1 B			0.3	3.5		1024	12.2	304.8	437	0.203		0.854
KL	14.77 ST			0.3	2.6		1378	8.4	304.8	582	0.152		0.844
KL	15.08 SB			0.3	2.7		1358	6.4	304.8	594	0.152		0.870
KL	19.86 ST			0.3	1.9		1841	10.6	304.8	782	0.152		0.849

exchangers, and then, to determine the near optimum loop flow rate using Eq. (3). With a defined loop flow rate, C_l, and heat exchanger areas, the effectiveness of the exhaust and inlet exchangers may be calculated, from which the loop temperatures ($T_{l,c}$ and $T_{l,h}$) of the LCHE system may be calculated using

$$T_{l,c} = \frac{\varepsilon_h C_{h,\min}\left(1 - \frac{\varepsilon_c C_{c,\min}}{C_l}\right) T_{h1} + \varepsilon_c C_{c,\min} T_{c1}}{\varepsilon_h C_{h,\min}\left(1 - \frac{\varepsilon_c C_{c,\min}}{C_l}\right) + \varepsilon_c C_{c,\min}} \quad (4)$$

$$T_{l,h} = \frac{\varepsilon_h C_{h,\min} T_{h1} + \varepsilon_c C_{c,\min}\left(1 - \frac{\varepsilon_h C_{h,\min}}{C_l}\right) T_{c1}}{\varepsilon_h C_{h,\min}\left(1 - \frac{\varepsilon_c C_{c,\min}}{C_l}\right) + \varepsilon_c C_{c,\min}} \quad (5)$$

The above formulas have been derived based on energy continuity across the LCHE system and assume that heat loss is minimal. Once the intermediate hot and cold loop temperatures are found, the overall duty of the system may be calculated.

3.2. Modelling fouling and its effects on heat transfer and pressure drop

3.2.1. Predicting fouling build-up on the exhaust heat exchanger

The inputs to the model that relate to the build-up of fouling are presented in Fig. 4. Elsewhere in the spreadsheet the user may also input a particle size distribution. Using these parameters the spreadsheet applies the deposition model from Walmsley et al. [12] to estimate the amount of powder that sticks for each time step. The model of Walmsley et al. [12] was originally based on a series of experiments of milk powder deposition on a flat plate in an impingement jet. This model has been recently successfully applied to predict the key deposition characteristics on round and elliptical tubes by Walmsley et al. [17].

The method for estimating the amount of deposition is explained in Fig. 5. After entering the required inputs, the spreadsheet calculates the overall heat recovery system duty and estimates the air temperature profile within the exhaust heat exchanger based on a constant average heat transfer coefficient for each tube row, which results in a constant *NTU* for all tube rows.

The temperature profile is used to calculate a critical impact angle using the deposition model on Walmsley et al. [12] for each combination of tube row and particle size. Once the critical impact is known, the position on the tube that is the boundary of particle's sticking and rebounding, and the frontal area of the sticking region (A_s), can be determined. A probability of sticking (ϕ_s), which is defined the probability that a particle which impacts a tube will stick, can be estimated by dividing the frontal area of the sticking region by the total frontal area of a row of tubes, i.e. A_s/A_F. To determine the total increase in foulant mass, the probability of impact (ϕ_i), which is the probability that a particle will impact a tube, must also be considered. For this work, the probability of impact is assumed constant and estimated as fraction of frontal tube area to total cross-sectional area of the duct, i.e. A_F/A_{tot}. Particles are assumed to be evenly distributed through-out the air flow and duct and, with presuming only minor deviations in a particle's flow path, particles that are aligned with the frontal area of a tube are likely to impact a surface, whereas particles in a gap are unlikely to impact the row. Using these assumptions, the fraction of particles impacting a tube can be estimated as A_F/A_{tot}. There is opportunity in future work to input a probability of impact that is row and particle size specific. In reality, smaller particles are expected to have lower probabilities due to the smaller particle relaxation times. At present, this is a limitation of the model.

The product of the probabilities of impact and sticking, i.e. $\phi_s \cdot \phi_i$, give the percentage of particle mass entering a row that will deposit. This process of calculating the mass deposited is repeated for each combination of particle size fraction and tube row within a single time-step using Visual Basic based macros. The effect of the

Fouling and Cleaning Parameters		
Concentration	3.5	mg/m^3
Run time	672	h
Time Step	5.0	h
Wash Length	1.0	h
Start Clean?	TRUE	
Optimum Clean?	FALSE	

Fig. 4. Screenshot from the spreadsheet model showing fouling and cleaning user defined parameters.

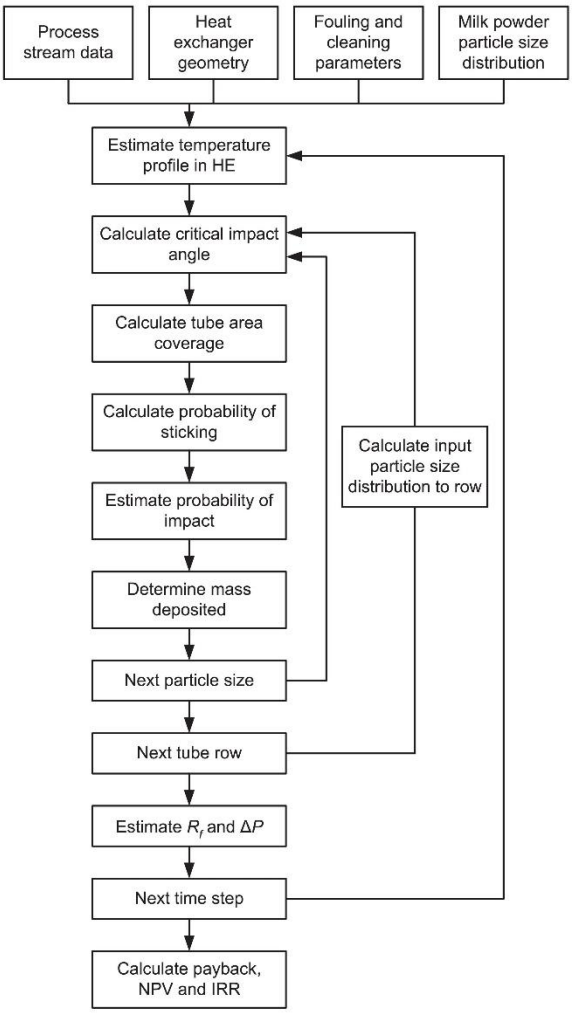

Fig. 5. Heat exchanger fouling model flow diagram.

fouling build-up on R_f and f is discussed in detail in the next two sections. For each new time-step, the performance of the heat recovery system and the exhaust heat exchanger temperature profile is recalculated. Once the run-time is complete, the model uses the cumulative heat recovery savings and costs to estimate the payback, NPV and IRR for the system.

The Excel spreadsheet tool incorporating the fouling model required 2.5 h on average to complete the analysis for one heat exchanger design using a time step of 5 h for a total cycle of 672 h. The fouling model was computed on an Intel™ i7 3.4 GHz processor. Test cases were used to determine the appropriate time step as to minimise its impact on the final solution.

The fouling build-up model makes several simplifications and assumptions. Uniform distribution along the length of each tube is assumed, although in recent experiments conducted by the authors [17], the particle distribution, which is often related to the airflow distribution, may be maldistributed causing a non-uniform profile along the length of a tube. Deposition is also likely to be heavier near the heat exchanger outer walls as shown in the experimental work of Walmsley et al. [17]. The probability of impact is constant for all rows and particle sizes. The probability of sticking has no respect for the surface condition and assumes the probability of a particle sticking to the tube wall is similar to a particle sticking to a particle. This simplification is supported by the work of Nijdam and Langrish [18], who found pre-coating the inside of a dryer with powder had little effect on the rate of deposition build-up.

3.2.2. Particle size distribution

Fig. 6 shows the particle size distributions of SMP (Skim Milk Powder) product compared to the size distribution collected in the bag house, which is assumed to be similar to the size distribution emitted out the exhaust duct. The particle size distribution was measured in iso-propanol using a Malvern Mastersizer 2000 according to the method of Pisecky [19]. The average particle size for bag house powder is significantly lower than bulk product, but the distributions span similar size ranges. The baghouse powder particle size distribution is entered into the spreadsheet tool as an input to the fouling model.

The particle size distributions in Fig. 6 were experimentally obtained using a light ray diffraction method using such instruments as a Malvern Mastersizer. Commonly food powders are added to a solvent and analysed. The standard method for analysis of milk powders is to place a small sample in isopropanol and test every two minutes until readings are constant [18,19].

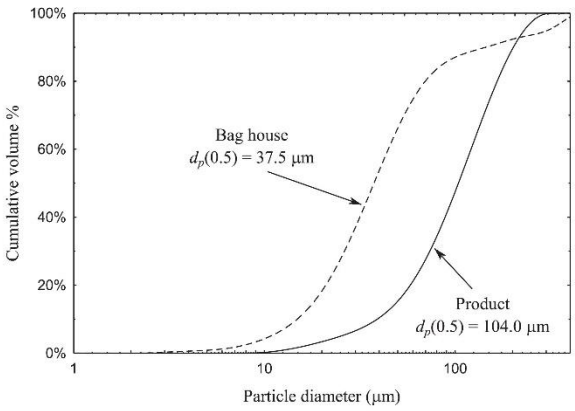

Fig. 6. Particle size distribution of baghouse and bulk product SMP.

3.2.3. The effect of fouling on heat transfer

Fouling affects heat transfer due to adding a layer of resistance. If the fouling was assumed to be perfectly uniform in thickness around a circular tube, the resistance due to fouling may be estimated using

$$R_{f,tube} = \frac{r_{tube}}{k_f} \ln\left(\frac{r_f}{r_{tube}}\right) \tag{6}$$

where $R_{f,tube}$ is the fouling resistance using the air-side tube area as the basis, k_f is the thermal conductivity of the foulant layer, r_f is the radius of the fouling and r_{tube} is the outside radius of the tube. As a simplification, it is assumed that the fouling build-up on the front of the tubes add a layer of thermal resistance approximately equal to the same volume of fouling uniformly spread around the outside of the tube. Thermal conductivity is taken as 0.1 W/(°C m) [20].

The heat transfer resistance due to milk powder deposition on the front of the tube is difficult to estimate without simplification. The presence of deposits in a heat exchanger are likely to significantly influence the airflow profile and the overall bulk average air velocity in the heat exchanger. The fouling layer acts as a thermal resistance, but it also improves h and A by channelling the air flow, which increases the average velocity in the heat exchanger, and enlarging the surface contact area between the air and the tube with fouling.

Fouling on the frontal face of fins has been shown to add little in the way of heat transfer resistance in other industries. Fouling does impact on the air flow resistance and, therefore, the velocity and distribution of the air flow experienced inside the heat exchanger. The added pressure drop can cause a reduction in the volumetric flow rate if the capacity of the fan has reached its zenith. The reduction in air flow through a heat exchanger has been shown to be the root cause of decreases in heat duty for particulate fouling on the frontal face of fins [21].

In this work, attempts are made to stay in heat recovery regions where powder deposition on the frontal face of fins is avoided. Walmsley et al. [22,23] presented a relationship between the velocity through the open area and milk powder stickiness. Using this relationship limits are placed on the outlet temperature of the exhaust heat exchanger, which is the point of greatest powder stickiness, to minimise the likelihood of fouling on the frontal face of fins. As a result only fouling on the frontal face of the tube is considered in the model. Future work will look in detail at the accuracy of this assumption between testing finned tubes of various pitches.

3.2.4. The effect of fouling on pressure drop

The effect of fouling pressure drop is estimated based on the experimental pressure drop data for single bare tubes in cross-flow from Walmsley et al. [17]. The experimentally examined fouling build up in Walmsley et al. [17] showed a asymptotic fouling behaviour, which data was analysed using a first order exponential equation containing a characteristic time constant. In this work, the first order approximation is differentiated with respect to obtain

$$\frac{d(\Delta P(\%))}{dt} = \frac{\Delta P_{final}(\%)}{\tau_f} \exp\left(-\frac{t}{\tau_f}\right) \tag{7}$$

For a small time step the change in pressure drop may be numerically estimated in the model using

$$\Delta(\Delta P(\%)) = \frac{\Delta P_{final}(\%)}{\tau_f} \exp\left(-\frac{t}{\tau_f}\right) \Delta t \tag{8}$$

Eq. (8) is applied to estimate how the pressure drop of the exhaust heat exchanger increases overtime. Experimental results of Walmsley et al. [17] yielded a time constant of 420 s based on a powder concentration of 1.8 g of powder per kg of air. In the model, the time constant is proportionally down-scaled to industrial situations where the powder concentration is significantly lower. Linear equations relating the final asymptotic value for the per cent pressure drop increase to stickiness are also obtained from the data presented in Walmsley et al. [17]. These equations are specific to the tube shape.

3.3. Utility and capital costing

Utility and capital cost estimates are made based on the parameters presented in Fig. 7. Capital cost equations are built into the spreadsheet and use the cost factor as a Lang factor. Based on these inputs together with the performance predictions, the spreadsheet calculates the cost benefit analysis shown in Fig. 8.

Literature and industrial documentation have very few capital cost estimation equations for finned tube heat exchangers. Furthermore the few equations that are present do not differentiate between heat exchangers with different fin pitches and tube or fin thickness and instead total area is used to estimate a capital cost. As a result the costs of the heat exchangers have been estimated using two different methods. Heat exchanger cost method A is based on calculating the total mass of stainless steel and aluminium required to make the heat exchangers multiplied by individual forming factors that reflect how easy a material will shape. Added to the material and forming costs is the cost of welding the heat exchanger together, which is dependent on the number of tubes in each exchanger, and the cost of putting fins on a tube. The sum of the various cost components relating to the construction of the heat exchanger is multiplied by a Lang factor of 3.5 [24]. Heat exchanger cost method B is based on the total area of the heat exchanger using

$$C_{HX,B} = 500A^{0.815} \tag{9}$$

Eq. (9) was fitted to data collected by the authors for recent industrial finned-tube heat exchanger installations. Capital and utility costs are calculated based on the New Zealand dollar. When simple payback, NPV and IRR are calculated, the spreadsheet uses the higher of the two heat exchanger cost estimates (either HX Cost A or HX Cost B in Fig. 8). Electrical power includes additional electricity consumed by the inlet fan for the new inlet exchanger, by the exhaust fan for the fouled exhaust heat exchanger, and by the water pump.

User Defined Cost Parameters		
Target Inlet Temp	200	°C
Steam Price	$ 30	/t
Electricity Price	$ 120	/MWh
$\eta_{Pump/Fan}$	0.60	
Cost for Cleaning	$ 5,000	/wash
Production Hours	5000	h/y
Utility Price Rise	5%	/y
Discount Rate	15%	/y
Accounting Period	10	y
Cost Factor	3.37	

Fig. 7. Screenshot from the spreadsheet model showing utility, capital and miscellaneous user defined parameters.

Cost/Benefit		
Estimated Savings	1289	kW
Steam Savings	$290,001	/y
Inlet Air Heat Req.	10,667	kW
%Main Air Heater Duty	12.1%	
Electrical Power	44	kW
Electrical Cost	$26,242	/y
Cleaning Cost	$ 0	/y
Profit	$ 263,759	/y
HX Cost A	$ 521,423	/y
HX Cost B	$ 339,528	/y
Pump & Fan Cost	$ 33,669	/y
Total Capital Cost	$555,092	
Payback	2.10	y
Net Present Value	$ 1,099,282	
IRR	54%	

Fig. 8. Screenshot from the spreadsheet model showing cost/benefit analysis results.

4. Industrial milk powder plant case study

The industrial case study for modelling exhaust heat recovery has an exhaust air temperature of 75 °C with a humidity of 48 g/kg before heat recovery flowing at 153 kg/s on a dry air basis. The inlet air is drawn in at 15 °C on average with a humidity of 10 g/kg at 117 kg/s on a dry air basis. The exhaust air flow includes air flow through the dryer and fluidised beds whereas the inlet air flow is only for the dryer. This same industrial plant was studied by Walmsley et al. [7].

In the analysis, a steam cost of $45/MWh and an electricity price of $120/GWh are used. The plant is assumed to operate for 5000 h per year and the dryer is washed every four weeks. At a minimum it is hoped that the exhaust heat exchanger will not require cleaning while the dryer is on product. Project economics are calculated using a typical industrial discount rate of 15% and an accounting period of 10 years. Utility prices are assumed to rise at a constant rate of 5% per year.

5. Results and discussion for industrial case study

5.1. Modelling heat exchanger performance with fouling

Heat exchanger performance has been modelled for a four week period with estimates for fouling build-up and its associated effects. Three tube types have been selected for comparison. The CF (circular finned tube), CF-9.05-3/4J, was selected from the available correlations in Kays and London [11] because it had the highest Goodness factor, i.e. *j/f*. The other tubes analysed include a bare round tube (CB), CB-1.5:1.25, and an EB (elliptical bare tube), EB-1.5:1.25. Fig. 9 plots one case where the inlet heat exchanger has 12 tube rows of CF-9.05-3/4J and the exhaust exchanger has 14 tube rows. Both heat exchangers have a face velocity of 4 m/s.

With no fouling, the finned tube exhaust heat exchanger recovered 3.2 MW, which is equivalent to a 14.4% reduction in steam use for the main dryer air heater. The duty of the finned tube exhaust exchanger system fell to 3.0 MW at the end of the dryer production cycle after fouling. The finned round tube had the greatest amount of deposition resulting in an 8% reduction in heat recovery, which is similar heat transfer reductions experienced in boilers [25], and an increase in pressure drop for the

exhaust exchanger of 5%, which is very modest. The bare round tube exhaust heat exchanger began with a duty of 2.7 MW, which fell to 2.6 MW at the end of the dryer run, and a pressure drop increase of 2%. The elliptical bare tube experienced very little fouling resulting in only a small change to its heat recovery and pressure drop. The low fouling property of elliptical tubes is well established in literature, e.g. Ref. [26], and is derived from the tube's small frontal area to perimeter ratio, which means that on average the particle impact angle is higher than for round tube. The exhaust exchanger with bare round tube recovers 17% less heat than with finned round tube. Fouling on the bare round tube is expected to be less than for the finned tube because the average temperatures experienced in the exhaust heat exchanger are higher due to less heat recovery compared to the finned round tube. The elliptical bare tube has a 41% lower pressure drop and a 3% higher heat recovery compared to the bare round tube. The elliptical tube is low fouling and is not expected to have much fouling after four weeks.

5.2. Optimisation of the liquid coupled loop heat exchanger system

The fouling with its associated effects has been modelled to analyse its impact on key economic indicators. In the optimisation, the tube geometries, number of tube rows in the exhaust exchanger (4–40), and face velocities for the exhaust heat exchanger (2–8 m/s), are methodically varied. In total over 25,000 time steps were modelled and the economics of the exhaust heat recovery system was analysed in terms of NPV and IRR based on average heat recovery and pressure drop values.

Fig. 10 plots the results for the finned round tube, bare round tube and elliptical round tube using the number of tube rows in the exhaust exchanger as the independent variable on the x-axis. Results show it is possible to design an economically favourable heat recovery system with a NPV reaching nearly $3 million over 10 years and IRR values greater than 50%. The face velocity of the exhaust heat exchanger in Fig. 10 is fixed at 4.0 m/s for all points. Furthermore each point in Fig. 10 takes into account fouling, which overtime lowers heat recovery and increases pressure.

Based on IRR the optimum number of exhaust tube rows is 6 tube rows whereas NPV indicates 12–14 tube rows is most profitable. This difference is important because IRR gives a good indication of the short-term payback of a project and NPV focuses on the long-term profit. As expected the finned tube exhaust heat exchanger offers better IRR and NPV values compared to the bare tubes.

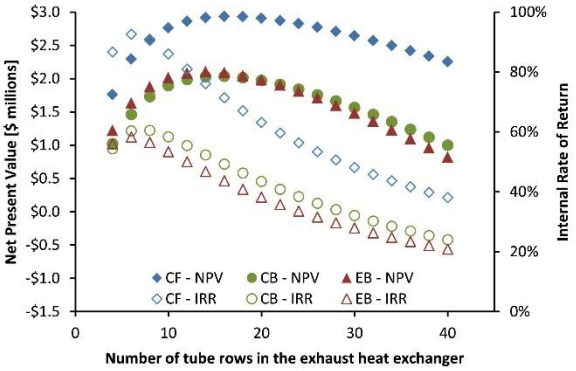

Fig. 10. Number of exhaust tube rows versus NPV and IRR.

The results may be also plotted using the exhaust outlet temperature as the x-axis as shown in Fig. 11. The deposition results on the frontal face of fins from Walmsley et al. [22] suggest fouling on the fins initiates and accelerates for exhaust temperatures below about 55 °C for an absolute humidity of 48 g/kg. In this particular case, the peak of the IRR and NPV curves all occur before 55 °C, which indicates deposition on the front of the fins should not occur. Fig. 11 shows the heat recovery savings achieved by basing the design on NPV is over 40% higher than basing the design on IRR.

Face velocity of the exhaust air heat exchanger is another important design parameter. Fluid velocity is often a parameter that is manipulated to reduce heat exchanger fouling at the expense of increased pressure drop. Fig. 12 plots the peak IRR and NPV values for the three heat exchanger geometries. In all cases the number of rows to achieve the peak IRR value compared to the peak NPV value is different. IRR analysis suggests a face velocity of about 6 m/s is advantageous whereas the NPV values support the selection of 4 m/s. Based on these results, the best LCHE system from a long-term investment viewpoint for the industrial case study is installation of a finned tube heat exchanger (CF-9.05-3/4J) to recover heat from the exhaust air with a face velocity of 4 m/s and 14 tube rows. For this system the NPV is NZ$2.9 million and an IRR of 71%.

6. Conclusion

Milk spray dryer exhaust heat recovery is economically justifiable based on an industrial case study with an exhaust temperature

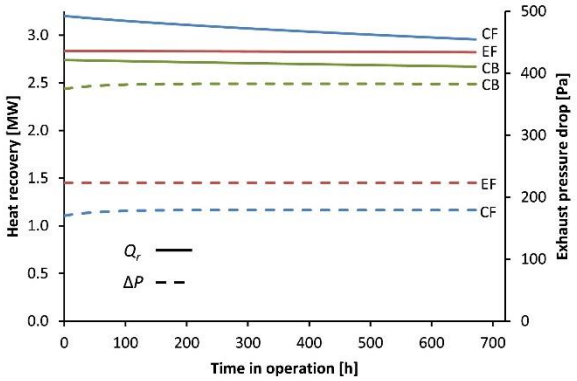

Fig. 9. Estimated heat recovery and pressure drop for a period of four weeks.

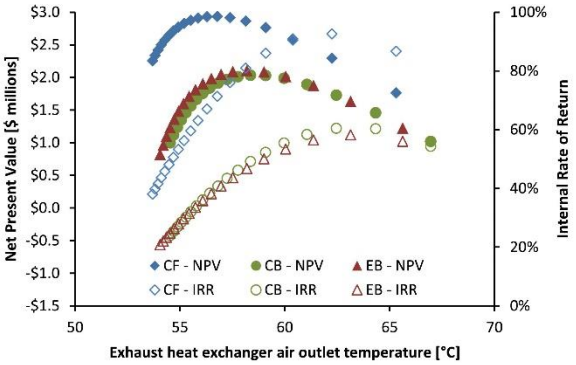

Fig. 11. Exhaust outlet temperature versus NPV and IRR.

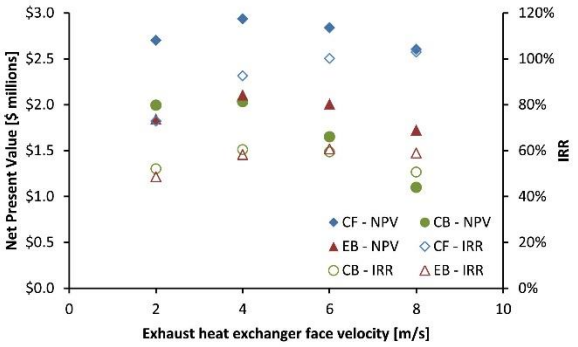

Fig. 12. Heat exchanger face velocity versus the peak NPV and IRR values.

of 75 °C. The exhaust heat recovery model applies literature correlations for finned-tube heat exchangers as the basis for determination of heat transfer and pressure drop. The impact of milk powder fouling in an exhaust heat recovery system is predicted to be able to be limited through smart heat exchanger design. Fouling predications are based on experimental correlations for milk powder deposition and fouling from literature. Results show that 4 m/s face velocity is the best trade-off between reducing fouling while maintaining an acceptable pressure drop. Internal rate of return analysis suggests the exhaust heat exchanger should contain only a few rows of tube (4–6 rows) whereas net present value analysis favours a larger exhaust heat exchanger with 12–14 rows. The developed thermo-economic assessment model has flexibility to be applied to any milk powder plant to optimise the economics of an exhaust heat recovery system.

Appendix. Site specific challenges facing economic implementation of milk spray dryer exhaust heat recovery

The economics for dryer exhaust heat recovery are highly site specific. For different industrial case studies, the optimum design of the exhaust heat exchanger may change; however the same thermos-economic analysis method may be applied. The operation, equipment, and construction are slightly different for each milk powder plant and spray dryer. The purpose of this section is to highlight some of the important factors that require consideration for industrial implementation of exhaust heat recovery in New Zealand milk powder plants by drawing upon the authors' collective experiences and observations.

- **Inlet air temperature and humidity to the dryer:** The temperature and humidity of the ambient is location specific. The temperature of the inlet air as the designated heat sink provides essential temperature driving to recovery exhaust heat, which is directly related to the size of the exhaust heat exchanger. The inlet temperature will vary during a day/night and over the production season. Less humidity air is advantageous in terms of dryer capacity, but it also has a lower heat capacity flow rate, which means less recovered heat and steam is needed to raise the temperature of the air to approximately 200 °C.
- **Exhaust air temperature and humidity:** Dryers with higher exhaust temperatures are better candidates for energy recovery due to a larger potential temperature driving force, which results in increase heat recovery and improved economics. Humidity is also an important factor because it affects the stickiness of the milk powder and, therefore, the amount of fouling. For ease of exhaust heat recovery, a lower humidity is desirable, but from an overall dryer efficiency perspective, lower exhaust temperatures at high humidity maximise the drying capacity of the air.
- **Inlet and exhaust fan capacity**: For existing sites it is important to understand where the inlet and exhaust fans are operating on the respective fan curves. Fans with sufficient spare capacity do not require replacement, which for retrofits is likely to be a significant cost. Where fans are likely pressure drop constrained, it is smarter to design the exhaust and inlet heat exchangers to meet a pressure drop target rather than a heat recovery target.
- **Existing pre-heaters using utility:** at many sites steam is used to preheat air entering the building to 30–35 °C. These heat exchangers are typically a few rows deep with a large frontal area and a low face velocity. Re-piping an existing inlet preheater exchanger to use heat from the dryer exhaust is likely the most economical opportunity for some sites.
- **Existing heat recovery to dryer inlet air:** some sites use waste heat from flue gas from the boiler or hot process condensate water to preheat the dryer inlet air. Because exhaust heat recovery is heating in similar temperature ranges, the full benefits of both heat recovery systems are not achievable.
- **Re-usable existing ducting:** if possible it is desirable to avoid the costs of fabricating and installing large sections of new ducting.
- **Price of energy:** heating costs can vary by 30–50% from site to site depending on the fuel source – either coal or natural gas – and the conversion efficiency. The supply of energy can strongly affect the price of energy.
- **Operating and production hours:** heat recovery savings is directly proportional to the hours of production per year.
- **Physical space:** the building housing the dryer needs to have the room for a heat recovery system. Modifications to buildings are very costly and risky potentially causing product contamination.
- **Inlet air heater bottleneck:** where the inlet air heater is the bottleneck to increased production, exhaust heat recovery would provide additional duty to allow for more airflow into the dryer and additional dryer capacity. In this case, exhaust heat recovery may prevent the need for increasing the capacity of the existing steam boiler to meet the higher process heat demand.
- **Bag filters:** efficient removal of milk particles from the exhaust air stream can decrease the risk and potential for exchanger fouling.
- **Good attitude to change:** the site needs a good attitude to change, particularly when a technology is being implemented for the first time.

References

[1] Reay D. A selection of heat recovery applications illustrated by means of case studies. J Heat Recovery Syst 1982;2:401–18. http://dx.doi.org/10.1016/0198-7593(82)90028-5.
[2] Mercer AC. Improving the energy efficiency of industrial spray dryers. J Heat Recovery Syst 1986;6:3–10. http://dx.doi.org/10.1016/0198-7593(86)90166-9.
[3] Laurijssen J, De Gram FJ, Worrell E, Faaij A. Optimizing the energy efficiency of conventional multi-cylinder dryers in the paper industry. Energy 2010;35:3738–50. http://dx.doi.org/10.1016/j.energy.2010.05.023.
[4] Han X, Liu M, Wang J, Yan J, Liu J, Xiao F. Simulation study on lignite-fired power system integrated with flue gas drying and waste heat recovery – performances under variable power loads coupled with off-design parameters. Energy 2014;76:406–18. http://dx.doi.org/10.1016/j.energy.2014.08.032.
[5] Tippayawong N, Tantakitti C, Thavornun S. Energy efficiency improvements in longan drying practice. Energy 2008;33:1137–43. http://dx.doi.org/10.1016/j.energy.2008.02.007.
[6] Linnhoff B, Hindmarsh E. The pinch design method for heat exchanger networks. Chem Eng Sci 1983;38:745–63.

[7] Walmsley TG, Walmsley MRW, Atkins MJ, Neale JR. Improving energy recovery in milk powder production through soft data optimisation. Appl Therm Eng 2013;61:80–7. http://dx.doi.org/10.1016/j.applthermaleng.2013.01.051.
[8] Walmsley TG, Walmsley MRW, Atkins MJ, Neale JR. Integration of industrial solar and gaseous waste heat into heat recovery loops using constant and variable temperature storage. Energy 2014;75:53–67. http://dx.doi.org/10.1016/j.energy.2014.01.103.
[9] Walmsley TG, Walmsley MRW, Atkins MJ, Fodor Z, Neale JR. Optimal stream discharge temperatures for a dryer operation using a thermo-economic assessment. Chem Eng Trans 2012;29:403–8. http://dx.doi.org/10.3303/CET1229252.
[10] Atkins MJ, Walmsley MRW, Neale JR. Integrating heat recovery from milk powder spray dryer exhausts in the dairy industry. Appl Therm Eng 2011;31:2101–6. http://dx.doi.org/16/j.applthermaleng.2011.03.006.
[11] Kays WM, London AL. Compact heat exchangers. 3rd ed. Malabar, USA: Krieger Pub. Co.; 1998.
[12] Walmsley TG, Walmsley MRW, Atkins MJ, Neale JR, Sellers CM. An experimentally validated criterion for skim milk powder deposition on stainless steel surfaces. J Food Eng 2014;127:111–9. http://dx.doi.org/10.1016/j.jfoodeng.2013.11.025.
[13] London AL, Kays WM. The liquid coupled indirect-transfer regenerator for gas turbine plants. Trans ASME 1951;73:529–40.
[14] Walmsley TG, Walmsley MRW, Atkins MJ, Hoffman-Vocke J, Neale JR. Numerical performance comparison of different tube cross–sections for heat recovery from particle-laden exhaust gas streams. Procedia Eng 2012;42:1476–90. http://dx.doi.org/10.1016/j.proeng.2012.07.527.
[15] Wang CC, Webb RL, Chi KY. Data reduction for air-side performance of fin-and-tube heat exchangers. Exp Therm Fluid Sci 2000;21:218–26. http://dx.doi.org/10.1016/S0894-1777(00)00005-4.
[16] Holmberg RB. Heat transfer in liquid-coupled indirect heat exchanger systems. J Heat Transf 1975;97:499–503.
[17] Walmsley TG, Walmsley MRW, Atkins MJ, Neale JR. Analysis of skim milk powder deposition on stainless steel tubes in cross-flow. Appl Therm Eng 2015;75:941–9. http://dx.doi.org/10.1016/j.applthermaleng.2014.10.066.
[18] Nijdam JJ, Langrish TAG. The effect of surface composition on the functional properties of milk powders. J Food Eng 2006;77:919–25. http://dx.doi.org/10.1016/j.jfoodeng.2005.08.020.
[19] Pisecky I. Handbook of milk powder manufacture. Copenhagen, Denmark: Niro A/S; 1997.
[20] MAF Quality Management. Physical properties of dairy products. 3rd ed. Hamilton, New Zealand: MAF Quality Management; 1996.
[21] Bell IH, Groll EA. Air-side particulate fouling of microchannel heat exchangers: experimental comparison of air-side pressure drop and heat transfer with plate-fin heat exchanger. Appl Therm Eng 2011;31:742–9. http://dx.doi.org/10.1016/j.applthermaleng.2010.10.019.
[22] Walmsley TG, Walmsley MRW, Atkins MJ, Neale JR. Fouling and pressure drop analysis of milk powder deposition on the front of parallel fins. Adv Powder Technol 2013;24:780–5. http://dx.doi.org/10.1016/j.apt.2013.04.004.
[23] Walmsley TG, Walmsley MRW, Atkins MJ, Neale JR. An investigation of milk powder deposition on parallel fins. In: Chemeca 2012. Wellington, New Zealand: IChemE; 2012.
[24] Bouman RW, Jensen SB, Wake ML, Earl WB. Process capital cost estimation for New Zealand 2004. Wellington, New Zealand: Society of Chemical Engineers New Zealand; 2005.
[25] Stehlík P. Conventional versus specific types of heat exchangers in the case of polluted flue gas as the process fluid – a review. Appl Therm Eng 2011;31:1–13. http://dx.doi.org/10.1016/j.applthermaleng.2010.06.013.
[26] Bouris D, Konstantinidis E, Balabani S, Castiglia D, Bergeles G. Design of a novel, intensified heat exchanger for reduced fouling rates. Int J Heat Mass Transf 2005;48:3817–32. http://dx.doi.org/10.1016/j.ijheatmasstransfer.2005.03.026.

CHEMICAL ENGINEERING TRANSACTIONS
VOL. 52, 2016
A publication of AIDIC
The Italian Association of Chemical Engineering
Online at www.aidic.it/cet
Guest Editors: Petar Sabev Varbanov, Peng-Yen Liew, Jun-Yow Yong, Jiří Jaromír Klemeš, Hon Loong Lam

ISBN 978-88-95608-42-6; **ISSN** 2283-9216
DOI: 10.3303/CET1652194

Impact of Hybrid Heat Transfer Enhancement Techniques in Shell and Tube Heat Exchanger Design

Ehsan Shekarian[a], Mohammad R. Jafari Nasr[b], Amir H. Tarighaleslami[c]*, Timothy G. Walmsley[c], Martin J. Atkins[c], Nadia Sahebjamee[d], Mohammad Alaghehbandan[e]

[a]Department of Chemical Engineering, College of Engineering, Adadshahr Branch, Islamic Azad University, Azadshahr, Iran
[b]Research Institute of Pertoleum Industry (RIPI), Tehran, Iran
[c]Energy Research Centre, School of Engineering, University of Waikato, Private Bag 3105, Hamilton 3240, New Zealand
[d]Department of Chemical Engineering, College of Engineering, Quchan Branch, Islamic Azad University, Quchan, Iran
[e]Applied Research Centre for Agricultural Inputs, Karaj, Iran
aht5@students.waikato.ac

Despite the advantages of shell and tube heat exchangers, one of their major problems is low thermal efficiency. This problem can be improved by using heat transfer enhancement techniques such as adding nanoparticles to the hot or cold fluids, and/or using tube inserts as turbulators on tube side as well as changing baffles to a helical or twisted profile on the shell side. Although all of these techniques increase the thermal efficiency; however, engineers still need a quantitative approach to assess the impact of these technologies on the shell and tube heat exchangers. This study attempts to provide a combination of such techniques to increase the impact of these improvements quantitatively. For this purpose, at first stage the thermal and hydraulic characteristics of pure fluid, Al_2O_3/water nanofluid in a plain tube equipped with and without twisted tape turbulator is evaluated based on a developed rapid design algorithm. Therefore, the impact of using enhanced techniques either in form of individual or in hybrid format and the increase of nanoparticle concentration in base fluid have been studied. The results show that using turbulators individually and in hybrid format with nanofluid can be effected on design parameters of a typical heat exchanger by reducing the required heat transfer area up to 10 %.

1. Introduction

Shell and Tube Heat Exchangers (STHE) are widely used in various industries such as oil, gas, petrochemical and power plants. Despite the increase in uptake of other types of Heat Exchangers (HE), which have better performance, STHEs remain the most widely used type of heat exchanger.
Iterative trial and error procedures are commonly applied in HE design procedures to achieve desirable heat loads subjected to the allowable fluid pressure drops. As a result, to ensure compliance with the allowable pressure drop and achieve a desired duty, HEs are designed larger than actually required. Polley et al. (1991) introduced a HE design algorithm, which could calculate simultaneously desirable heat load with consideration of maximum allowable pressure drops. The results are higher velocities on both the shell and tube sides, higher heat transfer coefficients and the minimum heat transfer area requirement, i.e. minimum capital cost. The method is called the Rapid Design Algorithm (RDA). Polley et al. (1991) introduced simple equations based on the Kern method (1950) for each stream, which correlated pressure drop, heat transfer coefficient of the fluid, and the heat exchanger area together. Combining pressure drop and basic heat exchange relationships led designers to avoid lengthy trial and error procedure. However, using Kern relations increases shell side errors due to inaccurate relationships. Later, Bell-Delaware equations were used to improve flow pattern in shell side and consequently achieved closer results of thermal-hydraulic analysis to experimental

Please cite this article as: Shekarian E., Jafari Nasr M. R., Tarighaleslami A. H., Walmsley T. G., Atkins M. J., Sahebjamee N., Alaghehbandan M., 2016, Impact of hybrid heat transfer enhancement techniques in shell and tube heat exchanger design, Chemical Engineering Transactions, 52, 1159-1164 DOI:10.3303/CET1652194

results (Serna and Jiménez, 2005). In this model, the amounts of leakage near the baffles and by pass flow were considered.
Various techniques have been applied to increase heat transfer rates in HEs and decrease heat and energy losses in process industries. These methods are known as Heat Transfer Enhancement (HTE). HTE can be applied in both shell side and tube side of STHEs. Helical baffles are more common in shell side (Wang et al., 2010). Jafari Nasr and Shafeghat (2008) presented a combination of HTE using helical baffles and RDA. Applying different types of turbulators and/or nanofluids are examples of HTE techniques in tube side. HTE techniques can be applied in both grassroots and retrofit designs to improve heat transfer characteristics of HEs. However, due to high revamp costs in large industries such as oil, gas, petrochemical and power plants, applying HTE techniques are more reliable and profitable in economical point of view.
Using nanofluids as service fluid in HEs is another HTE technique, which recently has been investigated for large industrial plants (Tarighaleslami et al., 2015). Nanofluids are prepared by distributing a nanoparticle through a base fluid, which helps increase its thermal conductivity (Shekarian et al., 2014). Bubbico et al. (2015) showed that different type of nanofluid may provide improved heat transfer efficiency. Elias et al. (2014) investigated the effect of different shape of nanoparticles on overall heat transfer coefficient of a STHE using different baffle angles and nanofluid. Sundar and Sharma (2010) studied the effect of increasing in heat load by using twisted tape inserts in laminar and turbulent flows. They used twisted tape inserts in presence of Al_2O_3/water nanofluid and proposed relationships for friction factor and Nusselt for simultaneous use of twisted tape insert and Al_2O_3/water nanofluid.
The aim of this paper is to develop the required inputs to RDA for three tube-side HTE scenarios for STHEs using the empirical correlations of Sundar and Sharma (2010). The three considered scenarios are: (1) Al_2O_3/water nanofluid, (2) twisted tape turbulators, and (3) a hybrid combination of both techniques.

2. Methodology

RDA method is one of the heat exchanger design methods that eliminates any trial and error calculations due to geometrical changes, leading to faster achievement of optimal design results. In RDA method, calculation of the heat exchanger area is based on the maximum usage of the given allowable pressure drop on both the shell- and tube-sides and solving the set of equations (1) simultaneously (Serna and Jiménez, 2004).

$$A = \frac{Q}{F_T \Delta T_{LM}}\left(\frac{1}{h_s} + \frac{1}{h_t} + \sum R\right)$$
$$\Delta P_t = K_T . A . h_t^n \qquad (1)$$
$$\Delta P_s = K_S . A . h_s^m$$

ΔP_s and ΔP_t are the maximum allowable pressure drop for shell and tube sides, K_T, K_S, m and n are dependent to the geometric parameters of the heat exchanger and physical properties of the fluid. K_T and n values are obtained based on semi-empirical equations that have been reported by reliable sources for the Nusselt number, friction factor and some mathematical simplifications. m and K_S are also available in terms of the shell side and based on the Bell-Delaware method.

2.1 The heat exchanger design algorithm and tube and shell sides equations

In each of the scenarios, the same shell-side correlations are applied. The Bell-Delaware equations that are needed as inputs to the RDA (Shenoy, 1995) are:.

$$\Delta P_s = (K_{S1} . A + K_{S2}) . h_s^2$$

$$K_{S1} = \frac{\left[(1+0.3N_{tcw}).\rho_s.R_l + 2.f_i.\rho_s.N_{tcc}.\left(\frac{\mu_s}{\mu_{sw}}\right)^{-0.14} R_l R_b\right]}{(\pi.D_t.N_t.L_{bc}.NS).\left[j_h \frac{k_s.\rho_s}{\mu_s}\left(\frac{C_{ps}.\mu_s}{k_s}\right)^{\frac{1}{3}}\left(\frac{\mu_s}{\mu_{sw}}\right)^{0.14} J_c J_l J_b J_r J_s\right]^2} \qquad (2)$$

$$K_{S2} = \frac{\left[2f_i\rho_s N_{tcc}\left(\frac{\mu_s}{\mu_{sw}}\right)^{-0.14}\left(1+\frac{N_{tcw}}{N_{tcc}}\right)R_s R_b - (1+0.3N_{tcw})\rho_s R_l - 4f_i\rho_s N_{tcc}\left(\frac{\mu_s}{\mu_{sw}}\right)^{-0.14} R_l R_b\right]}{\left[j_h \frac{k_s.\rho_s}{\mu_s}\left(\frac{C_{ps}.\mu_s}{k_s}\right)^{\frac{1}{3}}\left(\frac{\mu_s}{\mu_{sw}}\right)^{0.14} J_c J_l J_b J_r J_s\right]^2}$$

Scenario 1: No HTE - water flows in plain wall tube
In this case, water is used as the fluid on the tube side. Equations for Nusselt number and friction factor equations (Shenoy, 1995) are:

$$Nu = 0.023Re^{0.8}Pr^{1/3}$$
$$f = 0.184Re^{-0.2} \quad (3)$$

The relationship between pressure drop and heat transfer coefficient, therefore, is:

$$\Delta P_t = K_T . A . h^{3.5}$$
$$K_T = k_1 \frac{\rho_t D_i^2}{4M_t D_t} \left(\frac{1}{k_2}\right)^{3.5}$$
$$k_1 = 0.092 \left(\frac{\rho_t}{D_i}\right) \left(\frac{\rho_t D_i}{\mu_t}\right)^{-0.2} \quad (4)$$
$$k_2 = 0.023 Pr^{1/3} \left(\frac{k_t}{D_i}\right) \left(\frac{\rho_t D_i}{\mu_t}\right)^{0.8}$$

Scenario 2: Nanofluid HTE - Al_2O_3/water nanofluid in plain wall tubes
In this case, the object is to evaluate the effect of nanofluid on heat exchanger design parameters. Applied Nusselt number and friction factor (Pak and Cho, 1998) are:

$$Nu = 0.021Re^{0.8}Pr^{0.5}$$
$$f = 0.316Re^{-0.2} \quad (5)$$

The following equations express the relationship between pressure drop and heat transfer coefficient:

$$\Delta P_t = K_T . A . h^{3.5}$$
$$K_T = k_1 \frac{\rho_t D_i^2}{4M_t D_t} \left(\frac{1}{k_2}\right)^{3.5}$$
$$k_1 = 0.632 \left(\frac{\rho_t}{D_i}\right) \left(\frac{\rho_t D_i}{\mu_t}\right)^{-0.2} \quad (6)$$
$$k_2 = 0.021 Pr^{0.5} \left(\frac{k_t}{D_i}\right) \left(\frac{\rho_t D_i}{\mu_t}\right)^{0.8}$$

Scenario 3: Turbulent flow of water in tubes containing twisted tapes
In this case, the effect of turbulator on HE design parameters has been studied. For this scenario, suggested equations by Sundar and Sharma (2010), which are obtained from a regression of their experimental results, are used.

$$Nu = 0.02649Re^{0.8204}Pr^{0.4}(0.001 + \frac{H}{D})^{0.06281}$$
$$f = 2.068Re^{-0.4330}(1 + \frac{H}{D})^{0.004815} \quad (7)$$

This corresponds to the following relationships as RDA inputs:

$$\Delta P_t = K_T . A . h^{3.1290}$$
$$K_T = k_1 \frac{\rho_t D_i^2}{4M_t D_t} \left(\frac{1}{k_2}\right)^{3.1290}$$
$$k_1 = 4.136(1 + \frac{H}{D})^{0.004815} \left(\frac{\rho_t}{D_i}\right) \left(\frac{\rho_t D_i}{\mu_t}\right)^{-0.4330} \quad (8)$$
$$k_2 = 0.02649(0.001 + \frac{H}{D})^{0.06281} Pr^{0.4} \left(\frac{k_L}{D_i}\right) \left(\frac{\rho_t D_i}{\mu_t}\right)^{0.8204}$$

Scenario 4: Hybrid Al_2O_3/water nanofluid in a tube containing a twisted tape turbulators
In this case, the effect of the combination of nanofluid and turbulators is investigated. Again Sundar and Sharma (2010) equations are used.

$$Nu = 0.03666Re^{0.8204}Pr^{0.4}(0.001 + \phi)^{0.04704}(0.001 + \frac{H}{D})^{0.06281} \quad (9)$$

$$f = 2.068Re^{-0.4330}(1+\phi)^{0.01}(1+\frac{H}{D})^{0.004815}$$

The relation between pressure drop and heat transfer coefficient is:

$$\Delta P_t = K_T.A.h^{3.1290}$$

$$K_T = k_1 \frac{\rho_t D_t^2}{4M_t D_t}\left(\frac{1}{k_2}\right)^{3.1290}$$

$$k_1 = 4.136(1+\phi)^{0.01}(1+\frac{H}{D})^{0.004815}\left(\frac{\rho_t}{D_i}\right)\left(\frac{\rho_t D_i}{\mu_t}\right)^{-0.4330} \quad (10)$$

$$k_2 = 0.03666(0.001+\phi)^{0.04704}(0.001+\frac{H}{D})^{0.06281}Pr^{0.4}\left(\frac{k_t}{D_i}\right)\left(\frac{\rho_t D_i}{\mu_t}\right)^{0.8204}$$

3. Illustrative case study

To study the effect of HTE techniques, a case study is investigated for base case and three HTE scenarios. Allowable pressure drop in the tube and shell sides are 42,000 and 7,000 Pa. The HE is entirely made of carbon steel and consists of one shell pass and 6 tube passes. Shell side flow rate is 14.9 kg/s. Thermo-physical properties of the tube side fluids (service fluid, water and nanoparticle) and shell side fluid are presented in Table 1. Using the equations provided by Pak and Cho (1998), the thermo-physical properties of nanofluid can be calculated.

Table 1: Thermo-physical properties of fluids and nanoparticle, and flow stream data.

Fluid / Nanoparticle Direction	ρ (kg/m^3)	C_p (kg °C)	k (W/m °C)	μ (kg/m s)	Fouling Factor	T_{in} (°C)	T_{out} (°C)
Water / Tube	998	4,180	0.60	0.001	0.00015	15	25
Service Fluid / Shell	777	2,684	0.11	0.00023	0.00015	98	65
Al_2O_3	3970	880					

4. Results and discussion

4.1 Validation

To validate the result of RDA method, the result outcomes of this design has been compared with results of Kern and Bell-Delaware methods. Results show that in both RDA with Kern and RDA with Bell-Delaware methods acceptable ranges are achieved. Moreover, in Kern and Bell-Delaware methods, due to iterative trial and error calculations, it is not always possible to reach to the maximum allowable pressure drop, while it is a disadvantages of these methods compared with RDA.

4.2 Effect of nanofluid

Table 2 shows the effect of nanofluid by increasing of nanofluid concentration compared with water. According to the results, using nanofluid leads to a slight reduction in required heat transfer surface area. The reduction in heat transfer area is an advantage of nanofluids, which in some cases makes a reduction in initial investment cost compared to the cases that pure water is used. According to Table 2 it can be concluded that the use of nanoparticles only up to a certain concentration can cause an improvement; higher concentration has no benefit in the design parameters (most notably is the exchanger surface). The reason of this phenomenon is that the thermo-physical properties of nanofluid are different from the thermos-physical properties of the base fluid. Convective heat transfer coefficient of nanofluids is a function of the thermal conductivity and heat capacity of the base fluid and nanoparticles, flow patterns, Reynolds and Prandtl numbers, the volume fraction of nanoparticles in nanofluid, nanoparticle size and shape.

To increase the heat transfer coefficient in turbulent flow, both the conductive heat transfer coefficient and heat capacity should increase while the viscosity needs to be reduced. However, as it can be seen in Table 2, by increasing the concentration of nanoparticles in the base fluid, thermal conductivity and viscosity increase, and heat capacity decreases. As a result, there is a trade-off between these parameters. Hence it can be concluded that for concentration up to 0.1 % of nanoparticles causes the thermal conductivity to dominate heat capacity and viscosity. This results in the convective heat transfer coefficient increasing. By using more amounts of nanoparticles, the process demonstrates reversed behaviour. Thus a decline in the convective heat transfer coefficient of tubes happens and the surface increases.

Table 2: Effect of nanofluid and its concentration on the HE design parameters.

Parameter	Plain Tube	NF 0.1 %	NF 0.2 %	NF 0.3 %	NF 0.4 %	NF 0.5 %
Area (m^2)	15.695	15.487	15.514	15.541	15.569	15.596
h_t (W/m^2 °C)	10,247	11,016	10,908	10,802	10,699	10,599
M_t (kg/s)	31.572	31.597	31.622	31.647	31.672	31.697
V_t (m/s)	3.427	2.826	2.812	2.798	2.784	2.771
Re_t	52,665	41,889	40,238	38,663	37,168	35,748

4.3 Effect of a twisted tape turbulator

To investigate the influence of twisted tape turbulator on design parameters of HE, results are compared with an HE with the plain tubes (in both cases, the fluid is water). Results are summarised in Table 3, which shows, by using this type of turbulator, heat exchanger surface will decrease about 10 %. The turbulator disrupts the boundary layer. The tube-side fluid velocity slightly increases due to the reduction in cross sectional area because of the presence of the turbulator and constant flow rate. These changes cause convective heat transfer coefficient to increase and required surface to decrease.

Table 3: Effect of the twisted tape turbulator on design parameters of a HE

Parameter	Plain Tube	Pipe with Turbulator
Area (m^2)	15.695	14.190
h_t (W/m^2 °C)	10,247	20,675
M_t (kg/s)	31.572	31.572
V_t (m/s)	3.427	3.709
Re_t	52,665	56,998

4.4 Effect of the hybrid use of nanofluid and turbulator

According to Table 4, the hybrid use of nanofluid and turbulator decreases the required surface. There is also an optimum concentration for nanoparticles of 0.2 %, above which using more nanoparticles leads to increases in area.

Table 4: Effect of the hybrid use of different concentrations of nanofluid and turbulator on HE design parameters

Parameter	Plain Pipe	Insert + NF 0.1 %	Insert + NF 0.2 %	Insert + NF 0.3 %	Insert + NF 0.4 %	Insert + NF 0.5 %
Area (m^2)	15.695	14.166	14.161	14.165	14.173	14.183
h_t (W/m^2 °C)	10,247	21,024	21,088	21,036	20,923	20,775
V_t (m/s)	3.427	3.681	3.652	3.623	3.594	3.566
Re_t	52,665	54,583	52,269	50,070	47,984	46,007

4.5 Comparison of the different scenarios results

In this section the best results of four different scenarios are compared with each other. The best result appertains to the case of the simultaneous use of the twisted tape turbulator and the Al_2O_3/water nanofluid (at an optimal concentration of 0.2 %). However, the reduction in exchanger surface is negligible compared to the case of using only a turbulator. The more economical solution is there to use only turbulator.

5. Conclusions

The effects of Al_2O_3/water nanofluid, twisted tape turbulator and hybrid use of these two methods, which is considered as new method of HTE at the design parameters of STHE by the means of RDA have been successfully evaluated. The RDA is effective in designing for a specified pressure drop even with heat transfer enhancement techniques. In the case study, results illustrate that increases in nanofluid concentration up to an optimum level insignificantly reduces the heat transfer area and associated investment costs. It is likely that the cost of using nanoparticles in the system will out-weigh the benefits. Using a twisted tape turbulator reduces the required surface by up to 10 %.

Nomenclature

A : Heat Transfer Area (m^2)
C_p : Specific Heat (J/kg °C)
D : Diameter of the Tube (m)
f : Friction Factor
K : RDA Constant
L : Length of the Tube (m)
L_{tp} : Tube Pitch Length (m)
L_{bc} : Baffle Spacing Length (m)
M : Mass Flow Rate (kg/s)
N_b : Number of Baffle
NF : Nanofluid
Q : Heat Transfer Rate (W)
Nu : Nusselt Number
Pr : Prandtl Number
Re : Reynolds Number
T : Temperature (°C)
V : Velocity (m/s)
N_{tcc}: Number of Effective Tube Rows in Cross Flow
N_t : Number of Tube
F : Shell and Tube Correction Coefficient
h : Convective Heat Transfer Coefficient (W/m^2 °C)
H/D : Twist Ratio
k : Thermal Conductivity (W/m °C)
NS : Number of Shell Passes
R_l : Correction Factor for Baffle Leakage
R_b : Correction Factor for Baffle Bypass
h_{ic} : Heat Transfer Coefficient for Ideal Cross Flow
J_c : Segmental Baffle Window Correction Factor
J_l : Baffle Leakage Correction Factor
J_b : Bundle Bypass Correction Factor
J_r : Adverse Temperature Gradient Build up Correction Factor at Low Reynolds Number
J_s : Unequal Baffle Spacing Correction Factor
ΔP : Pressure Drop (Pa)
ΔT : Temperature Difference (°C)
ϕ : Nanoparticles Volume Concentration (%)
μ : Dynamic Viscosity (kg/m^2 s)
ρ : Density (kg/m^3)
ΣR : Resistance Summation

Subscripts

B : Baffle
bf : Base Fluid
I : Inner
o : Outer
LM : Log Mean
nf : Nanofluid
p : Nanoparticle
s : Shell
S : Shell Side
tp : Tube Pitch
t : Tube
T : Tube Side

Reference

Bubbico R., Celata G.P., D'Annibaleb F., Mazzarotta B., Menale C., 2015, Comparison of the Heat Transfer Efficiency of Nanofluids, Chemical Engineering Transactions, 43, 703–708.
Elias M.M., Shahrul I.M., Mahbubul I.M., Saidur R., Rahim N.A., 2014, Effect of different nanoparticle shape on STHE using different baffle angles and operated with nanofluid, Int. J. Heat Mass Transf., 70, 289–297.
Jafari Nasr M.R., Shafeghat A., 2008, Fluid flow analysis and extension of rapid design algorithm for helical baffle heat exchangers, Appl. Therm. Eng., 28, 1324–1332.
Kern D.Q., 1950, Process Heat Transfer. Mc-Graw-Hill, New York, USA.
Pak B.C., Cho Y.I., 1998, Hydrodynamic and Heat Transfer Study of Dispersed Fluids with Submicron Metallic Oxide Particles, Exp. Heat Transf., 11, 151–170.
Polley G.T., Panjeh Shahi M.H., Picon Nunez M., 1991, Rapid design algorithms for shell-and-tube and compact heat exchangers, Chem. Eng. Res. Des., 69, 435–444.
Serna M., Jiménez A., 2005, A Compact Formulation of the Bell–Delaware Method for Heat Exchanger Design and Optimization, Chem. Eng. Res. Des., 83, 539–550.
Serna M., Jiménez A., 2004, An Efficient Method for the Design of STHEs, Heat Transf. Eng., 25, 5–16.
Shekarian E., Tarighaleslami A.H., Khodaverdi F., 2014, Review of Effective Parameters on the Nanofluid Thermal Conductivity, J. Middle East Appl. Sci. Technol., 6, 776–780.Shenoy U.V., 1995, Heat Exchanger Network Synthesis: Processes Optimization by Energy and Resource Analysis, Gulf Publishing Company, Houston, USA.
Sundar L.S., Sharma K.V., 2010, Turbulent heat transfer and friction factor of Al2O3 Nanofluid in circular tube with twisted tape inserts, Int. J. Heat Mass Transf., 53, 1409–1416.
Tarighaleslami A.H., Walmsley T.G., Walmsley M.R.W., Atkins M.J., Neale J.R., 2015, Heat Transfer Enhancement in Heat Recovery Loops Using Nanofluids as the Intermediate Fluid, Chemical Engineering Transactions, 45, 991–996.
Wang Q., Chen G., Zeng M., Chen Q., Peng B., Zhang D., Luo L., 2010, Shell-side heat transfer enhancement for shell-and-tube heat exchangers by helical baffles, Chemical Engineering Transactions, 21, 217–222.